2010

Integration of paleotempestology with coastal risk and vulnerability assessment: case studies from the Dominican Republic and Nicaragua

Devyani Kar
Louisiana State University and Agricultural and Mechanical College, dkar1@lsu.edu

INTEGRATION OF PALEOTEMPESTOLOGY WITH COASTAL RISK AND VULNERABILITY ASSESSMENT: CASE STUDIES FROM THE DOMINICAN REPUBLIC AND NICARAGUA

A Dissertation

Submitted to the Graduate Faculty of the
Louisiana State University and
Agricultural and Mechanical College
In partial fulfillment of the
Requirements for the degree of
Doctor of Philosophy

In

The Department of Oceanography and Coastal Sciences

By
Devyani Kar,
B.Plan., School of Planning and Architecture, New Delhi, India, 2001
M.E.M., Duke University, 2003
December, 2010

To my parents,

Dr. Prabhat Kumar Kar

Dr. Sanghamitra Kar

ACKNOWLEDGEMENTS

I wish to offer my immense gratitude to Dr. Kam-biu Liu, my advisor and committee chair, for his guidance and support. This dissertation would not have been possible without his endless patience, persistence, and encouragement at every step.

I would like to thank Dr. Nina Lam, Dewitt Braud, Dr. Jaye Cable, and Dr. Melanie Gall for serving on my committee and assisting me with various aspects of this work.

Sincere thanks to Dr. Escobar, Dr. Jagger, and Dr. Elsner for discussing research ideas and for patiently explaining complicated statistical models.

I would like to acknowledge Inter American Institute for Global Change Research (IAI) for providing funding for this study. National Science Foundation (NSF), the Graduate School at Louisiana State University (LSU), and the Department of Oceanography at LSU helped with travel funds to present my work at national and international conferences. An award from American Association of Geographers (AAG) contributed toward the cost of Spanish immersion in Nicaragua to better prepare me for field work.

Thanks to Dr. Jaye Cable and Chris Whittaker for assistance with ^{137}CS and ^{210}Pb analysis; Floyd DeMers for help with grain size analysis; and to Dr. Terry McCloskey and Tom Bianchette for their help with loss-on-ignition analysis.

I am grateful to Dr. Lisa Kennedy, Allison LeBlanc, Pedro Martinez, and Dr. Terry McCloskey for helping with coring and data collection in the Dominican Republic. Research in Nicaragua would not have been possible without Claudia Taleno and Yelba Flores – a big Thank You!

I am also thankful to the wonderful people of the Dominican Republic and Nicaragua for their kindness and willingness to help. A special thanks to Aura Cruz, my wonderful Spanish

teacher, for her patience and good humor in teaching me to talk like a “Nicaragüense.”

Highland Coffees provided the caffeine fix for late nights and early mornings and Papa John’s and Atcha Bakery kept this family alive. I am indebted to all my friends who good-naturedly listened to my venting and forgave me for being an erratic, forgetful, social klutz. And much credit goes to my girlfriends for organizing lunches and “ladies’ nights” to keep me in good spirits.

These last few years would have been unbearable if not for my husband, Dr. Plamen Arnaudov; whose love, patience, and wonderful omelets kept me going; especially when I was overwhelmed and ready to quit. Thanks to my sister, Devangana, for believing in me and to my parents who made great sacrifices so I could come this far - I could never fully express my gratitude to them in words. And finally, thanks to Kaya for all the joy and laughter - everyday is worth waking up for!

TABLE OF CONTENTS

ABSTRACT

Hurricanes account for a significant portion of damages, injuries, and fatalities in the Caribbean. The Dominican Republic has had 3 major hurricane strikes in this century resulting in loss of lives for thousands of people and billions of US $ in economic loss. Major hurricanes had been relatively infrequent in north-eastern Nicaragua's modern history until Hurricane Felix, a Category 5 storm, made landfall in the north-east in 2007. It caused 130 confirmed deaths and brought devastation to many villages. These events highlight a need for re-evaluation of hurricane risk based on a more comprehensive and long-term hurricane history. Using paleotempestological methods, paleo- hurricane history of this region, going back 7,455 years in Nicaragua and 3,640 years in the Dominican Republic, was reconstructed. To achieve this, 27 cores of sediment from 4 coastal sites in the north-eastern part of Nicaragua and 5 sites on the coast of the Dominican Republic were collected. Presence of sand layers in a mainly lacustrine environment, were used as proxies to identify past storm events. Radiocarbon dating, ^{137}Cs, and ^{210}Pb analysis was used to establish chronology. Data from Nicaragua indicate a shift in the hazard regime occurring on a millennial scale - a high activity period in the last 950 years preceded by a low activity period between 950 - 3,350 BP. Using the average return period of hurricane landfall derived from prehistoric and historic data, Poisson probability of strikes was computed for all coastal provinces and municipalities in the study areas. Results reveal a redistributed likelihood of strike for the coastal areas. Vulnerability of coastal areas was determined using indicators and spatially represented. A hazard analysis was conducted by creating storm surge and wind speed models in ArcGIS. Ultimately, the probability information was combined with vulnerability and hazards data resulting in a comprehensive, spatial risk model for the case studies. Jurisdictions containing the seats of government for the Dominican Republic and RAAN face the highest risk.

CHAPTER 1
INTRODUCTION

1.1 Purpose of This Dissertation

This dissertation integrates paleotempestology with coastal risk and vulnerability assessment for the hurricane-prone communities of the Dominican Republic and Nicaragua. Currently, historical data spanning 160 years are used in estimating the return period of hurricane events. But by combining this historical data with paleotempestological data which extend further back to the later part of the Holocene, a return period estimation technique is created that reveals longer trends in the Caribbean.

A combination of the return period estimation with vulnerability and hazard assessment then culminates in a comprehensive risk assessment model for the Dominican Republic and Nicaragua presented in a spatial format using Geographic Information System (GIS) techniques. This is a multi-criteria composite model that can be applied in planning and policy formulation by decision makers in the region.

Quantifying risk and vulnerability and their spatial representation is helpful to resource managers and communities in predicting and preparing for future loss. A clear spatial representation of a risk model is beneficial to communities and resource managers who seek to prepare for longer-term mitigation and hazard reduction at the local level.

1.2 The Project

This project is funded by the Inter American Institute for Global Change Research (IAI) under the CRN2050: *Paleotempestology of the Caribbean region: a multi-proxy, multi-site study of the spatial and temporal variability of Caribbean hurricane activity.* Geologic records of prehistoric hurricanes are being studied by the Principal Investigator (PI) of the project, Dr. Kam-biu Liu at Louisiana State University and various other Co-Principal Investigators (Co-PIs)

throughout the pan-Caribbean region. This region is an area of high hurricane activity and CRN2050 attempts to "understand the climate mechanism" through records of past hurricanes and to evaluate future risk based on that understanding (IAI, 2010).

1.3 Background

Hurricanes and cyclones account for a significant portion of the damage, injury, and loss of life from natural hazards. They are the costliest natural catastrophe in the US as well as other countries (Elsner and Kara, 1999). In the United States, the normalized average economic damage from hurricanes was $10 billion each year between 1900 AD and 2005 AD (Pielke *et al.,* 2008). With rising sea levels, the threat they pose to coastal areas increases exponentially (Lam *et al.,* 2009). Hurricane variability is important for economic considerations including insurance and other policy decisions (Murnane, 2004). These fluctuations in hurricane activity are also of obvious importance to society, especially as populations of afflicted coastal areas increase year to year.

A majority of the Caribbean population lives within 1.5 km from the coast (Mimura *et al.*, 2007), which makes it vulnerable to hurricanes. With increased land loss from sea level rise and increase in storm intensity as a consequence of global warming (Emanuel, 2005), Caribbean countries are further exposed to the threat of hurricanes. They are heavily dependent on tourism, and because of limited resources, they rely on external trade for most of their needs. This dependence, coupled with weak political and economic infrastructure, worsens their vulnerability to natural disasters (Briguglio, 1995).

1.4 Hurricanes and Paleotempestology

Paleotempestology is defined as the study of past storm activities. Using paleotempestological techniques, identification of extreme storm events such as hurricanes is

possible by studying sedimentary or erosional evidence left by wave and wind action associated with these events (Nott, 2004; Donnelly *et al.*, 2001a, 2001b; Liu and Fearn, 1993, 2000; Liu, 2004, 2007). These evidences or signatures left behind by storms are then dated to form a chronology of past events which helps in understanding past trends and variability in storm activity.

It is noted that mainly events of great magnitude and intensity (Category 3-5) leave a signature in the sedimentary record (Nott, 2003), but weaker storms (Category 1 and 2) can also leave a record if a site is very sensitive (Liu, 2004). Paleo records of sand layers are generally available for the later part of the Holocene when the marine transgression slowed (Nott, 2004; Liu, 2004); prior to this the rising sea levels erased the records. The paleo time frame is thus limited to the last 5,000 years in most cases (Frappier *et al.*, 2007b), but longer records have been found in some locations.

1.5 Risk Analysis and Prediction Using Paleotempestology

Most risk assessment studies consider available historical data that go back at most a few centuries in estimating the return period of an extreme event. While recent data are more accurate and provide a better modern analog, this may not be sufficient to demonstrate changes in trends that are apparent in data sets spanning the prehistoric time frame (Nott, 2003). Predicting future events based on a relatively short time period excludes all possible events that may occur within a longer "hazard regime" (Nott, 2003).

1.6 Study Areas

The Caribbean region has an extremely low tidal range such that the surge height is almost entirely due to the physical parameters of the event itself (Donnelly, 2005). Sea level change in the Caribbean has been studied and well documented (Digerfeldt and Hendry, 1987;

Milne *et al.* 2005; Toscano and MacIntyre, 2003) and can be used for calibration of overwash deposits from historic storm surges.

The two countries - Dominican Republic and Nicaragua - were chosen to provide a contrast between the vulnerability to hurricanes based on a range of characteristics including:

i. The Mosquito Coast of Nicaragua, which consist of the Región Autónoma del Atlántico Norte (RAAN) and Región Autónoma del Atlántico Sur (RAAS), has a diverse ethnicity including Creoles, Miskitos, Ladinos, Sumu, Garífuna, Chinese, and Rama. The Dominican Republic on the other hand has a relatively more homogenous population consisting of mixed race, whites, and blacks.
ii. Nicaragua's government is located in Managua, which is on the western side of the continental interior and is not affected by hurricanes. Santo Domingo, the capital of the Dominican Republic, is a coastal city and impacted by coastal risks.
iii. Nicaragua is developed than the Dominican Republic.
iv. The Caribbean coast of northern Nicaragua is a vast plain with low relief, susceptible to storm inundation. The Dominican Republic coastline in contrast has diverse topography and greater relief.

1.7 Research Questions

This study aims to answer the following questions:

1. How does forecasting of future storm probability based on historic and prehistoric proxy data differ from forecasting based solely on historic data?
2. Based on historic and prehistoric data, how is probability of strike, vulnerability, and risk distributed spatially for the Dominican Republic and RAAN in Nicaragua?

1.8 Document Structure

This dissertation aims to better understand the risk and vulnerability of this region by studying the spatial and temporal dimensions of hurricane hazard. It describes the steps used to apply paleotempestology to the Caribbean coast of northern Nicaragua and the Dominican Republic and examines the spatial distribution of vulnerability in both. A flow diagram (Figure 1.1) illustrates the dissertation structure.

The document is divided into nine chapters which are briefly described below: Chapter 2 provides a literature review of paleotempestology, risk analysis, and hurricane risk prediction using past hurricane data. Chapter 3 is a detailed description of all the techniques and methods applied in the study. Chapters 4 and 6 describe the study sites and the collection of cores; and provide loss on ignition analysis and the dating results from hurricane markers in the Dominican Republic and Nicaragua respectively. Return period estimation based on the results are also provided in Chapters 4 and 6. Chapters 5 and 7 address the vulnerability of the Dominican Republic and Nicaragua correspondingly to hurricanes and present a spatial representation of the components of risk and of the composite risk. These chapters also integrate the information from paleotempestology of the two countries with the historic records of hurricanes. Finally, Chapters 8 and 9 discuss the results, the potential for future work, and provide the conclusion to the dissertation.

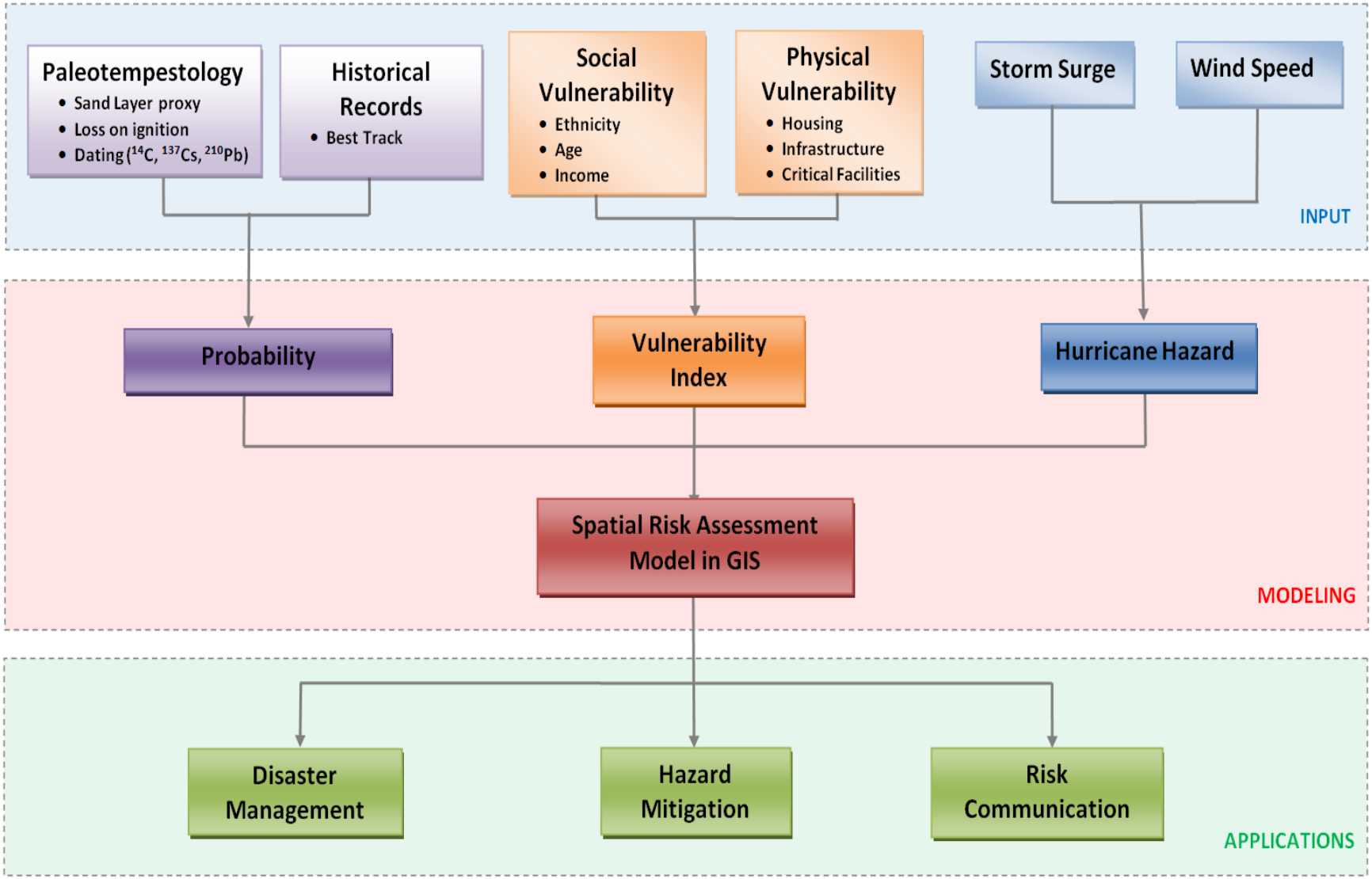

Figure 1.1: Diagram showing overview of the dissertation structure.

CHAPTER 2
LITERATURE REVIEW

2.1 Proxies and Methods Used in Paleotempestology

Pre-historic hurricane strikes can be identified by studying proxies such as clastic deposits of marine origin in coastal lakes; microfossils such as foraminifera (Scott *et al.*, 2003) phytoliths (Lu and Liu, 2005), pollen and dinoflagellates (Liu *et al.*, 2008); Oxygen isotopic changes recorded by stalagmites (Frappier *et al.*, 2007a), corals (Frappier *et al.*, 2007b) and tree rings (Liu, 2004; Miller *et al.*, 2006); and the presence of coal particles (Liu *et al.*, 2008) indicating fires after hurricanes. Often more than one technique is used to validate findings. Two examples of the proxies are briefly described below:

a. Palynology or Pollen Analysis

Pollen grains are highly resistant and do not decay over thousands of years. This makes them excellent markers for climatic and vegetative reconstructions. Vegetation response to changes in climate, a major event (like a hurricane), or any other stressor can be recorded by the pollen that has been preserved in lake sediment and can be studied. Paleoclimatic studies are done by using pollen of a few indicator species that are limited by certain climatic conditions e.g., salinity, temperature, or humidity (Birks, 1993). Presence of pollen from species that can tolerate higher salt levels just above a sand layer indicates an overwash from a hurricane that brought in ocean water (Liu, 2007).

b. Dinoflagellates

Dinoflagellates are unicellular microorganisms that are found in marine environments. During a part of their life cycle, they are in a vegetative state in the form of a "cyst" (Sluijs *et al*., 2005). These cysts have a calcareous or siliceous covering which is not easily destroyed (Sluijs *et al*., 2005). The presence of these dinoflagellates or their fossilized cysts in the sand layers

indicates intrusion of sea water into a mostly freshwater environment of the coastal lake and thus the sand layer can be inferred to be of marine origin (Liu *et al.*, 2008).

Another recent addition to the ever expanding science of paleotempestology is to finding evidence of fires in the form of charcoal particles. A recent study by Liu *et al*. (2008) in the Gulf Coast of Alabama shows that there is a higher probability of fires occurring after a hurricane as trees are uprooted and limbs broken, providing ready fuel for a fire to breakout. Thus the presence of charcoal particles in the sediment indicates the occurrence of a fire following a hurricane (Liu, 2007; Liu *et al.*, 2008).

2.1.1 Hurricane Overwash

One of the most useful proxies in paleotempestology is the identification and interpretation of extreme storm events such as hurricanes by studying sedimentary or erosional evidence left by wave and wind action associated with these events (Nott, 2004; Donnelly *et al.*, 2001a, 2001b; Liu, 2004, 2007; Liu and Fearn, 1993).

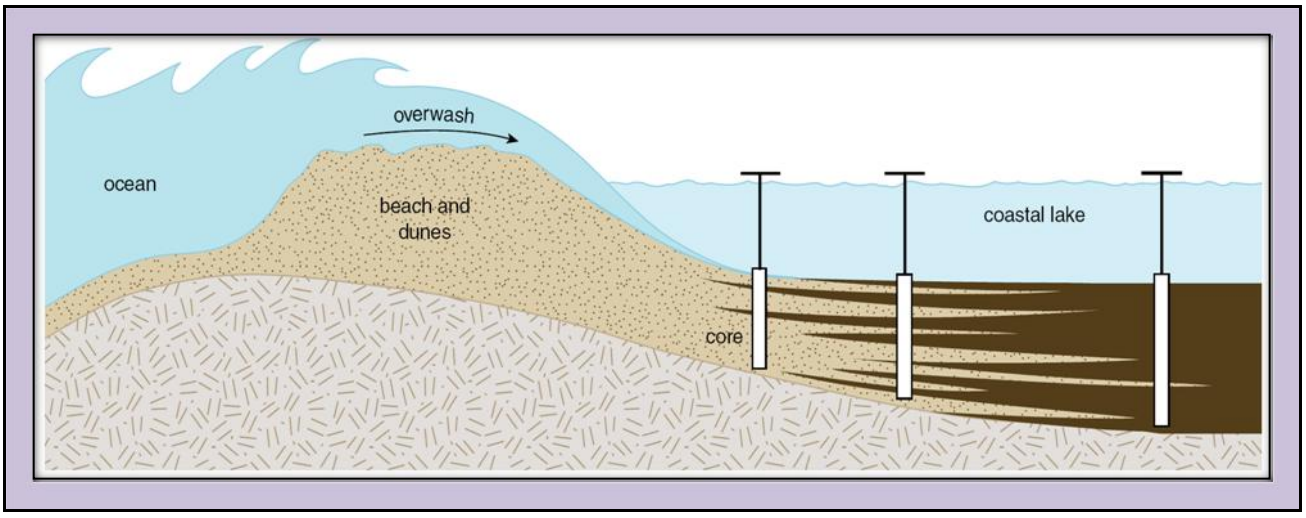

Figure 2.1: Overwash Deposition in a Coastal Lake (Liu, 2007).

During a hurricane, intense winds and storm surge transport material inland from marine sources and sandy barriers such as beaches and dunes (Figure 2.1). Coastal lakes and lagoons

behind these barriers register the overwash events as a layer of clastic material deposited in a lacustrine environment. Each of these layers is considered a possible signature of a storm event. Utilizing paleotempestological dating techniques, origin and the chronology of the event record can be determined.

The thickness of the sand layer combined with the spatial extent of sand towards the middle of the lake (signifying the distance of transport) could be indicative of the storm intensity (Liu and Fearn, 1993, 2000a, 2000b; Donnelly *et al.*, 2004). Estimation of storm return periods and of future strike probability can be arrived at by identifying and dating these sand layers.

In addition to paleo-records, it is important to calibrate results based on modern analogs (i.e., comparing signatures left by known hurricane events) (Liu, 2004). Modern analogs help in the understanding of the conditions of the site and the strength of hurricanes that can leave a signature at that location.

2.1.2 Dating

Various dating techniques are used in determining the age and chronology of overwash events. The main ones are: Radiocarbon (^{14}C) dating of sediments older than 200 years (Liu, 2004); Cesium -137 (^{137}Cs) dating is useful in dating sediments deposited in last ~50 years (Ritchie and McHenry, 1990); and Lead – 210(^{210}Pb) dating which is useful in dating sediment deposited in the last 110-130 years (Donnelly *et al.*, 2001a).

2.1.3 Reservoir Effect

When carbonate samples of marine origins are dated, sometimes they are considerably older than expected due to a phenomenon called the "reservoir effect" (Dix *et al.*, 1999). Deep waters are depleted in ^{14}C due to radioactive decay since they are not as effectively mixed as surface waters. The inorganic carbonate in these waters exhibits an older radiocarbon date. When

these carbonates are used by organisms in their shells, the shells are effectively "older." This effect is different for different seas based on the rate of depletion of ^{14}C (Mangerud, 1972). A database called the *Marine Reservoir Effect Database* provides the correction values for different areas on the Earth (http://intcal.qub.ac.uk/marine/index.html?ORDERBY=C14age%20asc).

2.2 Why Don't All Storms Leave a Signature?

There are various factors that determine whether a storm will leave a marker. Two main factors are: (a) the relative height of the surge that transports the material for the storm marker and (b) paleotempestological sensitivity of the lake that records the storm.

2.2.1 Relative Height of the Storm Surge

The distance and the quantity of transported sand depend primarily on the height of storm surge in relation to the height of the beach barrier (Morton and Sallenger, 2003). The height of the surge is a consequence of the strength/intensity of the storm as well as the geomorphology of the coastline (Morton and Sallenger, 2003; Liu, 2004). Another factor that influences the surge height is the tidal influence during landfall (Liu, 2004). In this case, the Caribbean coast is micro-tidal in nature, thus astronomical tides have a negligent effect on the surge height (Donnelly, 2005).

A hurricane track's direction as well as the position of the eye in reference to the coastline is one of the factors that determine the amount of water pushed against the coast and the height of the surge (Fletcher *et al.*, 1995). Hurricanes have an anti-clockwise circulation in the northern hemisphere and therefore the water pileup is the maximum on the right side of the eye wall (Liu, 2004). However this is true only if the hurricane hits the coast at a perpendicular angle. If the track is not perpendicular then the surge height will differ based on the angle of the hurricane track in relation to the coastline. Other characteristics of the hurricanes such as wind

speed, central pressure, as well as the speed of the hurricane itself will also determine the surge height (Stone *et al.*, 2005).

2.2.2 Paleotempestological Sensitivity of the Lake

Liu (2004) warns that the height of the surge (and the possibility of finding a sand deposit) may not always be a function of the intensity of the storm. For example, right after a barrier has been breached or eroded by a major storm, the sensitivity of the lake will be higher and even a small storm can leave a signature (Liu, 2004).

Paleotempestological sensitivity of a lake is defined as "the minimum intensity of a hurricane whose impacts will be recorded in the sediments of the lake" (Liu, 2004). This sensitivity is determined by the height of the barrier in front of the lake and the distance of the lake from the sea. The height of the barrier determines the relative surge height. Barriers that have been washed away or eroded can take decades to centuries to re-establish (Leatherman, 1983). The return period of storms will determine how fast and high the barrier can grow (Ritchie and Penland, 1990).

Relative sea level rise (RSL) can change the distance of the lake from the sea and thus affect the paleotempestological sensitivity of the lake. For example, a sand record left by a major storm while the sea stand is low (and the lake is farther from the coast), may be the same thickness as the one left by a smaller hurricane when the sea level is higher (and the lake is closer to the coast).

However, since the distance from the shoreline should also change the environmental characteristic of the lake by changing its salinity and organic content, this would potentially reflect in the loss-on-ignition analysis and fossil content of the cores extracted from the lake site (Liu, 2004).

2.3 Sea Level Change

The most recent low stand in the eustatic history of sea level change was ~18,000 BP, a time which coincides with the Last Glacial Maximum. Sea level was shown to be as much as 150 m below the present level (Douglas *et al.*, 2001). A study done in Barbados found the sea level to be 121 +/- 5 m below present level (Fairbanks, 1989). In the Holocene period ice began to melt and the sea level rose rapidly until about 6,000 BP; from then on, this rise was fairly constant (Douglas *et. al.*, 2001; Toscano and Macintyre, 2003).

There are two mechanisms that supply us with "markers" for measuring sea level change.

a. Transgressive phase is relative sea level rise (Roy, et al., 1997). As transgression continues, the barrier islands begin retreating landward and start losing their sediment supply. Eventually, they become submerged shoals and then disappear. Radiocarbon dating of barrier sand sediment has provided data on sea level change.

b. Regressive phase is when the sea level falls and the coast "progrades" towards the sea (in theory). This, in turn, creates beach ridges and peat marshes that can be used for radiocarbon dating (Douglas *et al.,* 2001). The regressive phase is responsible for the formation of shoreline features that can date back to the last glacial age.

In general, Holocene sea levels can be inferred from geologic features such as ridges and other relict geologic forms. Radiocarbon dating is used to corroborate such evidence. Global Positioning Systems (GPS) are used to get accurate readings of the elevations (Tornquist, *et al.*, 2006). But dating obtained from peat has many problems; mainly, that over time it collapses under its own weight and thus cannot be stratified according to age (Douglas *et al.*, 2001). However, this problem can be solved by using only the basal peat that forms the contact layer with the upland surface (Douglas *et al.*, 2001).

2.3.1 Caribbean Sea Level Change

By studying mangrove peat and salinity of the sediment, Holocene sea level changes were determined. Change in salinity changed the vegetation composition and was one of the factors for distribution of mangroves species (Torrescano and Islebe, 2006). Calibrating these results with sea level studies done earlier (Fairbanks, 1989) further confirmed the changes in sea level in the Caribbean basin.

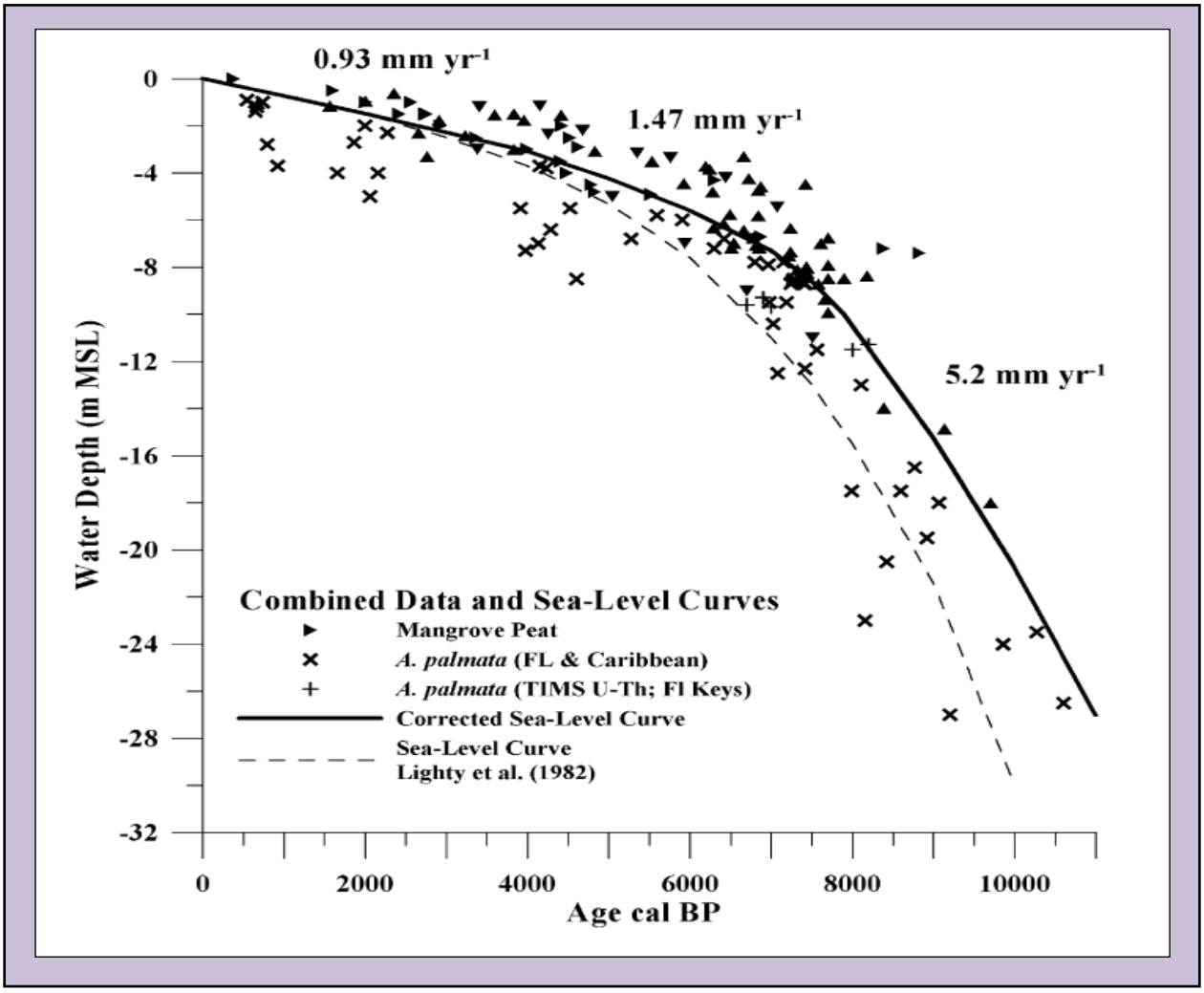

Figure 2.2: Sea level curve for the south-western Atlantic and the Caribbean region based on peat and coral data (Toscano and Macintyre, 2003).

No specific study exists for the study areas presented in this dissertation, i.e., the

Dominican Republic and Nicaragua, but the two countries are part of the Caribbean plate and the basin is believed to have a homogeneous sea level curve without much local/isostatic influences. A comprehensive sea level curve for the south-western Atlantic and the Caribbean based on red mangrove peat (*Rhizophora mangle*) and coral (*Acropora palmata*) data (Toscano and Macintyre, 2003) is presented in Figure 2.2. This curve shows a rapid sea level rise of 5.2 mm/yr in the early part of Holocene (10,000-7,000 BP) which then slowed down to 0.93 mm/yr in the last 6,000 years. Due to this slowing down of the sea level, paleotempestology can generally provide hurricane records up till the last 5,000-6,000 years.

2.3.2 Global Warming and Sea Level Rise

Research done in the last few decades shows that sea level rise rates are increasing at a pace that can be correlated with the increase in levels of CO_2 (Douglas and Kearney, 2001; IPCC, 2007). Climatic models have predicted that in the next century, the best estimate rise in temperature will be between 1.8˚ C to 4.0˚ C (IPCC, 2007). With this range of increase in temperatures, the rate of sea level rise is projected to increase from 0.18 m to 0.59 m (IPCC, 2007). Though some of the increase in CO_2 can be absorbed by the global oceans up to a point, with the increase in temperature, the solubility of CO_2 will decrease and the ocean will stop acting as a "sink" (Geophysics Study Committee, 1990).

2.3.3 Global Warming and Change in Intensity and Frequency of Hurricanes

Recent studies (Bender *et al.*, 2010; Emanuel, 2005) connect an increase in hurricane strength and frequency to the rise in sea surface temperatures (SST). The effects of both storm intensification and rising sea levels are of immediate concern to low-lying areas; together the two compounds the devastation that hurricanes can bring to coastal areas.

Studies by Emanuel (2005) show that warmer waters lead to more intense storms. A clear

trend of increase (Figure 2.3) in hurricane intensity is visible in the last 50 years (Emanuel, 2006). This rise is strongly correlated with the average rise in sea surface temperatures (SST). However, Landsea (2005) and Landsea *et al*. (2006) challenge the reliability of limited data used in detecting increase in frequency and intensity in the Atlantic basin.

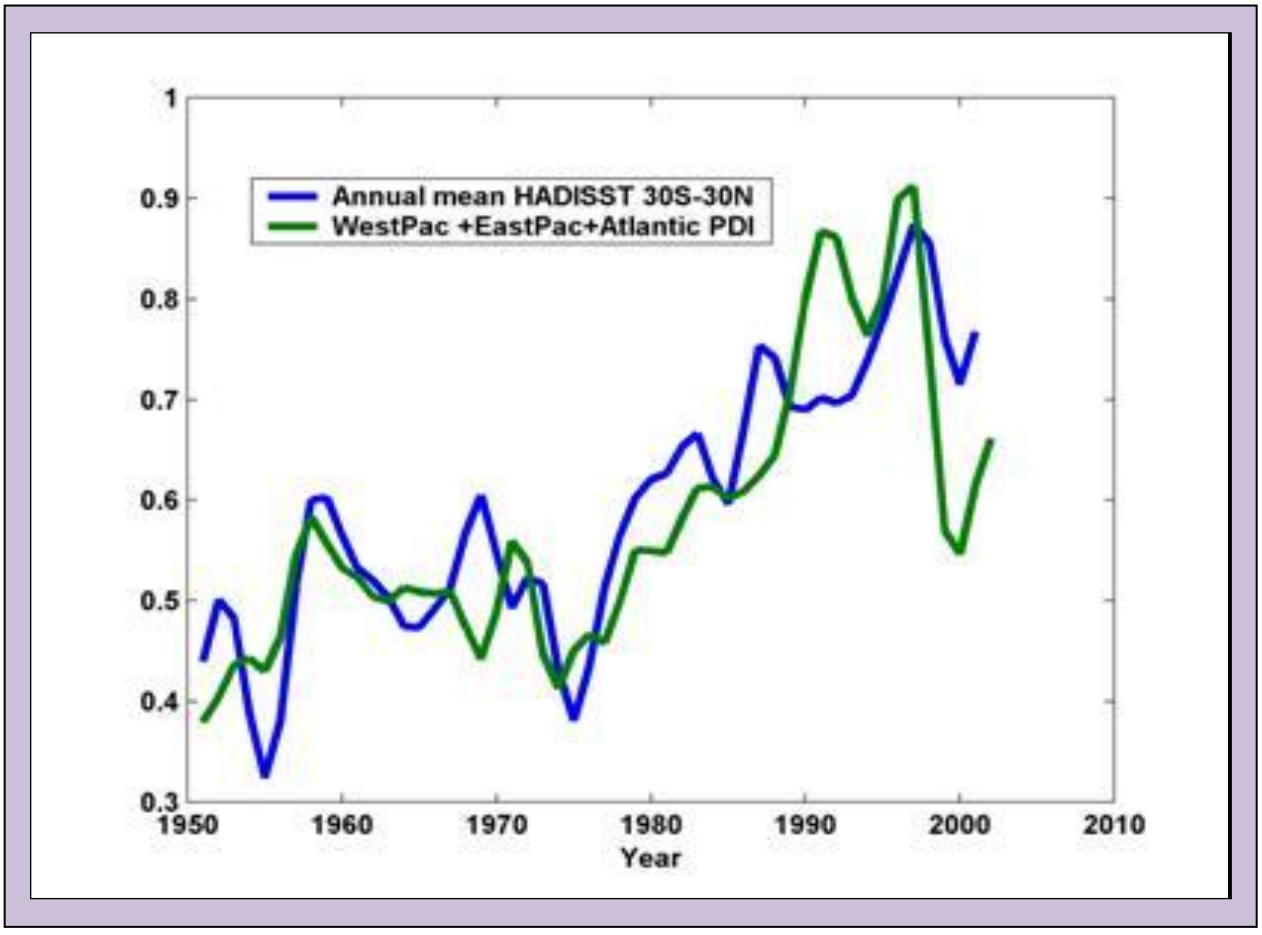

Figure 2.3: Increase in Hurricane Intensity with rise in SST (Emanuel, 2006).

Studies by Knutson and Tuleya (2004) have also proven that hurricanes simulated with higher temperatures and CO_2 conditions are more intense. Records show a linear increase of 11% in CO_2 levels over a period of 80 years and from 10.88^{o} C to 12.48^{o} C in temperatures (Knutson and Tuleya, 2004). Using these values, different models project an average of 6% increase in wind speeds, 14% decrease in central pressure, and 18% increase in precipitation (Knutson and

Tuleya, 2004).

According to Pielke (2007), for 2050, the range of intensity increase due to global warming is projected to fall between 0–18%; and for 2100, between 0–36%. This projection indicates a considerable change in the strength of storms (Pielke, 2007). His calculations show that the damage by hurricanes in the year 2050 would be more than four-fold if a worst-case scenario of an 18% increase in intensity is adopted.

A recent study done by Bender *et al.* (2010) suggests a two to three-fold increase in frequency of category 4 and 5 hurricanes respectively in the Atlantic basin between 20^{o} and 40^{o} latitudes. This leads to about 30% increase in damages from the strong hurricanes (Bender *et al.*, 2010) in this region. On the contrary, the number of days of all categories of hurricanes in the Caribbean is shown to decrease in the same study (Bender *et al.*, 2010).

2.4 Climate Change in the Caribbean

Paleoecological study conducted by Hodell *et al.* (1991) indicates great variations in the climate of the Caribbean region in the last 10,500 years. This study conducted in Lake Miragoane in Haiti (in the island of Hispaniola), shows alternating wet and dry climate conditions that were based on oxygen isotope ratios from ostracods and pollen records from the lake sediments (Hodell *et al.*, 1991). Results from this study correspond with the general climatic conditions of the broader Caribbean, Africa, and Mesoamerica (Hodell *et al.*, 1991).

Another study done by Islebe and S´anchez (2002), using mangrove pollen analysis in the Caribbean coast of Mexico, shows similar changes in the climatic conditions, shifting between wet and dry conditions during the late Holocene (Islebe and S´anchez , 2002). One of the explanations for this change in climatic conditions and wet/dry cycles is the shift in Bermuda High (Liu 2004) which is a high pressure system in the Atlantic (Knowles, 2008).

2.5 Seismology of the Caribbean Basin

Due to the presence of three plate boundaries, the Caribbean basin is an area of high seismic activity (McCann, 2006). There have been 127 records of volcanic activities and shallow earthquakes in the last 500 years in this region (O'Loughlin and Lander, 2003). As evident from Figure 2.4, the island of Hispaniola has a "high potential" of earthquakes and tsunamis.

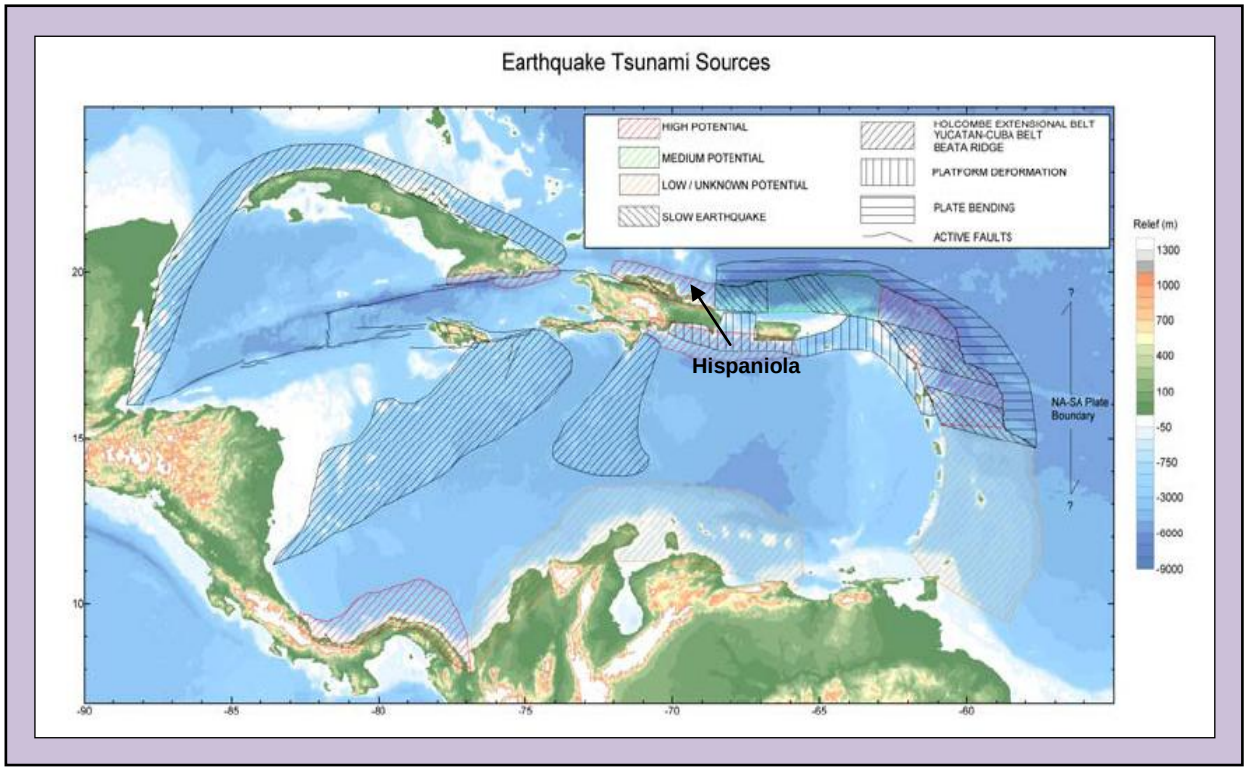

Figure 2.4: Tectonic feature of the Caribbean region (McCann, 2006).

There were numerous earthquakes (Figure 2.5.A) in and around the island of Hispaniola in the 18th century; since then it had been very quiet (Figure 2.5.B) and the stress has been building up (Kerr, 2010). Experts have predicted major earthquakes that are waiting to happen in the future. The recent devastating earthquake in Haiti (western part of the island of Hispaniola), in January 2010, is thought to be the first of a series of more intense earthquakes that can affect the island of Hispaniola (Kerr, 2010). The recent Port-au-Prince earthquake is considered to be a

"moderate" earthquake even though the damage to life and property was immense due to the ground being built on not too stable sediments, poor infrastructure, and high vulnerability of the population (Kerr, 2010).

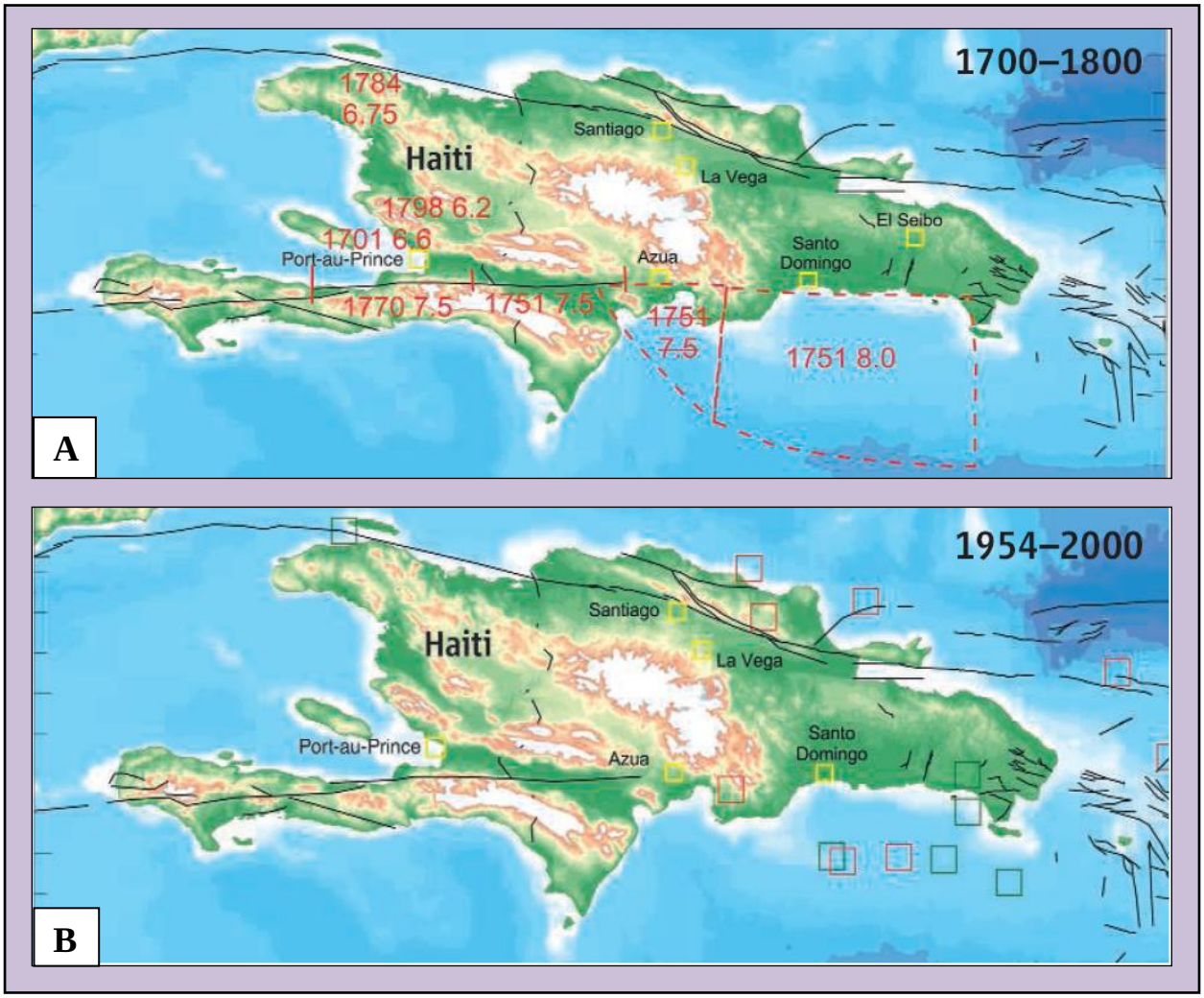

Figures 2.5: Earthquakes in Hispaniola (A) in the 18th century and (B) in the 20th century (Kerr, 2010).

2.6 Tsunamis in the Caribbean

There have been eight tsunami events (1751, 1775, 1842, 1897, 1910, 1918, 1946 – August 4th and 8th) recorded in the Dominican Republic that have resulted in deaths (O'Loughlin and Lander, 2003). While fewer instances of tsunami are recorded for Nicaragua, a recent event

in 1992 on the western (Pacific) coast, resulting in 170 deaths, confirms that Nicaragua too is affected by tsunami hazard (Kikuchi, 1995; Gonzales, 1999). No recorded tsunami events are available in the eastern Caribbean coast and in the study area –RAAN.

2.7 Distinguishing Between a Tsunami and a Hurricane

In case of both hurricanes and tsunamis, a surge is created, bringing overwash material (sand) in the landward direction. In locations where sand layers have been deposited by tsunamis and hurricanes that occurred at separate times, it is theoretically possible to distinguish them.

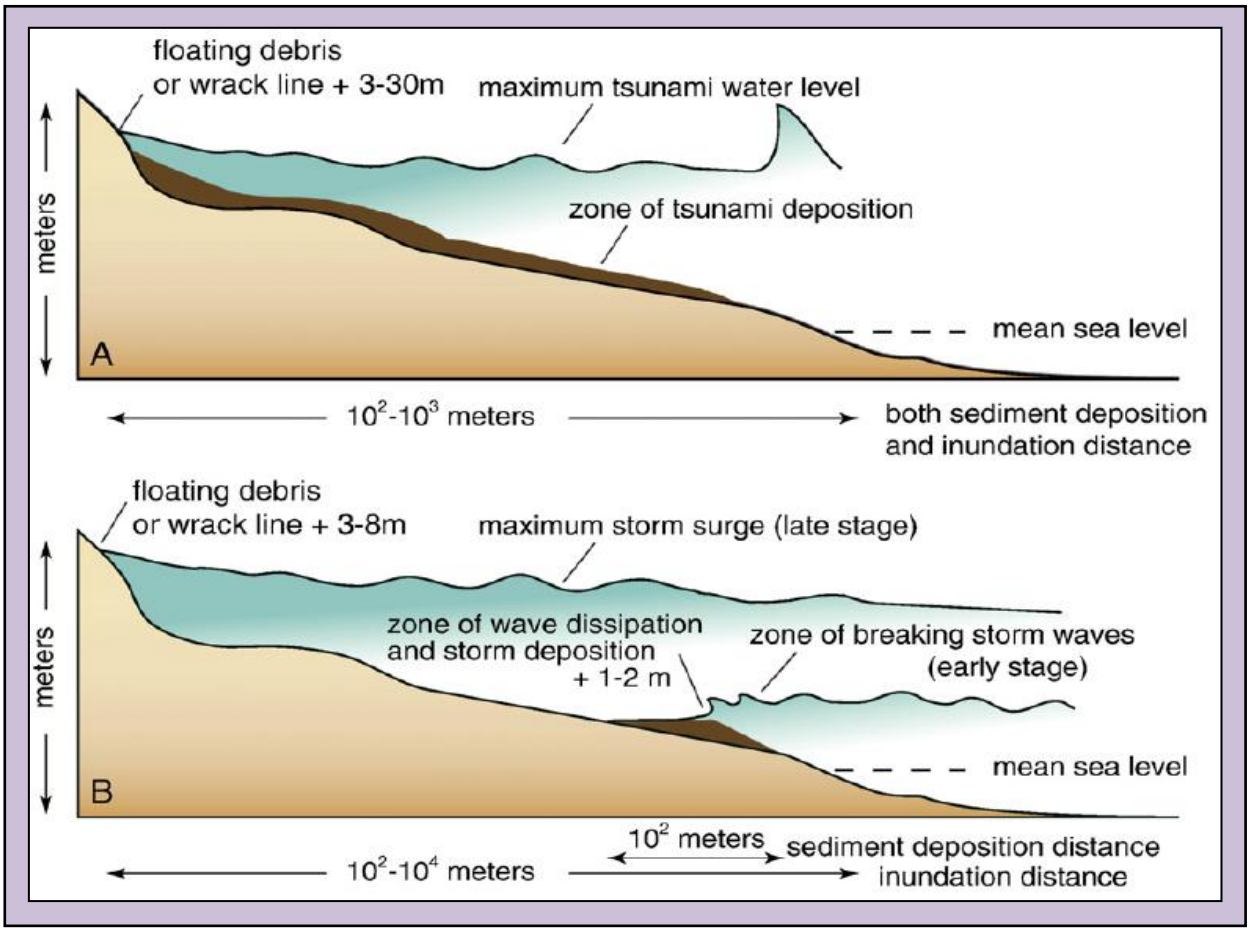

Figure 2.6: Difference between the inundation, sediment transport, and deposition between (A) tsunamis and (B) hurricanes (Morton *et al.*, 2007).

Tsunamis and hurricanes have different hydrodynamic processes leading to differences in sediment transport and the eventual sorting and deposition of those sediments on land. Tsunamis

have sediments suspended in the water column and deposit the sediments over a large area on land (Figure 2.6.A.) (Morton *et al.,* 2007). On the other hand, hurricane surge carry coastal sediments (like sand) landward and deposit them on land at a comparatively closer distance to the coast (Figure 2.6.B) (Morton *et al.,* 2007).

In St. Lucia, Scheffers *et al.* (2005) found that the tsunami deposits contained materials of various sizes ranging from mud to boulders along with gravel and pieces of coral. Kelletat *et al.* (2004) reports similar findings in the Bahamas. Kortekas and Dawson (2007) found in Martinhal, Portugal, that the main differences between tsunami and hurricane deposits were the presence of boulders and rip-up clasts along with the large extent of depositional area seen after the tsunami of 1755. In Puerto Rico, Moya (2006) discovered that tsunami deposits were laminated and contained haematite (an iron mineral produced due to volcanic activity in seismically active oceans) and *Halemida sp*. (a calcareous alga found in the bottom of the shallow marine platform) indicating massive tsunami induced waves of marine origins. This could be distinguished from hurricane induced storm surges that are coastal in nature.

Hurricane overwash has sand which is better sorted than tsunami deposits. Tsunami deposits exhibit multiple layers due to an alternating land-ward and sea-ward flow of the water carrying marine and non-marine materials respectively. In contrast, hurricane deposits show only a land-ward flow with coastal material (Nayanama *et al.*, 2000; Dawson and Stewart, 2007; Morton *et al.,* 2007).

Most of these studies compare tsunami and hurricane deposits in different locations but there is no research yet in the Caribbean which illustrates the difference between the deposits at the same location. Nevertheless, two distinctions seem to be common in all studies and are visually apparent: (a) varying grain size and lack of sorting (Scheffers *et al*., 2005; Kelletat *et al.,*

2004) and (b) an alternating composition (Nayanama *et al.*, 2000, Dawson and Stewart, 2007; Morton *et al*., 2007). These two criteria have been used for preliminary identification of sediment origin in this work.

Although much work has been done in the recent years to differentiate tsunamis from hurricane deposits, it is still problematic and difficult in less-than-ideal conditions. Especially distinguishing small tsunamis from large storms (which may have comparable carrying capacities) in which large materials (an indication of tsunami) may not be present (Kortekas and Dawson, 2007). Tsunami and hurricane distinction in greater depths of cores is also problematic as bioturbation and compression of deposit layers can hide sorting and layering due to bi-directional flow (McCloskey, 2009).

2.8 Hazard Regimes

Hazard regimes are defined as clearly identifiable periods of time within which the frequency of a hazard remains more or less constant (Nott, 2003). Current hurricane return period forecasting techniques are based on a homogeny in the past records but various studies indicate that shifts in hazard regimes occur on both temporal and spatial scale. Temporally, storm frequency has been studied on an inter-annual, decadal, or millennial timeframe (Nott, 2003).

a. Inter-Annual Variability due to ENSO and NAO: Variability due to El Niño Southern Oscillations (ENSO) activity happens every 3-5 years. The effects last for about a year and dampen hurricane activity in the Atlantic Basin. Hurricane records from 1985 till 2003 suggest that ENSO has greatest effect on inter-annual variability (Frank and Young, 2007). The primary explanation for the decline in hurricane frequency during El Niño years is increased wind shear in the environment. In the Caribbean, hurricane activity is lower in the El Niño years (Chu, 2004). North Atlantic Oscillation (NAO) is another phenomenon that controls the strength and

direction of hurricane tracks across the North Atlantic (Elsner, 2000; Elsner, 2006).

b. Decadal Variability: Multi-decadal variations in hurricane frequency are attributed to Atlantic Multi-decadal Oscillation (AMO). The Gulf of Mexico and the Atlantic see alternating lulls and peaks spanning 20-25 years. When hurricane activity at high latitudes is above average, it is below average at low latitudes and vice versa. Plots show an inverse relationship between activity in the Gulf of Mexico and in the Atlantic (Elsner, 2000; Goldenberg *et al.*, 2001).

c. Millennial Variability: "Bermuda High" is defined as a "persistent atmospheric high-pressure system in the North Atlantic" (Liu, 2004) whose change in positions may explain the change in hurricane activity in the last 5,000 years (Liu, 2004).

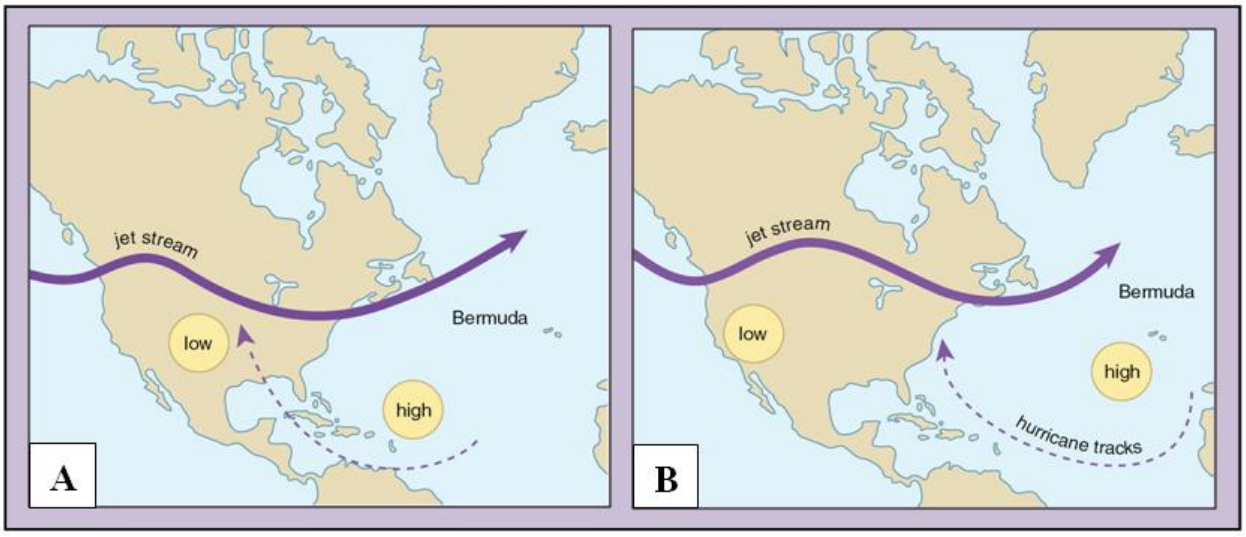

Figures 2.7: Bermuda High Hypothesis (Liu, 2007). (A) Southwest position of Bermuda High. (B) Northeast position of Bermuda High.

Between 1,000 to 3,800 years ago, this high-pressure system may have been positioned more to the southwest, causing storms to strike the Gulf Coast and the Caribbean (Figure 2.7.A). In the last 1,000 years the Bermuda High has shifted towards the northeast, thus pushing the storms towards the East Coast (Figure 2.7.B). Hence, the last millennium has been a period of relatively low activity for the Gulf Coast and the Caribbean (Liu, 2004).

2.9 Risk Analysis and Prediction Using Paleotempestology

Risk assessment quantifies the level of exposure a society faces to a given hazard (Cutter *et al.*, 2003). Risk combines the likelihood of an event occurring with the impact this event may have on the people and their environment. Thus the three components of risk are:

a. Probability of occurrence: is the likelihood of a hazard event happening; a part of risk assessment is the quantification *and estimation* of that likelihood (Cutter, 2003). Based on the "probability of event" calculations, yearly potential of occurrence determining the level of impact can be predicted for the future (Cutter *et al.*, 2003; Nott, 2003; Nott, 2004).

b. Hazard: are defined as "a threat to people and the things they value" (Cutter et al., 2003). In this study the hazard is identified as hurricanes (and associated storm surge and winds).

c. Vulnerability: is the susceptibility of people or systems to be exposed to and harmed by a hazard.

2.9.1 Probability of Occurrence

Predictive return period modeling or probability modeling is based on empirical data. Past storm records can be divided into two broad categories: (a) "best-track" records (from the last 160 years collected by the Coastal Services Center at NOAA (CSC, 2010), and (b) proxy records for the last ~5000-6000 years analyzed by using paleotempestological techniques (Liu, 2007).

A simple probability can be calculated by using a ratio of total occurrence over total time. This method assumes uniformity in the geologic records, i.e., it does not account for changes in climatic conditions (Elsner *et al.*, 2008; Woodruff *et al.*, 2008a, 2008b; Nott, 2003). The simple

probability also does not take into consideration that some years may have more than one storm and some none. A method developed by Elsner *et al.* (2008) is capable of providing return periods for storms above a certain threshold of intensity and wind speed if modern analogs are available.

Older records have higher uncertainty but by using Bayesian methods, this uncertainty can be addressed in the models (Elsner and Bossak, 2001; Jagger and Elsner, 2006; Solow and Moore, 2000). Poisson distribution is used to model the likelihood of hurricanes using historical data (Elsner and Bossak, 2004). While using historical data for predictive modeling has been attempted before in a hierarchical Bayesian model (Elsner and Jagger, 2004), this has not been done yet for paleo-hurricane records which have high degree of uncertainty.

Using statistical methods proposed by researchers in the field, a modified probability of occurrence is estimated based on combined historic and prehistoric data (Solow and Moore, 2000; Elsner *et al.*, 2008; Elsner and Bossak, 2001; Elsner and Kara, 1999). Poisson distribution (Equation 1) is a distribution of rare events over a long period of time; it assumes that the mean (λ) is unchanging over time. Here $\hat{h}$ is the number of hurricanes being forecasted and T is the time period of the past record (Elsner and Bossak, 2001).

$$f_{\text{Poisson}}(\hat{h} \mid \lambda,\ T) = \exp(-\lambda T)\frac{(\lambda T)^{h}}{h!} \quad \text{for } h = 0,\ 1,\ 2,\ \ldots, \quad \lambda > 0, \quad \text{and} \quad T > 0.$$

Equation 1

But when we consider two time periods of hurricane occurrence, λ is variable due to missing data or other factors. A mixture of Gamma density with a Poisson distribution is then proposed leading to a negative binomial distribution (Epstein, 1985). In this case the "gamma density is considered the conjugate prior" (Elsner and Bossak, 2001; Elsner and Kara, 1999) for

the Poisson process.

Using this method with a prior function, predictions for varying time periods (e.g., 5, 10, 20, 50 years) could then be made by using the following formula (Equation 2) where $\hat{T}$ is the time period we are forecasting for and $\hat{h}$ is the number of hurricanes being forecasted; T'' is total time period (certain and uncertain) and $h''$is the total number of hurricanes in the uncertain and certain periods (Elsner and Bossak, 2001).

$$f_{\mathrm{nb}}\left(\hat{h} \mid h'', \frac{T''}{\hat{T} + T''}\right) = \frac{\Gamma(\hat{h} + h'')}{\Gamma(h'')\hat{h}!}\left(\frac{T''}{\hat{T} + T''}\right)^{h''}\left(\frac{\hat{T}}{\hat{T} + T''}\right)^{\hat{h}}.$$

Equation 2

2.9.2 Hazard Analysis

a. Wind speeds

Along with the frequency of hurricanes, using wind damage assessment of past storms to predict future impacts is also a part of hazard analysis. Reconstructing hurricane speeds for historical storms is more involved and requires extensive research in the archives and other documentary sources for reports of damage due to hurricane winds (Boose, 2004). U.S. National Hurricane Center has reconstructed data for the wind speed and intensity for hurricanes for the last ~160 years (CSC, 2010).

Wind speeds for prehistoric storms are even harder to determine due to a large uncertainty in the record. Recently this has been attempted by using modern analogs in the geologic records to identify intensity and wind speeds of storms that are capable of leaving a record (Elsner *et al.*, 2008). Modern storms of known intensities which leave a signature in the coastal lakes are used to infer the threshold intensity required to leave a proxy record at the same

location, assuming geologic conditions have not changed considerably over time (Elsner *et al.*, 2008). A Fujita scale for wind damage can be used to correlate historically reported damage with wind speeds to prehistoric storm data (Donnelly *et al.*, 2001a; Boose 2004).

b. Storm Surge

Numerical storm surge models are used to estimate the surge height at a hurricane landfall location for historic and prehistoric storms (Nott, 2003). These models employ variables such as bathymetry, sea-level at the time of event, the topography at the site, and the estimated intensity established from sand layer records (thickness and distance from shoreline).

In case of historic records, wind speeds from written accounts (Hsu, 2004; Cheung *et al.*, 2007; Woodruff *et al.*, 2008a, 2008b) are inferred. Apart from historical events that have been documented, oral histories obtained through ethnographic methods provide valuable information regarding storm conditions and impacts (Frappier *et al.*, 2007b).

2.9.3 Vulnerability

"Vulnerability is the degree to which a system, subsystem, or system component is likely to experience harm due to exposure to a hazard, either a perturbation or stress/stressor" (Turner *et al.*, 2003). A community's vulnerability indicates its lack of resiliency to disasters or lack of ability to cope and recover after the disaster (Cutter, 2003a).

The concept of vulnerability has been around for a long time, but only recently have efforts been made to quantify it by using models. Since vulnerably is based mainly on qualitative characteristics, quantifiable and conceptually robust indicators are used to measure it.

There are different aspects of a community that contribute to its vulnerability. Even though everyone in a hazard prone area will be impacted by a hurricane, certain demographics are more at risk and will require additional assistance during the storm and after in the recovery

phase.

2.10 Emergence of Vulnerability Science

Two classic frameworks that were proposed to study vulnerability in the early days of the vulnerability analysis were: the risk-hazard (RH) model and the pressure and release (PAR) model. The RH model is defined as a function of the hazard, exposure to the hazard, and the sensitivity of the entity that was exposed (Turner *et al.*, 2003). This model lacked information about the interactions between the social/physical characteristics of the system as well as the differential exposure and consequent impacts to the hazard (Turner *et al.*, 2003).

The PAR model improves upon this limitation and incorporates the existing vulnerability of the system creating a disproportionate effect of the exposure within the system (Blaikie *et al.*, 1994). However, this model lacks the "human –environment" interactions that may reduce or increase vulnerability (Turner *et al.*, 2003).

2.11 Vulnerability Modeling Approaches

Based on extensive research done on various vulnerability models and approaches, Cutter (1996) categorized vulnerability approaches into three broad groups – vulnerability as a pre-existing condition, vulnerability as a tempered response, and vulnerability as a hazards of place (Boruff, 2005). Boruff (2005) describes five models of note (including PAR) that employ the aforementioned three approaches for studying vulnerability:

i. Pressure and release model (Blaikie *et al.*, 1994);
ii. Hazards dimensions of vulnerability model (Tobin and Montz, 1997);
iii. Circle of vulnerability model (Alexander, 2000);
iv. Human ecology of endangerment model (Hewitt, 1997); and
v. Vulnerability of place model (Cutter, 1996).

First four of the five models lack either a feedback mechanism, a geographic variability of vulnerability, a socio-economic variability, or an interaction between social and biophysical vulnerability (Boruff, 2005).

In addition to varying characteristics within the system (Phillips *et al.*, 2006) that may contribute towards uneven impacts of a hazard, there is also disparity in vulnerability due to location (Turner *et al.*, 2003; Boruff, 2005). A place-based model for vulnerability (Cutter, 1996) comprises of a modeling framework that integrates all three approaches and characteristics of vulnerability to determine the comprehensive vulnerability of a geographic location. The vulnerability of place model (VPM) allows for comparison between geographic locations and their vulnerability. It also has a feedback mechanism that monitors change in vulnerability over time (Boruff, 2005).

A place based vulnerability model was first employed by Cutter *et al.* (2000) in a spatial, multi-hazard assessment for Georgetown County, South Carolina. Although most of the work has been limited to the United States, recently Boruff and Cutter (2007) applied a comprehensive multi-hazard place based vulnerability model outside of the United States to two islands in the Caribbean - Barbados and St. Vincent.

2.12 Vulnerability Indicators

Since vulnerability is a multi-dimensional concept and cannot be measured directly, quantifiable indicators are used to measure it**.** Indicators are useful tools in monitoring and assessing complex social and environmental issues because they combine data and observations to create quantifiable measures (Cutter *et al.*, 2003; Birkmann, 2007). Different approaches in defining vulnerability to hazards lead to different methods in selecting indicators that best represent it. While identifying the most vulnerable populations and spatially exploring variations

in vulnerability within different regions, the use of indicators based on "human exposure" (Adger *et al.,* 2004) is common. This generally is known as "social vulnerability" (Adger *et al*., 2004) which is a component of the overall "biophysical vulnerability" (Adger *et al.,* 2004). Cardona (2005) calls this the "predisposition to be affected" regardless of the nature of hazard. This is also known as the Prevalent Vulnerability Index (*PVI*) (Cardona, 2005).

Traditional methodologies consider social indicators, e.g., gender, age, income, ethnicity, and disability (Cutter *et al.*, 2003; Cardona, 2005) that reveal an inherent susceptibility to perils. The built environment (roads, housing, infrastructure, and critical facilities) are also vulnerable to hazards and are an intrinsic part of a vulnerability assessment study.

Table 2.1: Fifteen indicators that were used for vulnerability index calculation in St. Vincent and Barbados (Boruff, 2005).

Concept of Vulnerability	Variable	Effect on Vulnerability
Age	Percent of population under five	Increase
	Percent of population attending primary school	Increase
	Percent of population 65 years of age or over	Increase
Gender	Percent female	Increase
Employment	Percent of population employed	Decrease
Family Structure	Average number of persons per household	Increase
Social Dependents	Percent of population retired	Increase
Special Needs	Percent of population disabled	Increase
Development	Housing unit density	Increase
Infrastructure	Percent of housing units possessing radios	Decrease
	Percent of housing units possessing televisions	Decrease
	Percent of housing units cooking with gas or kerosene	Increase
	Percent of housing units cooking with electricity	Decrease
	Percent of housing units lighting with electricity	Decrease
Rural/Urban	Percent of land used for agriculture	Increase

Fifteen such indicators (Table 2.1) were used for social vulnerability in St. Vincent and

Barbados (Boruff and Cutter, 2007). These indicators were combined to produce a composite index for each of the parishes in Barbados and the census districts in St. Vincent and were then mapped on GIS to illustrate the comparative vulnerability (Boruff and Cutter, 2007).

2.13 Normalization of Vulnerability Indicators

Indicators used for vulnerability research have different units and cannot be combined in a justifiable manner. By using normalizing and standardizing techniques, they can be converted to quantifiable units that are comparable and can be integrated. There are many methods that are used for normalization and based on recent works done in vulnerability (Nardo *et al.*, 2005; Briguglio, 2003), three of the commonly used (often together) methods are described below:

a. Ranking method: this is the simplest way to normalize qualitative data. Number of ranks is specified and qualities are arranged as ordinal numbers. The same number of ranks is used for all the indicators and then combined. Although this method is the quickest and easiest to use, there is considerable loss of information (Briguglio, 2003).

b. Standardization (Z-Score) method: indicators in different units and scale are hard to compare and combine. Statistical standardization of data puts them on a uniform scale with a mean of zero and standard deviation of one. However, there is a bias towards extreme values which have the largest effect on the index (Nardo *et al.*, 2005).

c. Rescaling method: this method uses the range of the indicator values and converts them to values between 0 and 1. It is simple and effective while retaining data information. Again, the index can be distorted by outliers or extreme values (Nardo *et al.*, 2005).

2.14 Spatial Representation of Risk

Risk assessment is best conducted with multi-criteria analysis using Geographic Information System (GIS) (Boruff, 2005; Carrara, 1991; Cutter, 2003b; Cutter *et al.*, 2000).

Interactive models in GIS that simulate hazard scenarios are useful in studying the impacts of hurricanes before they happen. They also help in delineating areas and identifying populations that are particularly susceptible to storm damage. Risk assessment modeling is done in GIS by overlaying different layers that demonstrate the geographic variations in vulnerability and impacts from hurricanes.

2.14.1 Spatial Representation of Vulnerable Population

An important aspect of vulnerability studies is finding out the total number of people that will be affected. Though this information is available from the census at district, provincial, or municipal levels, it does not capture the exact number of people who live within a certain distance of the coast and will be impacted by a hurricane more than the people who live inland. LandScan population data (LandScan™, 2010) has been used to map the population that will be susceptible to the surge or hurricane winds without considering the jurisdictional boundaries (Lam *et al.*, 2009).

2.14.2 Spatial Representation of Probability of Strike

Spatial representation of probability of strike was made possible by the advent of GIS. One of the initial works in this area using GIS was done by Elsner and Kara (1999) who represented return periods of all categories of hurricane strike for the east and south coastal counties of the US. With this method, there is possibility of misrepresentation of hurricane strikes depending upon the length of a county's coastline (Keim *et al.*, 2007), as well as the location of strike.

An alternative method proposed by Keim *et al.,* (2007) uses a point of strike without using jurisdictional boundaries. This seems to be more effective in representing the probability of strike. This method too has its own limitation; it is not possible to combine it with for boundary

based analysis such as vulnerability analysis which uses indicators that are measured for jurisdictions.

A representation technique created by Knowles and Leitner (2007), where past historic tracks were used to create a "Choropleth Map" of density distribution **(**Knowles and Leitner, 2007; Knowles, 2008), uses the "kernel density interpolation" tool available in GIS, to map weighted densities of hurricane strike locations. This method nonetheless requires a large number of data points and cannot be applied to this study.

2.14.3 Spatial Representation of Hazards

There are various models that can create maps of hurricane surge and wind field. Though these models provide very detailed information, none of them work in real-time which is a limitation for all hazard models. A wind-speed model based on data from past hurricanes is mapped using spatial interpolation techniques such as Kriging, Spline, and Inverse Distance Weighing (IDW). These are geo-statistical techniques that use the relative distance between points to assign weights while interpolating missing data points (Lam, 1983). The values being interpolated can be any attribute of the past hurricane. In this dissertation, wind speed in knots was used and classified into categories based on the Saffir-Simpson Hurricane Wind Scale.

Models such as ADCIRC Coastal Circulation and Storm Surge Model; Sea, Lake and Overland Surges from Hurricanes (SLOSH) model; provide potential surge information based on the topography, bathymetry, central pressure, wind speed, tides, etc. But they require immense computing power and time. A simple flooding model is proposed in this dissertation that calculates the potential inundation by a storm surge after it has reached the coastline. The flooding is then based on the height of the surge and the elevation of the coastal area.

CHAPTER 3
METHODOLOGY

3.1 Field Methods

A criterion of finding lacustrine environments behind sandy barriers was used for choosing coring sites after an initial reconnaissance. Cores were extracted using a modified Livingstone Piston Corer or a Russian Peat Borer (RPB). Livingston Piston Corer is 5 feet (approximately 1.5 m) long plastic tube fitted with a piston, a core head, and a cutting shoe. When it is pushed in the lake/swamp bed and pulled back up, it captures 130 cm of sediment in the tube at a time. The second kind of corer is the RPB which can obtain sediment sections that are hemispherical and 0.5 m in length.

For shallower areas, coring was done by standing in water; in deeper waters, coring was carried out by standing on a wooden platform between two inflatable boats. Global Positioning System (GPS) readings and salinity measurements were noted. Finally, core tubes with the sediments inside were labeled, sealed, and transported back to LSU.

3.2 Laboratory Methods

After opening, the cores were scanned and a visual analysis performed detailing stratigraphy of the sediment layers. Loss-on-ignition (LOI) was performed at a cm resolution to determine the percentages of water, organic matter, and carbonate (Dean, 1974). In cases where the sand layer was not detectable through LOI but was visually apparent, an additional grain size analysis was done to verify its presence. If the sediment layer signified an event (i.e., was composed of sand), dating techniques were used to determine its age and chronology (Donnelly *et al.*, 2004).

3.2.1 Loss-on-Ignition

Loss-on-ignition (LOI) is an inexpensive yet efficient method that estimates the differential

loss of matter by combustion technique and is used to study the composition of lake-core sediment. It is a widely used method that helps to roughly identify the percentage composition of water, organics and carbonates in the sediment sample (Dean, 1974).

First, the crucibles were weighed empty to get the tare weight. Next, sediment was sampled at an interval of 1 cm and weighed with the tare weight to get the gross weight of the sample. Crucibles with sediment in them were dried overnight at 100^{o}C and weighed again to determine the water percentage. After weighing the dried samples, they were burnt at 550^{o}C during which organic matter was oxidized (Heiri *et al.*, 2001; Dean, 1974). Weighing this sample after ignition at 550^{o}C gave the amount of organics in the sediment. Finally, the samples were ignited at 1000^{o}C, at which temperature the carbonates in the sediments were oxidized to carbon dioxide and ash (Heiri *et al.,* 2001; Dean, 1974). The remaining substance was the residual matter which is mainly composed of silicates. Weighing the samples after this last step gave the amount of carbonates in the sediment.

Storm overwash events were inferred from sand layers found in the cores based on the LOI analysis. A sharp dip in the organic content in the LOI curves indicated a clastic layer. In case of the presence of clay, the water content was not reduced noticeably. On the other hand, where sand was present, water as well as the organic content showed a steep reduction.

3.2.2 ^{14}C Dating

Once the hurricane records were identified by a visual inspection and loss-on-ignition analysis; bulk organic sediment samples from just under or above the event layer, and from the basal layer (to determine age of the core) were collected, dried overnight and sent to the National Ocean Sciences Accelerator Mass Spectrometry (NOSAMS) Facility at Woods Hole Oceanographic Institution for analysis of ^{14}C. In cases where a faster turnaround time was required, organic samples were sent to Beta Analytic, Inc., which is a commercial facility in

Miami, Florida. An Accelerator Mass Spectrometry (AMS) technique was used at NOSAMS and Beta Analytic to date the samples. A total of 21 samples from the Dominican Republic and RAAN, Nicaragua, were dated using radiocarbon.

The radiocarbon dates received from Beta Analytic were already calibrated but those received from NOSAMS were calibrated into calendar years by using CALIB 6.0 program (Stuiver and Reimer, 1993) (http://calib.qub.ac.uk/calib/calib.html) which was written by Quaternary Isotope Lab at the University of Washington. Intercept dates were calculated using the calibration plot obtained from Calib 6.0.

3.2.3 ^{137}Cs and ^{210}Pb Dating

^{137}Cs ($t_{1/2}$ = 30.2 years) analysis was done to determine the hurricane events in the last 50 years based on the fallout of this fission byproduct around 1952 to1958, 1963, and 1964 from atomic testing (Ritchie and McHenry, 1990). The 1963 peak was used in this analysis due to the maximum atmospheric delivery during this time.

^{210}Pb was used to estimate the accumulation rate of sediments in the lake. It is part of the ^{238}U decay series and has a half life of 22.3 years. It falls into the lakes and oceans from the atmosphere and gets fixed with the sediment material. Age of the sediment is determined by the ^{210}Pb activity in it; it takes about 110-130 years for it to decay completely.

Cores LIM 4 core from the Dominican Republic and DAK 3 from RAAN, Nicaragua were selected for ^{210}Pb and ^{137}Cs dating. Samples at 3 cm resolution were extracted from the top 30 cm of each of the two cores. Each sediment sample was weighed, dried at 60˚C, and weighed again until the dry weight was constant. The oven-dried samples were pulverized, packed into vials and sealed. After a 3 to 4 week period when the ^{210}Pb parent isotope ^{226}Ra reached equilibrium with its daughters ^{214}Bi ($t_{1/2}$ = 19.9 m) and ^{214}Pb ($t_{1/2}$ = 26.8 m), ^{210}Pb and ^{137}Cs

activities were detected using gamma spectrometry on a Canberra well germanium detector for ≥ 24 hours each. This analysis was done in the laboratory of Dr. Jaye Cable in the Department of Oceanography and Coastal Sciences at Louisiana State University.

A constant flux: constant sedimentation rate (CF: CS) model was used, which assumes a constant ^{210}Pb flux from the atmosphere and a constant sedimentation rate. The excess amount of ^{210}Pb activity is graphed on a log scale against the depth (cm) where the slope indicates the sedimentation rate of the core (e.g.,Pempkowiak *et al.,* 1988; Tylmann, 2004). The model was then solved for time (since deposited) to obtain the age of a sediment layer at a certain depth.

Sedimentation rates obtained from the above analysis were used to determine the cut-off between the historic period (160 years) and the prehistoric period in the core. This removed the overlap in the core for historic storms so Bayesian statistical analysis could be performed using a superposition of two separate time lines.

Recent hurricane event chronology was estimated for the Dominican Republic and RAAN, Nicaragua, using known hurricanes around these years as baseline coupled with the sedimentation rate data. Modern analogs were created for events identified in the core that were correlated in the historical records.

3.2.4 Grain Size Analysis

Grain size analysis was done on selected cores that had very low levels of organic matter and lacked event layers clearly identifiable in the LOI analysis. Core sediments were analyzed for grain size using a nested sieve technique. The analysis was done in-house in Dr. Harry Robert's laboratory using a GILSON Performer III, model SS-3 sieve shaker. Nine sieves were used ranging from numbers 18-230. They were stacked on top of each other with the largest mesh size on the top and the smallest at the bottom.

After tapping the sediments for 10 minutes in the sieve shaker, each sieve was removed and material was weighed to get a grain size profile. Statistical analysis was performed to understand the grain size distribution in the sample and to determine levels of sand (Folk and Ward, 1957). A smoothened frequency curve was created in Microsoft Excel; highest frequency in the 3-1 Φ (or 125- 500 microns) indicated presence of sand (Krumbein and Sloss, 1963).

3.3. Analytical Methods

3.3.1. Probability (P) Estimation

To arrive at an empirical probability from the prehistoric data with greater uncertainty and a more certain and complete historic data, a Bayesian model using Poisson distribution (Elsner and Bossak, 2001; Solow and Moore, 2000) was used. A method using a "Gamma Density" function (Elsner and Bossak, 2001) was vetted but could not be used for the paleo records of hurricanes as there was no distribution available to calculate the variance and hence the distribution parameters could not be established.

A simple superposition (Nelson, 1995) of two Poisson processes was considered by combining the time periods and occurrences. Historic and prehistoric hurricanes were both treated as two *separate* Poisson events with *non overlapping time frames*. (For this, using a sedimentation rate from dating of the core, the top 160 years of the core was removed.) Their superposition then yielded a Poisson distribution (Nelson, 1995).

$$f_{\text{Poisson}}(\hat{h} \mid \lambda, T) = \exp(-\lambda T)\frac{(\lambda T)^h}{h!}$$

$$\text{for } h = 0, 1, 2, \ldots,$$

$$\lambda > 0, \quad \text{and} \quad T > 0.$$

(Elsner and Bossak, 2001)

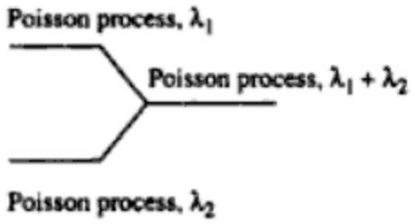

(Nelson, 1995)

First, return periods were calculated for historic hurricanes by counting the number of hurricane strikes from the HURDAT (CSC, 2010) database. The historic return period was combined with that of paleo-hurricanes by adding the total events and dividing by the total time to arrive at an integrated mean rate of return. Historical events that were duplicated in the prehistoric records were counted only once.

All categories of hurricanes were used from the historical records (CSC, 2010). Prehistoric records were also assumed to be of all categories as there is uncertainty regarding the sensitivity of study sites. Hurricane strikes divided by the total time was used in the Poisson distribution to calculate the expected probability of a hurricane making landfall in the future.

Expected probability of hurricane strikes was calculated using the following formula (Klotzbach *et al.*, 2004):

$$EP = (e^{-p})\ (p^{x})\ /\ x!$$

Where:
EP = Expected Poisson Probability
p = Annual average number of tropical cyclones that have occurred in the past.
x = Number of storms expected in the upcoming year based on the Poisson formula.
x! = Factorial
e = 2.71828

Annual hurricane probability calculation along with that of longer time frames and of multiple hurricane strikes is useful for calculating future losses in the insurance and building industry (Elsner and Kara, 1999). These calculations are used to estimate damage and loss from single and multiple hurricane strikes for varying time periods (Appendix B-2 and B-4). Predictions for varying time periods (e.g., 5, 10, 20, and 50) were made by using the following formula (Klotzbach *et al.*, 2004):

$$T\ Year\ Prob = 1 - (1 - One\text{-}Year\ Prob.)^{T}$$

Where:
T = Time Period under consideration

Similarly predictions were made for multiple storms occurring over varying time periods.

3.3.2 Vulnerability (V) Assessment

Vulnerability indicators for the Dominican Republic and RAAN in Nicaragua were selected based on a social vulnerability methodology which was applied in the Caribbean countries of St. Vincent and Barbados (Boruff, 2005; Boruff and Cutter, 2007) (see Chapter 2). However in this dissertation, total values were considered instead of percentages as they provide the total number of vulnerable persons that have to be moved from harm's way, provided for, and rehabilitated. Additionally, only those indicators that were available from the national census records and national statistical office (as they were considered reliable) were used for analysis in the Dominican Republic and Nicaragua.

In case of the Dominican Republic, the following indicators were used as proxies for vulnerability at the province level: total population, poverty, disability, women, children younger than 5 years, building stock, households with access to roads, and population with access to medical facilities (in terms of Beds/1000 persons). For the department of RAAN, Nicaragua, the indicators used at the municipal level were: total population, number of women, and extremes in age group. Other information was available at the department level for Nicaragua but not at the municipal level.

3.3.3 Normalization

There are various methods that are used in normalizing of indicators. The most commonly used method is the rescaling method because it is simple and effective. It is calculated as (Briguglio, 2003):

$$Vij = (Xij - MinXi) / (MaxXi - MinXi)$$

Where:

Vij = normalized vulnerability score with regard to vulnerability component i, for country j;

Xij = observed value of the same component for the same country;

MaxXi and MinXi = maximum and minimum value of the observed range of values of the same component, for all countries in the index.

3.3.4 Integration of Vulnerability Indicators

After normalization, the indicators were separated; those that contribute towards vulnerability (+) and those that reduce vulnerability (-) they were then combined (added) together to provide a composite index of vulnerability (Cutter *et al.*, 2003; Boruff and Cutter, 2007) which is:

$$\textit{Vulnerability} = \sum(V_1, V_2, V_3, V_4, \ldots)$$

Where $V_{(1,2,3,\ldots)}$ are the rescaled indicators of vulnerability; for example, V_1 is poverty, V_2 is disability, etc. Cutter *et al.* (2003) and Boruff and Cutter (2007) use an aggregate method without assigning weight to the indicators to calculate the index. Using a similar approach, a composite index was created for each coastal province in the Dominican Republic and each municipality in RAAN. This was then spatially represented using GIS.

3.4. Spatial Representation Methods

Risk for the coastal areas was geographically represented by overlaying potential storm surge, vulnerability, and probability of hurricane strike maps.

a. Potential Storm Surge

Potential storm surge inundation was mapped for each category of hurricane ranging from 5 feet (1.5 meters) representing surge for Category 1 hurricanes to 25 feet (7.6 meters) for Category 5 hurricanes. A similar method has been used by Lam *et al.* (2009) to delineate inundation areas based on distance from coast (1 km) and inundation levels of 3 and 6 meters, respectively.

Detailed bathymetric data were not available for the coast of Nicaragua or for the Dominican Republic. Since wave setup is almost all due to the storm in the Caribbean due to a

negligible tidal range (Donnelly, 2005), a simplified flooding approach (NOAA, 2009) was used to create potential surge map.

Digital Elevation Maps obtained from Nicaragua and the Dominican Republic (at 30 m X 30 m resolution) were first converted into raster format in ArcGIS 9.3. Surge height thresholds were set for each category of storm and pixel elevation values above this height was converted to "1" and below the height to "0". A seed pixel with value "0" was created on the coastline. "Cost Distance" function was used to create areas of surge that are theoretically all pixels with a value of "0". Flooding stopped when a pixel value of "1" was encountered. Thus all the areas that are flooded are below the threshold level set for elevation.

b. Vulnerability

Vulnerability indices calculated earlier were used for mapping each province and municipality. Additionally, the population that was directly at risk from hurricane strikes (and resulting flood from storm surge) was mapped (Lam *et al.*, 2009) by using raster grid data available from LandScan (LandScan™, 2010). A function in GIS called "raster math" was used to calculate the population that would be affected by the potential surge.

c. Spatial Interpolation of Hurricane Wind Speed

Using historical hurricane strike data (HURDAT) for the last 160 years, available from NOAA, a raster surface was created for the Dominican Republic and for northern Nicaragua using wind speed as the input value. This map was used to represent the potential wind speed from future storms.

Three interpolation techniques- Kriging, Spline, and Inverse Distance Weighing (IDW) - were considered but due to very few data points over large distances (which do not allow the use of Kriging and Spline interpolation), IDW was used. IDW is an interpolation technique that uses

the distance between data points to assign weights (Lam, 1983). Points farther out have less weight than those nearer. Furthermore, IDW suited the wind speed analysis as speeds decrease as the distance from landfall locations increases. "Geostatistical Analyst Wizard" was used in ArcGIS 9.3 to create an IDW surface using the historic hurricane strike points. Winds-speed at landfall was used as the value that was being interpolated. The resulting map shows predictive surface for wind speeds of hurricanes making landfall on the coast.

All categories of historic hurricanes were taken into consideration for a comprehensive spatial analysis. Since not enough information about the exact point of strike and the intensity of storm could be inferred from the analysis of the proxy records, prehistoric hurricanes were not used in the analysis.

d. Probability of Strike

Probability of strike calculated earlier (see section 3.3.1), was mapped for each district in the Dominican Republic and each municipality in RAAN, Nicaragua. This map shows the likelihood of a hurricane strike in the future based on the combined Poisson probability calculations.

3.5 Data Collection Methods

Data used in this dissertation were collected primarily during two field trips undertaken in 2009. Data were solicited from universities and agencies in the study areas. The rest were collected by utilizing free, public resources available on the internet, such as the LandScan Dataset (LandScan™, 2010).

3.5.1 LandScan ™ Dataset

A request was made and datasets were downloaded from the Oakridge National Research Laboratory website (http://www.ornl.gov/sci/landscan/) which maintains population data for 2007 in a

30”X 30” Latitude/Longitude grid format.

3.5.2. Data from Nicaragua

A fieldtrip lasting two weeks to Nicaragua (Managua and Puerto Cabezas) was undertaken in February 2009 with the help of a local guide who is familiar with the study area and speaks fluent Spanish and English. The first part of the trip was spent in Managua and Puerto Cabezas visiting national and regional government agencies; non-government agencies such as Sistema Nacional para la Prevención, Mitigación y Atención de Desastres, (SINAPRED - Managua), Instituto Nicaragüense de Estudios Territoriales (INETER), Instituto Nicaragüense de la Pesca y Acuicultura (INPESCA), The Nature Conservancy (TNC); and universities including La Universidad Nacional Autónoma de Nicaragua, (UNAN – Managua), and La Universidad de las Regiones Autónomas de la Costa Caribe Nicaragüense (URACCAN – Puerto Cabezas).

Socio-economic, risk, and vulnerability data were requested and obtained from each of these agencies. The following are some examples of data that were obtained from the above agencies

1. Latest official national census data from 2005.
2. Geographic Information System (GIS) data such as roads, jurisdictional boundaries, population of communities, elevation maps, etc.
3. Photos from Hurricane Felix.

3.5.3. Data from the Dominican Republic

A three week trip was undertaken between April 12, 2009 and May 1, 2009 to collect hazard and vulnerability data from the Dominican Republic and to extract additional cores from a coastal lake site that was deemed promising in the initial reconnaissance trip in 2008. A local guide’s help was used in visiting agencies for data collection. Solicitation letters were prepared, delivered, and interviews scheduled with the respective contact persons at the agencies.

The first week was utilized in obtaining permits for coring in Lake Alejandro (near Barahona in the western part of the Dominican Republic) from the Ministry of Environment (Medio Ambiente). Various other agencies were approached for information and data on risk, hazards, and vulnerability. The Main agencies that were contacted for information are: Medio Ambiente, Defensa Civil, United Nations Development Program (UNDP), and The Nature Conservancy (TNC).

Additional cores were collected from Lake Alejandro in the second week of the trip. This trip was undertaken in collaboration with Dr. Lisa Kennedy of the Department of Geography Virginia Tech.

The third week of the trip was spent collecting the socio-economic, hazard, risk, and vulnerability data requested earlier. The following are some examples of data that were obtained from the above agencies:

1. Official national census data from 2002.
2. Geographic Information System (GIS) data such as roads, elevation, population of communities, etc.
3. Photos from recent hurricanes and tropical storms such as Olga (2007) and Noel (2007).

CHAPTER 4
PALEOTEMPESTOLOGY OF THE DOMINICAN REPUBLIC

4.1 Background

The Dominican Republic (19^{o} N, 70.66^{o} W) is on the eastern part of the island of Hispaniola which is a part of the Greater Antilles that lies in the Caribbean basin between the Caribbean Sea and the Atlantic Ocean. It occupies two thirds of the island while sharing the rest with Haiti. It has a rugged topography and high elevations (3,175 m). The total area of the Dominican Republic is 48,730 km^{2}.

The capital of the Dominican Republic is Santo Domingo which is located on the southern coast of the country. The climate is tropical maritime with average maximum temperature of 25^{o}C. The Dominican Republic has an annual average precipitation of 150 cm, mostly during the months of May – August.

4.2 Geologic Setting

The island of Hispaniola was developed from the early Cretaceous period and it forms an intricate island-arc structure (Lewis and Draper, 1990) along the boundaries between the Caribbean plate, the North American plate, and the South American plate. The Caribbean basin is also an area of high seismic activity (McCann, 2006). The island of Hispaniola has two fault systems running parallel through it, creating a seismically unstable environment (Kerr, 2010). Due to considerable plate activity in the island of Hispaniola, there is evidence of folding and lifting of rocks. The island has gone through gradual uplifting and this continues to this day (Lewis and Draper, 1990).

Prominence of conglomerates and other clastic sediments in the northern and southern parts of the island (Figure 4.1) indicates a lower sea level in the past (Lewis and Draper, 1990).

The eastern end of the island (Figure 4.1) is a Pliocene and Pleistocene reef consisting of Coralina/Coralstone (Draper *et al.*, 1994).

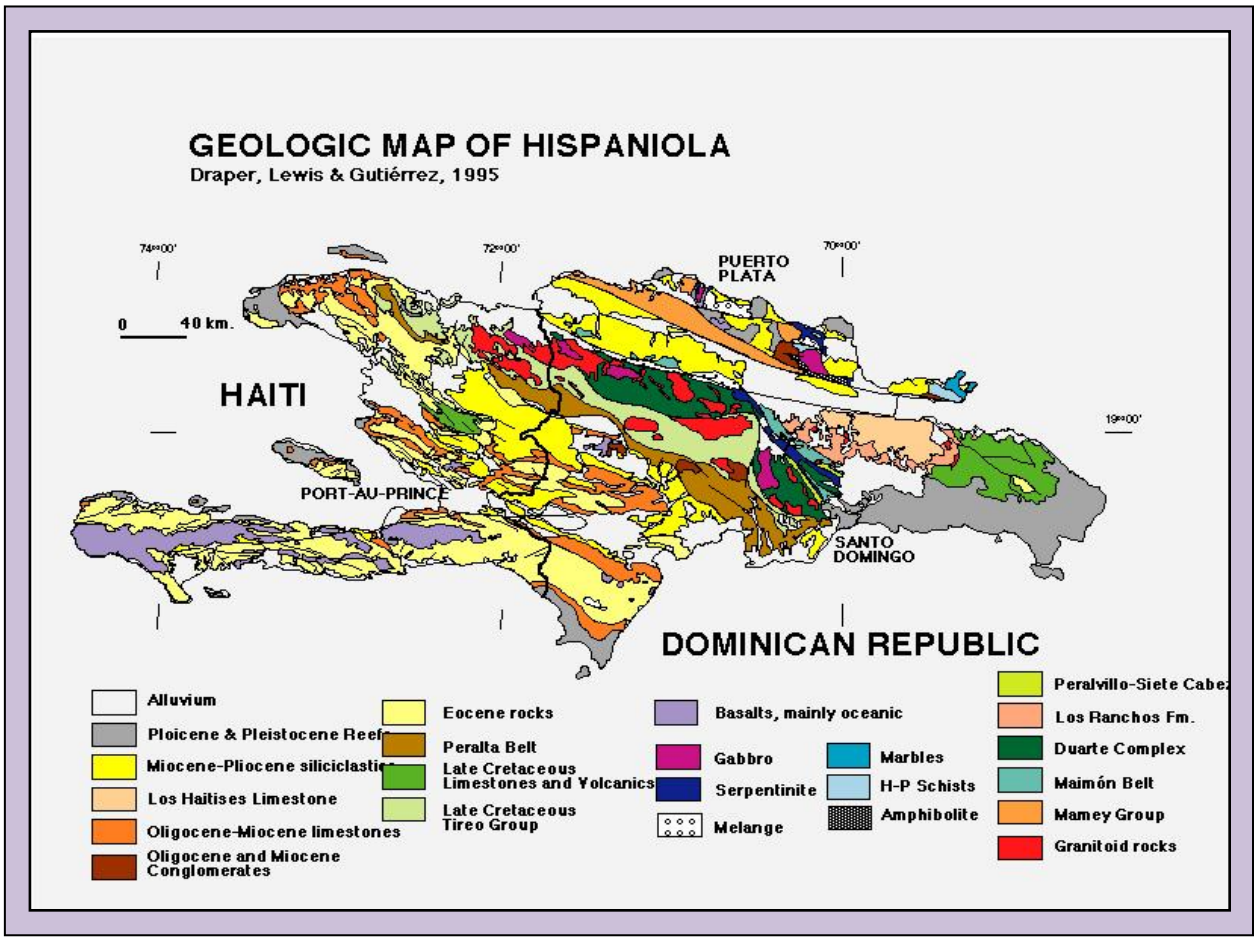

Figure 4.1: Geology of the Dominican Republic (map drawn by Gabi Gutierrez-Alonso, http://palaeo.gly.bris.ac.uk/palaeofiles/Lagerstatten/DomAmber/geoSet.jpg).

4.3 Dominican Republic and Hurricanes

The Dominican Republic is frequently affected by intense hurricane activity (Figure 4.2). Most of the coastline of the Dominican Republic has been hit by hurricanes; the only areas that have not had hurricane strikes are the extreme northwest part of the country, next to the Haiti border.

Based on historical records, the Dominican Republic lies in the region of at least 10% annual probability of hurricane strikes (Pielke *et. al.*, 2003). Figure 4.2 shows the hurricane

tracks and landfall locations of the hurricanes. Twenty-six hurricanes, of which 12 were major (Category 3-5) hurricanes, have hit the Dominican Republic since 1851 (CSC, 2010). The most destructive hurricanes to hit the country in this century are Hurricane San Zenon in 1930, Hurricane David in 1979, and Hurricane Georges in 1998 (see Chapter 5 for the description of these hurricanes).

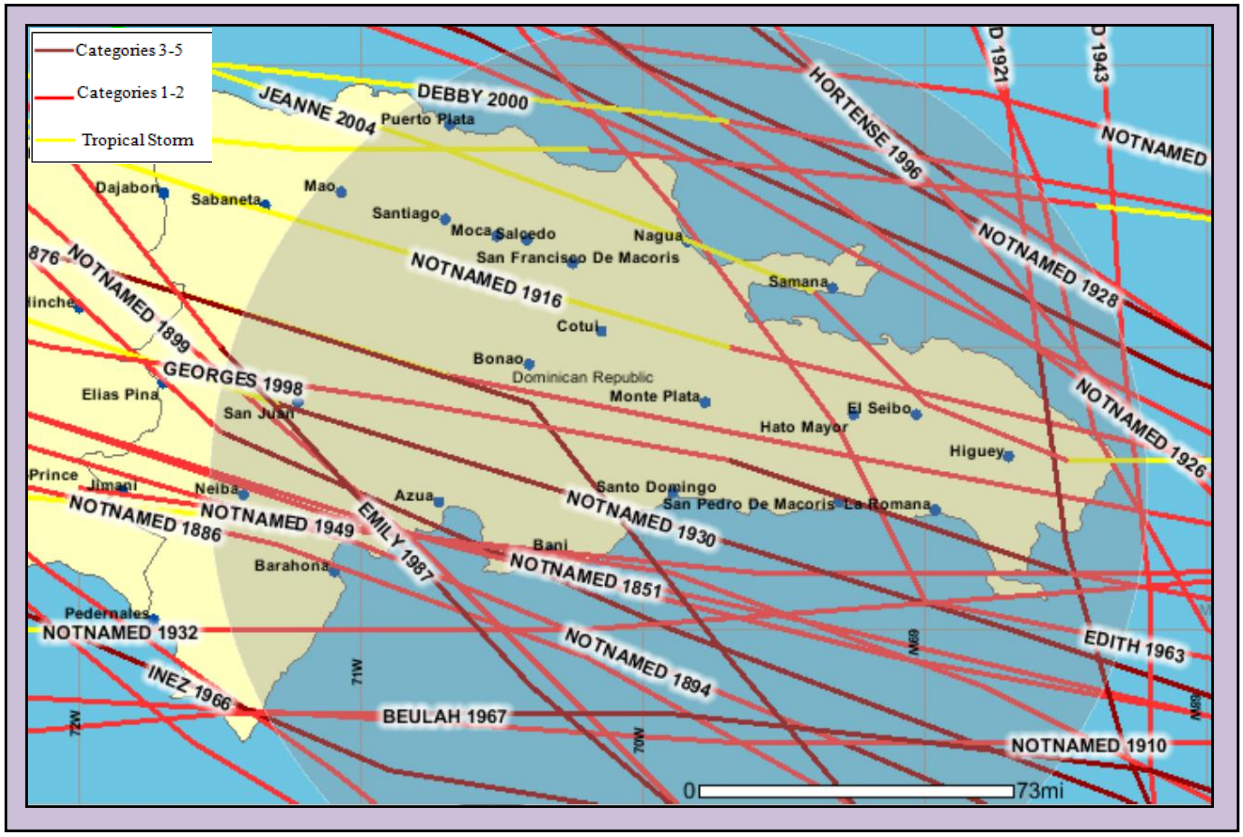

Figure 4.2: Hurricane strikes in the Dominican Republic since 1851(CSC, 2010).

4.4 Paleotempestology in the Dominican Republic

Based on the criterion of lakes behind sandy barriers, and knowledge of previous hurricane strikes, suitable locations were chosen for coring in the Dominican Republic. Coring was done in February of 2008 and April of 2009. Twenty-five cores were obtained measuring 32 m of sediment. After opening, the cores were scanned by using a table-top digital scanner and a visual analysis was performed detailing stratigraphy and visible sand layers. All of the cores

obtained from the field were analyzed using loss-on-ignition (LOI) to determine the percentage of water, organic matter, and carbonate. Due to budget constraints, only some of the cores that showed prominent hurricane layers were selected for radiocarbon dating. A hurricane history was reconstructed using those dates.

4.5 Study Sites

Six sites: Laguna Oviedo, Lake Alejandro, Alijibe, Lake Mala Punta, mouth of Yuna River, and Lake Limon were selected in the coast of the Dominican Republic (Figure 4.3).

Figure 4.3: Coring sites in the Dominican Republic.

4.5.1 Laguna Oviedo

Laguna Oviedo is a large lake located in the southern part of the Barahona peninsula in the southwest part of the country. Cores were extracted from two smaller coastal lakes in this area: Laguna Hediendo (Lake Stinky) and Laguna Playa Ingles (Figures 4.4.A and 4.4.B).

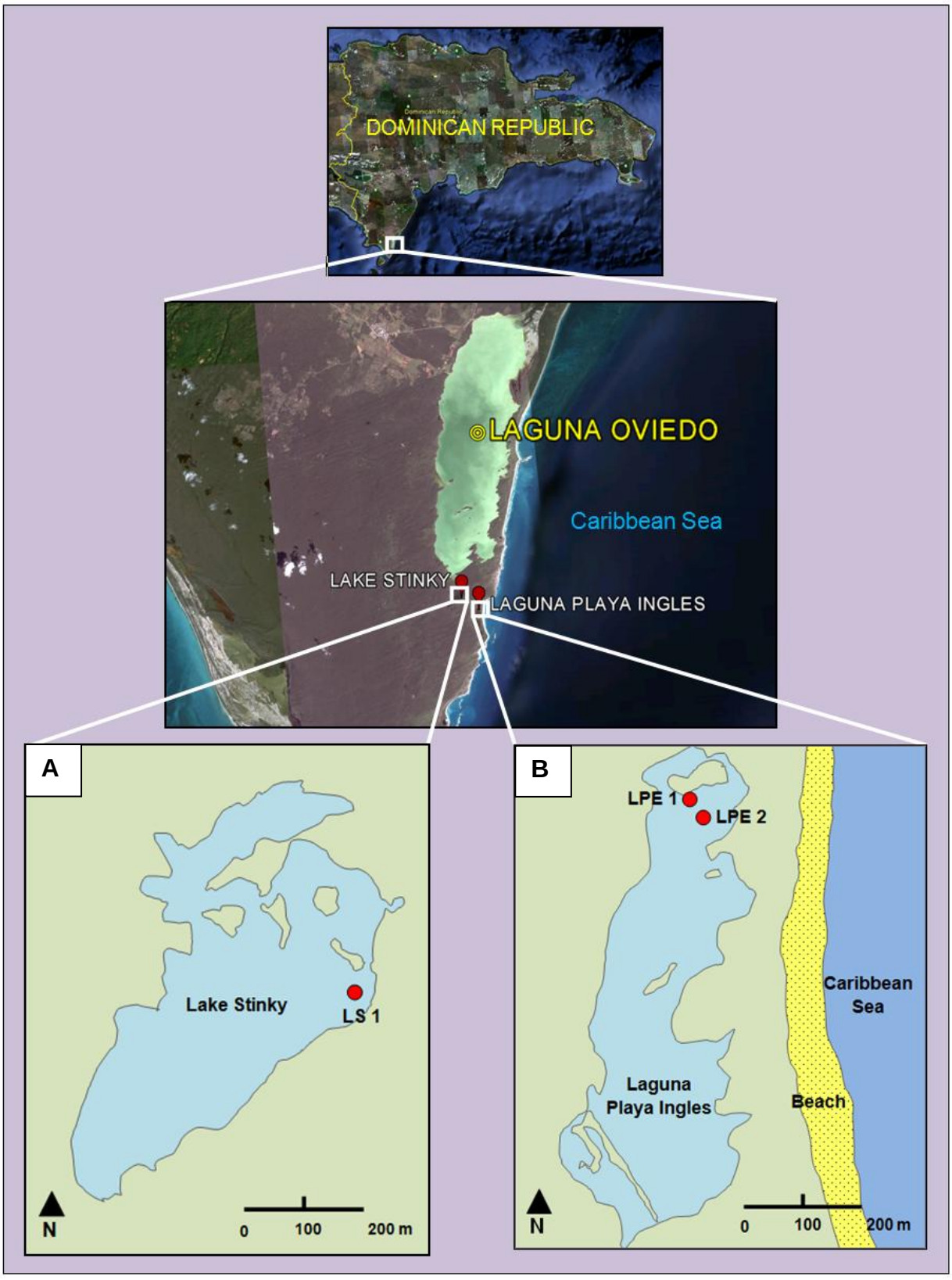

Figure 4.4: Coring locations for LS 1, LPE 1 and LPE 2 near Laguna Oviedo.

Laguna Oviedo is separated from the beach by a vegetated sand ridge which is anchored to a limestone headland about 50 m high to the north (Figure 4.5.A). Due to the presence of this rocky headland, it is most likely that this area has maintained a fairly stable relief through the Holocene.

4.5.1.1 Laguna Playa Ingles

Laguna Playa Ingles is an ideal setting for paleotempestology. It is separated from the sea by a sandy beach ridge (Figure 4.5.B). It is a shallow lake and seems likely to dry up; mudflats were already in formation.

The rocky ridge next to Laguna Oviedo (Figure 4.5.A) continues as an 8-10 m high beach ridge and according to the fishermen who live around there, it is regularly topped during storms. The salinity of this lake was 36.2 ppt (same as that of the sea) in January, 2008, indicating either a continuous exchange with the sea water or a higher salinity due to its shallow depth.

Two cores were extracted from this lake: LPE 1 (Figure 4.6) measured 115 cm and was extracted 200 m from the coast. Sediment stratigraphy reveals the presence of clay on top 5 cm of the core followed by sand below it until the depth of 58 cm (Figure 4.6). Below that there are mixed sediments with intermittent layers of sand. The loss-on-ignition analysis (Figure 4.6) of the core supports the presence of these sand layers. The other four layers of sand which indicate hurricane events were found in the bottom 60 cm of the core at the depths of 70-75 cm, 86-91 cm, 96-100 cm, and 104-109 cm.

LPE 2 measured 100 cm and was extracted 165 m from the coast. LOI results for LPE 2 correspond with the visible sand layers in the core photographs taken in the field (Figure 4.7). The top 10 cm of the core consists of clay and the next 45 cm of the core is sand (similar to LPE 1) with bigger grain sizes in the 50-55 cm depth (Figure 4.8). In the bottom 45 cm of the core,

the sand layers were recorded at 63-66 cm and at 95-98 cm depth.

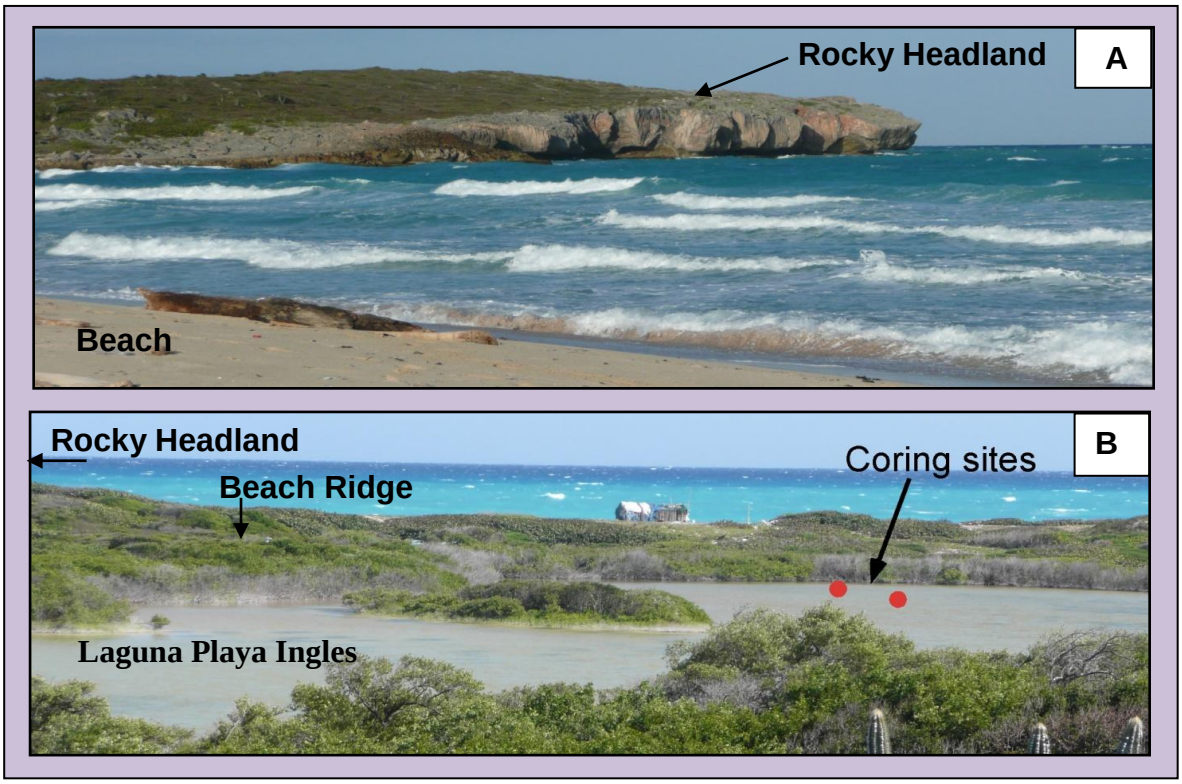

Figure 4.5: (A) A limestone rocky headland anchors the ridge in the north. (B) Laguna Playa Ingles is separated from the beach by a vegetated beach ridge.

Both cores (LPE 1 and LPE 2) have 5 cm of clay and then 45-50 cm of sand on the top (Figures 4.6 and 4.7). This is surprising as no recent hurricanes have made landfall in this area. The last hurricanes to hit this area were Inez (Category 4) in 1966 and Beulah (Category 3) in 1967. The alternative explanation is an overwash deposit from a tsunami. However the last tsunami to hit the Dominican Republic was in 1946 (from National Geophysical Data Center at National Oceanic and Atmospheric Administration, NOAA, http://www.ngdc.noaa.gov/nndc/struts/form?t=101650&s=167&d=166) which mainly affected the northeastern part of the country. While this was caused by a strong earthquake of magnitude 7.4, the maximum water height was a mere 0.6 m in the Dominican Republic.

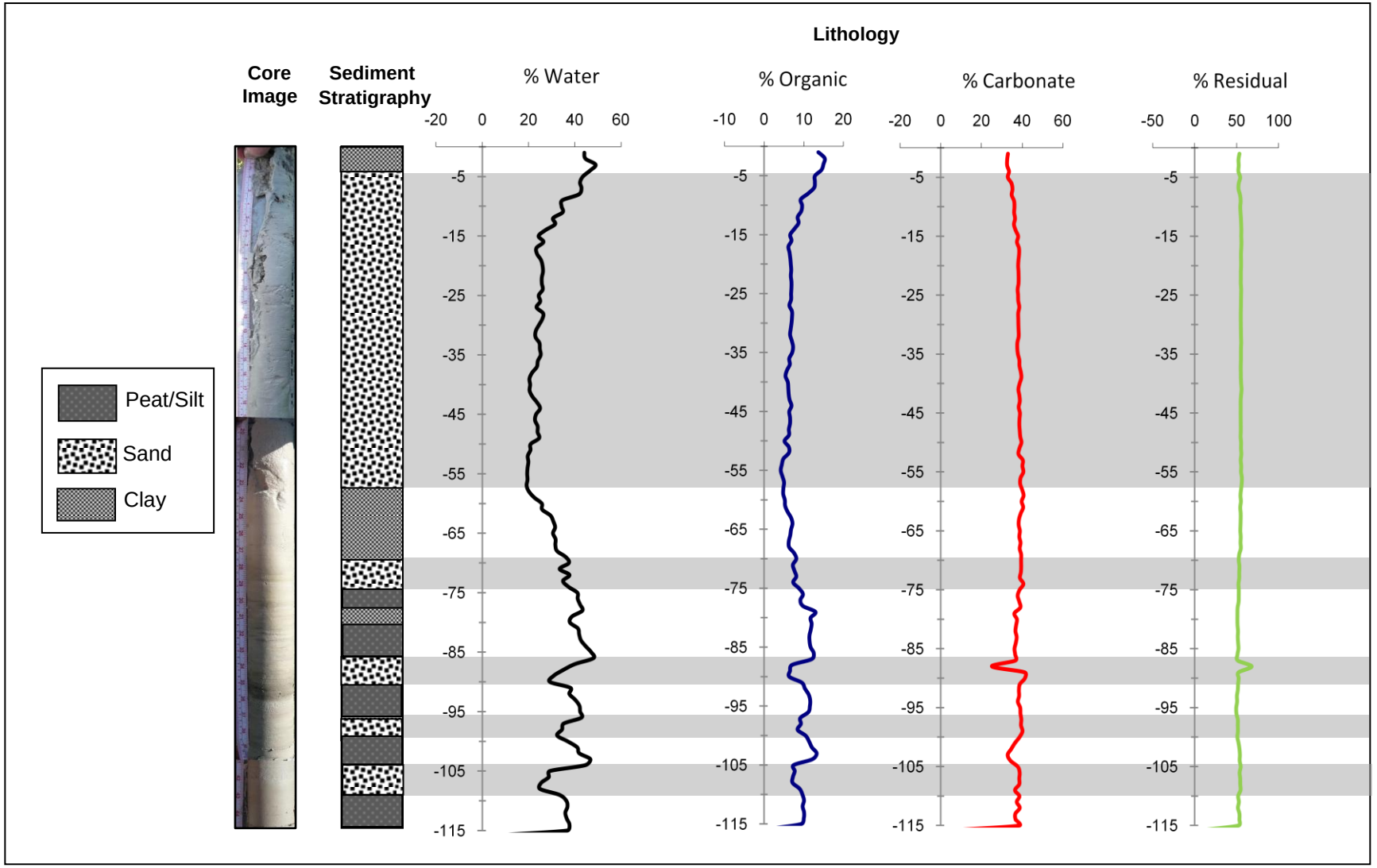

Figure 4.6: Loss-on-ignition and sedimentological analysis of Laguna Playa Ingles core LPE 1.

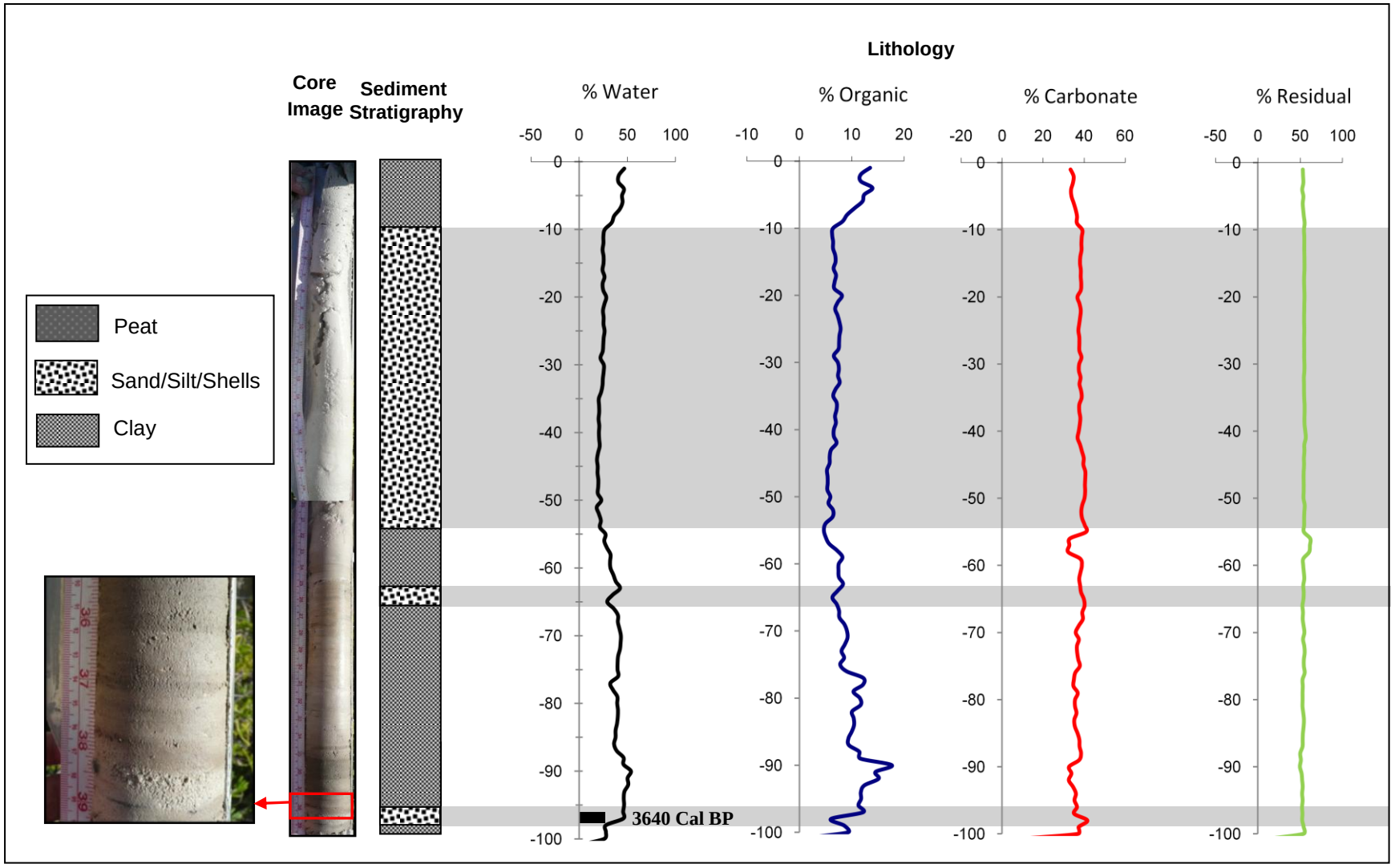

Figure 4.7: Loss-on-ignition and sedimentological analysis of Laguna Playa Ingles core LPE 2.

Organic matter could not be obtained from the bulk sediment below the sand layers; instead a shell fragment was extracted from the basal layer (97 cm) and sent for radiocarbon dating. Results show that the event occurred in the conventional date of 3,820 +/- 30 ^{14}C yr BP. Reservoir effect was factored in for the shell fragment (Dix *et al.*, 1999). While there are no reservoir effect studies in the Dominican Republic, those in Jamaica show a value of 423 years with an error of +/- 42 years (http://intcal.qub.ac.uk/marine/index.html?ORDERBY=C14age%20asc). By using this correction factor, the radiocarbon age for LPE 2 basal layer is about 3,400 ^{14}C yr BP. This date was calibrated (Table 4.1) using CALIB 6.0 program (Stuiver and Reimer, 1993). References for calibration datasets are from Reimer *et al*. (2009). An intercept date was calculated using the calibration plot obtained from Calib 6.0.

Table 4.1. ^{14}C and calibration results for LPE 2 at 97 cm depth using Calib 6.0 (Reimer *et al.*, 2009).

Core	Depth (cm)	Laboratory Number	Material Dated	Radiocarbon Age BP	Cal BP (2σ)	Probability	Intercept Date
LPE 2	97	OS-79619	Shell	3400 +/- 30	**3567 -3718**	**1.0**	**3,640 BP**

Grain size analysis was done on the lower part of the core LPE 2 to identify the sand layers which may be potential hurricane events. A dry sieving method was utilized to measure the size of grain of the sediment layers. Sampling was done at 5 cm resolution. The grain sizes of samples were measured in percentage and plotted as separate curves for each sample (Figure 4.8.B). The grain size of sand ranges between 3-1 Φ (125- 500 microns) with the extreme values of the range overlapping with the grain size of gravel at the higher end and silt on the lower end.

The gray area in Figure 4.8.B represents the range within which the three peaks are present, indicating a higher percentage of medium-grained sand. There were three prominent

layers in the core that are candidates for hurricane events. These are at: (1) 50-55 cm, (2) 60-65 cm, and (3) 95-100 cm (Figure 4.8). The sample at 50-55 cm is from the bottom portion of the top section (10-55 cm) of the core LPE 2 (Figure 4.7) which primarily consists of sand. Analysis at a higher resolution of 1 cm for both cores will provide a better portrayal of the stratigraphy.

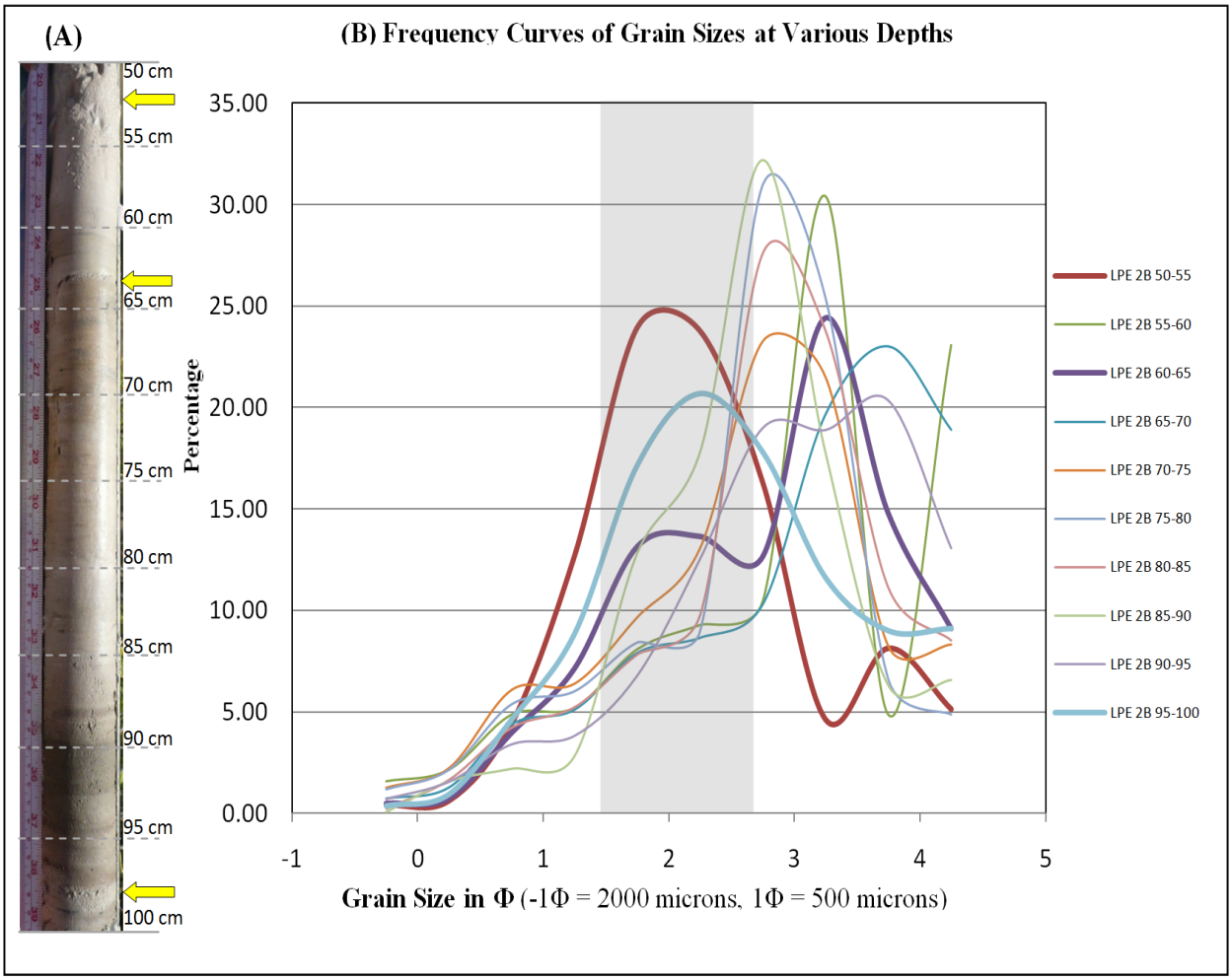

Figure 4.8: Grain size analysis of LPE 2B (A) Core photo of LPE 2B showing sand layers indicated by yellow arrows.(B) Grain size analysis curves for LPE 2B. Red, blue, and purple curves (50-55 cm, 60-65 cm, and 95-100 cm) with the highest peaks in the medium sand size range (area in gray) suggest hurricane events. The highest percentage of medium-grained sand is at the 50-55 cm depth (shown in red).

4.5.1.2 Laguna Hediondo (Lake Stinky)

Lake Stinky is about 1 km from the ocean (Figure 4.4) and was chosen for coring to assess the reach of a hurricane surge. The beach ridge in front of the lake is 30-40 meters high (Figure 4.9.A). One core was extracted from this lake (Figure 4.9.B) measuring 65 cm. Even though this lake is further inland, it shows a similar stratigraphy as LPE 1 and LPE 2 cores (Figures 4.6 and 4.7) and has ~ 35 cm of sand on the top (below a 5 cm layer of peat) (Figure 4.10). There are two more layers of coarser sand at 43-45 cm and 63-65 cm. The sand layer at 63-65 cm corresponds with the layers at 70-75 cm in LPE 1 and 63-66 cm in LPE 2.

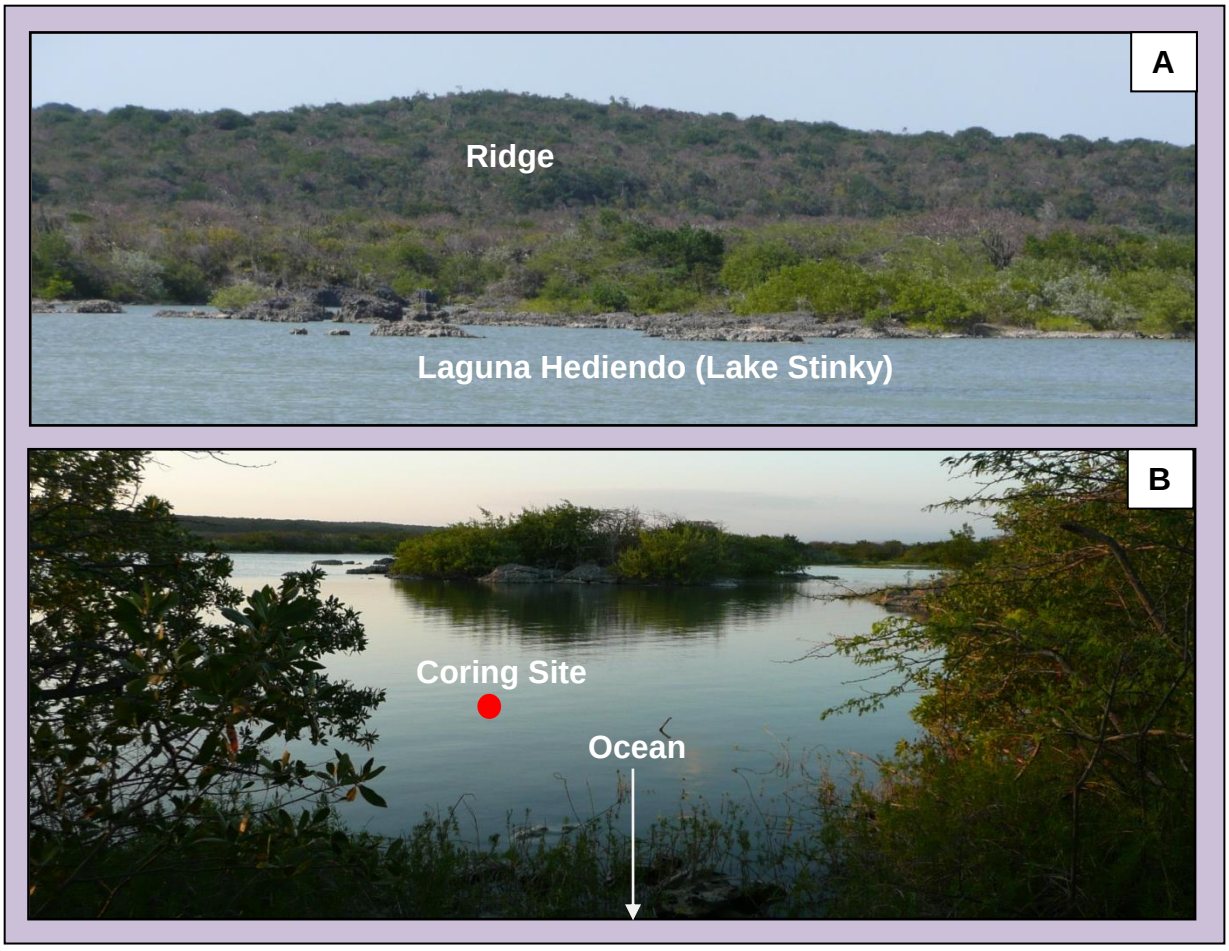

Figure 4.9: (A) 30-40 m high ridge in front of the lake towards the ocean. (B) Laguna Hediendo (Lake Stinky) coring site.

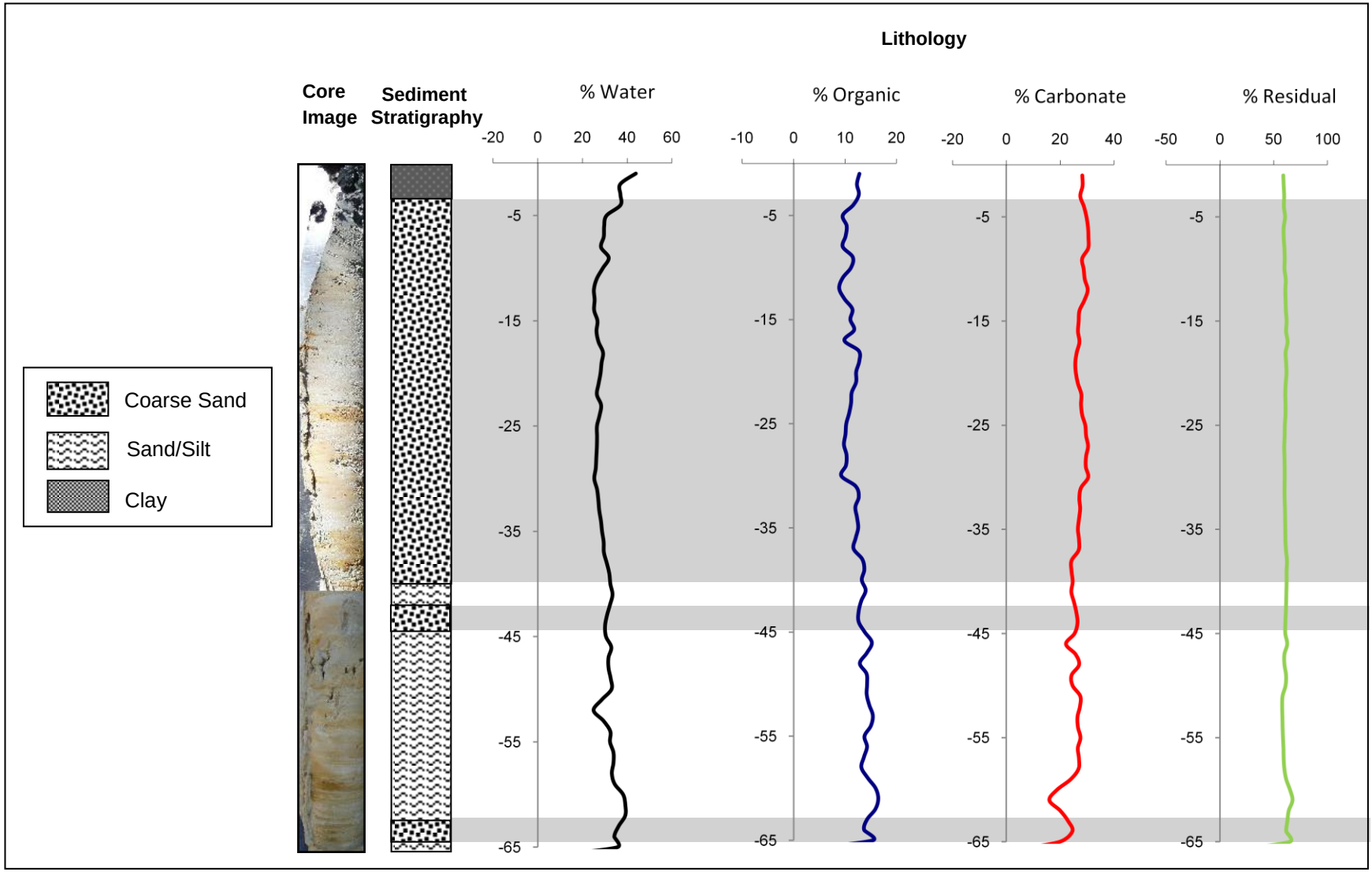

Figure 4.10: Loss-on-ignition and sedimentological analysis of Lake Stinky core LS 1.

4.5.2 Lake Alejandro and Fish Lake

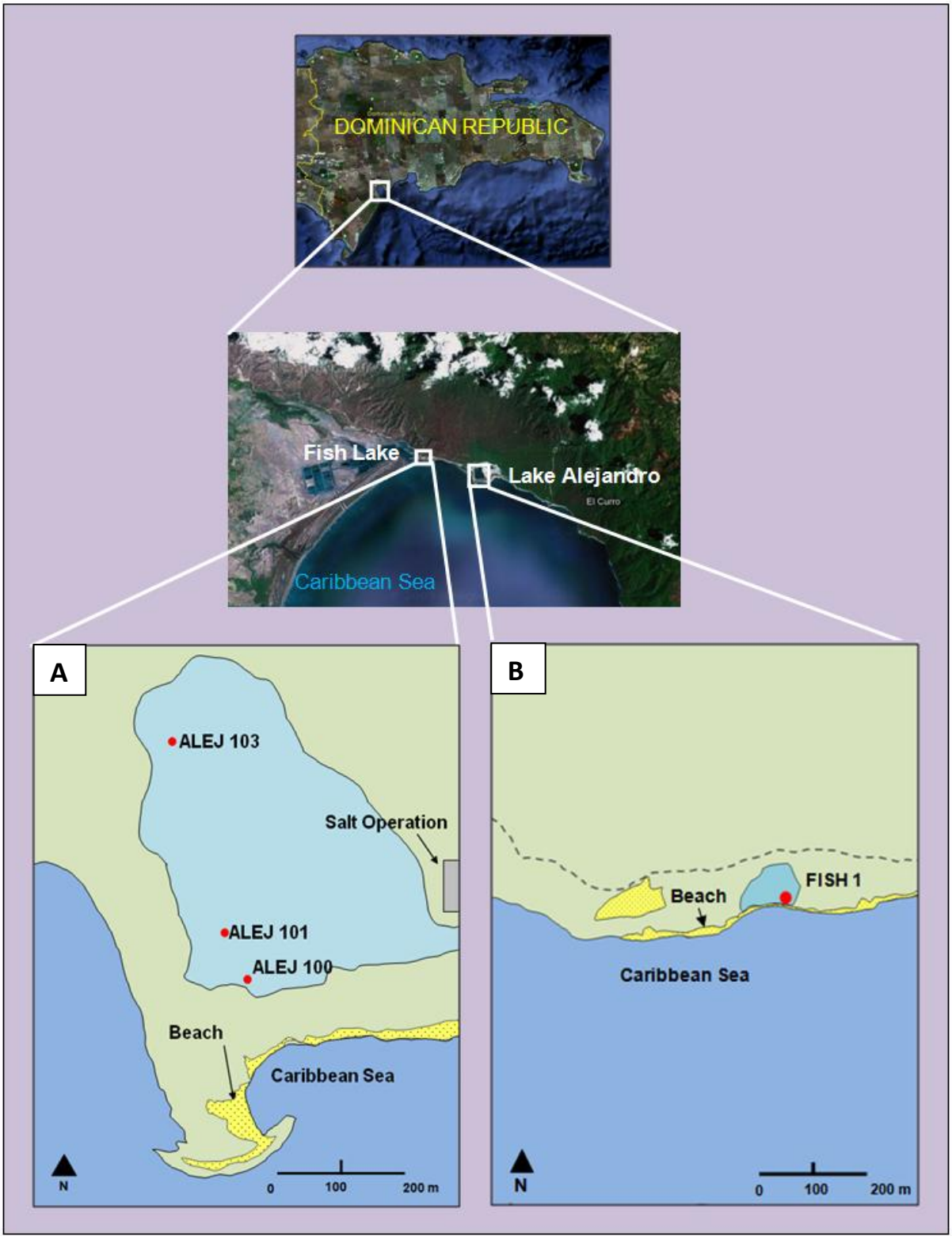

Figure 4.11: Satellite map and diagrams showing coring locations for (A) Lake Alejandro cores, ALEJ 100, ALEJ 101, and ALEJ 103; and (B) Fish Lake core, FISH 1.

4.5.2.1 Lake Alejandro

Lake Alejandro is north of Oviedo and it is a saline lake located in a bay formed between the Barahona peninsula and the main southern shoreline (Figure 4.11.A).This lake was open to the ocean in the past and became a separate lake (Desjardins, 2007), at around 1,173 -935 cal yr BP.

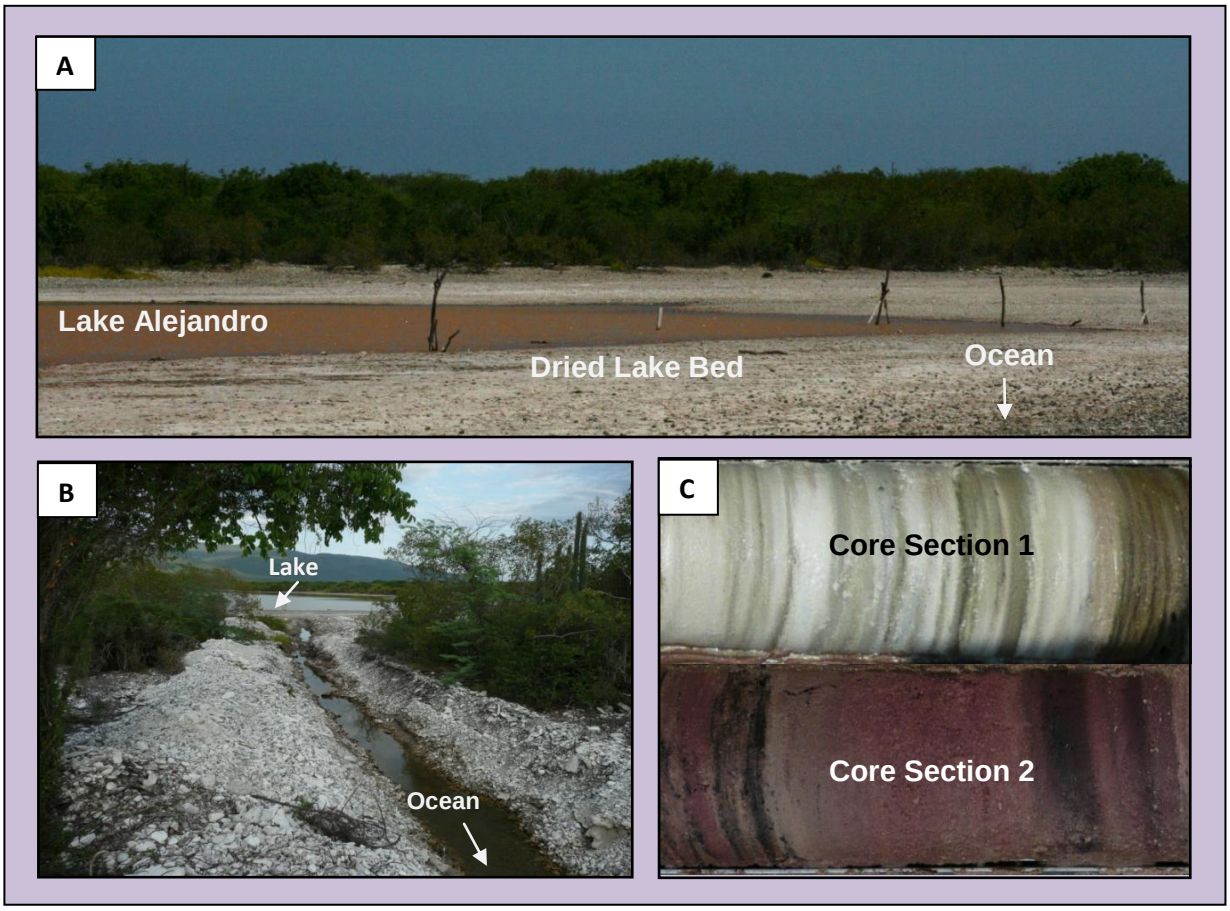

Figure 4.12: (A) Lake Alejandro in April 2009. Much of the lake has dried either due to human actions (salt manufacturing) and/or in the dry season. (B) Dug out channel on the western side of the lake connecting it to the sea. (C) Sections of cores illustrating: 1.White and green bands of gypsum and clay. 2. Peat ranging in color from red to black.

Two sets of cores were extracted from this lake: first in February, 2008 and second in April, 2009. Cores from 2008 could not be used and another trip was conducted in 2009 to

extract new cores. This trip was undertaken in collaboration with Dr. Lisa Kennedy at the Department of Geography at Virginia Tech.

There is a salt operation (Figure 4.11.A) close to the lake, on the eastern part of the lakeshore. Under a new management, it had expanded operation further into the lake as compared to 2008. The western half of the lake was still undisturbed and deemed appropriate for coring. During the second trip, which was in the dry season, the lake level was very low (Figure 4.12.A). The lakeshore has gravel similar to the gravel on the beach. This could be due to an open inlet from the sea in the past. The salt factory had also recently dug a channel connecting the lake to the sea on the western part of the lake (Figure 4.12.B).

Four cores were extracted; three were brought back to LSU and analyzed. Core ALEJ 100 measured 250 cm, core ALEJ 101 measured 260 cm, and core ALEJ 103 measured 365 cm. Core ALEJ 100 was taken 5 m from the lake shore and has nine layers of sand (differentiated based on a dip in organic and water content). The first two layers of sand are mostly gray sand and the seven below those are mixed with silt and gravel (Figure 4.13). The first layer is at 10-37 cm, second is at 46-70 cm, third layer is at 90-100 cm, fourth at 125-130 cm, fifth at 155-167 cm, sixth at 182-192 cm, seventh layer is at 205- 212 cm, eighth layer at 225- 233 cm, and finally towards the bottom of the core is the ninth layer of sand at 240-245 cm. These seven sand layers indicate overwash from hurricanes.

ALEJ 101 was obtained 70 m from the lake shore. The first 10 cm section of this core was lost during extraction. Another segment, at 155-165 cm is also missing; most likely this section fell off during transport. Similar to ALEJ 100 core, it has sand in the top 10-25 cm of the core and there are two smaller sand layers below it, at 40-45 cm, and at 223-230 cm (Figure 4.14). The rest of the core has white gypsum, red/black peat, and green bands of clay (Figure

4.12.C).

Core ALEJ 103 was extracted 50 m from the western lake shore. Ten sand layers (Figure 4.15) were identified at: 1-7 cm, 16-26 cm, 34-42 cm, 76-90 cm, 110-122 cm, 150-160 cm, 190-203 cm, 240-255 cm, 317-330 cm, and 343-346 cm. As in the cases of cores ALEJ 100 and ALEJ 101, there is a layer of sand on the top indicating a more recent overwash event. This could be Hurricane Emily, a Category 3 storm in 1987, which was the last hurricane to make landfall in this area.

In a study done by Desjardins in 2007, two samples obtained from the proxy event layers were dated: one at 1057-794 CAL BP and the second one at 1147-958 CAL BP. ALEJ 100 and ALEJ 101 both exhibit multiple layers of sand indicating such overwash events in the past. Radiocarbon dating of the event layers in these cores will assist in establishing a timeline of the overwash events and correlate them with the event layers found in the cores studied by Desjardins (2007) earlier.

4.5.2.2 Fish Lake

Fish Lake is a small, shallow lake east of Lake Alejandro (Figure 4.11.B). On the south of the lake there is a high energy beach with a 1.5 m beach ridge with cobblestones and pieces of coral in front of the lake (Figure 4.16. B).

The coring site is 25 m from the high tide mark. One core was extracted from this lake measuring 135 cm. The top 52 cm of this core is clay. Five sand layers were found below this clay layer indicating hurricane events in the past. These sand layers were at the following depths: 54-58 cm, 69-74 cm, 85-88 cm, 94-106 cm, and 120-135 cm (Figure 4.17). The sand layers at 94-106 cm and at 120-135 cm are thicker than the rest which may mean higher sensitivity of the lake in the past or occurrence of more intense storms bringing a larger sand load.

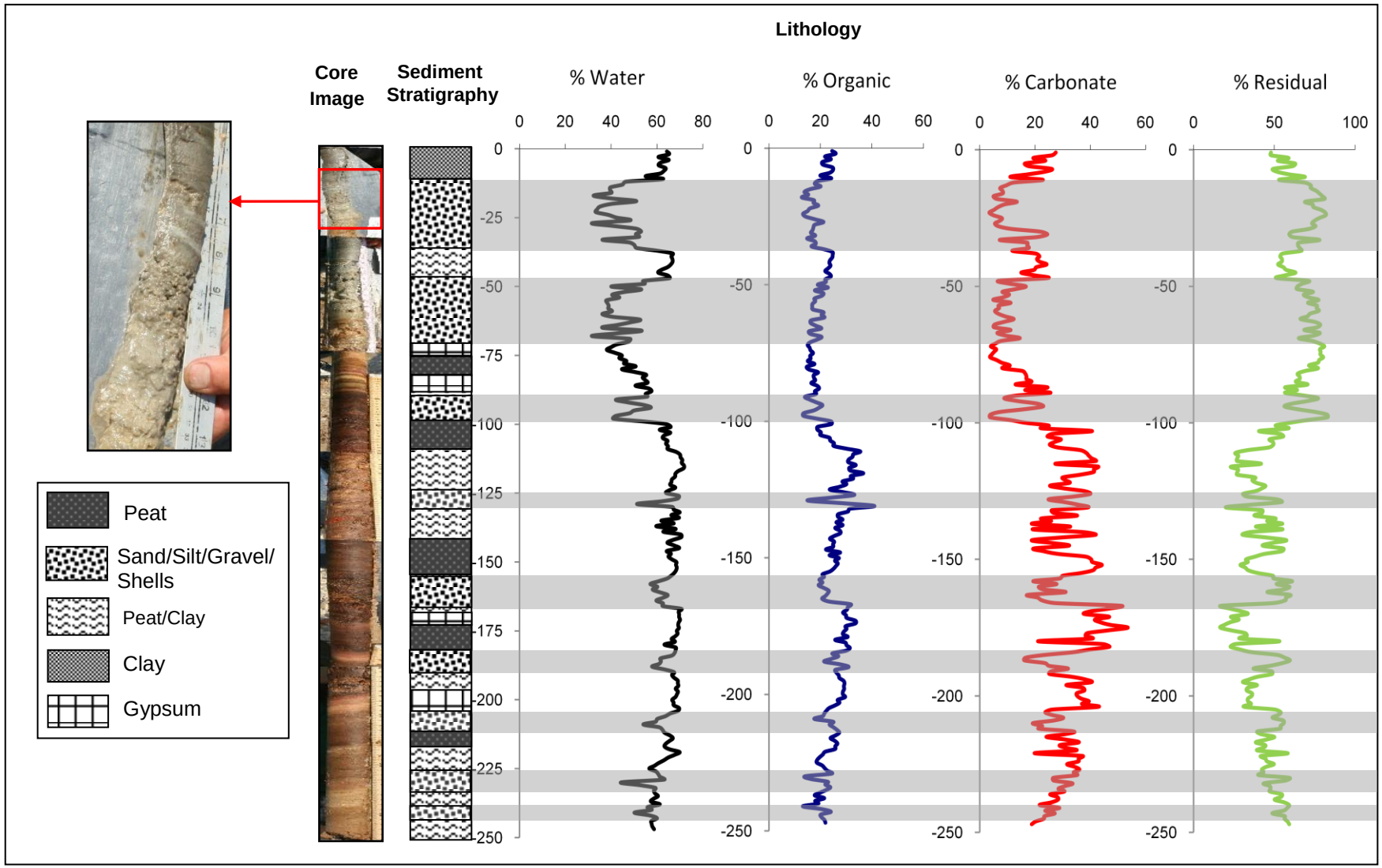

Figure 4.13: Loss-on-ignition and sedimentological analysis of Lake Alejandro core ALEJ 100.

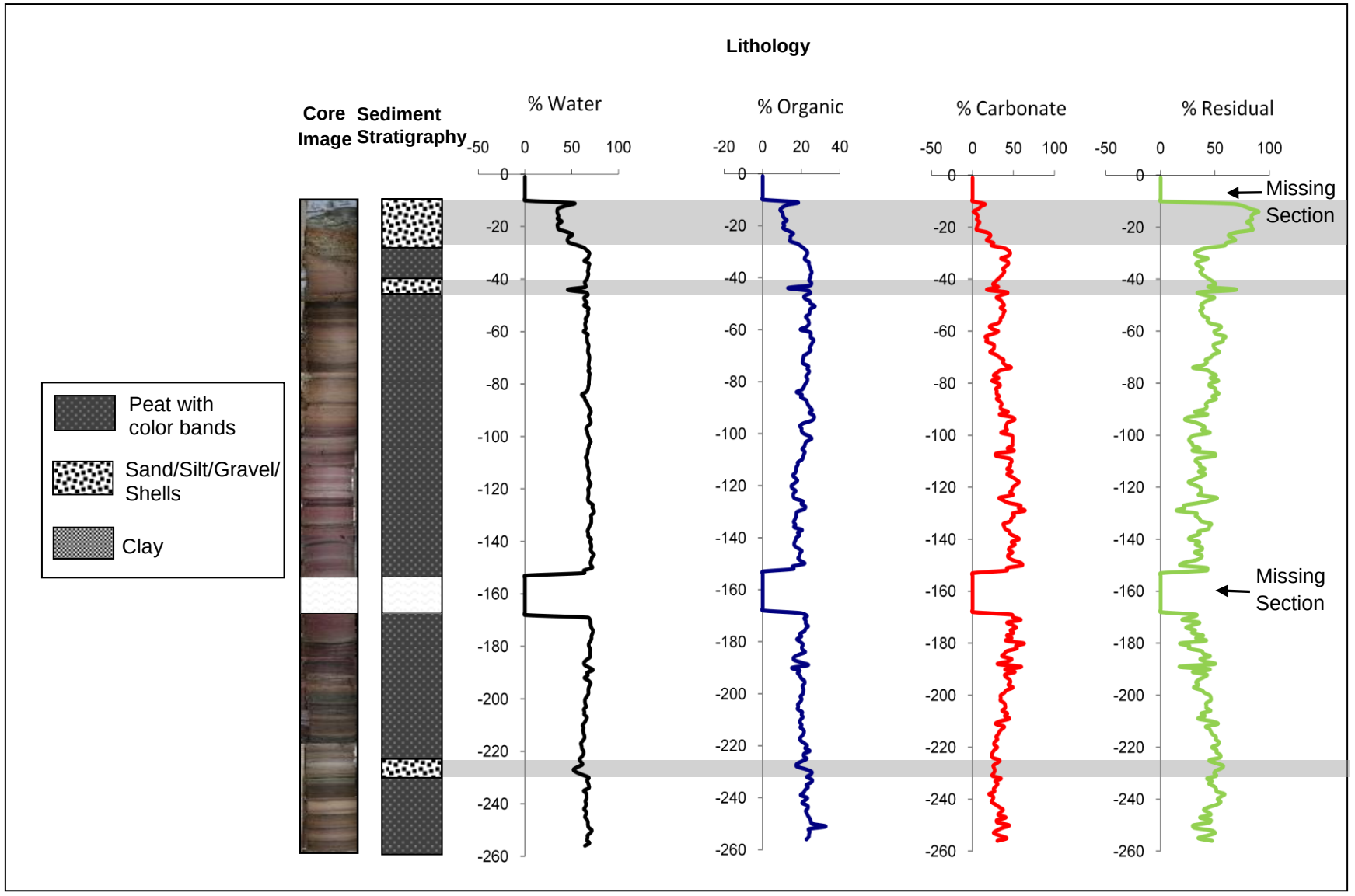

Figure 4.14: Loss-on-ignition and sedimentological analysis of Lake Alejandro core ALEJ 101.

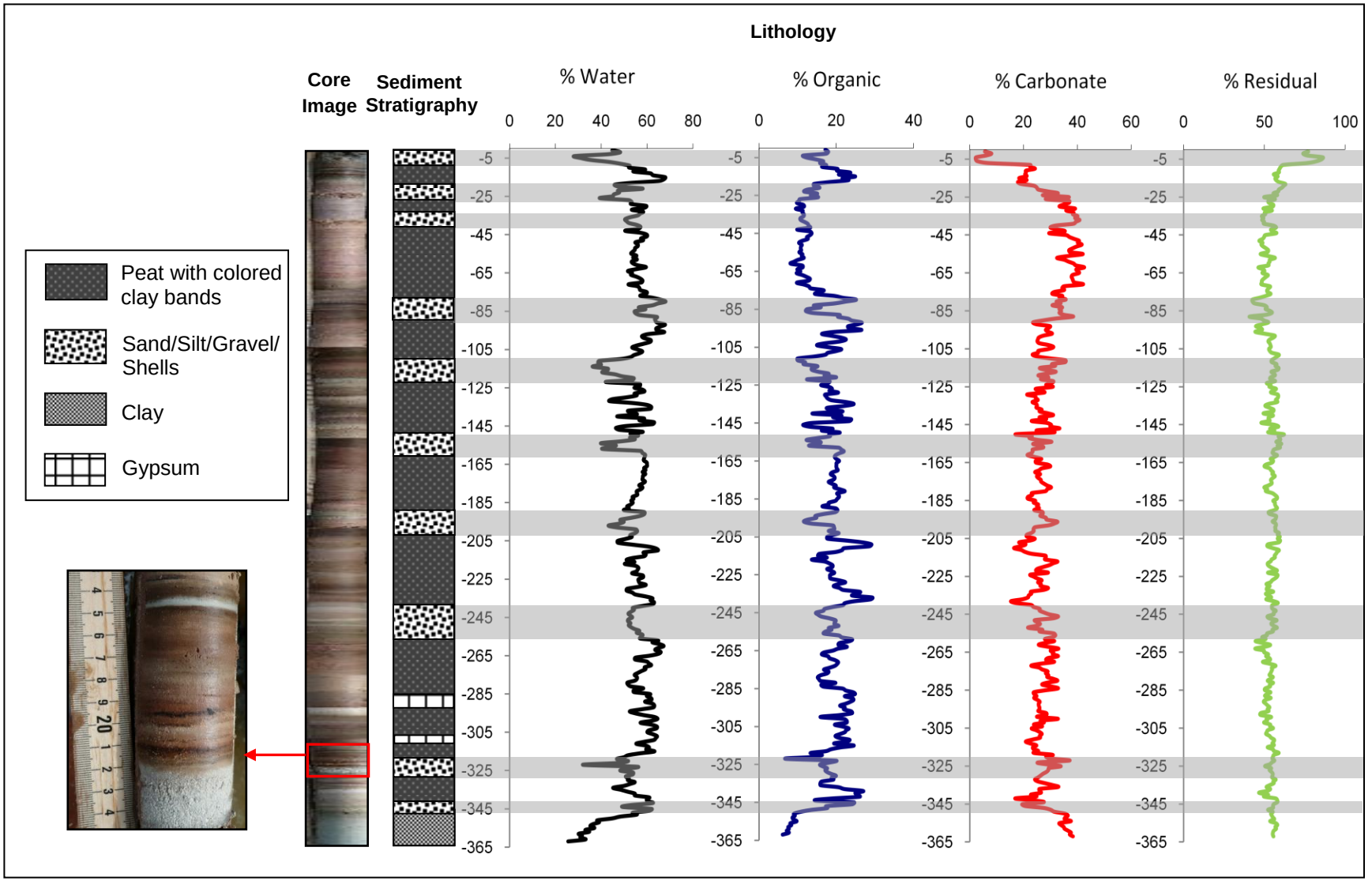

Figure 4.15: Loss-on-ignition and sedimentological analysis of Lake Alejandro core ALEJ 103.

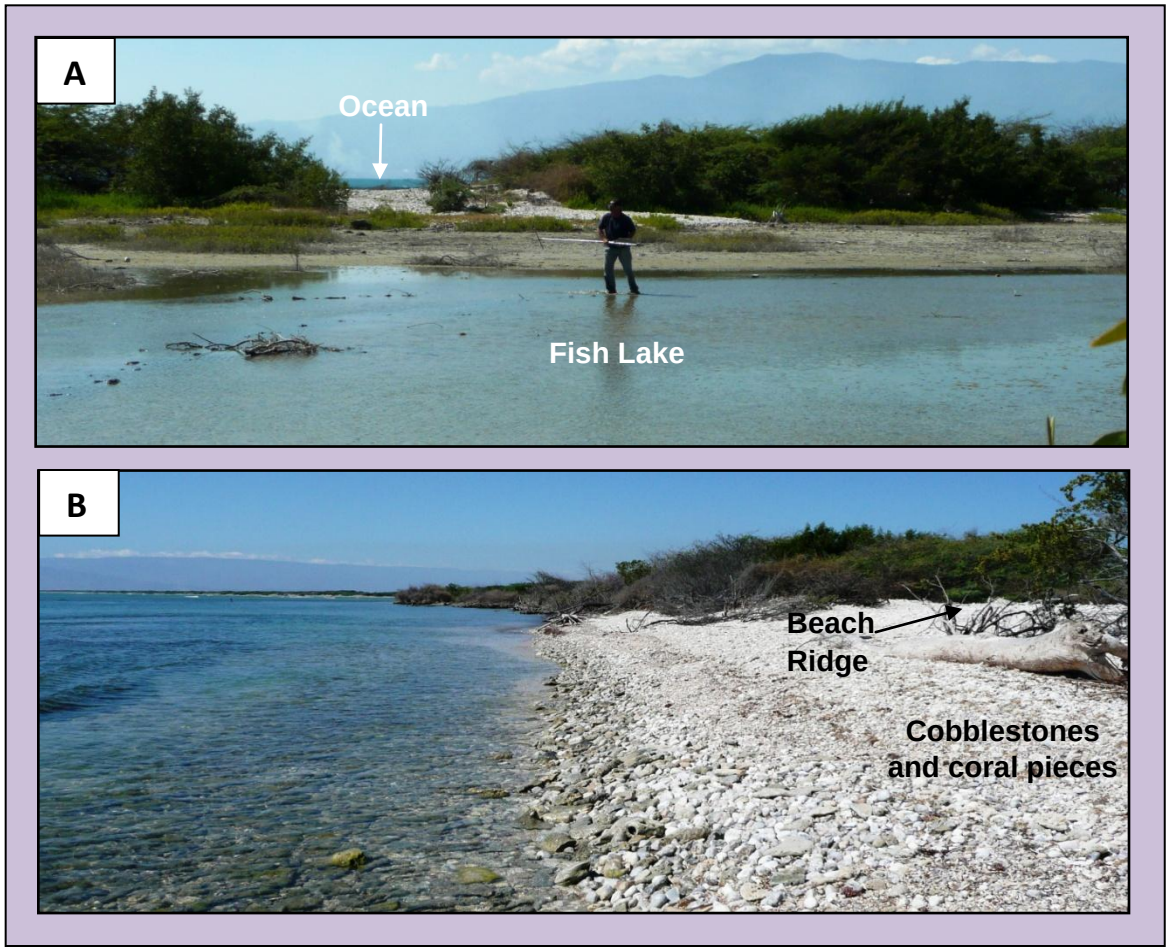

Figure 4.16: (A) Fish Lake. (B) High energy beach with a 1.5 m high beach ridge.

4.5.3 Alijibe

The Alijibe site is in a mangrove/salt pan area on the southern tip of a peninsula which is part of the vast carbonate (Coralina/Coralstone) area (Figure 4.18). There is a narrow beach in front of the site and mangroves forming a barrier next to the sea (Figure 4.18). A salt pan is present 20 m inland (Figure 4.19) which has shallow bodies of water.

Five cores were extracted from the Alijibe site ranging from 35 cm to 180 cm. The first core, ALI 1, was obtained close to the edge of the mangroves near the sea (Figure 4.18). This

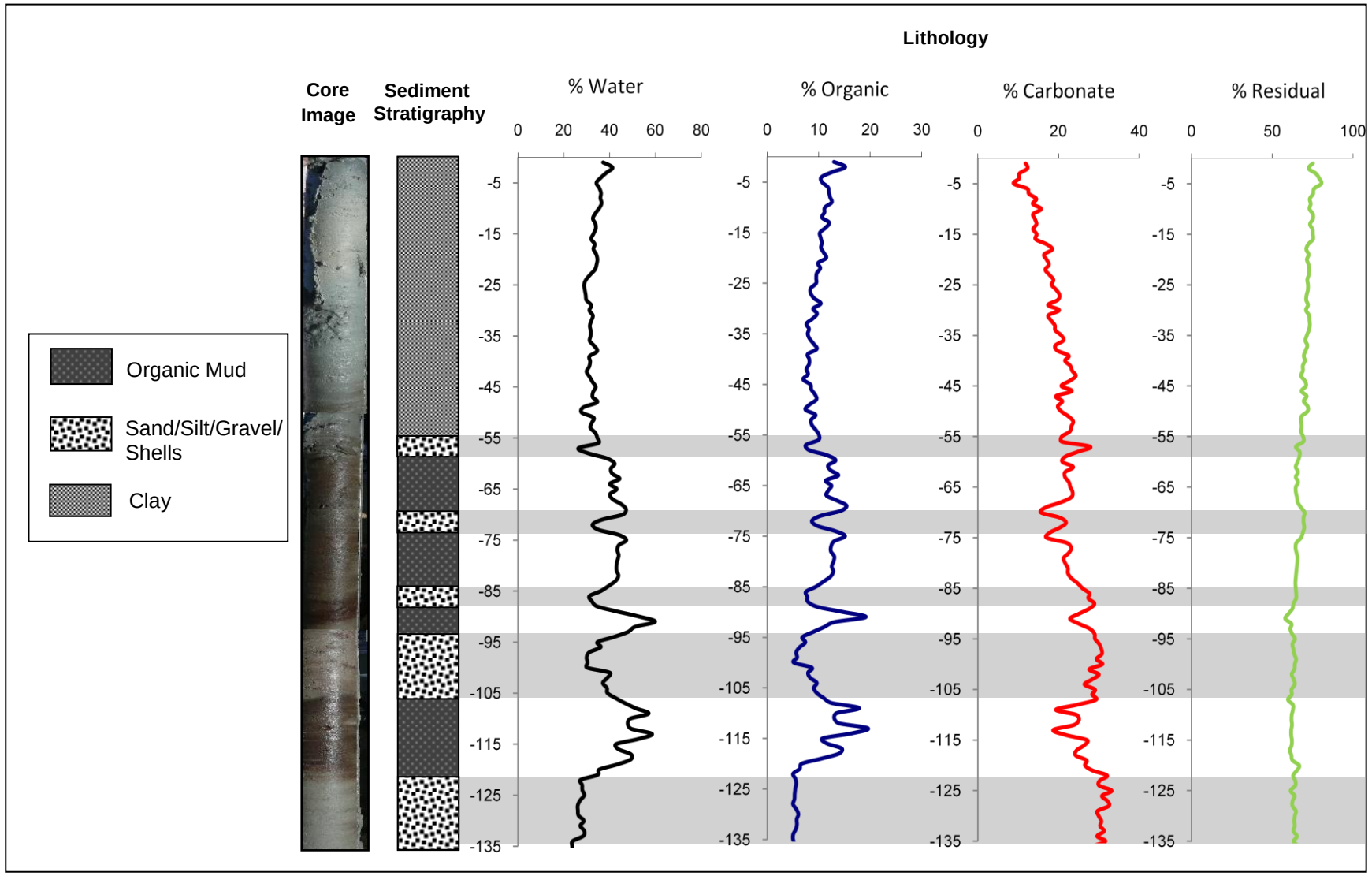

Figure 4.17: Loss-on-ignition and sedimentological analysis of Fish Lake core FISH 1.

Figure 4.18: Alijibe coring site for cores ALIJ 1-5.

core is 35 cm long and contained mostly peat mixed with some sand and gravel. Bottom of the core has a 3 cm layer of sand mixed with gravel from the ocean floor (Figure 4.20). ALI 2 is a 140 cm long core and was obtained 45 m from the sea. This core consists of clay and peat and in some sections, a peat with layers of clay (Figure 4.21). Core ALI 3 was taken 30 m from the sea and is a 95 cm long core. Similar to ALI 2, this core also contained clay, peat, and peat with layers of clay (Figure 4.22).

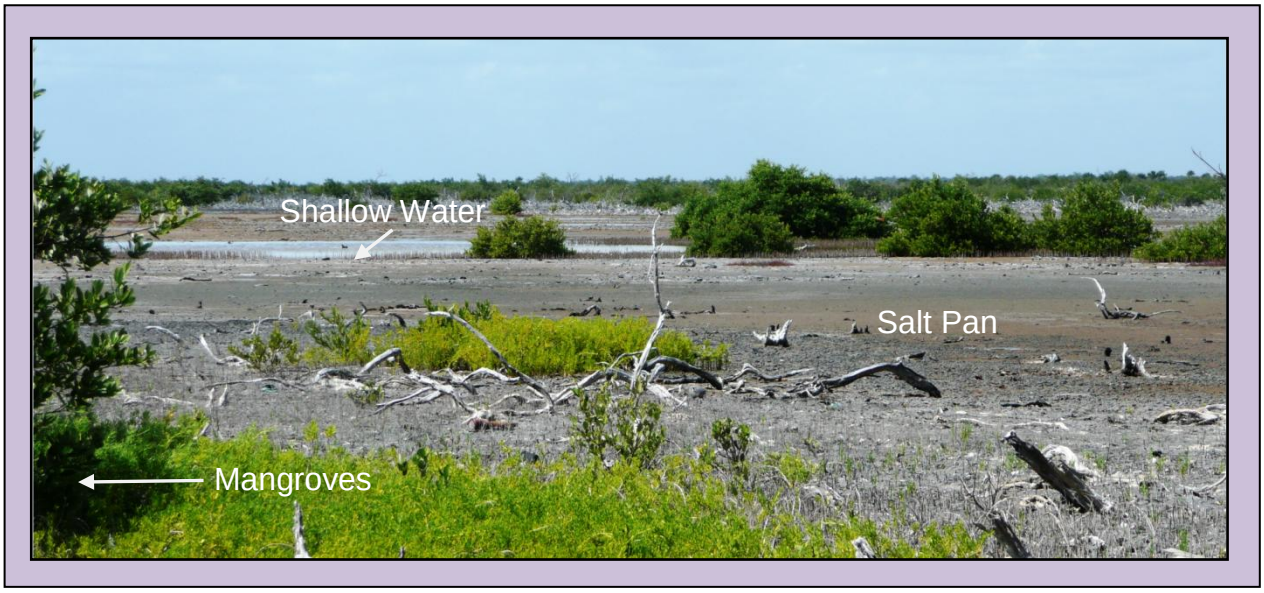

Figure 4.19: Alijibe site photo showing mangroves, salt pan, and shallow water bodies.

ALI 4 was extracted 20 m from the shore and is 105 cm long. This core had two layers of sand and the rest was a peat with layers of clay. The first layer is at 15-25 cm and the second at 48-56 cm (Figure 4.23). The fifth core, ALI 5, is the longest and measures 180 cm. This core consists of clay with some sections of peat (Figure 4.24).

4.5.4 Mala Punta

Mala Punta is a shallow lake located behind a 2-3 m high beach ridge north of Alijibe on the far eastern coast of the island (Figure 4.25). The salinity of the lake is 16.4 ppt.

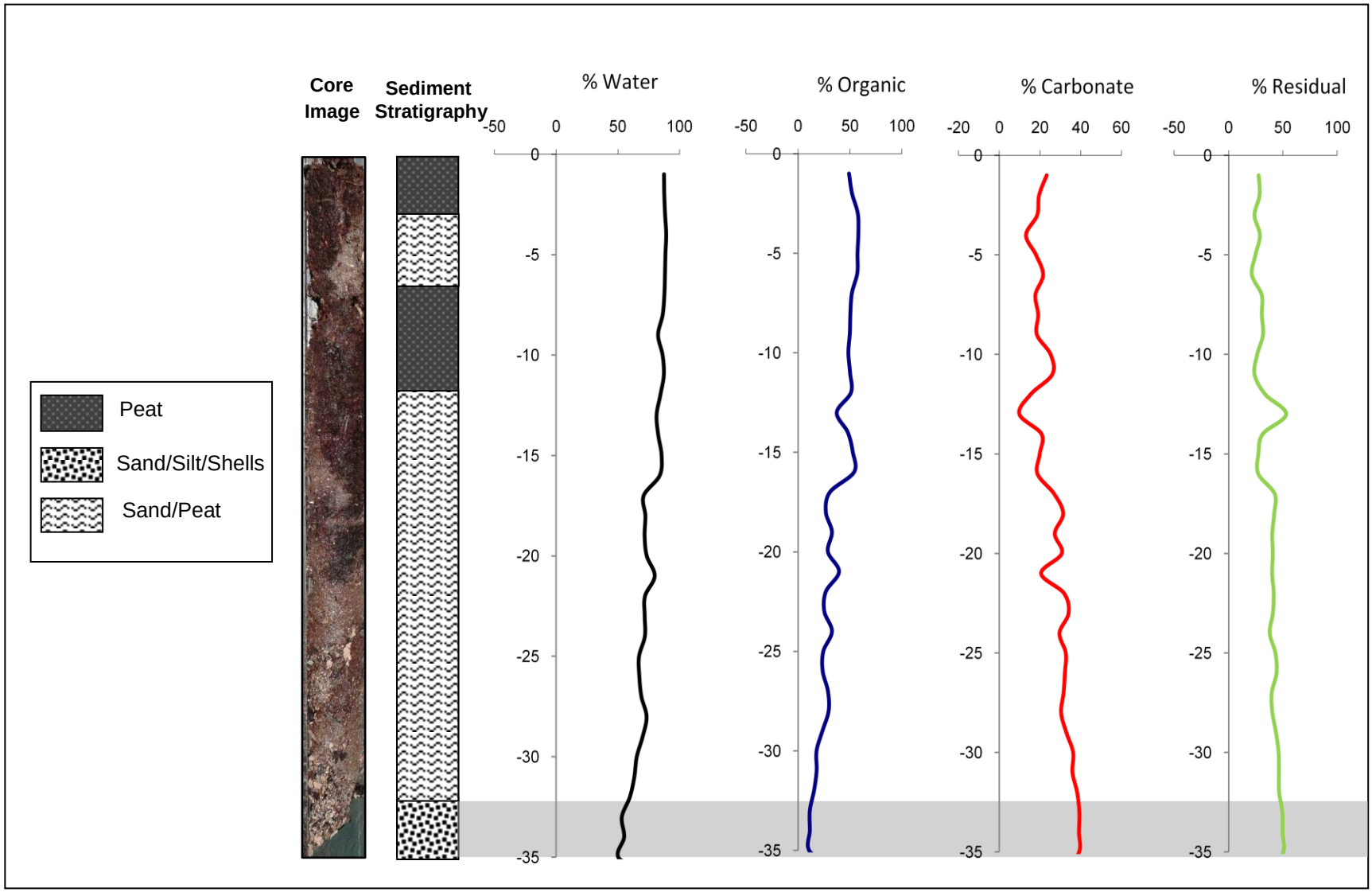

Figure 4.20: Loss-on-ignition and sedimentological analysis of Alijibe core ALI 1.

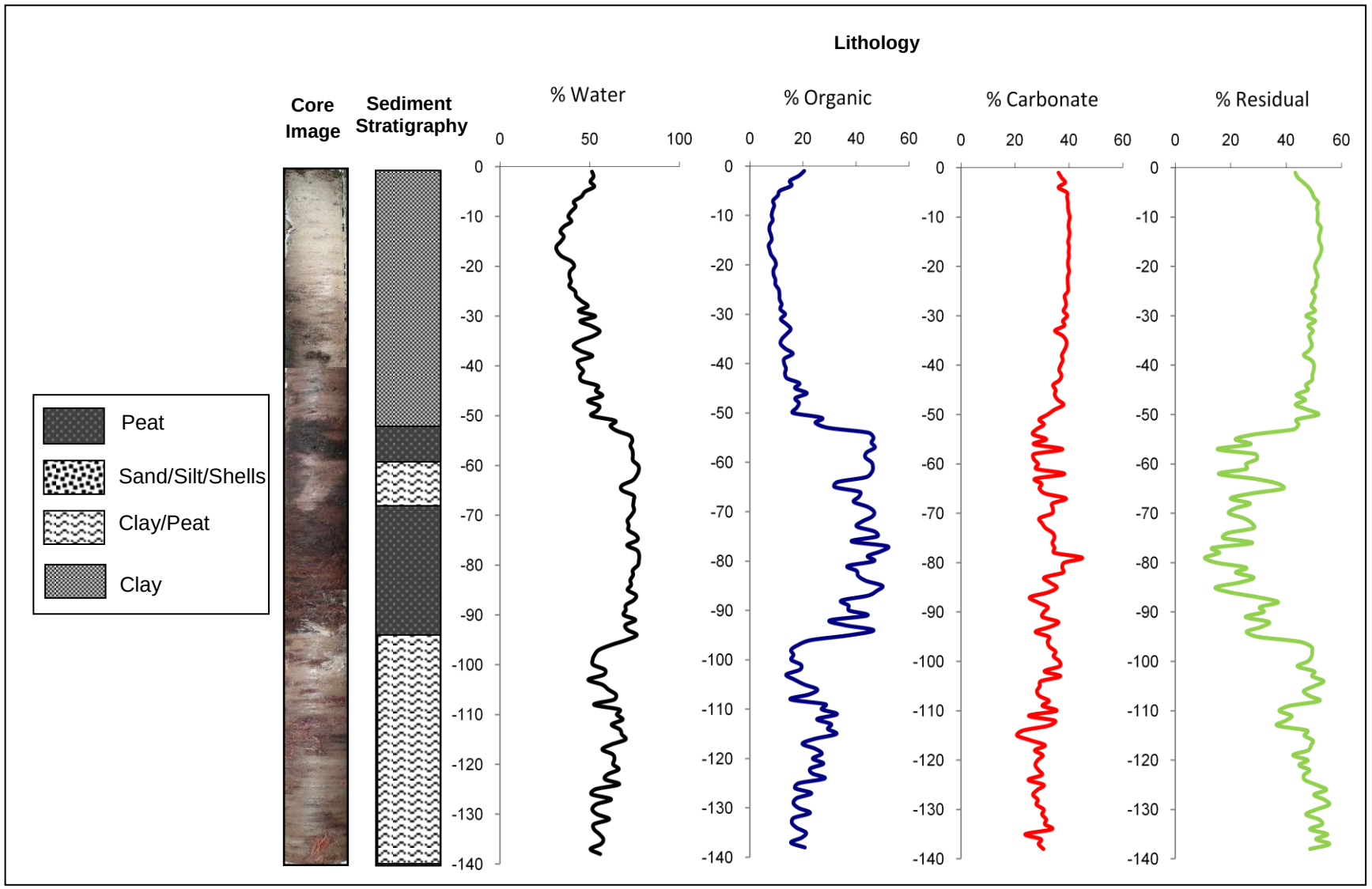

Figure 4.21: Loss-on-ignition and sedimentological analysis of Alijibe core ALI 2.

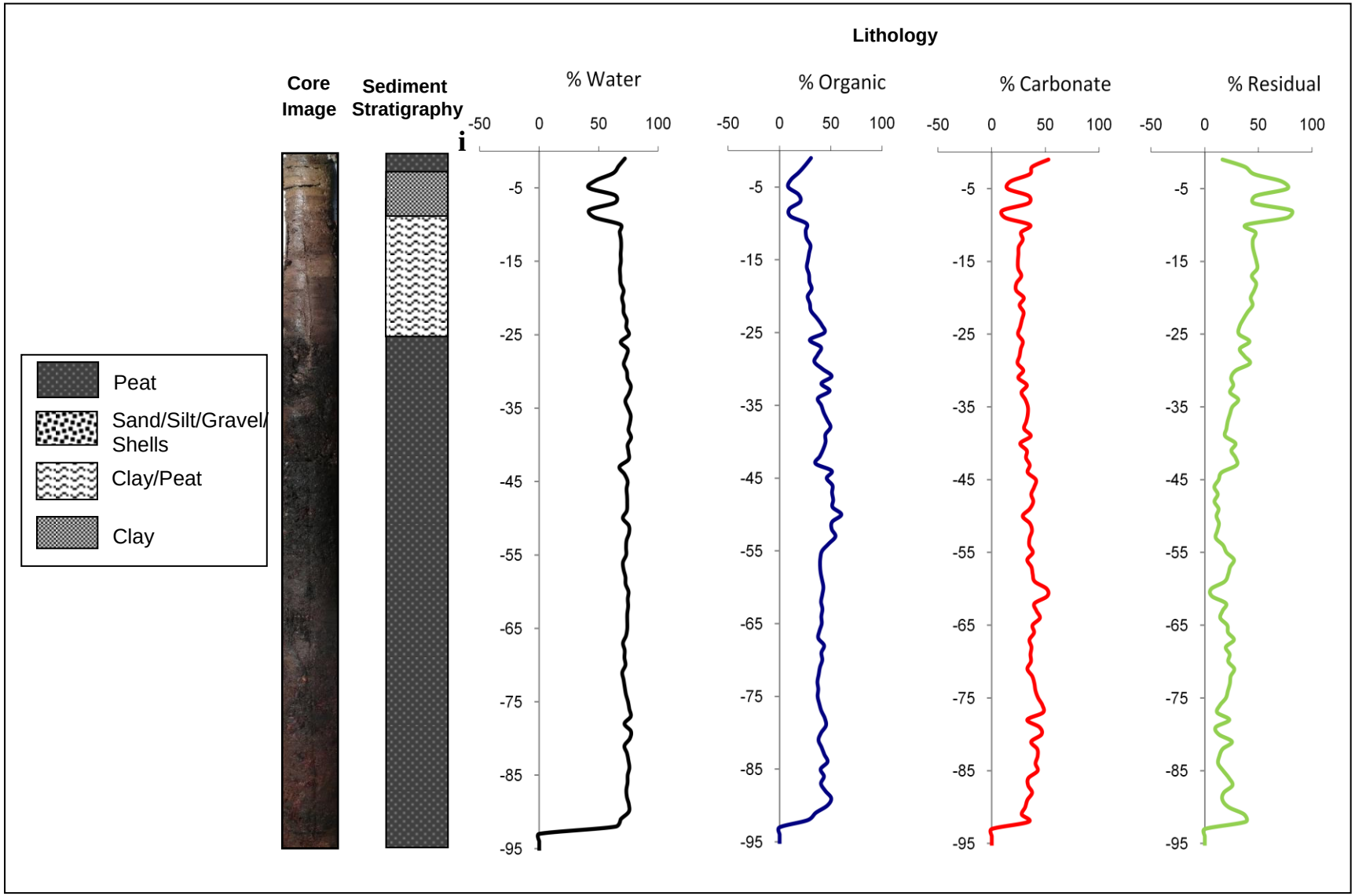

Figure 4.22: Loss-on-ignition and sedimentological analysis of Alijibe core ALI 3.

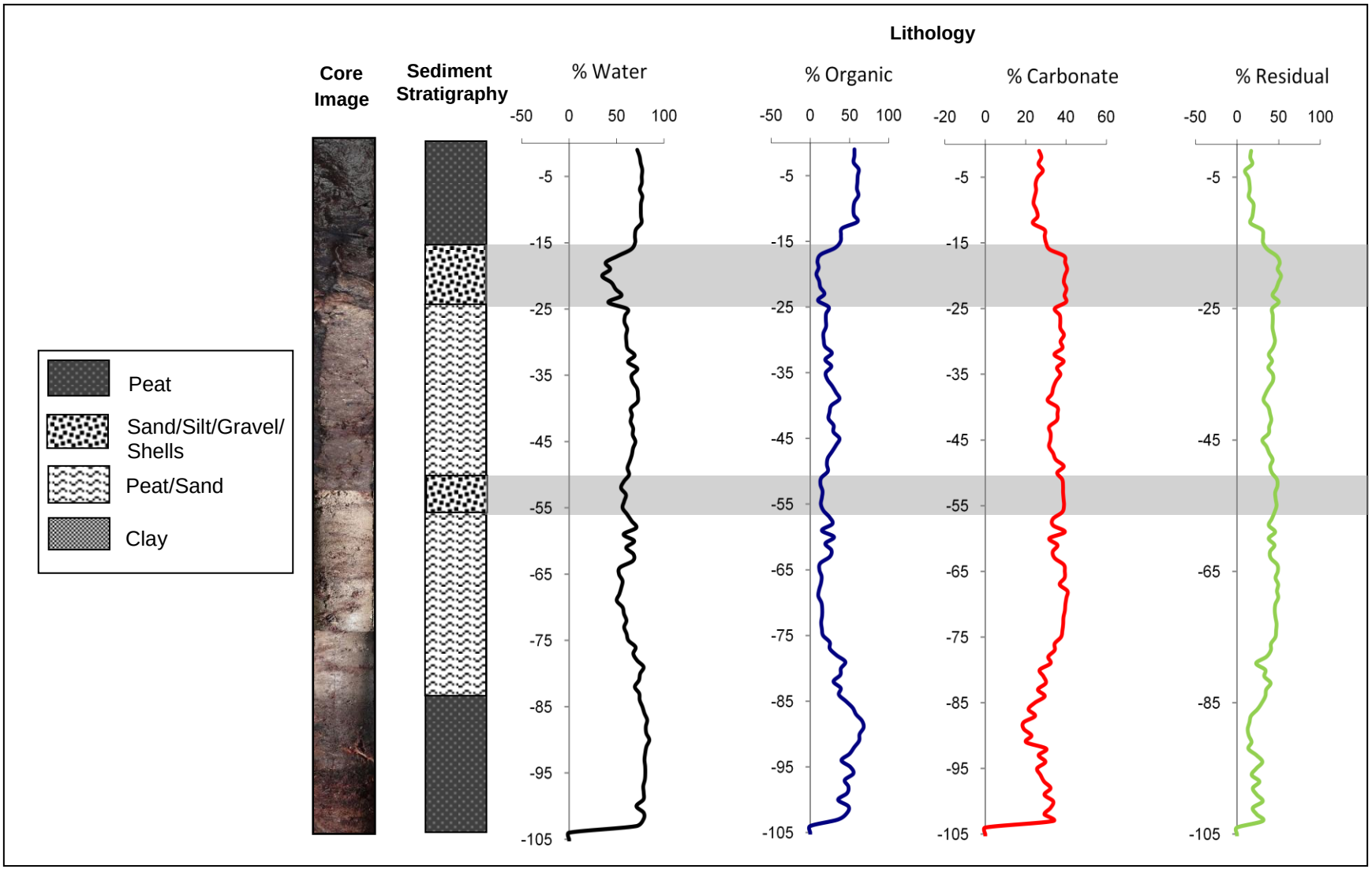

Figure 4.23: Loss-on-ignition and sedimentological analysis of Alijibe core ALI 4.

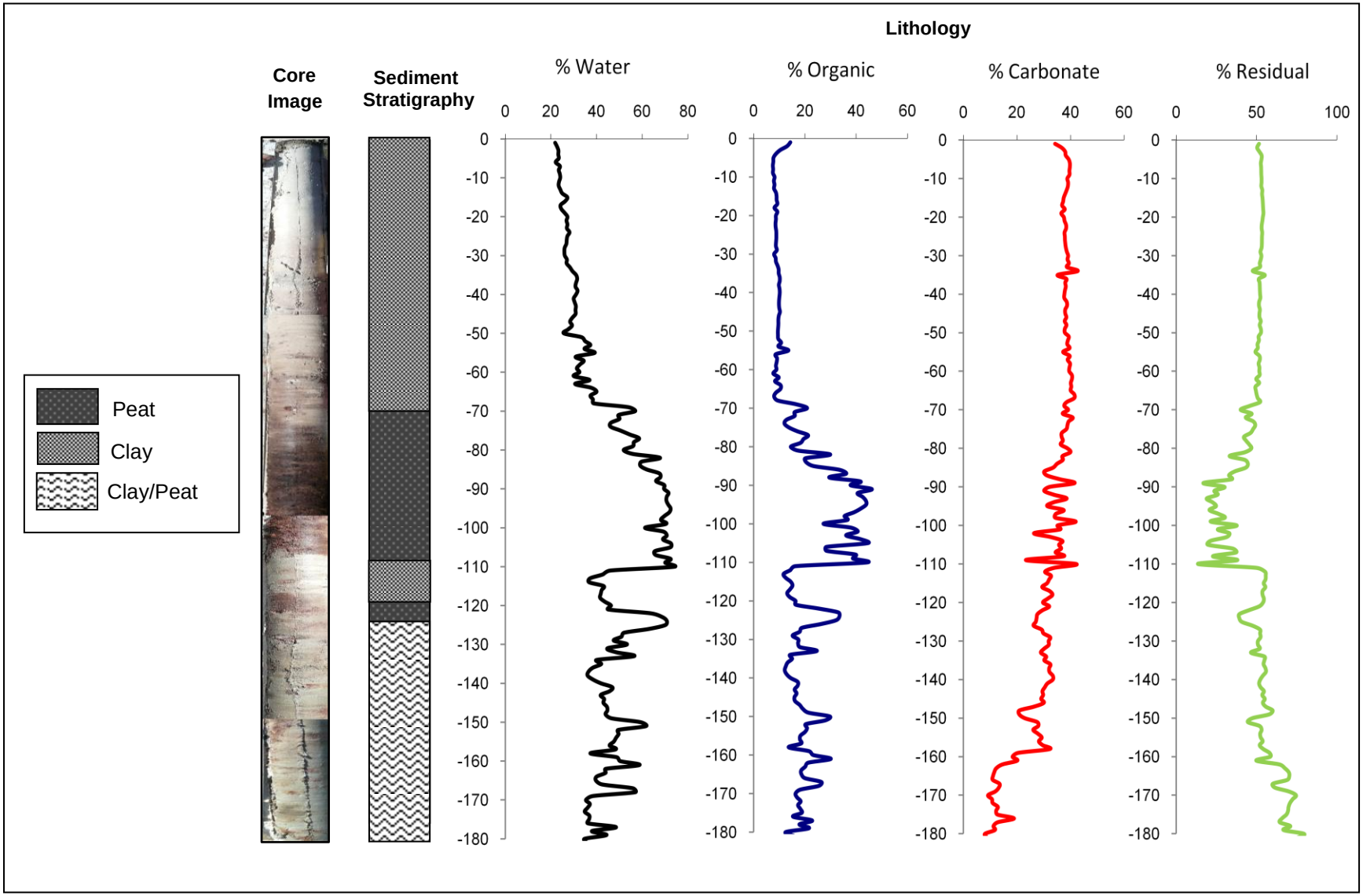

Figure 4.24: Loss-on-ignition and sedimentological analysis of Alijibe core ALI 5.

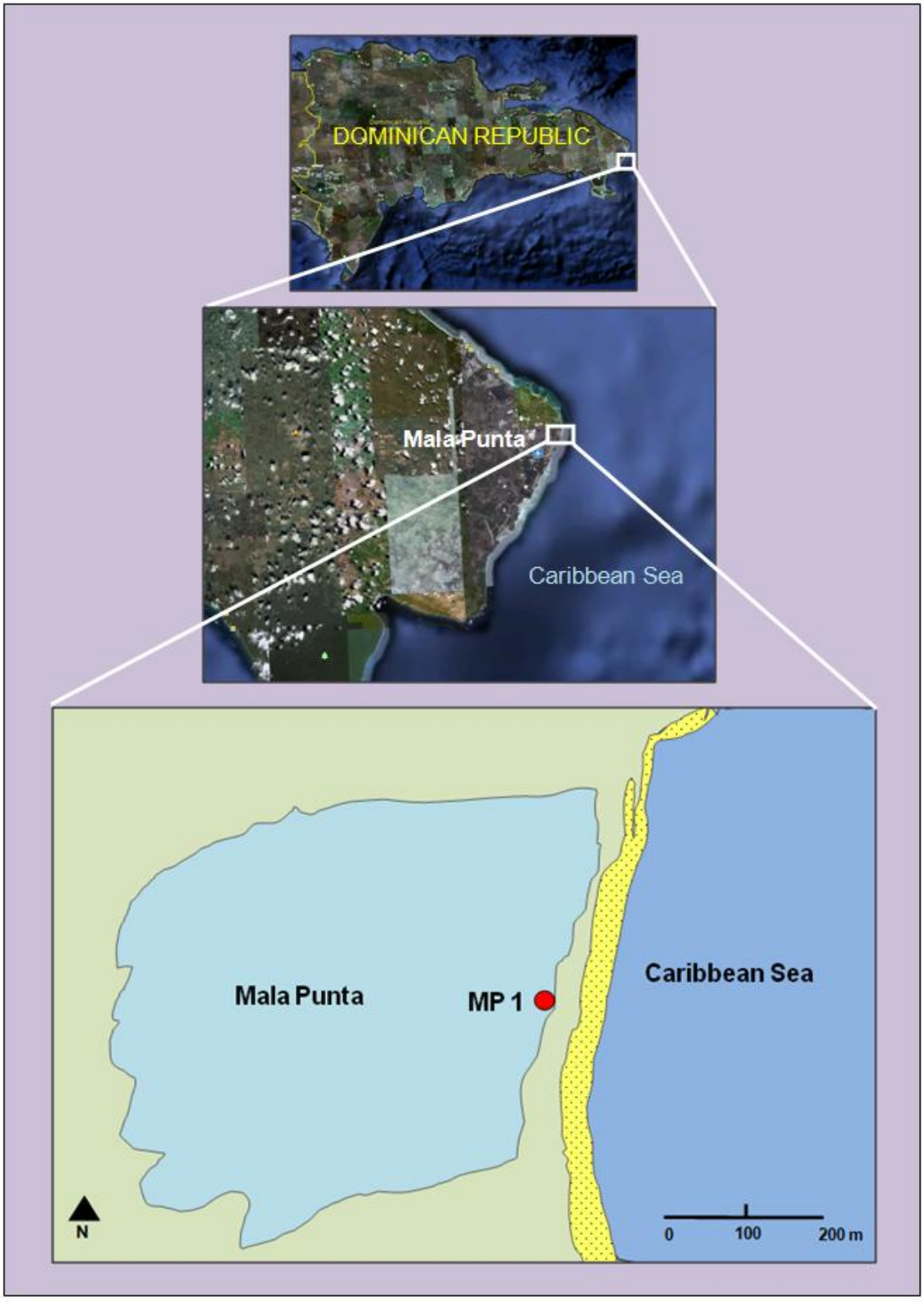

Figure 4.25: Mala Punta coring site.

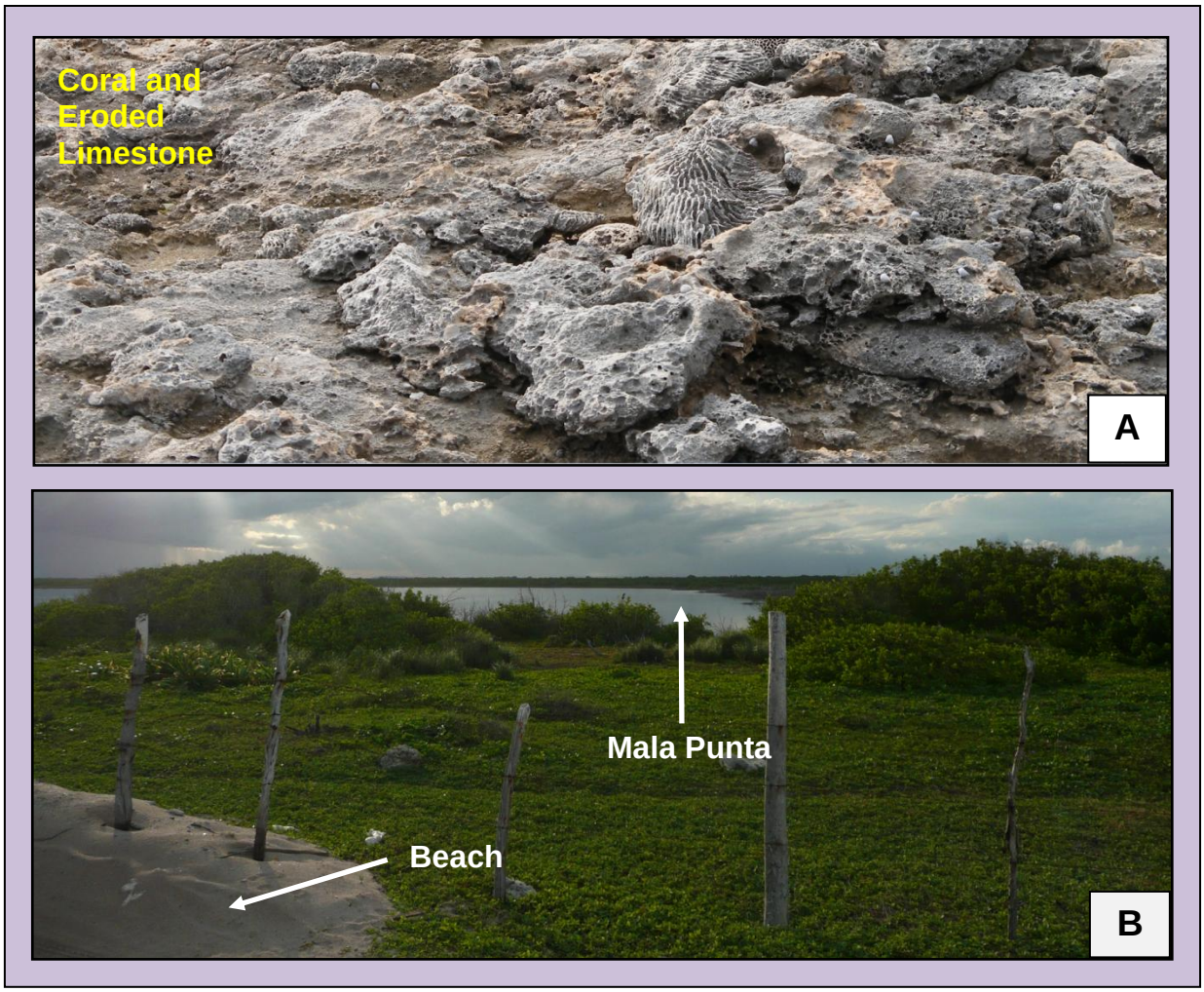

Figure 4.26: (A) Pieces of coral and eroded lime stone on beach. (B) Mala Punta coring site.

The beach close to the site has eroded limestone and pieces of coral due to high energy waves (Figure 4.26.A). The sandy ridge (that also serves as a road) between the ocean and the lake is stabilized by vegetation (Figure 4.26.B).

One core, MP 1, measuring 100 cm was extracted from Lake Mala Punta. This core was taken 80 m from the shore line (Figure 4.25). Sediment stratigraphy and loss-on-ignition profile shows that the core contains mainly clay with some peat in the bottom half (Figure 4.27).

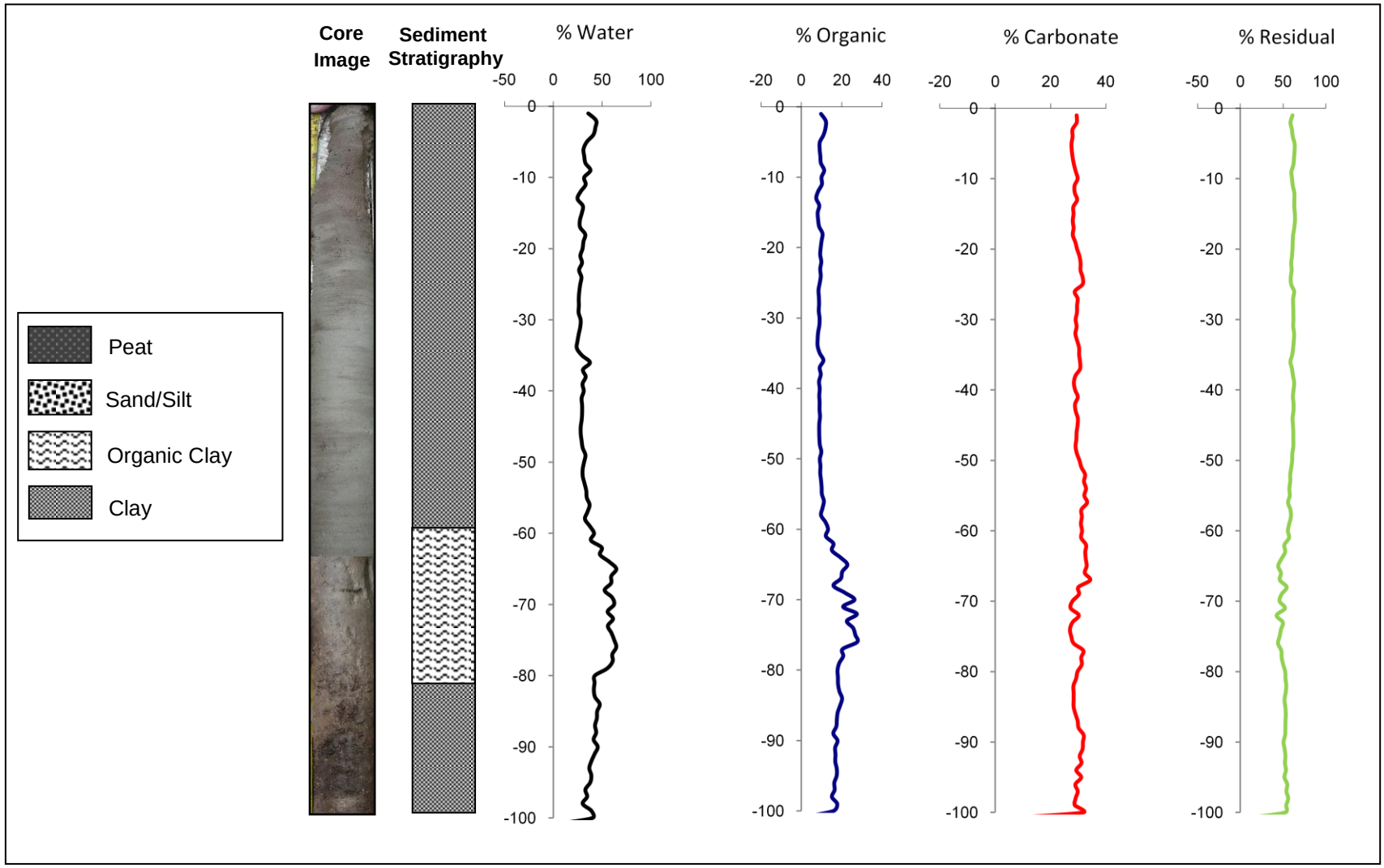

Figure 4.27: Loss-on-ignition and sedimentological analysis of Lake Mala Punta core MP 1.

4.5.5 Yuna River

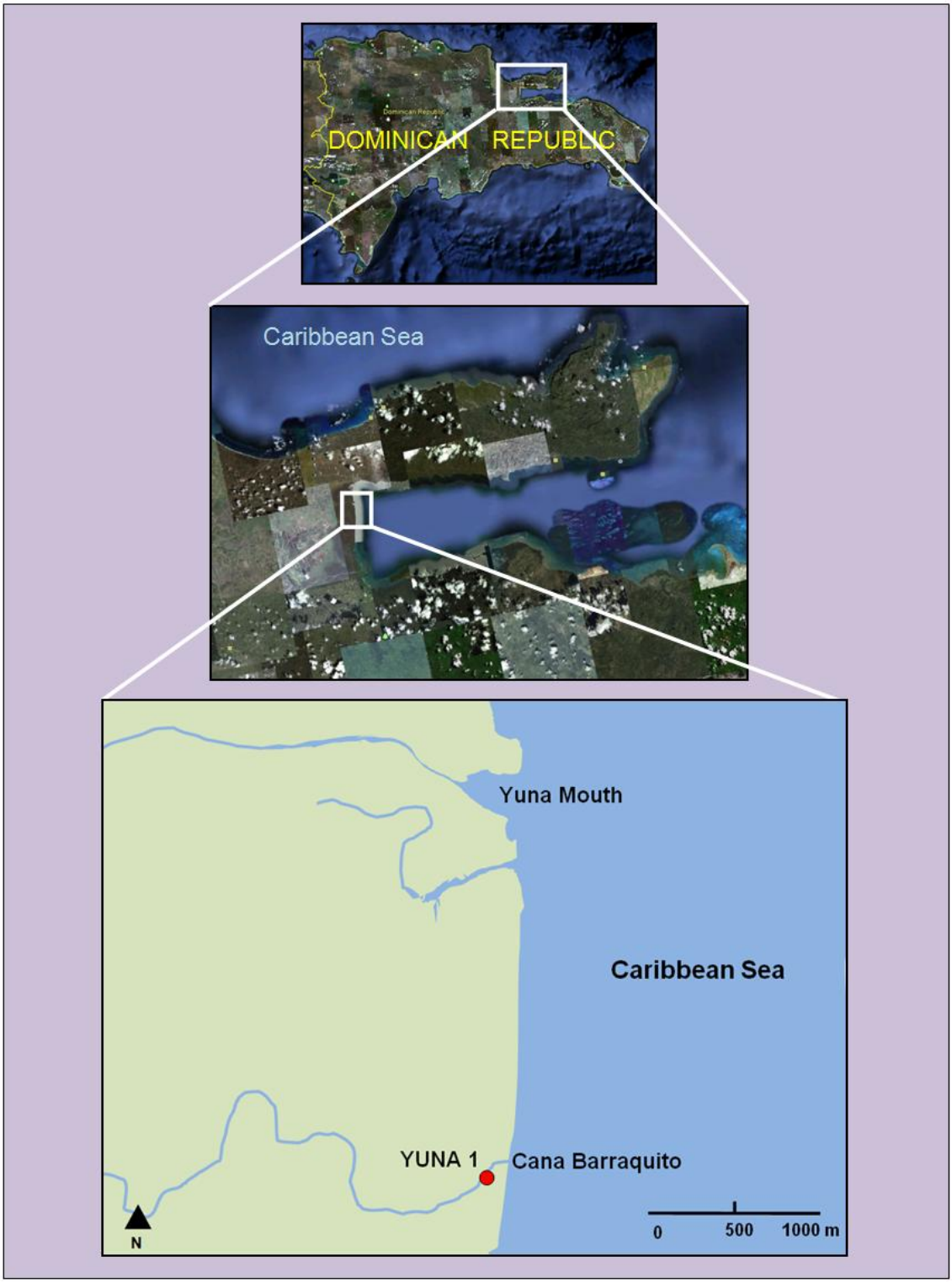

Figure 4.28: Yuna River coring site.

Yuna River is the second longest river in the Dominican Republic. It starts at the mountains of Cordillera Central and drains in the Samana bay, in the north-eastern part of the island. Yuna core was taken inland in a shorter distributary of Yuna, Cana Barraquito (Figure 4.28). This is a narrow channel (~10 m), 2.5 km south of the Yuna Mouth. This location has mainly red mangroves (Figure 4.29).

Figure 4.29: Site photo showing Cana Barraquito channel with red mangroves.

YUNA 1 core is a 185 cm long core and was extracted 80 m inland from the mouth of Cana Barraquito. This core consists of clay and some peat at 55-75 cm. In the bottom there is a 9 cm thick layer of sand from 175-184 cm (Figure 4.30). Organic matter from this layer at 177 cm was sent for radiocarbon dating to NOSAMS. Results show that the radiocarbon age of the basal layer is 95+/-30 ^{14}C BP (calendar age of 145-20 cal yr BP). However this is not a reliable date because it is less than 200 years (Liu, 2004) and therefore was not used for further analysis.

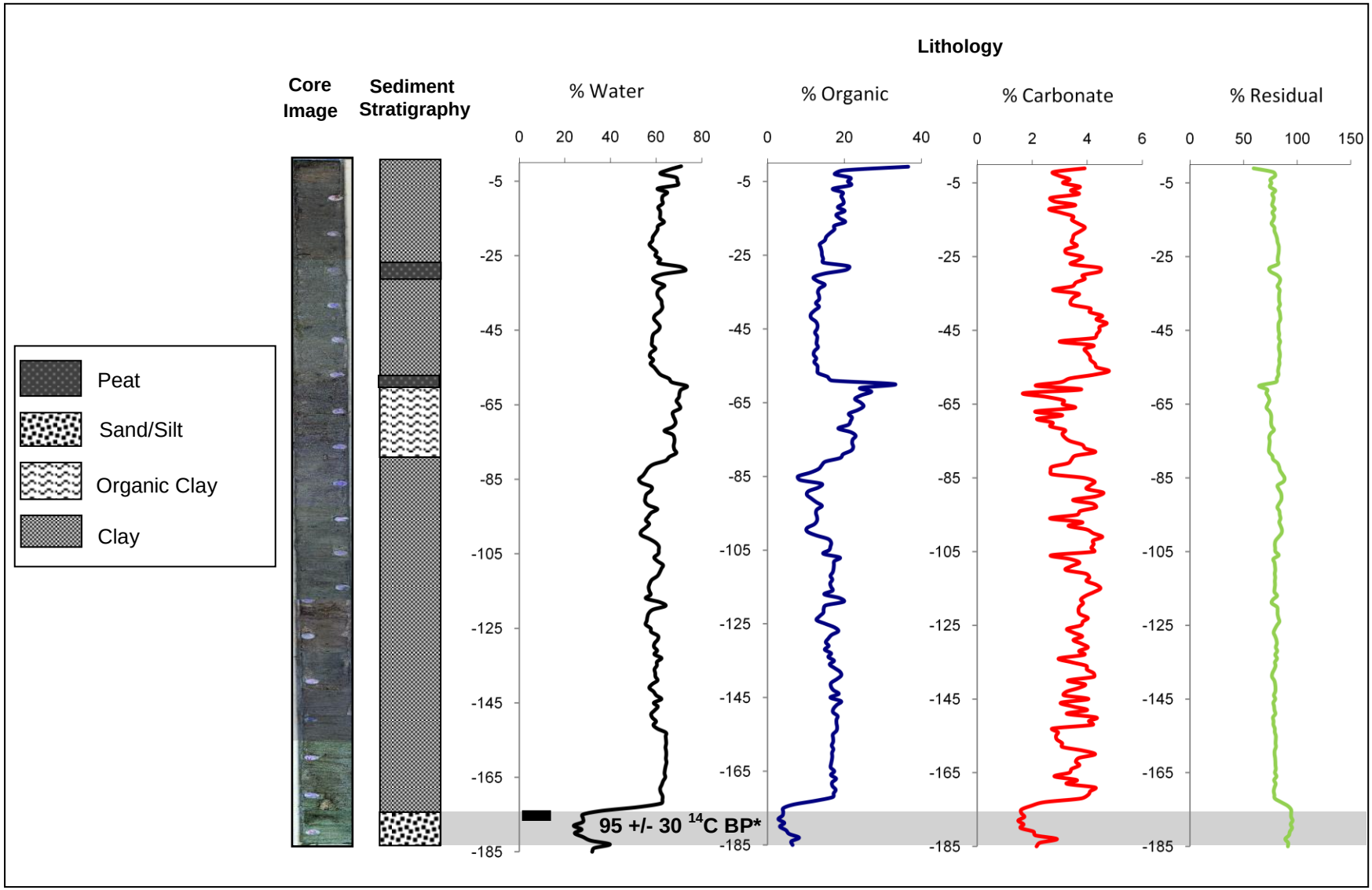

Figure 4.30: Loss-on-ignition and sedimentological analysis of River Yuna core YUNA 1.

4.5.6 Lake Limon

Figure 4.31: Lake Limon coring sites.

Lake Limon is in a depression and close to the ocean (Figure 4.32.B). There is a small section of coral reef and a coconut grove in front of the lake (Figure 4.32.A). Presence of the coral reef suggests that the coastline has been stable in the past. All species (red, black, and white) of mangroves grow on the eastern side of the lake and a *Typha* marsh (Figure 4.32.C) is on the northwest corner (Figure 4.31).

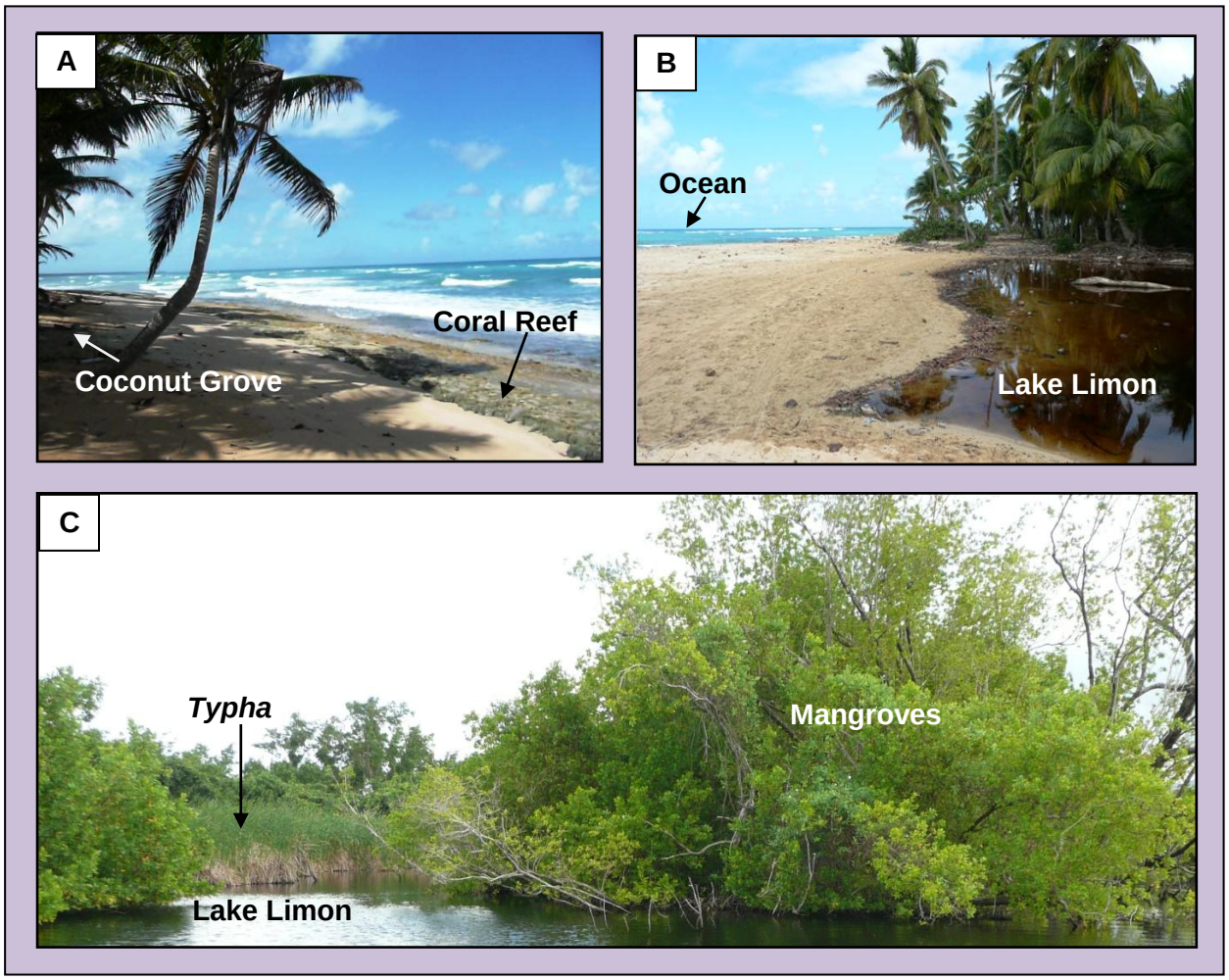

Figure 4.32: (A) Beach in front of Lake Limon is anchored by a coral reef. (B) Proximity of Lake Limon to the ocean.

Four cores were extracted from this site. Core LIM 1, which was obtained 55 m inland from the sea, is a 90 cm long core (Figure 4.34). There are 5 distinct sand layers present in it and the rest is mostly peat. The first layer is from the top of the core (0 cm) until a depth of 23 cm. The second layer is at 32-41 cm, third at 44-48 cm, fourth at 53-58 cm, and fifth at 84-89 cm

depth. Organic matter from just below the fourth sand layer at 58 cm was sent for AMS radiocarbon dating to Beta Analytic Dating Laboratory. Results show that the event has a conventional radiocarbon age of 1,610 +/- 40 which is calibrated to the calendar age of 1,570 cal yr BP (Table 4.2).

LIM 2 is a 175 cm long core and was obtained 50 m from the sea. There are 5 layers of sand present in this core and the rest is mainly peat. Similar to LIM 1, this core also has a layer of sand on the top at 0-14 cm (Figure 4.35). The second layer of sand is at 25-30 cm, third at 45-52 cm, fourth layer at 146-150 cm, and the fifth is at 115-125 cm. A bulk organic sample was collected from just below the sand layer at 50 cm and was sent for radiocarbon dating to Beta Analytic Dating Laboratory. The sample was dated at 1,690+/- 40 ^{14}C yr BP and calibrated to a calendar age of 1,640 cal yr BP (Table 4.2).

Core LIM 3 was extracted farthest from the shoreline at 130 m and this is a 95 cm core (Figure 4.36). This core has a 30 cm layer of clay on the top. In the first 10 cm the clay is organic clay. A section of the core at 60-75 cm has peat with bands of clay. A sand layer is present at 45-48 cm, and the bottom of the core has a layer of sand at 90-95 cm.

The last core obtained from Lake Limon was LIM 4. It is a 190 cm long core (Figure 4.37) which was extracted 35 m from the high tide line. This core is mostly peat with five layers of sand in it. The first is at 15-25 cm and is mixed with silt. The second layer is from 86 cm to 98 cm. An organic sample was collected from this layer at 90 cm and has a calibrated age of 925 cal yr BP (Table 4.2). The third layer is at 102-105 cm and the fourth layer is at 134-139 cm. At the bottom of LIM 4 is a 13 cm thick layer of sand from 176-188 cm. A sample was collected at 170 cm and dated at 2,330 cal yr BP (Table 4.2).

The radiocarbon dates were calibrated (Table 4.2) using CALIB 6.0 program (Stuiver and Reimer, 1993). Intercept dates were calculated for the purpose of using one date for probability

analysis using the calibration plot obtained from Calib 6.0.

Table 4.2: Calibration results for LIM 4 at 90 cm and 170 cm depth using Calib 6.0 (Reimer *et al.*, 2009).

Core	Depth (cm)	Laboratory Number	Material Dated	Radiocarbon Age BP	Cal BP (2σ)	Relative Area under Probability Distribution	Intercept Date
LIM 4	90	OS-78261	Plant/Wood	995 ± 30	818 - 797	0.08	
					870 - 821	0.25	
					964 - 898	**0.67**	**925 BP**
LIM 4	170	OS -78262	Plant/Wood	2270 ± 25	2169 -2160	0.02	
					2244 - 2177	0.429	
					2346 - 2301	**0.551**	**2,330 BP**
LIM 1	58	Beta-250731	Plant/Wood	1610 ± 40	**1540 - 1370**		**1,570 BP**
LIM 2	53	Beta-250732	Plant/Wood	1690 ± 40	**1701 - 1524**		**1,640 BP**

4.5.6.1 ^{137}Cs and ^{210}Pb Dating of LIM 4

Top 30 cm of the LIM 4 core was sampled at 3 cm intervals for ^{137}Cs and ^{210}Pb activity by using gamma spectrometry for ≥ 24 hours each. A ^{137} Cs peak was found at 10 cm depth (Figure 4.33) that indicated deposition of sediment at this depth in 1963.

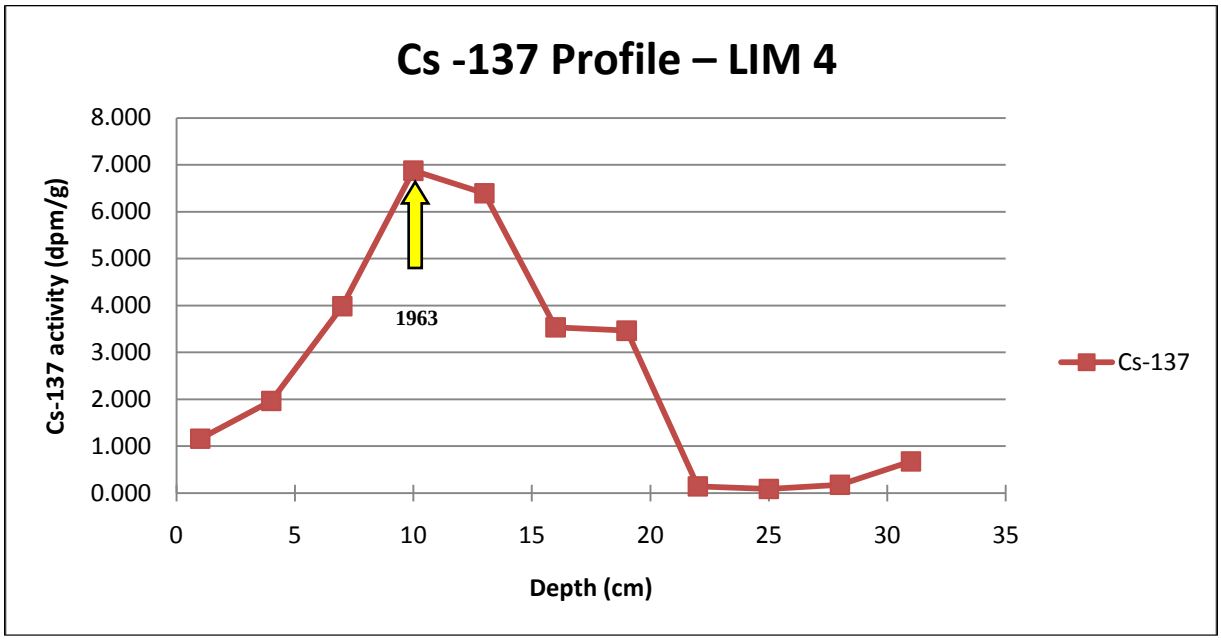

Figure 4.33: ^{137}Cs activity versus depth plot.

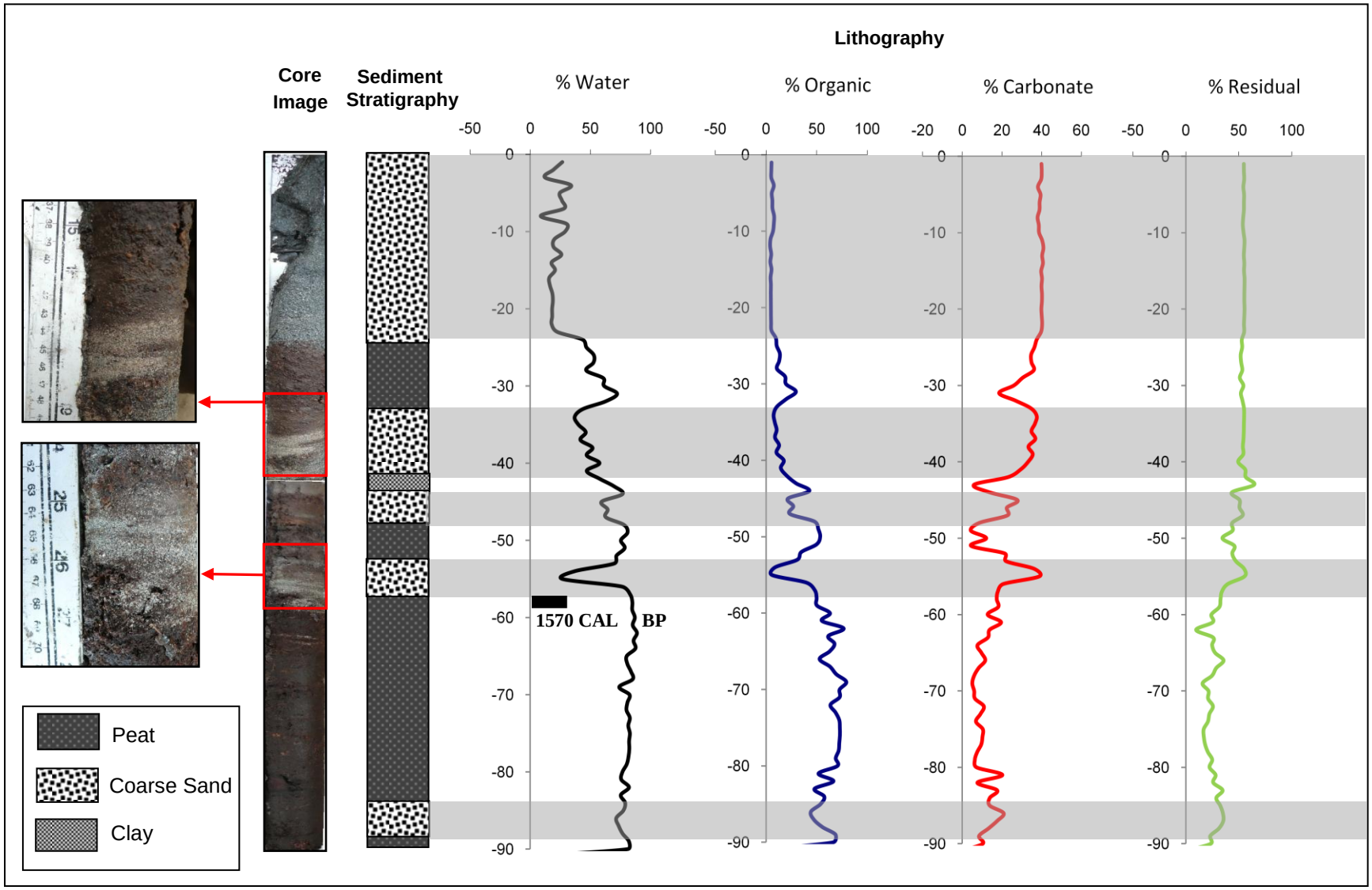

Figure 4.34: Loss-on-ignition and sedimentological analysis of Lake Limon core LIM 1.

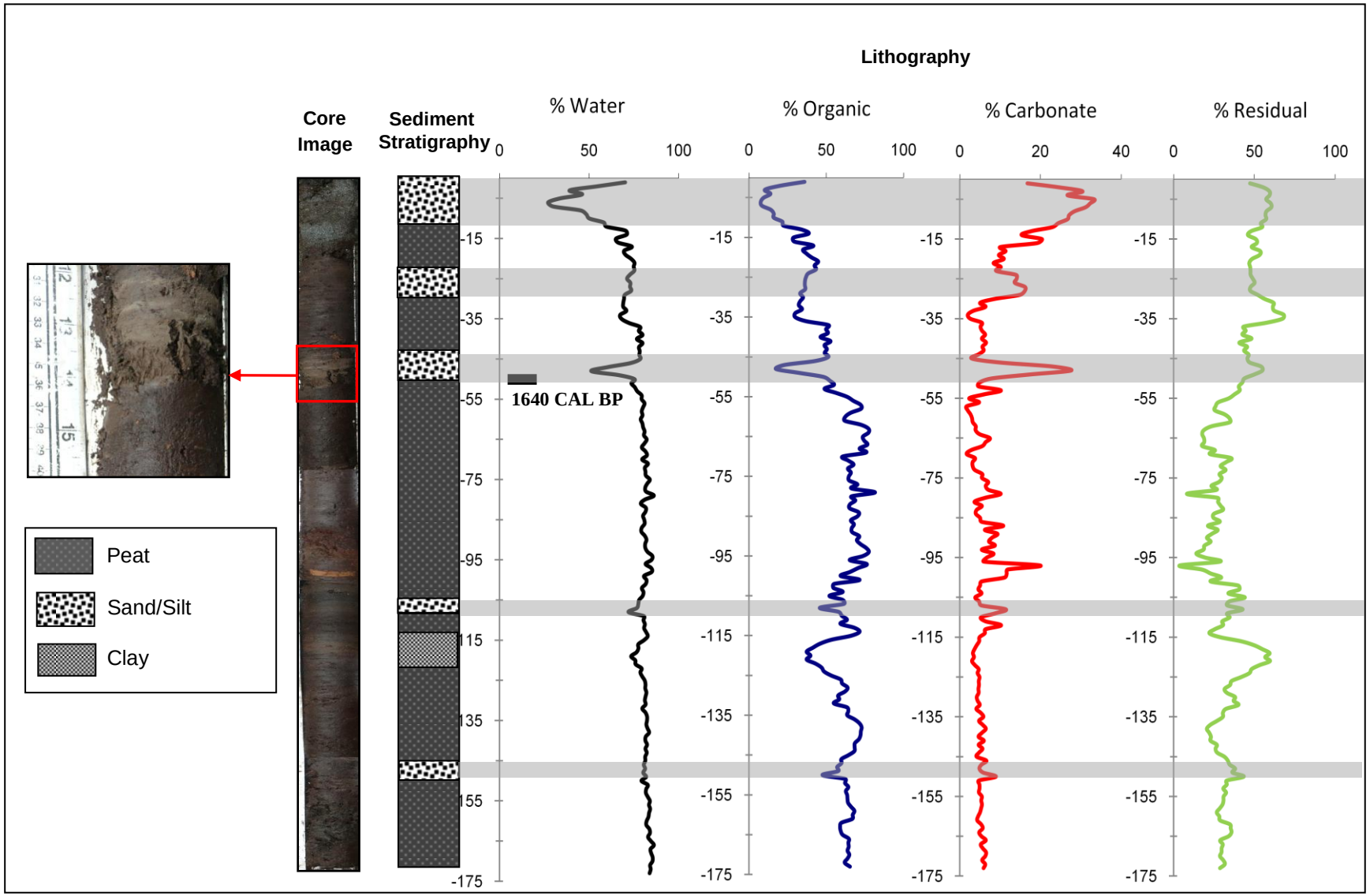

Figure 4.35: Loss-on-ignition and sedimentological analysis for Lake Limon core LIM 2.

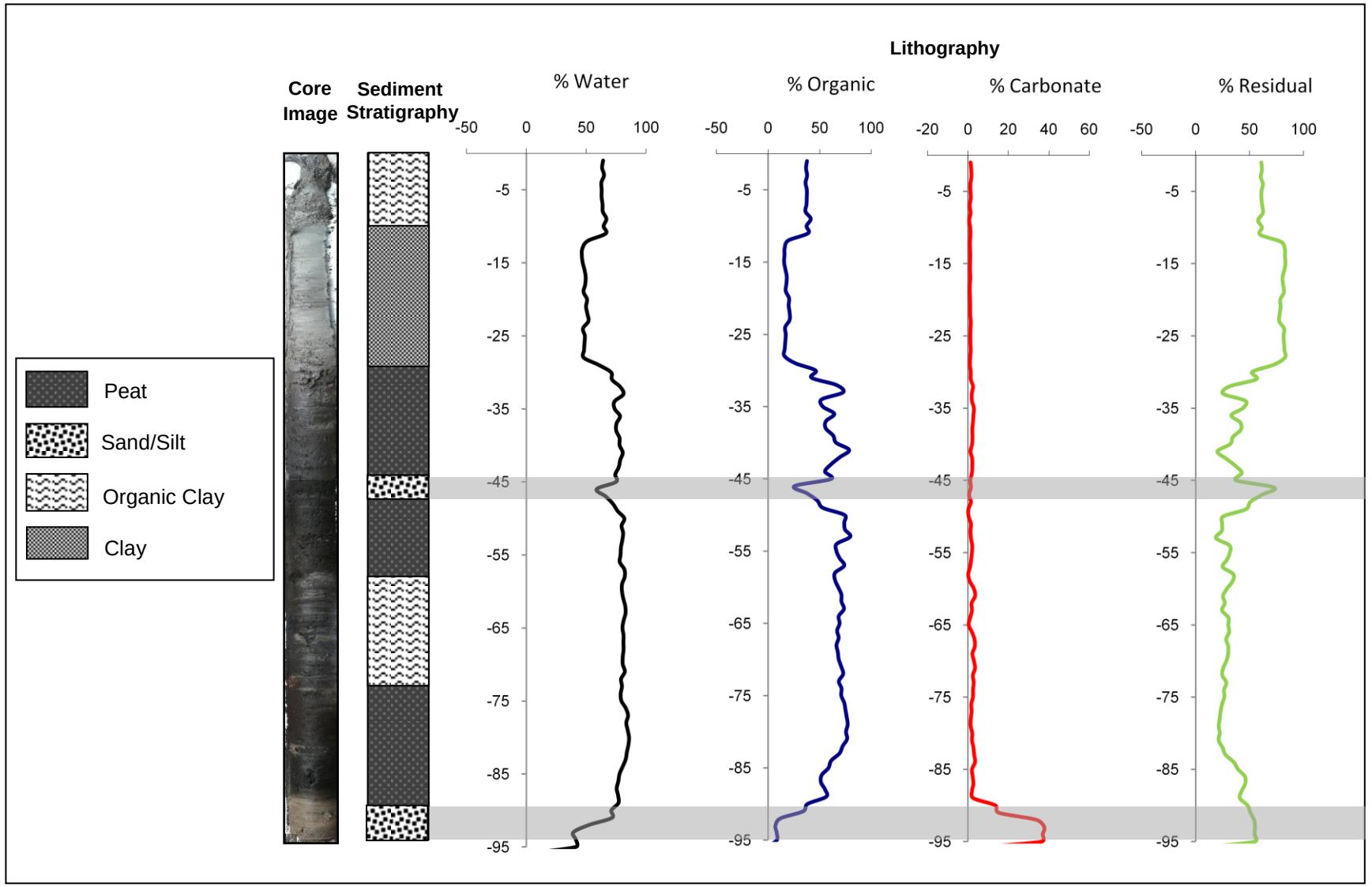

Figure 4.36: Loss-on-ignition and sedimentological analysis of Lake Limon core LIM 3.

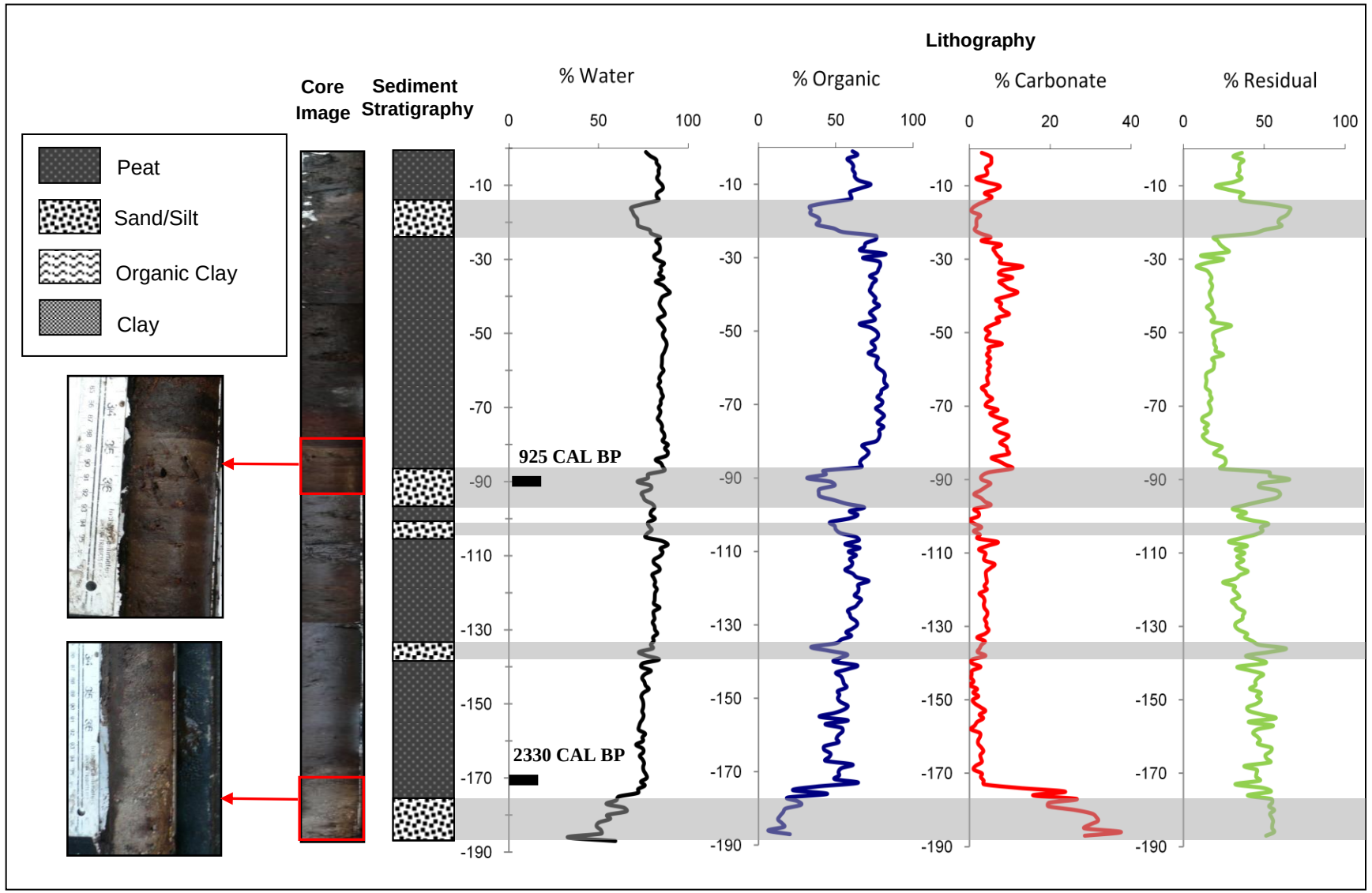

Figure 4.37: Loss-on-ignition and sedimentological analysis of Lake Limon core LIM 4.

^{210}Pb decay constant λ (0.03114 yr^{-1}) divided by the slope (-0.1182) (Figure 4.38) gave the sedimentation rate of 0.263 cm/year. This rate is in agreement with the ^{137}Cs derived rate of 0.213 at this depth. ^{210}Pb rate was used for calculating year of occurrence for recent storms as it can be used for the last 110-130 years as opposed to for the last ~50 years for ^{137} Cs dating.

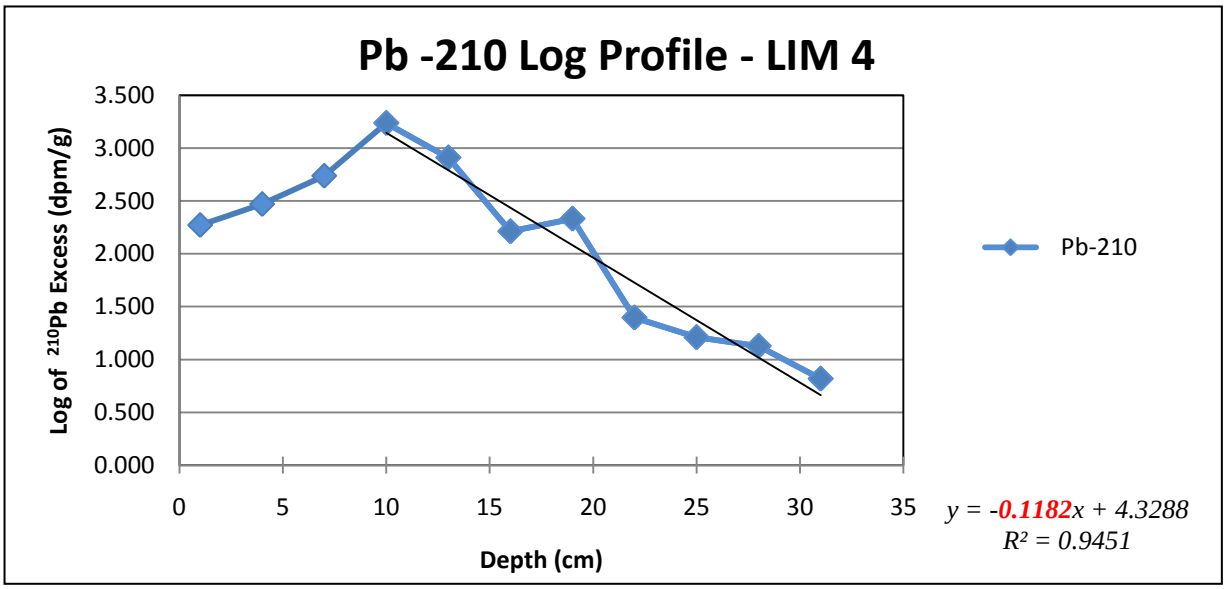

Figure 4.38: Log of excess ^{210} Pb versus depth plot.

A sand layer at 15-25 cm in LIM 4 (Figure 4.37) indicated an overwash event. A sedimentation rate of 0.263 cm/yr derived from ^{210}Pb was used in calculating the date for the depth of 15 cm. This layer of deposit was dated at 1950 AD. Only one hurricane – Hurricane Betsy in 1956- passed at a distance of 120 km from the site (CSC, 2010). This was a Category 1 storm and not likely to register at the lake site due to its distance and low intensity. A tsunami in 1946 affected the northeastern part of the Dominican Republic. Though this tsunami was of magnitude 7.4, the maximum water height produced was only 0.6 m and hence it is improbable that it deposited a sand layer at the site.

The layer of sand at the bottom of LIM 3 at 90-95 cm (Figure 4.39) corresponds with the layer in LIM 2 at 45-52 cm, LIM 1 at 53-58 cm, and LIM 4 at 134-139 cm which was calibrated

at ~1,600 cal yr BP. LIM 3 also registers an overwash deposit at 45-48 cm which corresponds with the deposit at 25-30 cm in LIM 2, 32-41 cm in LIM 1, and 86-98 cm in LIM 4. This was calibrated at 925 cal yr BP (Figure 4.39). These two sand layers might have been deposited by an overwash from a stronger hurricane than Category 1, capable of reaching the LIM 3 location which is farther inland. The overwash event of 2,330 cal yr BP (at 176-188 cm), dated from LIM 4, is visible in LIM 1 at 85- 89 cm and LIM 2 at 106-110 cm as well (Figure 4.39). LIM 3 is a shorter core and hence it is not known whether the hurricane deposited sand at this site.

Cores LIM 1 and LIM 2 have a layer of sand on the top which is most likely from a recent event as there is no sediment above this layer in both the cores. This layer was not visible in LIM 3, indicating that this was a hurricane of a higher intensity than the ones in 925 cal yr BP and ~1,600 cal yr BP. No comparable modern analog, capable of depositing this layer, could be found in the historical data.

4.6 Summary

Of all the cores extracted from the Dominican Republic, those from two locations, Lake Limon and Laguna Playa Ingles which showed distinct event deposits, were dated. These sites are in the eastern and western part of the country respectively. None of these layers were found to be tsunami deposits based on the two preliminary criteria discussed in Chapter 2. Additionally, sediment composition of the event layers matches the composition of sand from the beach (Appendix A-1). These sand layers have a high percentage of carbonates similar to the beach sand, supporting the view that the sand was transported from the beach and the overwash came from the sea side.

A core from Laguna Playa Ingles - LPE 2 (Figure 4.7) - contains sedimentary records of 3 hurricanes. The oldest deposit layer was dated at 3,640 cal yr BP. Grain size analysis showed

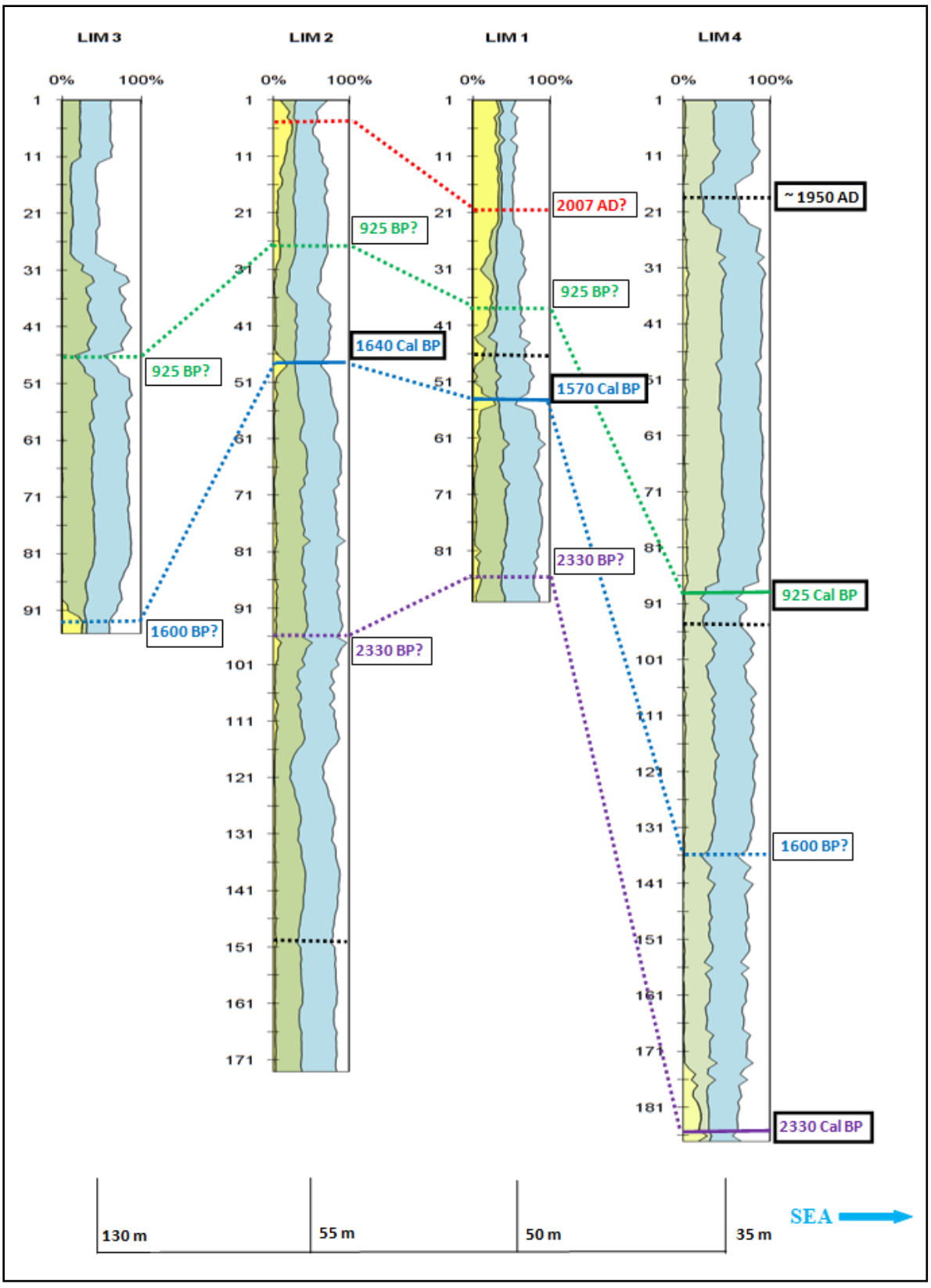

Figure 4.39: Transect showing the four LOI curves and correlation of event layers.

these event signature layers to be composed of medium-grained sand indicating overwash events. Core LIM 4 (Figure 4.37) indicates deposits from 5 events, 2 of which were dated using radiocarbon. One occurred around 925 cal yr BP and one around 2,330 cal yr BP. Since no modern analogs were found in the historical records, it is not possible to interpolate the intensity of prehistoric hurricanes for Laguna Playa Ingles and Lake Limon sites.

Based on the chronology obtained from radiocarbon dating, the western part of the island has had three storms in the last 3,640 years and the eastern part has had five in the last 2,330 years. This signifies a return period of 1,213 years in the western part and 466 years in the eastern part. This means a Poisson probability of hurricane strike of 0.0824% for the eastern part (Lake Limon), and 0.21% for the western part (Laguna Playa Ingles). Paleo-hurricane records from LPE 2 and LIM 4 cores are used as a "prior" for Bayesian statistical analysis (Elsner and Bossak, 2001) of future probability of hurricane landfall computed in Chapter 5.

CHAPTER 5
RISK ANALYSIS OF THE DOMINICAN REPUBLIC

5.1 Background

The Dominican Republic lies in the zone of moderate activity for hurricanes (Pielke *et al.*, 2003). By virtue of being on an island, it is susceptible to hurricane strikes from three sides. The coastal population of the Dominican Republic is extremely vulnerable to Hurricanes as almost 56% of the total population lives in the coastal provinces (La Oficina Nacional de Estadística, 2010). The country has a high poverty rate of 42.2% (CIA, 2010) and a low level of access to medical facilities due to lack of roads and personal vehicles. Additionally, one of the biggest sectors in terms of GDP in the Dominican Republic is tourism (CIA, 2010); since most of the tourism is in the coastal areas, the nation's economy is also vulnerable to hurricanes which can disrupt tourism.

Even though the recent devastating earthquake in Haiti did not affect the Dominican Republic directly, lying on the cusp of three tectonic plates, the Dominican Republic is also prone to earthquakes and tsunamis. While earthquakes are rarer events that cannot be predicted with accuracy, hurricanes on the other hands are of more immediate concern to the Dominican Republic.

5.2 Hurricane History

The Dominican Republic has been affected by numerous hurricanes in the last 160 years. Of these, the most destructive hurricanes to have made landfall are: San Zenon Hurricane in 1930, Hurricane David in 1979, and Hurricane Georges in 1998. In addition to these devastating hurricanes, tropical storms such as Olga and Noel in 2007 have also caused extensive flooding damage (Figures 5.1.A and 5.1.B) in the country.

Figure 5.1: (A) and (B) Tropical storm Noel in 2007 and the extensive flooding caused by it (Defensa Civil, the Dominican Republic).

Hurricane San Zenon (1930)

Hurricane San Zenon was a Category 4 hurricane and considered to be the deadliest of the Atlantic Hurricanes. This hurricane made landfall with peak winds between 150 mph to 200 mph (Hartwell, 1930) on September 3rd, 1930. It killed 4,000 people in the capital city of Santo Domingo (Hartwell, 1930). Historians later put the death toll at close to 8,000 (Government of the Dominican Republic, 1958). Damages were estimated at $50 million in 1930 US dollars (Hartwell, 1930).

Hurricane David (1979)

Hurricane David was a Category 5 hurricane and the second most destructive to have hit the Dominican Republic in this century. It made landfall on August 31st, 1979 with peak wind speed of 175 mph (Hebert, 1980). Hurricane David killed about 2,000 people in the Dominican Republic and caused damages of well over $1 billion (Hebert, 1980).

Hurricane Georges (1998)

Hurricane Georges made landfall in the eastern part of the Dominican Republic on

September 22nd, 1998 as a Category 3 storm. It had peak winds of 120 mph and brought surges of 7 feet along with heavy precipitation that caused widespread destruction due to landslides and flooding. More than 438 people were killed and it cost the country about $1.2 billion in damages (Geerts *et al.*, 2000).

5. 3 Socio-Economic Setting

The population of the Dominican Republic (projected) in 2010 is 9,884,371 with 4,935,282 men and 4,949,089 women (La Oficina Nacional de Estadística, 2008). This is a 15.4% population increase from the last census of 2002. The population of the Dominican country is mostly young with a median age of 22 years (La Oficina Nacional de Estadística, 2008).

A large population is more vulnerable in a disaster due to limited availability of resources such as water, food, and shelter. It also faces slow recovery post disaster. Women are more vulnerable to disasters because they are (usually) economically less stable and have to care for children and family (Cutter *et al.*, 2003). The elderly and young children are less capable of caring for themselves during disasters and this makes them more vulnerable (Cutter *et al.,* 2003). They also may be less mobile and are dependent on other people. While statistics were available for children under the age of 5 for each province, none was available for the elderly population. Thus "children under 5 years" is the indicator used for extremes in age group which is dependent on the rest of the population. There were a total of 645,513 children under the age of 5 in the coastal provinces (La Oficina Nacional de Estadística, 2008). Even though the Dominican Republic is considered to be one of the "small countries with signs of progress" by the World Bank (Helwege and Birch, 2007), 42.2% (CIA, 2010) of its population is under the poverty line and 29% is considered to be extremely poor (USAID, 2005).

Only 38.65% of the country's population is connected to asphalted roads (La Oficina Nacional de Estadística, 2008). Access to private vehicles and connectivity to roads are important for voluntary/self evacuation before a hurricane landfall. Most (more than 85%) of the population in the Dominican Republic does not own a vehicle (La Oficina Nacional de Estadística, 2008). Vehicle ownership information was not available for individual provinces.

There are 1,994,194 buildings in the coastal provinces of the Dominican Republic. Damage to residential buildings can put additional pressure on the displaced population. It may prolong their return to their homes after an event and cause further economic hardship. Structural losses can impede post-disaster recovery and redevelopment of the provinces. Funds have to be diverted to shelter displaced population instead of utilizing all resources towards getting infrastructure and other essential services back in order (Cutter *et al.*, 2003).

Disabled population includes people who are blind, deaf, mute, have no arms, have no legs, are mentally disabled, and "others" (La Oficina Nacional de Estadística, 2008). Of the total population in the Dominican Republic, 4.2% are disabled.

There is limited access to healthcare facilities in the Dominican Republic, especially in the rural areas. In 2006, there were 1,439 health care centers in the country including hospitals and clinics. There are total 9,517 beds available (La Oficina Nacional de Estadística, 2008) for the entire populace. Assuming that this count has not changed in 2010, this translates to about one available bed for every 1000 persons.

5.4 Calculation of Vulnerability Index

Census data obtained from the La Oficina Nacional de Estadística (2008) provided information about the various indicators of vulnerability used for mapping. Coastal areas were mapped at the provincial level. Six of the indicators (population, gender, children, disability,

poverty, and building stock) contributed towards increasing the vulnerability and two (access to roads and medical facilities) towards decreasing it.

Using a rescaling methodology proposed by Brugglio (2003) (see Chapter 3), the indicators were normalized such that each ranged from 0 to 1 (Figure 5.2) and then combined and normalized again to create a composite index for each coastal province (Figure 5.3). This technique assigned equal weights to all indicators (Cutter *et al.*, 2003) before adding them (Appendix B-1).

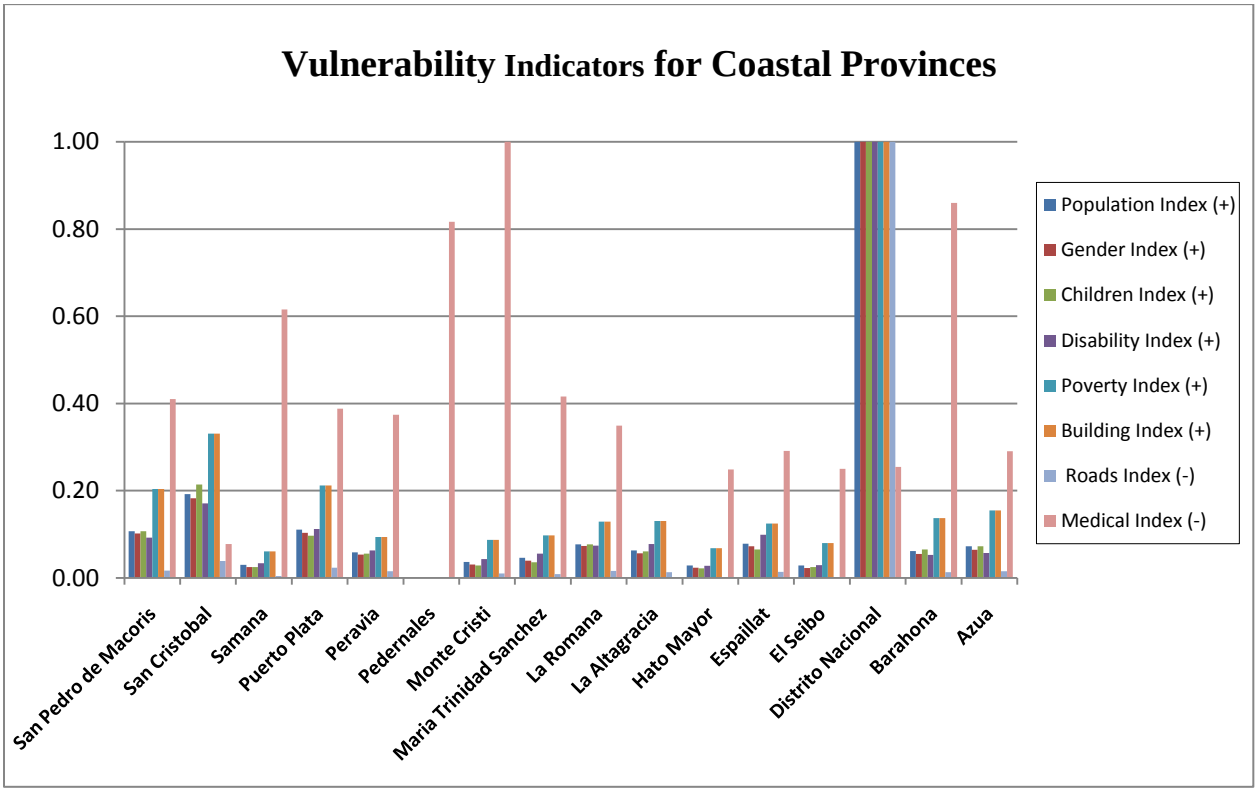

Figure 5.2: Histogram showing normalized vulnerability indicators for each coastal province.

Distrito Nacional has the highest score for all the vulnerability indicators (Figure 5.2). While six of them increase the total vulnerability, two decrease the vulnerability. Even with the assuaging factors, it has the highest vulnerability to hurricanes due to its high population (Appendix B-1). This province has almost 27% of the total population of the country and 49% of

all the coastal population. The second most vulnerable district is San Cristobal which is next to Distrito Nacional on the west (Figure 5.3).

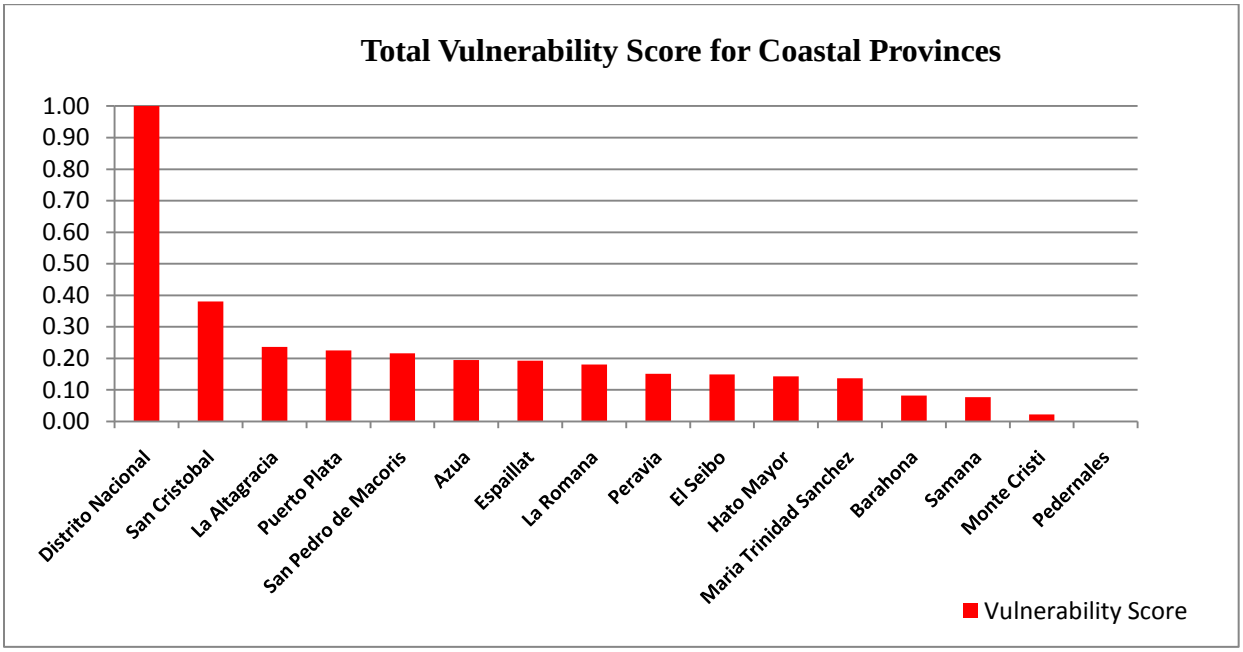

Figure 5.3: Histogram showing normalized total vulnerability score for each coastal province.

5.5 Calculation of Probability of Strike

There have been a total of 26 hurricanes that made landfall in the Dominican Republic since 1851 (CSC, 2010). Using these past strikes, an average rate of return can be derived for future hurricane landfall by dividing number of strikes by the number of years.

A Poisson distribution model was used to predict future hurricanes based on past hurricane data from all coastal provinces in the Dominican Republic. This distribution was based on the return periods of hurricanes calculated from the historic records as well as from prehistoric records (where available).

Data for historic records were obtained from hurricane database - HURDAT - which has records of all North Atlantic hurricanes since 1851(CSC, 2010). Prehistoric records of hurricane strikes that were obtained from paleotempestological analysis (see Chapter 4) were used for the

probability calculation in the provinces where coring was done. For the rest of the provinces, only the historic records were used for probability calculations (Table 5.1).

Table 5.1: Annual probability of occurrence of hurricanes in the coastal provinces of Dominican Republic. La Altagracia has the highest Poisson probability of strike. (NA represents locations where no paleo-records were found and/or dated)

Province	Historic Landfalls	Rate of Return (Historic Hurricanes)	Prehistoric Hurricanes	Rate of Return (Including Prehistoric Hurricanes)	Poisson Probability
San Pedro de Macoris	2	0.0125	NA	0.0125	0.0123
San Cristobal	4	0.0250	NA	0.0250	0.0244
Samana	1	0.0063	NA	0.0063	0.0062
Puerto Plata	0	0.0000	NA	0.0000	0.0000
Peravia	3	0.0188	NA	0.0188	0.0184
Pedernales (LPE)	**2**	**0.0125**	**3**	**0.0014**	**0.0014**
Monte Cristi	0	0.0000	NA	0.0000	0.0000
Maria Trinidad Sanchez	0	0.0000	NA	0.0000	0.0000
La Romana	0	0.0000	NA	0.0000	0.0000
La Altagracia	**5**	0.0313	NA	0.0313	0.0303
Hato Mayor	0	0.0000	NA	0.0000	0.0000
Espaillat	0	0.0000	NA	0.0000	0.0000
El Seibo (Lake Limon)	**0**	**0.0000**	**5**	**0.0021**	**0.0021**
Distrito Nacional	0	0.0000	NA	0.0000	0.0000
Barahona	2	0.0125	NA	0.0125	0.0123
Azua	8	0.0500	NA	0.0500	0.0476

El Seibo which has a 0.0 probability of strike based on historical data, has a higher likelihood by adding prehistoric hurricane data (Table 5.1). Conversely, the probability of strike for Pedernales is lower when prehistoric records were added (Table 5.1).

Figure 5.4 shows the probability of at least one hurricane making landfall in the future in each of the provinces. The highest likelihood of hurricane strike is in Azua province followed by La Altagracia. While Distrito Nacional has not had a direct landfall within its boundaries, it was greatly affected by the deadly hurricanes, San Zenon in 1930, and Hurricane David in 1979.

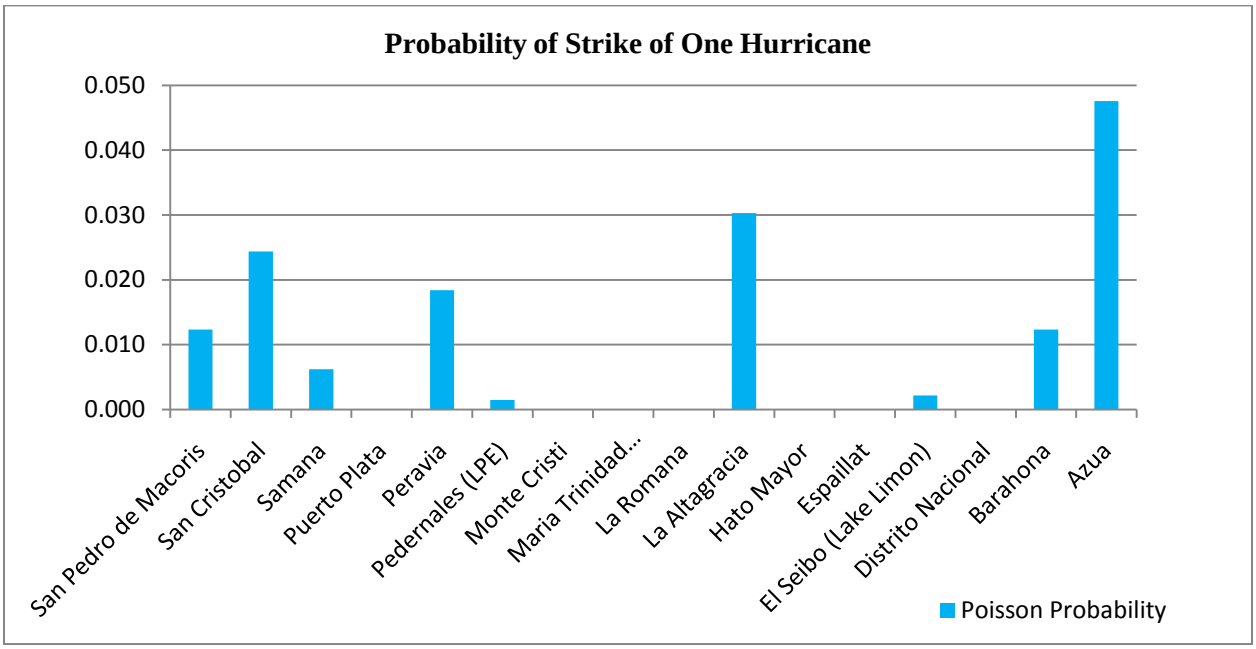

Figure 5.4: Histogram showing the annual probability of occurrence of a hurricane in coastal Dominican Republic.

Finally, annual hurricane probability calculations, along with that of multiple hurricane strikes over longer time periods, were made (Appendix B-2). This kind of prediction is very useful in calculating future losses in the insurance industry (Elsner and Kara, 1999).

5.6 Spatial Components of Risk for Coastal Dominican Republic

5.6.1 Mapping of Vulnerable Populations

Coastal provinces are ranked from highest to lowest in terms of their aggregate vulnerability index (Appendix B-1). They are represented spatially in Figure 5.5 for each of the sixteen coastal provinces of the Dominican Republic. Note that these scores provide a relative index and are not absolute scores.

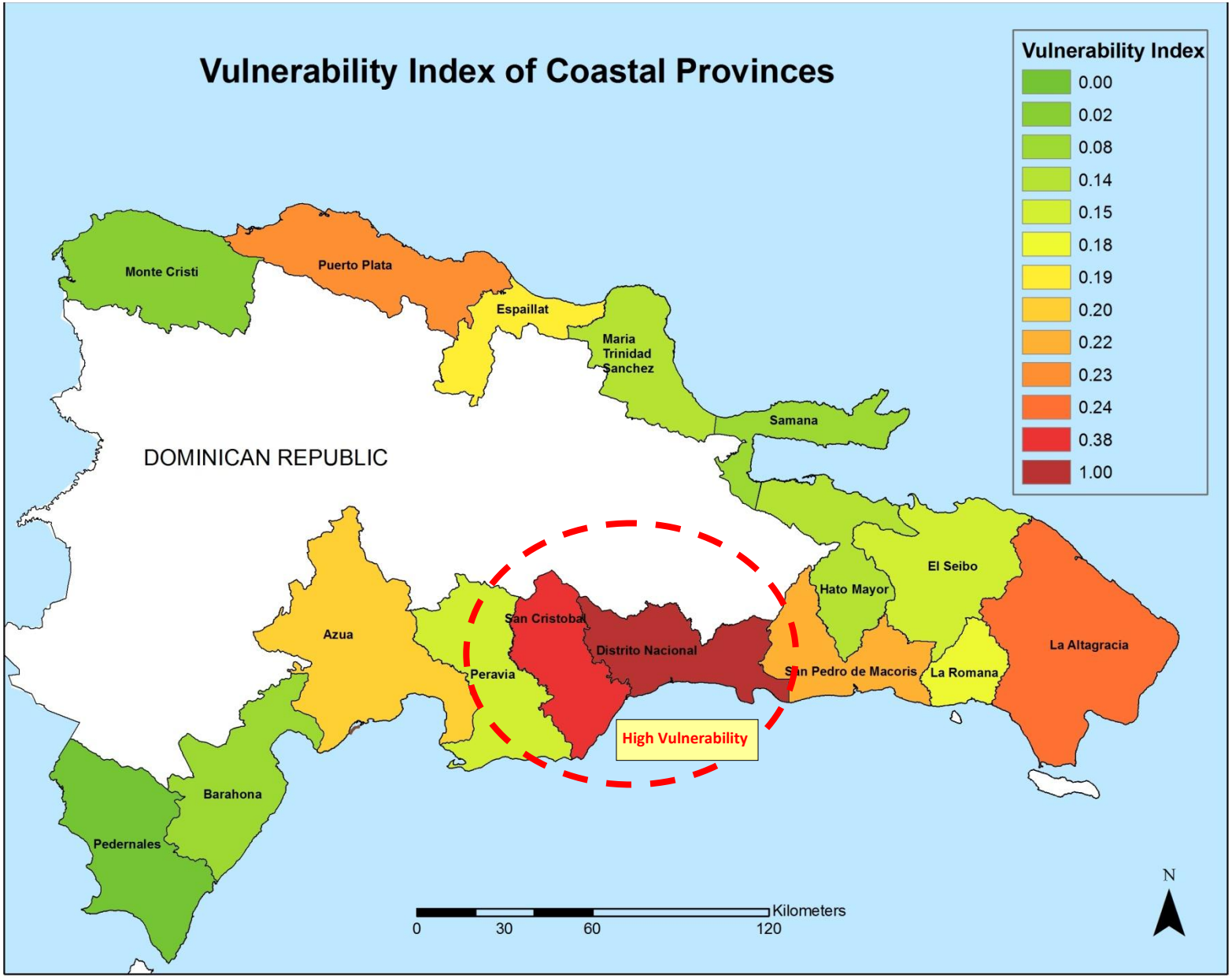

Figure 5.5: Composite vulnerability score of the 16 coastal provinces. Distrito Nacional has the highest vulnerability index.

5.6.2 Mapping of Surge Inundation Potential

A simplified flooding approach (see Chapter 3), utilizing cost-distance analysis technique available in ArcGIS 9.3, was used to arrive at the inundated areas for different surge thresholds based on storm categories (Figure 5.6). This potential surge model is a simplistic view of the inundation after the surge has reached land. It does not take into consideration the bathymetry of the coast; the pressure, or the wind speed of the hurricane. Nevertheless, it helps illustrate the flooding potential of coastal areas in the Dominican Republic to delineate areas for mitigation efforts. There is considerable likelihood of flooding from hurricanes in Distrito Nacional which is extremely vulnerable due to its high population. Likewise, Samana, Sanchez, Barahona, Monte Cristi, and San Pedro de Marcoris have low lying areas that flood easily.

Flooding of roads

Most of the coastal roads in the Dominican Republic lie in flood-prone areas and are flooded during storm events (Figure 5.7). In some parts they are also flooded from heavy precipitation, making evacuation difficult for the coastal population. The road network in the Dominican Republic is concentrated in coastal areas, mainly due to tourism. Not many highways can be used to travel inland directly. The few that do go across the country are expensive toll roads and less frequently used by people. However, in case of an approaching hurricane, these may be used for evacuation.

5.6.3 Mapping of Potential Wind Speed

Wind speeds were interpolated using only historic hurricane landfalls (Figure 5.8) as the intensities of paleo-hurricanes are not known. Using an Inverse Distance Weighting (IDW) technique, the missing data points were interpolated. Distrito Nacional shows the highest wind speed potential due to its proximity to the landfall location of Hurricane David (1979) and Hurricane San Zenon (1930) which were both Category 5 storms.

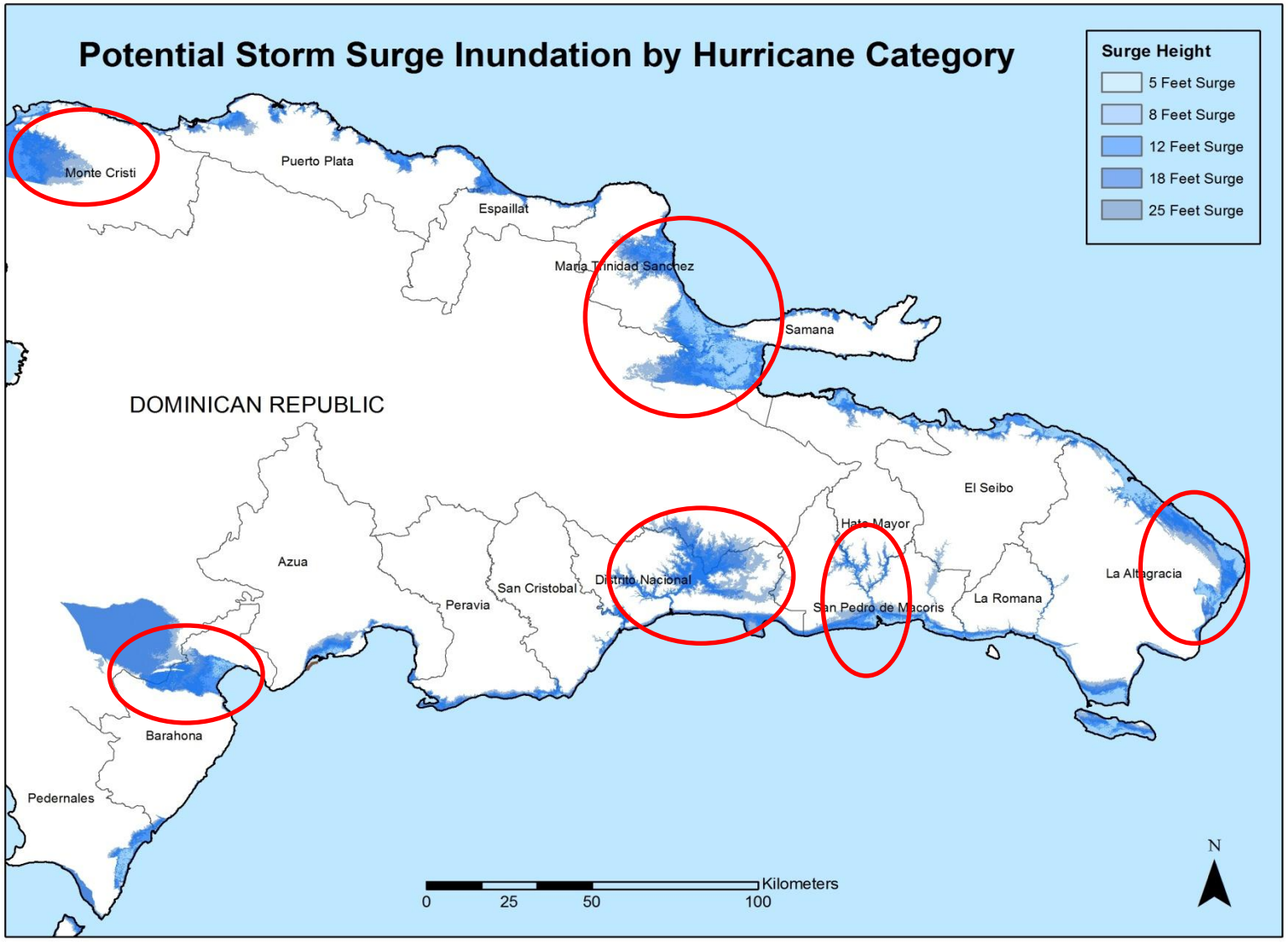

Figure 5.6: Potential inundation by storm surge from different categories of hurricanes.

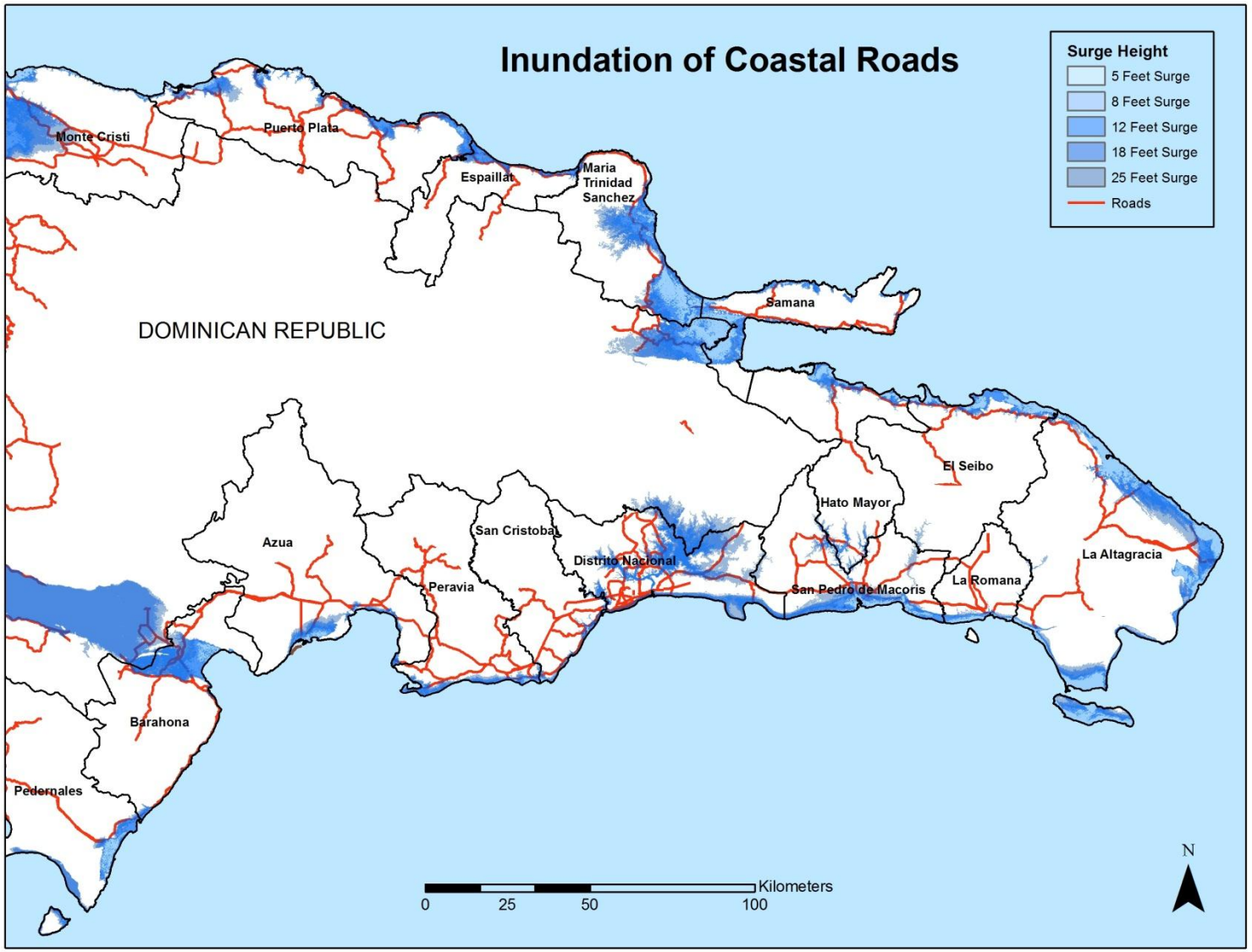

Figure 5.7: Flooding of coastal roads from hurricane surge.

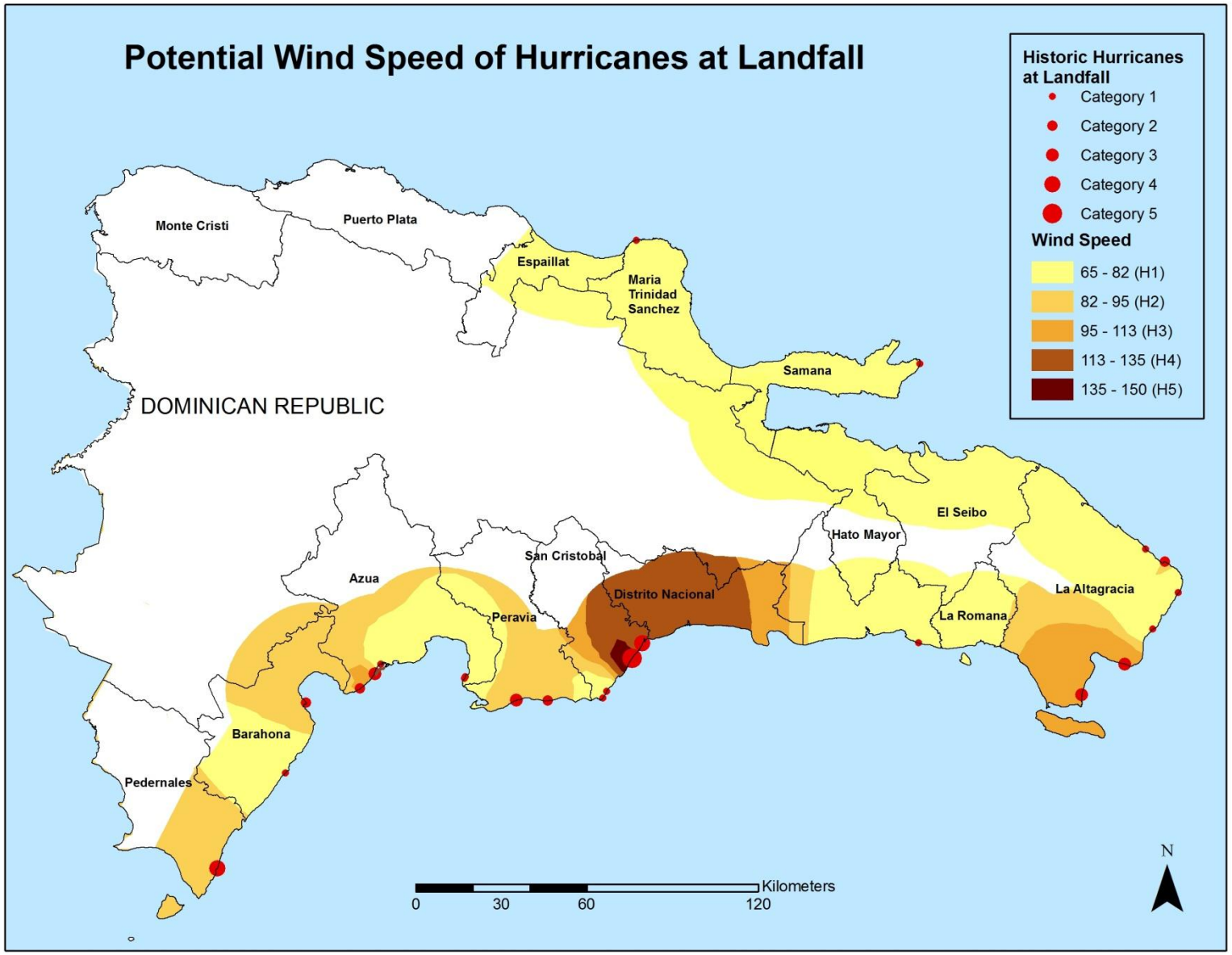

Figure 5.8: Potential wind speed of hurricanes at landfall based on historic storms.

Since hurricanes dissipate as they travel inland, they are not expected to affect the interior population directly. Thus potential wind speed is shown only for the coastal areas and is limited to 25 km inland based on the maximum distance of the potential storm surge inundation.

5.6.4 Mapping of Hurricane Strike Probability

Strike probabilities were calculated for each province using a Poisson distribution model. Each province was mapped based on the Poisson probability of hurricane strike. The hurricane landfall probability is useful for planning for each province as a whole and may not be representative of the varying risk within the province or in the areas near the boundary of two provinces. For example, a hurricane that strikes a province *A* near the border will also affect the neighboring province *B* but the actual threat to province *B* is not captured as the strike location is restricted to province *A.*

The highest probability of strike is in La Altagracia followed by Peravia because of multiple historic landfalls in these provinces (Figure 5.9). Distrito Nacional, Monte Cristi, Espaillat, La Romana, and Hato Mayor have not been hit by a hurricane in the past (based on historic records) and therefore have a zero probability of future strike (Figure 5.9). If more sites are cored within these provinces and prehistoric records of storms found, their probability of hurricane strike may increase.

5.6.5 Hurricane Risk Mapping for the Coastal Population

An amalgamation of the three components of risk; vulnerability, likelihood of hurricane landfall, and hurricane hazard (storm surge and wind); leads to a comprehensive risk map (Figure 5.10) that shows areas most susceptible to hurricane peril by virtue of their socio-economic status (including demographic composition), location, and elevation.

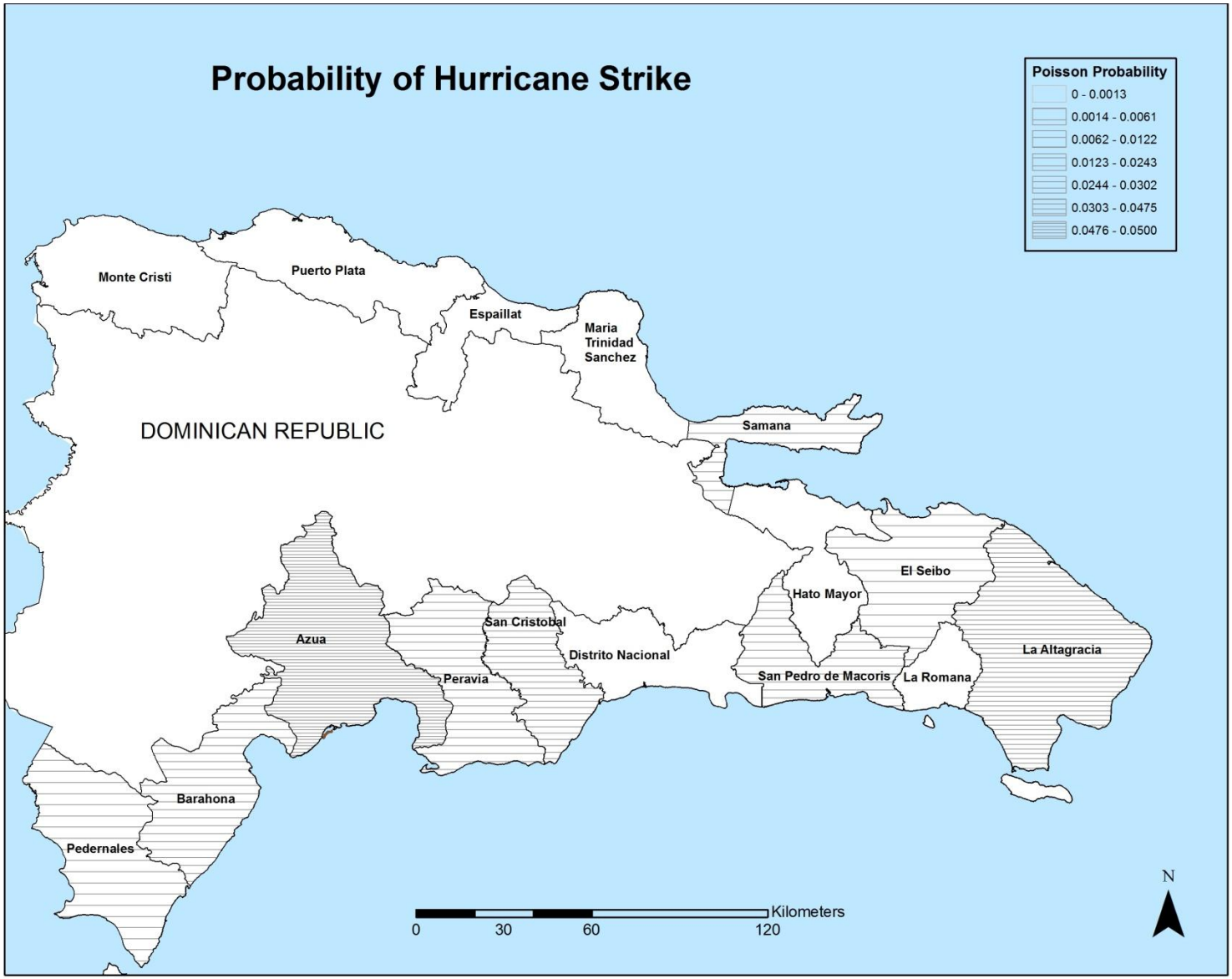

Figure 5.9: Poisson probability of strike based on historic and prehistoric hurricane records.

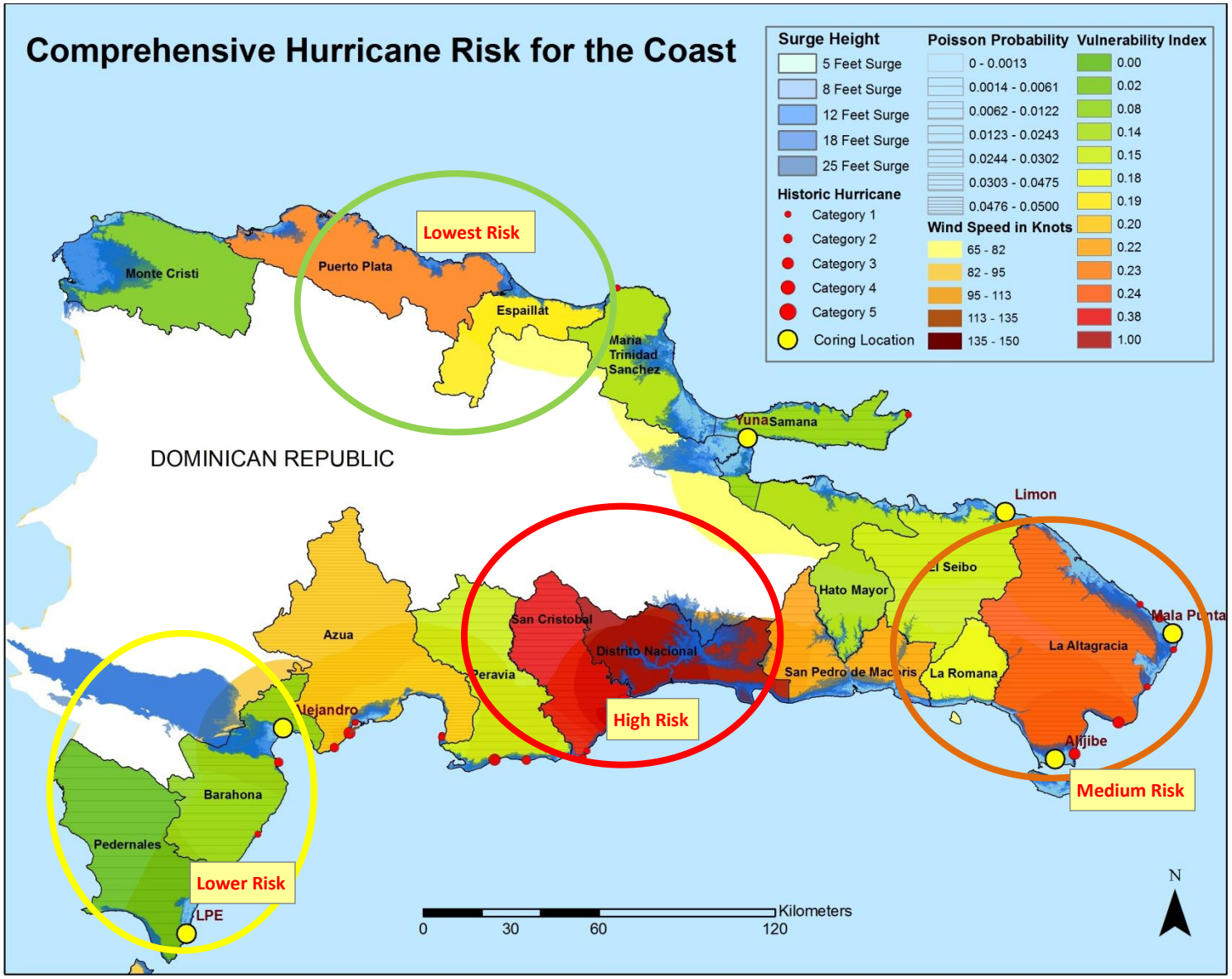

Figure 5.10: Comprehensive risk for coastal Dominican Republic. Distrito Nacional and San Cristobal face the highest risk followed by La Alta Garcia in the east and Puerto Plata in the north.

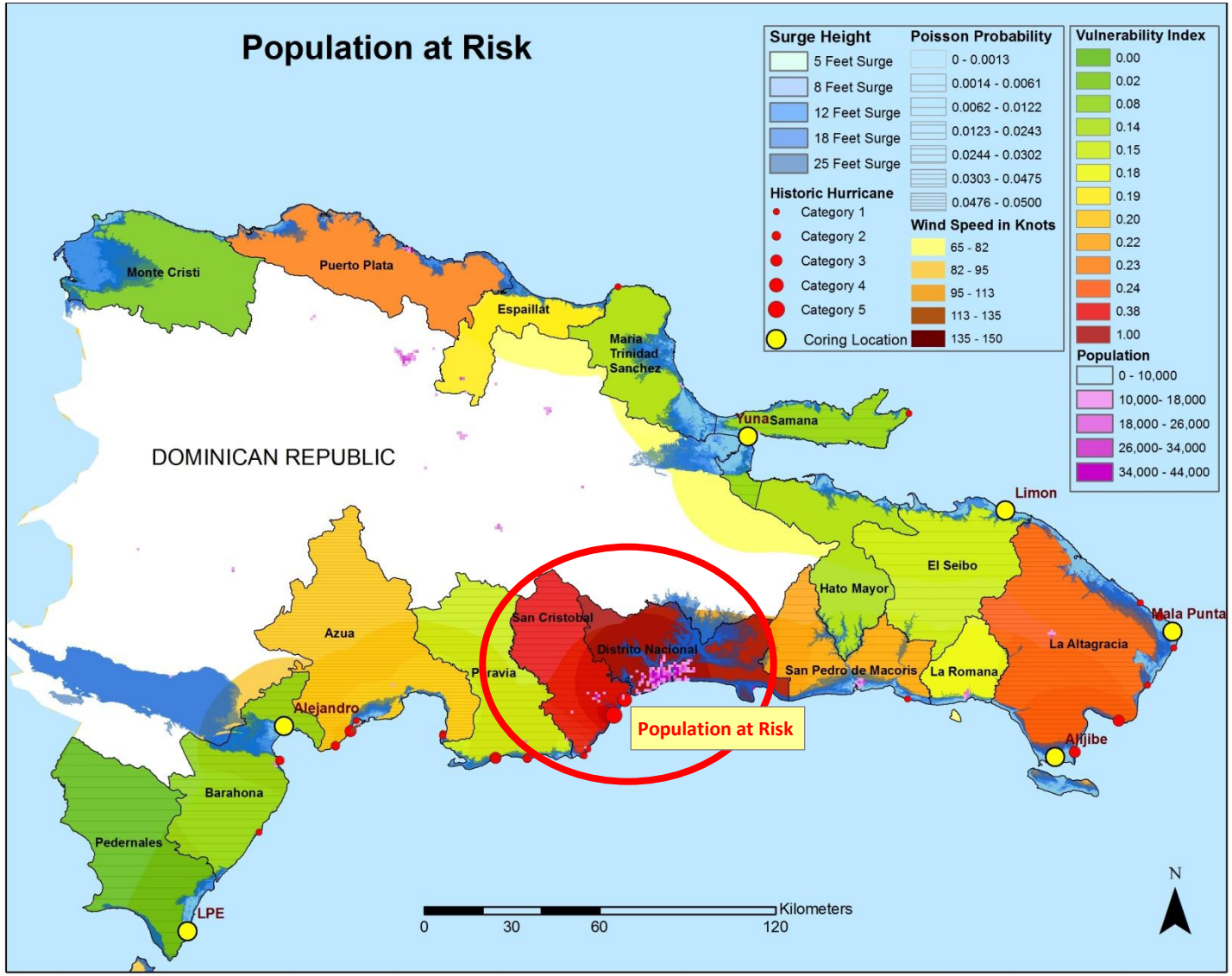

Figure 5.11: Population at risk from hurricanes. There is a high population concentration in the Distrito Nacional area which is most at risk.

It is worth noting that the province with the highest probability of strike (Peravia) has a lower total risk (Figure 5.10) due to its low vulnerability score (Figure 5.5). Conversely, Distrito Nacional has a 0.0 probability of strike (Figure 5.9), but it faces the highest risk due to a high vulnerability score, a high inundation potential, as well as a high wind speed potential.

LandScan grid data were utilized for the population count, and based on potential categories of hurricanes, the population that would be directly affected was mapped (Lam *et al.,* 2009). The population in LandScan data base is counted for each pixel and illustrated as the total population that would be in harm's way while not being limited by jurisdictional boundaries. Figure 5.11 shows the total population affected by potential hurricanes along with the accompanying surge and wind from the different categories of hurricanes.

There are 589,151 people who would be impacted by a surge of 5 feet; 772,713 by a surge of 8 feet; 1,446,672 by a surge of 12 feet; a surge of 18 feet will affect 2,021,765 people; and a surge of 25 feet plus, created by a Category 5 hurricane, will affect 2,505,416 people. This translates into 6% of the country's population that will be directly affected by a Category 1 hurricane, 8% by a Category 2, 14.5% by a Category 3 hurricane, 20% by a Category 4 hurricane, and finally, 25% or a quarter of the country's population will be impacted by a Category 5 hurricane.

5.7 Summary

Based solely on historical data, the likelihood of hurricane strike for La Altagracia province is the highest and second highest for Pedernales province (Table 5.1). But when prehistoric records are added, the probability of strike is reduced considerably for Pedernales (from 0.025 to 0.0020). Similarly, El Seibo has a 0.125 probability of strike based on historical records. By adding the prehistoric data, the likelihood of hurricane strike in this province goes

down to 0.0021 (Table 5.1). In the above two cases, the Poisson probability has decreased by adding the prehistoric records. But depending on the site and its sensitivity, the probability could also increase if additional prehistoric hurricane records were found.

Although Distrito Nacional has a 0.0 probability of a direct strike based on past records, it is the most 'at risk' province due to its high population. A hurricane landfall even in the vicinity of this province is likely to create substantial damage to life and property as was the case with Hurricane David in 1979. The hurricane storm surge and wind speed maps (Figures 5.6 and 5.8) illustrate the high level of threat to Distrito Nacional. Additionally, the capital city Santo Domingo, which is one of the biggest ports in the region, is located in this province. This area is the economic hub of the country owing to tourism and trade. Distrito Nacional is also the seat of the central government and a major hurricane landfall in this area could cripple the entire country.

The province with the lowest vulnerability score is Pedernales which has a small population and thus gets low scores on each of the indicators of vulnerability. Surprisingly, this province also has the highest per capita medical facilities (Appendix B-1). While the vulnerability of this province is low, it has a high likelihood of hurricane strikes based on historical records. This makes the total risk of hurricanes in the province moderately high.

CHAPTER 6
PALEOTEMPESTOLOGY OF RAAN, NICARAGUA

6. 1 Background

Nicaragua (13 ^{o} N, 85 ^{o} W) is the largest Central American nation with a total area of 129,494 sq km. The country is bordered by the Pacific Ocean on the west, the Caribbean Sea on the east, Honduras on the north, and Costa Rica on the south. The capital is Managua which is located in the western part of the country.

There are three different climate zones: Pacific lowlands, North-Central highlands and Atlantic lowlands. Nicaragua has an average maximum temperature of 28 ^{o}C and average precipitation of 100 -150 cm between the months of May and October. The North-Central highlands are cooler and wetter than the Pacific lowlands. The Atlantic lowlands get the most rain, between 250 cm and 650 cm, in the months of May through December. The eastern part of Nicaragua including the Mosquito Coast is part of the Atlantic lowlands.

This coastal area is politically separated into the Region Autonomista Atlántico Norte (RAAN) in the north, and the Region Autonomista Atlántico Sur (RAAS) in the south. The study area, RAAN, is an autonomous region with an area of 32,159 sq km. The capital of this region is Bilwi which is part of the municipality of Puerto Cabezas.

6.2 Geologic Setting

Nicaragua is located on top of the Chortis block of the Caribbean plate (Figure 6.1) and is tectonically active (Dengo, 1969). The coastal alluvial plain (Figure 6.2) that comprises the Mosquito Coast is 150 km wide. Mosquito Coast is a flat lowland with savannah vegetation (pine savannahs), mangrove swamps, and tidal lagoons (Mills and Hugh, 1974; Parsons, 1955; Marshall, 2007).

This depositional environment was formed in the Late Cenozoic with erosional material from the central highlands in the west. “Coarse, clastic sedimentation” (Marshall, 2007) was formed along with deep river channels due to the Neogene uplift of the Chortis highland in the west (Marshall, 2007). This area is part of the largest sedimentary basins in Central America, which extends about 240 km offshore as the Mosquita Banks (Mills and Hugh, 1974).

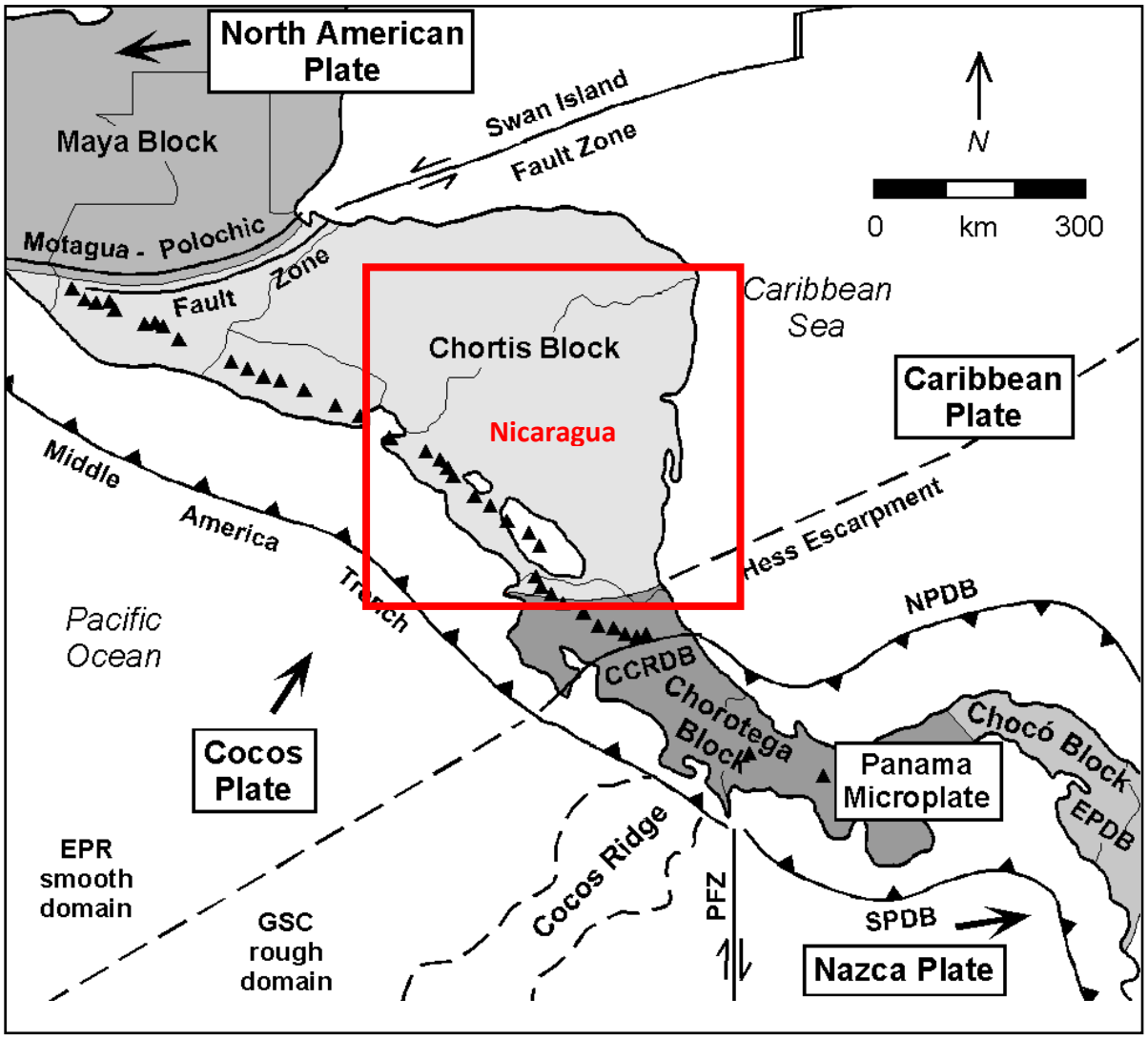

Figure 6.1: Geologic Map of Nicaragua (Marshall, 2007).

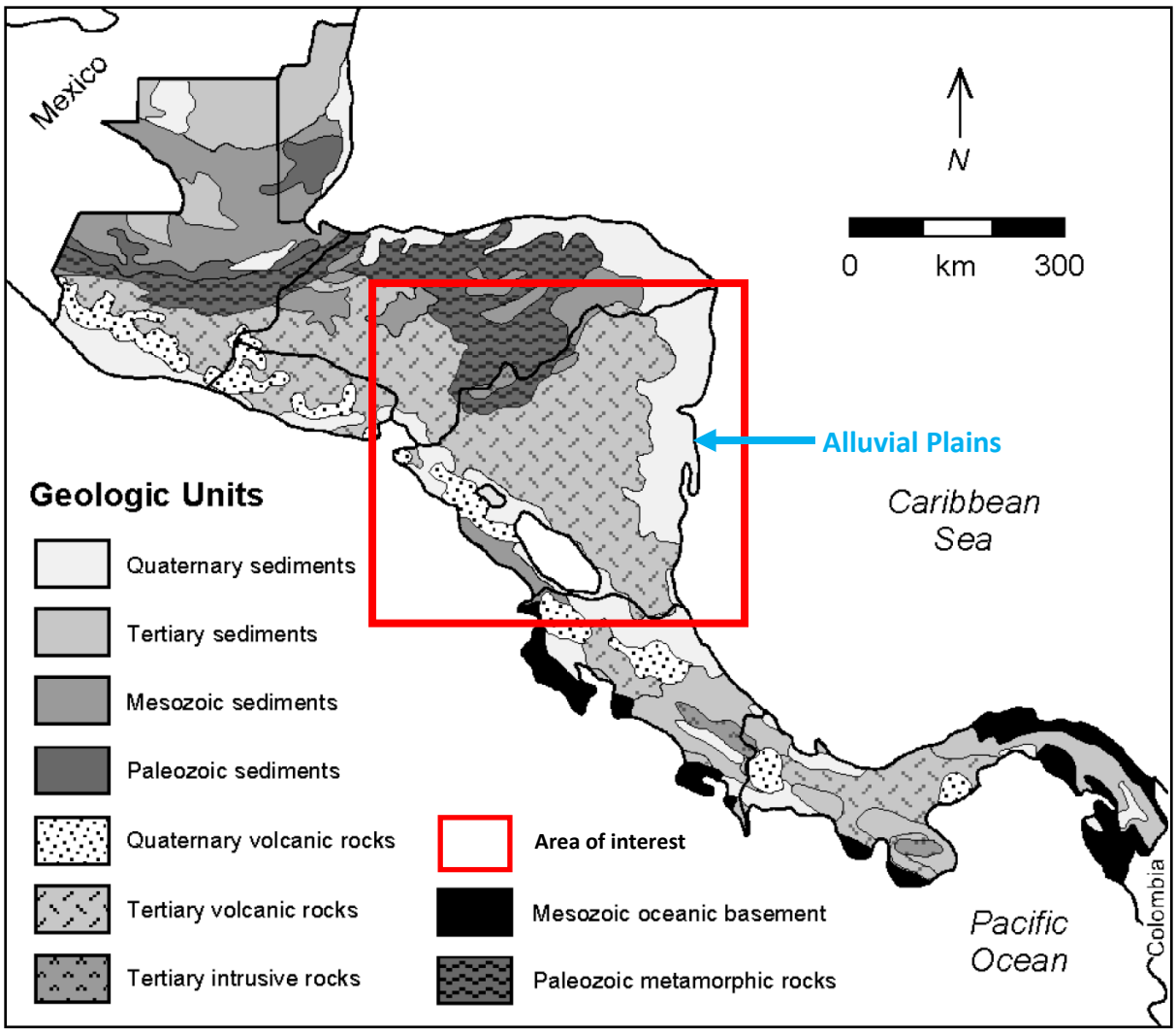

Figure 6.2: Geologic Map of Nicaragua (Marshall, 2007).

6.3 Nicaragua and Hurricanes

Nicaragua's Caribbean coast is in the area of low hurricane activity compared to the Central American mainland and the Caribbean islands farther north and east. Nicaragua lies in the region of 1-5% (Pielke *et al.*, 2003) annual probability of hurricane landfall. Although lying slightly south of the main hurricane pathway and experiencing fewer hurricanes than areas farther north, Nicaragua has been hit by 13 hurricanes since 1851 (Figure 6.3.B.), 6 of which were Category 3 or higher.

Five of the 13 hurricanes made landfall in RAAN (CSC, 2010) (Figure 6.3.A), they are: Hurricane "Notnamed" in 1890, Hurricane "Notnamed" in 1893, Hurricane "Notnamed" in 1941, Hurricane Edith in 1971, and Hurricane Felix in 2007.

Hurricane Felix, a Category 5 hurricane, was one of the most destructive hurricanes to have struck this region. (See Chapter 7 for more details about this hurricane.) Figure 6.3.A shows the five historic hurricane strikes that have affected RAAN, Nicaragua, based on National Hurricane Center's "best track" database - HURDAT (CSC, 2010).

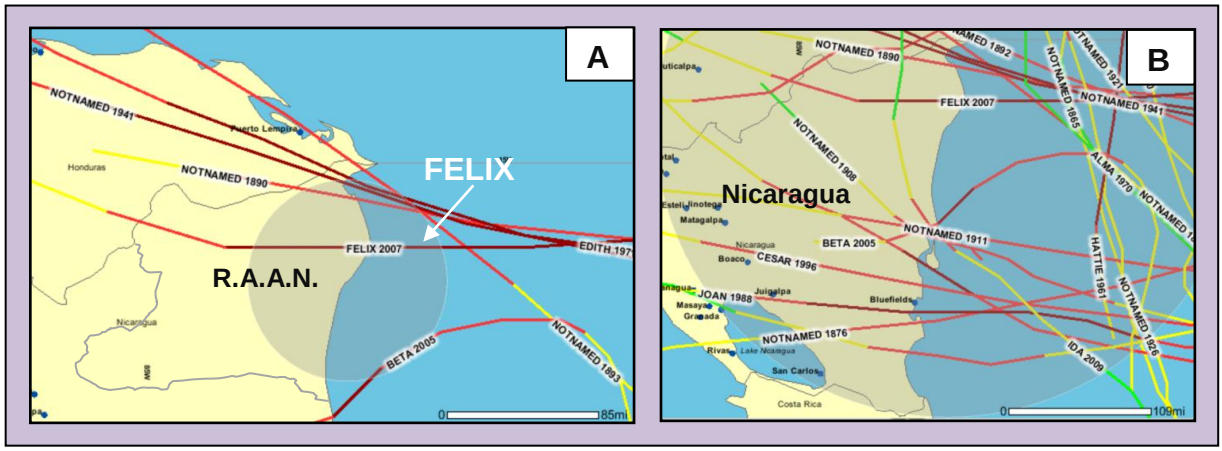

Figure 6.3: (A) Five hurricane strikes in RAAN, Nicaragua, since 1851(CSC, 2010). B) Thirteen hurricane strikes in eastern Nicaragua, since 1851(CSC, 2010).

6.4 Paleotempestology in RAAN, Nicaragua

Four coring sites were chosen on the coast of RAAN. Site selection was based on a criterion of lakes behind sandy barriers, and knowledge of previous hurricane strikes. These sites are: near Dakura village; at Haulover; at Lake Lakun Tara, and at Puerto Isabel (Figure 6.4). Ten cores, measuring 31m of sediment were extracted. Coring was done in February of 2008 before the start of the wet season.

6.5 Study Sites

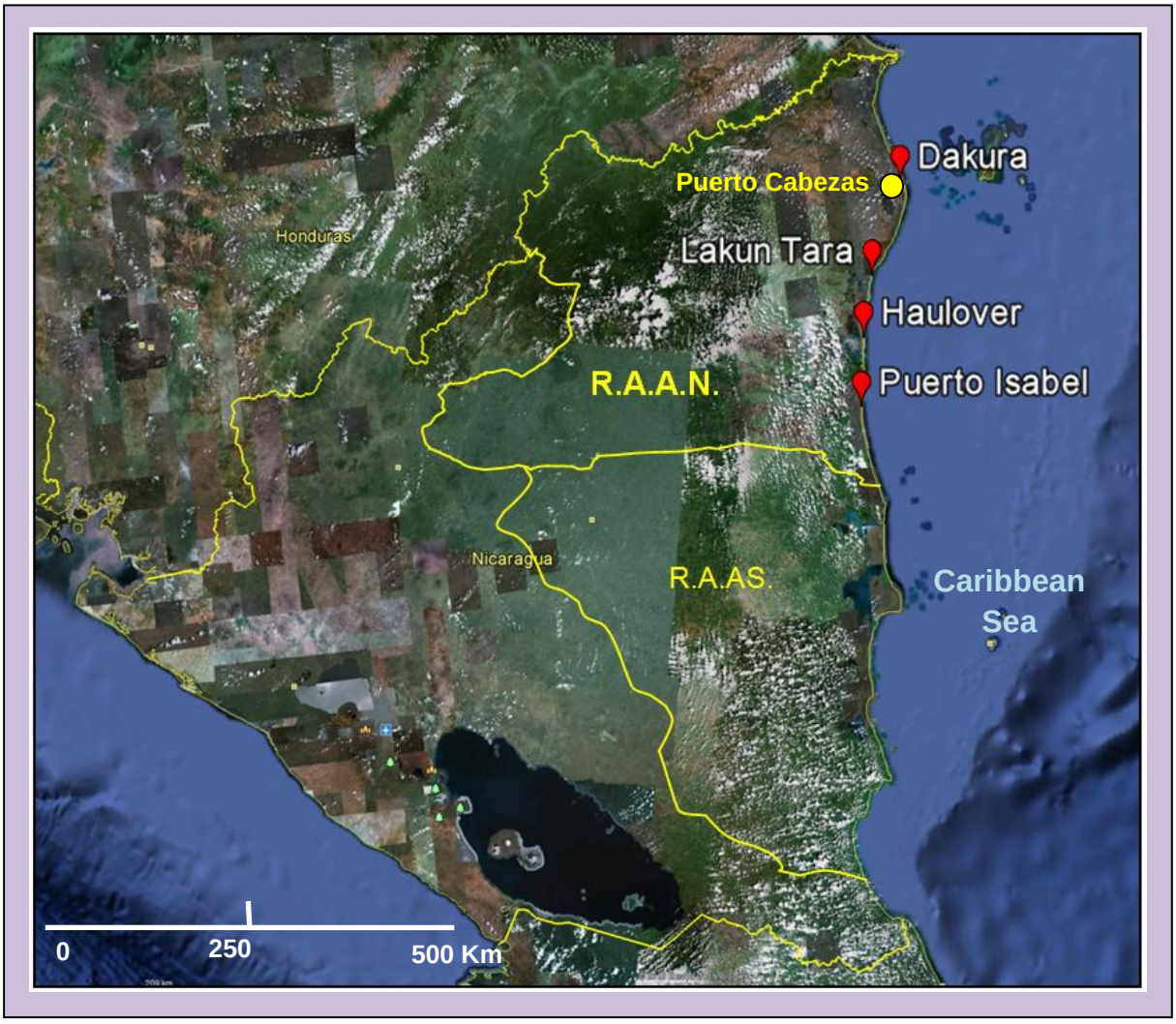

Figure 6.4: Coring Sites in RAAN, Nicaragua.

6.5.1 Dakura

The coring sites are near the village of Dakura which is about 40 km north of Puerto Cabezas (Figure 6.4). Lake Dakura is a lagoon connected to the sea by a narrow channel (Figure 6.5). There are seasonal marshes around this area with low bushes in the front of the ocean and higher bushes towards the back. This area had extensive damage from Hurricane Felix which made landfall in 2007

Figure 6.5: Coring locations for DAK 2 and DAK 3 near Lake Dakura.

Coring for DAK 2 and DAK 3 were done in mud holes (areas of depression filled with water) (Figures 6.6). DAK 2 is a 220 cm long core and was extracted 250 m from the sea. There is a sand field in front of this location (between the sea and the coring site). This core has 9 layers of sand that indicate hurricane events (Figure 6.7). The first is at the top of the core and is about 7 cm thick (0-7 cm). Since Hurricane Felix in 2007, there hasn't been another hurricane strike in this area. For this reason this layer is assumed to be an overwash deposit from Hurricane Felix. The other 8 layers are at: 27-33 cm, 78-82 cm, 98-102 cm, 134-144 cm, 162-166 cm, 170-173 cm, 180-185 cm, and 210-215 cm.

Figure 6.6: Coring site for Lake Dakura cores is a water-filled depression where DAK 2 and DAK 3 were extracted.

Three organic samples were dated from this core and calibrated to conventional ages. The first sample was taken from 75 cm depth and was dated at a radiocarbon age of 1,250+/-30 ^{14}C BP and a calibrated age of 1,220 cal yr BP (Table 6.1). The second sample at 145 cm was dated at 1,290+/-30 ^{14}C BP and calibrated date of 1,265 cal yr BP, and the third sample (basal) was obtained from 217 cm depth and dated at 1,300+/-30 BP radiocarbon age and the conventional

age of 1,270 BP (Table 6.1). The close dates of 1,265 cal yr BP and 1,270 cal yr BP at a 75 cm difference in depth indicate an error in estimation of one of those dates. If the date of 1,265 cal yr BP is correct at 145 cm, then there are 5 events that are indicated in the core above it. This means that this area experienced a hurricane return period of 253 years. On the other hand if the 1,270 cal yr BP date is correct at 217 cm then the return period of hurricanes is 141 years. For probability analysis in this dissertation, the date of 1,265 at 145 cm was used as it seems more probable considering that the sediment at 75 cm was dated at 1,220 cal yr BP.

DAK 3 location is about 6 km north of DAK 2 and is 150 m inland. This core is 295 cm long and contains mostly clay with some peat and sand layers (Figure 6.8). Four sand layers were found in this core using visual and LOI analysis. These layers were at: 0-8 cm, 10-20 cm, 30-35 cm, and a thick layer at the bottom of the core at 243-300 cm. Both cores exhibit two sand layers on the top that are presumably from the same events as they are found at consistent depths in the two cores.

Other than these layers, the stratigraphies of DAK 2 and DAK 3 cores are very different. The reason for the difference in stratigraphies of DAK 3 from that of DAK 2 is most likely because DAK 2 site has a sand field in front of it making it more sensitive to overwash deposits. DAK 3 is near the mouth of water channel and the presence of clay in most of the core indicates frequent flooding of the inlet.

Table 6.1: Calibration results for DAK 2 at 75 cm, 145 cm and 220 cm depth using Calib 6.0 (Reimer *et al.*, 2009).

Core	Depth (cm)	Laboratory Number	Material Dated	Radiocarbon Age BP	Cal BP (2σ)	Relative Area under Probability Distribution	Intercept Date
DAK 2C	75	OS-80987	Plant/Wood	1250 +/- 30	1114 -1082	0.083	
					1273-1120	**0.917**	**1,220 BP**
DAK 2D	145	OS-74958	Plant/Wood	1290 +/- 30	**1287-1175**	**1**	**1,265 BP**
DAK 2E	217	OS-74959	Plant/Wood	1300 +/- 30	1215-1178	0.34	
					1289-1220	**0.66**	**1,270 BP**

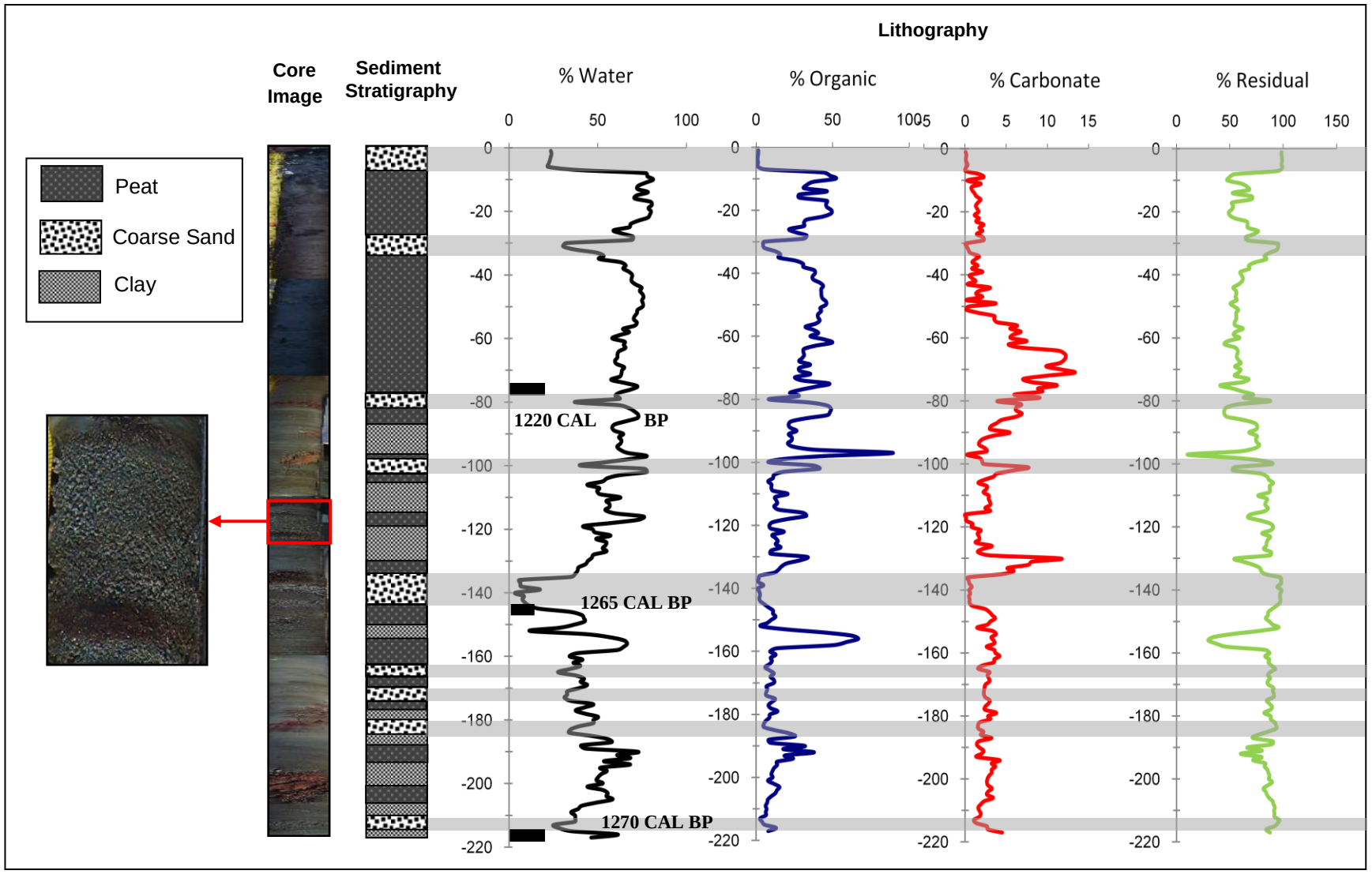

Figure 6.7: Loss-on-ignition and sedimentological analysis of Dakura core DAK 2.

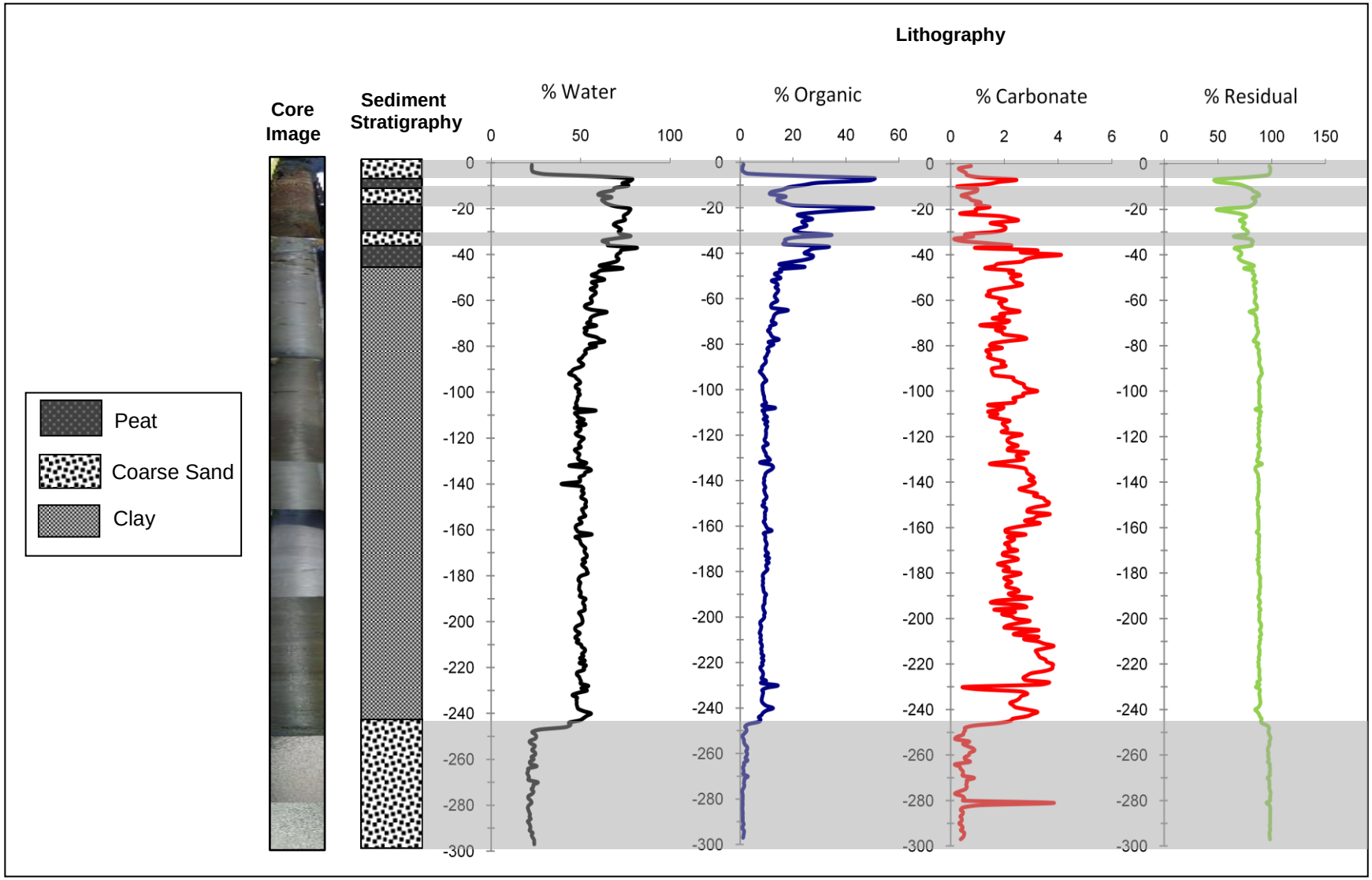

Figure 6.8: Loss-on-ignition and sedimentological analysis of Dakura core DAK 3.

6.5.1.1 ^{137}Cs and ^{210}Pb Dating of DAK 3

The top 30 cm of the DAK 3 core was sampled at 3 cm intervals for ^{137}Cs and ^{210}Pb activity determination by using gamma spectrometry for ≥ 24 hours each. A ^{137} Cs peak was found at 7 cm depth (Figure 6.9) indicating that the sediment at this depth was deposited in 1963.

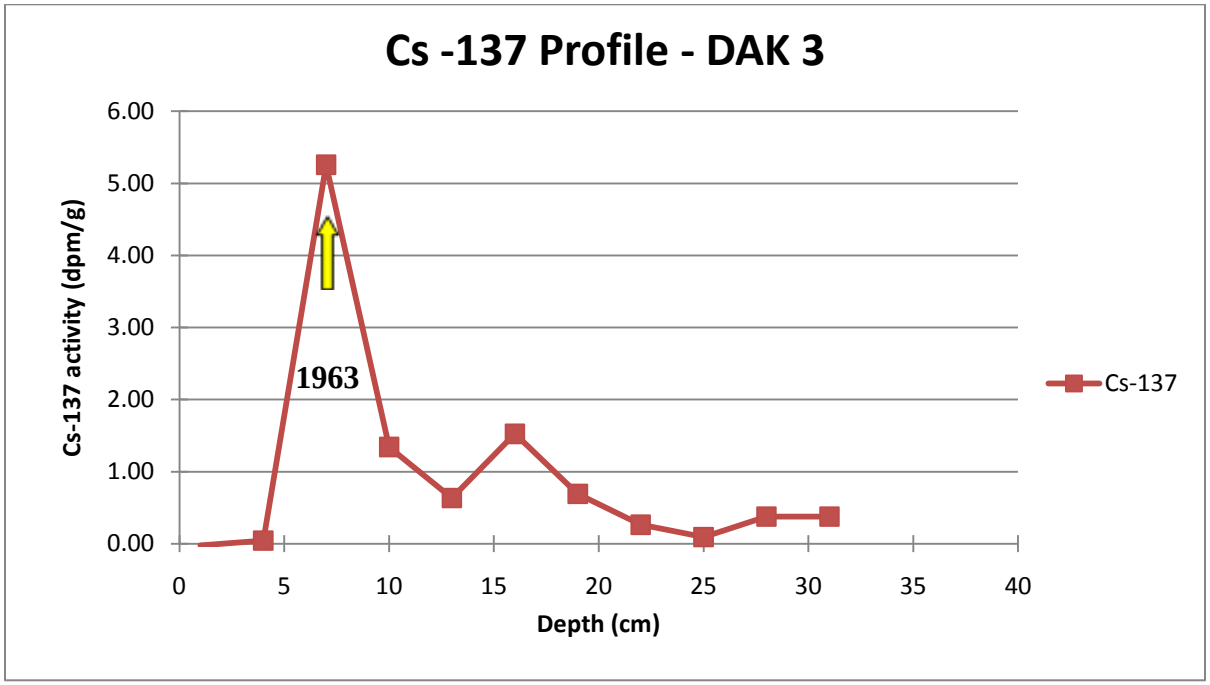

Figure 6.9: ^{137}Cs activity versus depth plot. The peak at 7 cm indicates 1963 as the year of deposition of the sediment at that depth.

The slope derived from the log of excess ^{210}Pb activity versus depth line (Figure 6.10) is used in calculating the sedimentation rate of the top 30 cm of the core. ^{210}Pb decay constant λ (0.03114 yr^{-1}) divided by the slope (-0.049) gives the sedimentation rate of 0.177 cm/year. This rate is in agreement with the ^{137}Cs derived rate of 0.149 at this depth. ^{210}Pb rate is used for calculating the year of occurrence for recent storms as it can be used for the last 110-130 years as opposed to for ~50 years for ^{137} Cs dating.

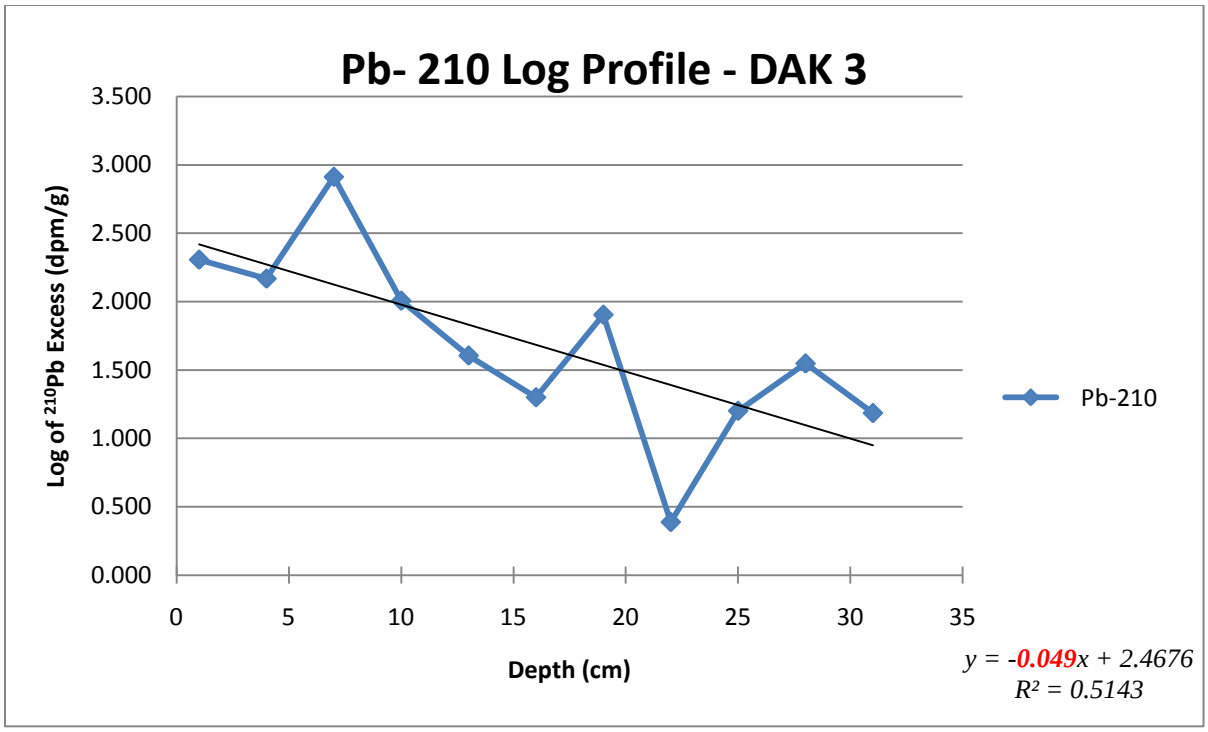

Figure 6.10: Log of excess ^{210}Pb versus depth plot.

6.5.2 Lake Lakun Tara and Llano de German

6.5.2.1 Lake Lakun Tara

Lakun Tara is an inland lake 130 m from the sea. It is close to the Laguna De Karata which is a large freshwater lake (Figure 6.11). It is a waist deep lake surrounded by red mangroves and a *Typha* island at the entrance (Figure 6.12). According to locals, the entrance to the lake was open to the sea about 10 years back but is closed now by the *Typha* island.

One core measuring 250 cm was extracted from this site at a distance of 135 m from the sea. This core contains mainly clay, peat, and sand (Figure 6.13). The first 50 cm of this core is sand with two layers of peat in it. This sand could be attributed to the open entrance of the lake to the sea 10 years ago. There are 11 layers of sand in the core that indicate hurricane events in the past (Figure 6.13). The eleven layers are as follows: 0-10 cm, 15-40 cm, 46-52 cm, 96-102 cm, 110 -116 cm, 130-138 cm, 182-187 cm, 195-199 cm, 205-210 cm, and at 228-234 cm.

Figure 6.11: Coring locations for Lake Lakun Tara and Llano de German cores, LKT 1, LLGM 1, and LLGM 2.

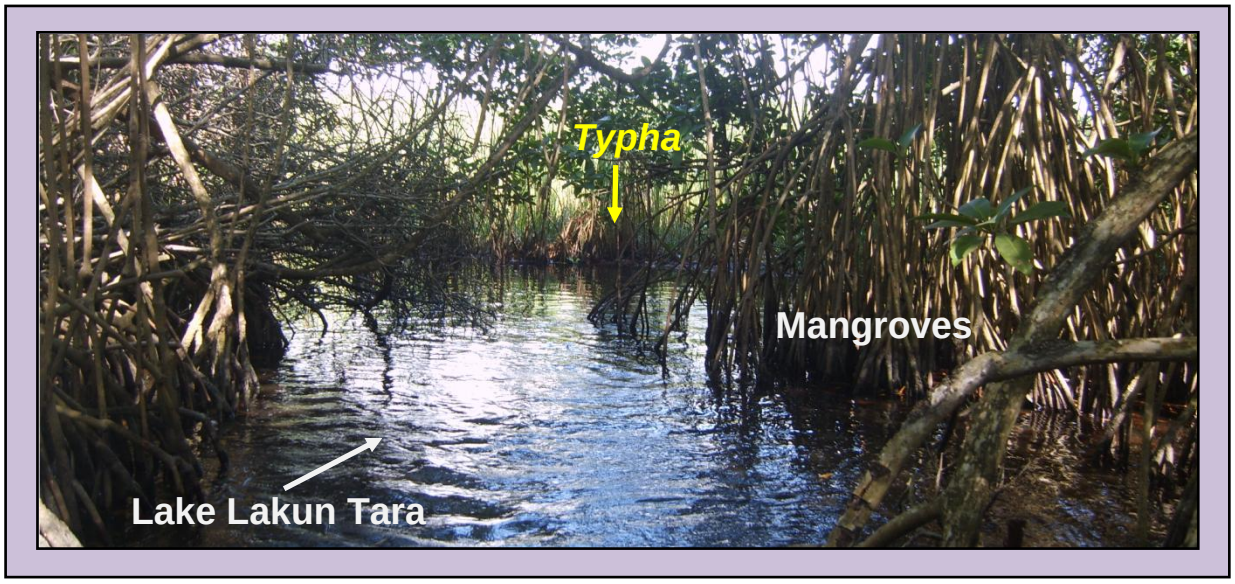

Figure 6.12: Lake Lakun Tara surrounded by red mangroves and *Typha* at the entrance of the water body.

Two organic samples were dated and calibrated from this core; one at 185 cm and a basal sample at 246 cm (Table 6.2). Sample at 185 cm was dated at 3,890 cal yr BP. The sample at 246 cm was dated at 4,545 cal yr BP. A return period of 413 years was calculated by taking into account the 11 event records over a course of 4,545 years.

Table 6.2: Calibration results for LKT 1 at 185 cm and 246 cm depths using Calib 6.0 (Reimer *et al.*, 2009).

Core	Depth (cm)	Laboratory Number	Material Dated	Radiocarbon Age BP	Cal BP (2σ)	Relative Area under Probability Distribution	Intercept Date
LKT 1D	185	OS-74953	Plant/Wood	3590 +/- 40	3748-3728	0.021	
					3792-3765	0.033	
					3987-3823	**0.929**	**3,890 BP**
					4065-4047	0.017	
LKT 1E	246	OS-75018	Plant/Wood	4070 +/- 45	**4652-4426**	**0.79**	**4,545 BP**
					4704-4669	0.062	
					4809-4757	0.148	

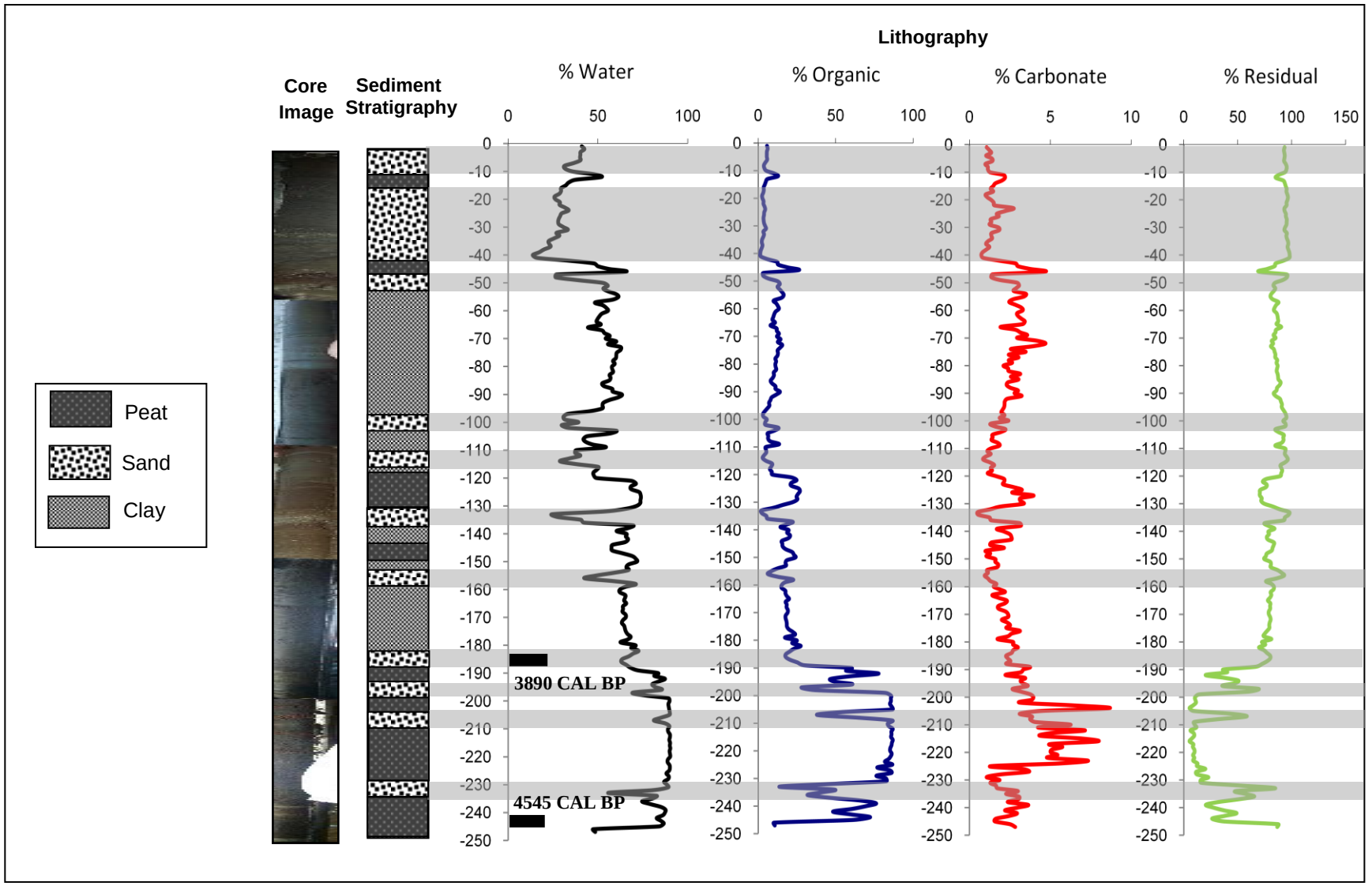

Figure 6.13: Loss-on-ignition and sedimentological analysis of Lake Lakun Tara core LKT 1.

6.5.2.2 Llano de German

Llano de German site is about 2 km north of Lake Lakun Tara (Figure 6.11). Two cores were extracted from Llano de German, LLGM 1 and LLGM 2. The coring location for LLGM 1 is dominated by mangroves and LLGM 2 site has mostly *Typha* vegetation (Figures 6.14 A and B).

Figure 6.14: Coring sites for Llano de German (A) LLGM 1 was extracted in allocation with mangroves. (B) LLGM 2 was extracted in further inland in a location with *Typha*.

LLGM 1 coring site was 70 m inland from the sea (Figure 6.11) and it is a 345 cm long core. This core consists of mainly sand, peat, and clay. This core has 10 layers of sand at: 34-39 cm, 50-58 cm, 60-70 cm, 85-91 cm, 95-102 cm, 115-119 cm, 212-222 cm, 272-280 cm, 320-330 cm, and 340-345 cm (Figure 6.15).

An organic sample was extracted at 107 cm which is right below the event layer at 95-102 cm. This sample was dated at a radiocarbon age of 2,490 +/- 25 ^{14}C BP and an intercepted date of 2,590 cal yr BP (Table 6.3). Five event layers above the date of 2,590 BP at 107 cm depth indicate a return period of 518 years.

Table 6.3: Calibration results for LLGM 1 at 107 cm depth using Calib 6.0 (Reimer *et al.*, 2009).

Core	Depth (cm)	Laboratory Number	Material Dated	Radiocarbon Age BP	Cal BP (2σ)	Relative Area under Probability Distribution	Intercept Date
LLGM 1C	107	OS- 74960	Plant/Wood	2490 +/- 25	2719-2467	1	**2,590 BP**

LLGM 2 is a 300 cm long and was extracted 170 m inland from the sea (Figure 6.11). This core consists of mainly peat and clay with 5 layers of sand. The layers of sand are at: 11-15 cm, 20-24 cm, 26-30 cm, 248-254 cm, and 288-294 cm (Figure 6.16).

The top three layers (at 11-15 cm, 20-24 cm, and 26-30 cm) of sand in LLGM 2 (Figure 6.16) seem to correspond with the top three layers of sand (at 34-39 cm, 50-58 cm, and 60-70 cm) in LLGM 1 (Figure 6.15). However the stratigraphies of the two cores are less similar here-on possibly due to the location of LLGM 2 site which is farther inland and thus has not registered all the overwash sand layers visible in LLGM 1.

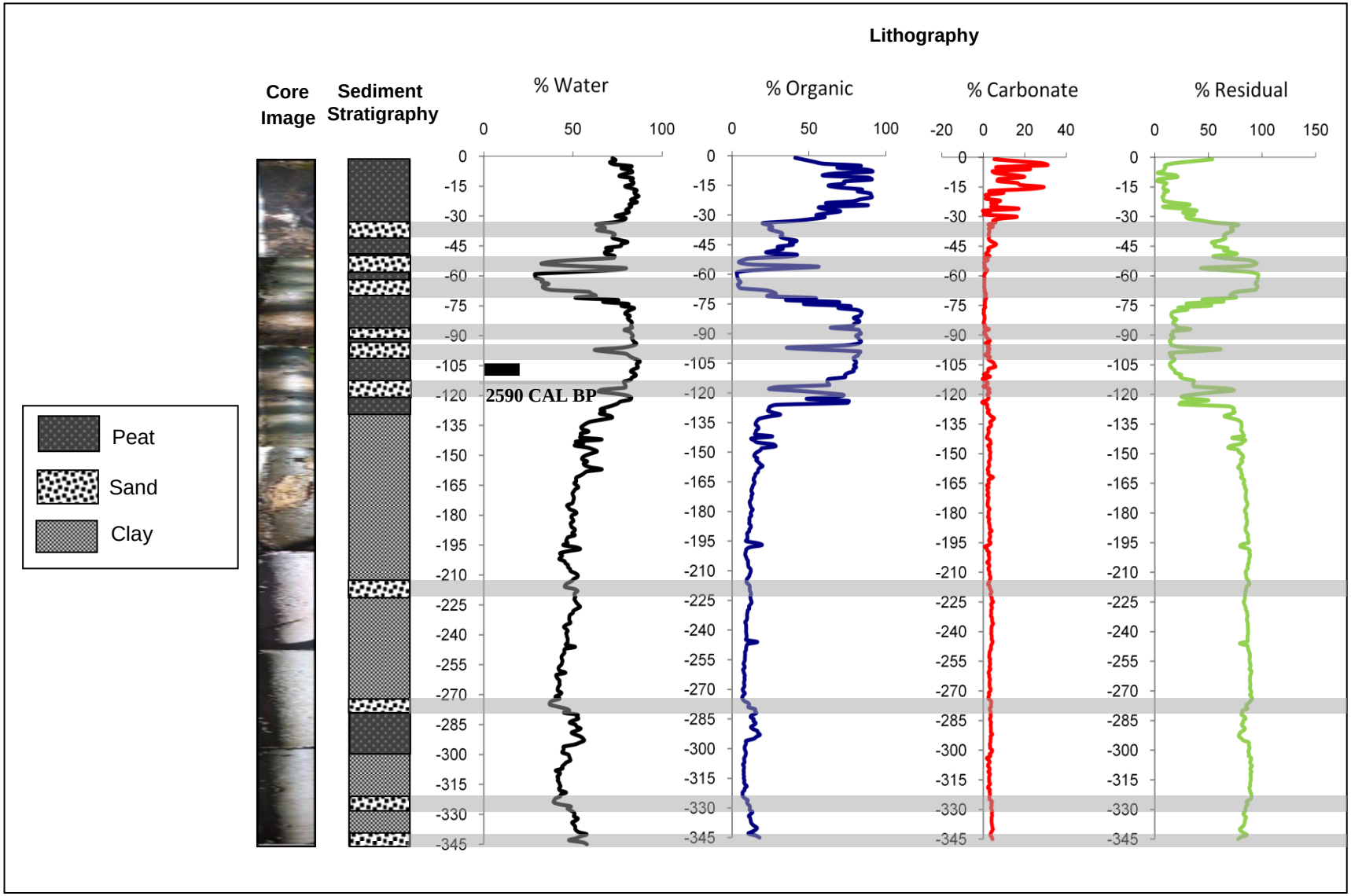

Figure 6.15: Loss-on-ignition and sedimentological analysis of Llano de German core LLGM 1.

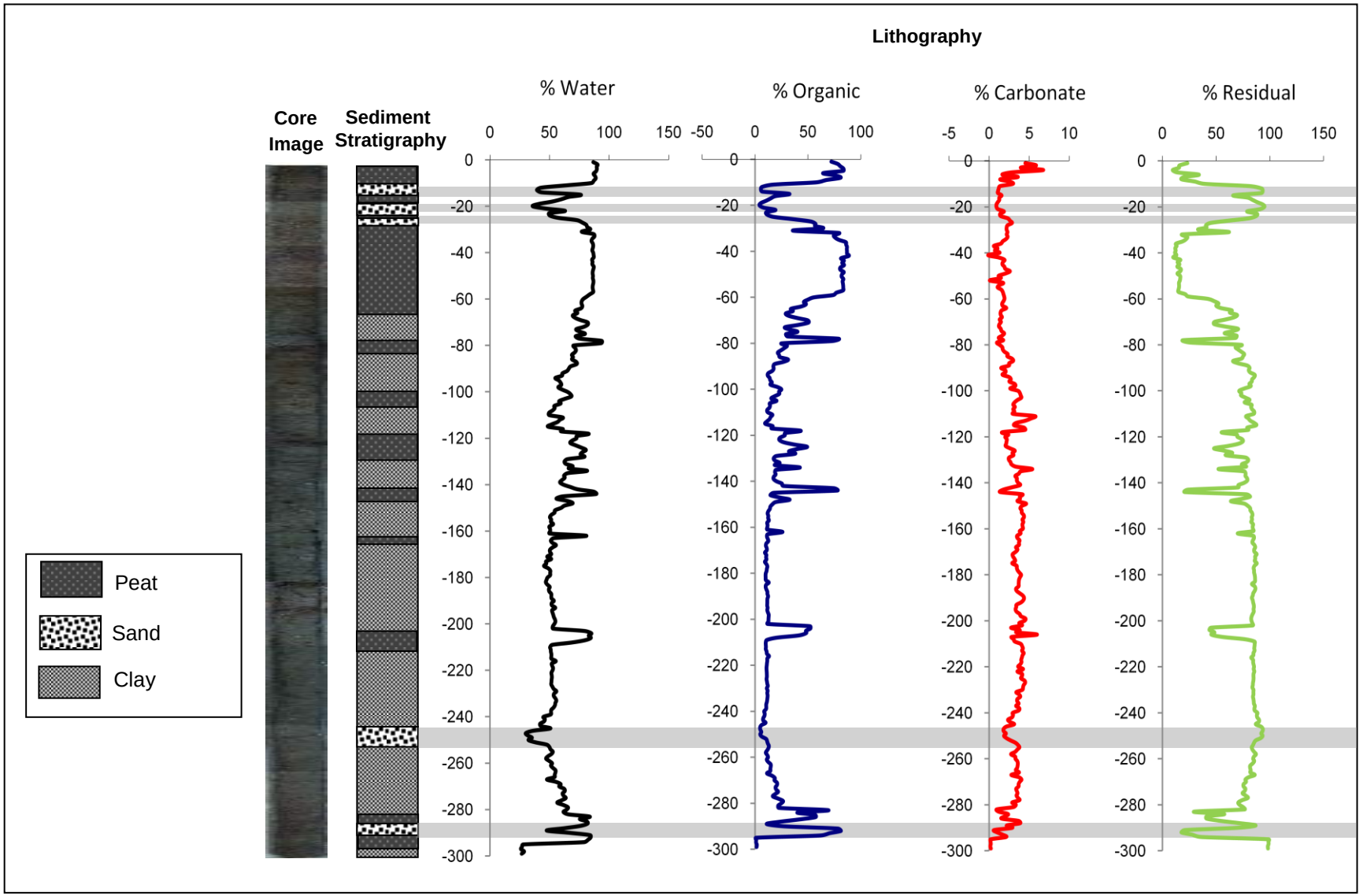

Figure 6.16: Loss-on-ignition and sedimentological analysis of Llano de German core LLGM 2.

6.5.3 Haulover

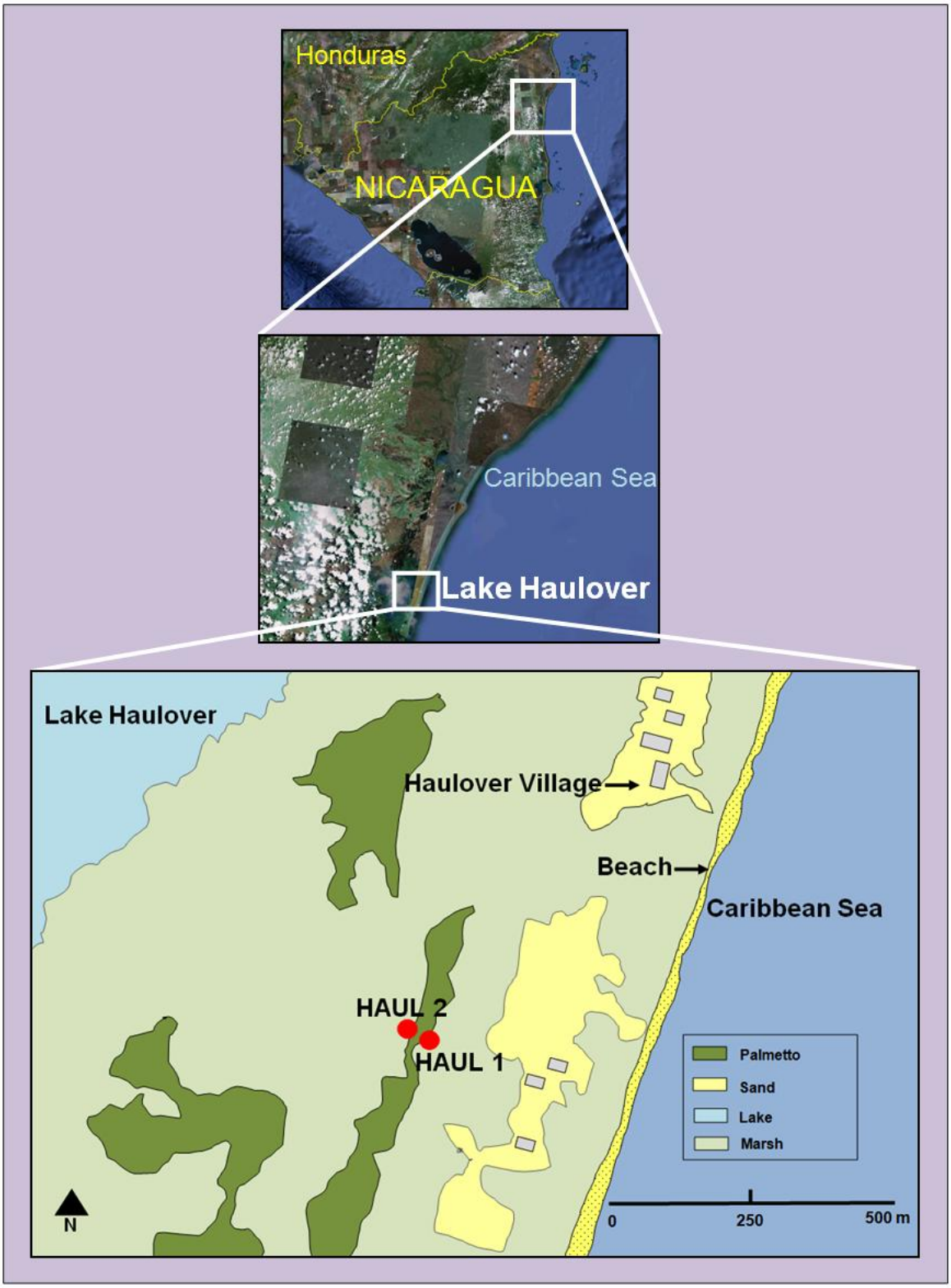

Figure 6.17: Coring locations for HAUL 1 and HAUL 3 near Lake Haulover.

Lake Haulover site is south of Lakun Tara and is close to the Haulover village (Figure 6.17). The coring sites are between the lake and the sea and dominated by palmetto and marsh (*Typha*) vegetation (Figure 6.18). There are sandy areas behind the beach which have thatched buildings which are most likely seasonal tourist shacks (Figure 6.17).

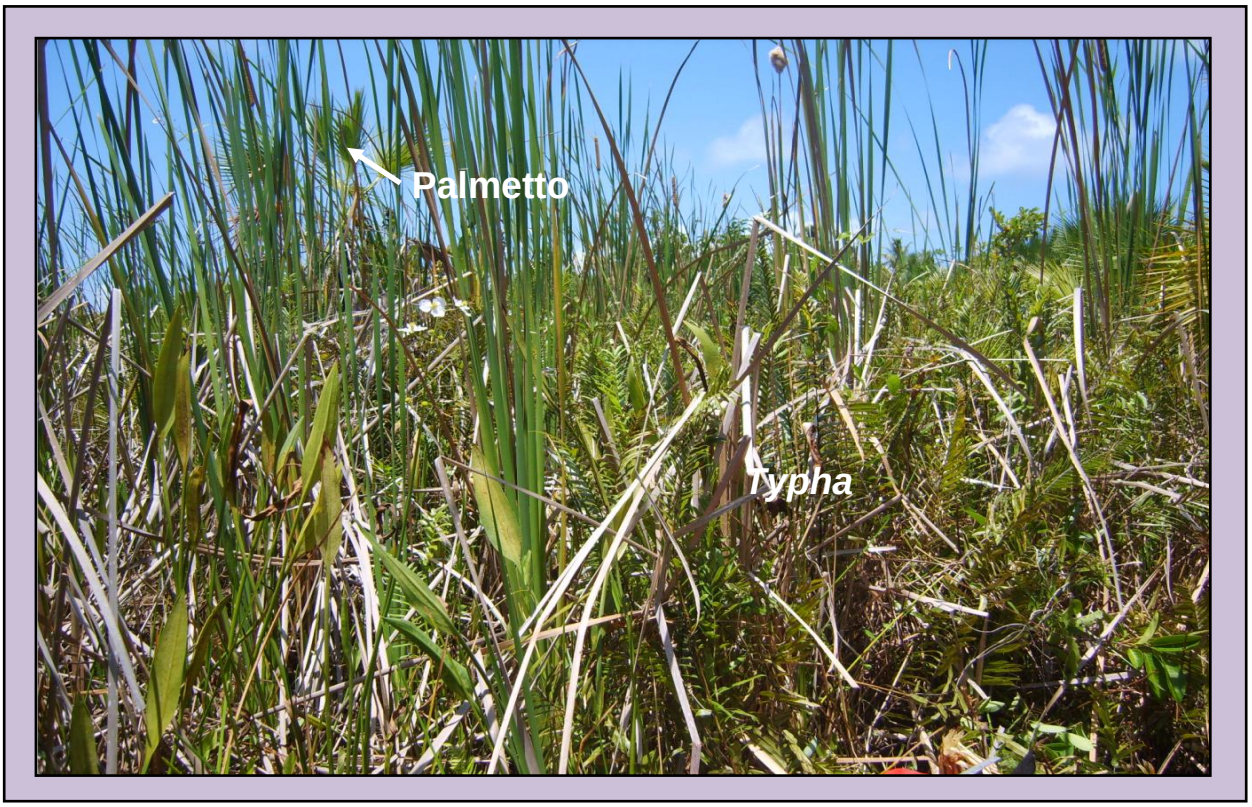

Figure 6.18: Coring location for Haulover cores HAUL 1 and HAUL 2.

Two cores were extracted from this site, HAUL 1 and HAUL 2. The two coring locations are close to each other (within a distance of 15 m). HAUL 1 is a 280 cm long core and was obtained 175 m from the sea. This core contains mainly peat and clay with 5 layers of sand (Figure 6.20) at 25-29 cm, 80-85 cm, 86-90 cm, 95-100 cm, and 259-262 cm.

HAUL 2 coring site is 185 m from the sea and the core extracted from here is 260 cm long. This core is similar to HAUL 1 in sediment composition. It too has mainly peat and clay with 4 layers of sand in it. The sand layers are at 35-38 cm, 75-80 cm, 90-94 cm, and at 105-115

cm (Figure 6.21). Four organic samples from HAUL 2 core were sent for radiocarbon dating. The result obtained and calibrated (Table 6.4) are as follows: the first sample at 35 cm was dated at the conventional age of 304 BP, second at 75 cm was dated at 3,200 BP, third at 106 was dated at 4,580 BP, and the fourth sample at 124 cm was had a conventional age of 4,845 BP. Four hurricane events in the last 4,845 years gave a return period of 1,211 years. Dates are consistent with depth R^2 =0.955 (Figure 6.19).

Table 6.4: Calibration results for HAUL 2 at 35 cm, 75 cm and 106 cm, and 124 cm depths using Calib 6.0 (Reimer *et al.*, 2009).

Core	Depth (cm)	Laboratory Number	Material Dated	Radiocarbon Age BP	Cal BP (2σ)	Relative Area under Probability Distribution	Intercept Date
HAUL 2B	35	OS- 80873	Plant/Wood	265 +/- 25	168-153	0.073	
					324-283	**0.635**	**304 BP**
					366-361	0.005	
					428-376	0.287	
HAUL 2B	75	OS- 80883	Plant/Wood	2970 +/- 30	3014-3006	0.006	
					3050-3030	0.019	
					3259-3060	**0.975**	**3,200 BP**
HAUL 2C	106	OS- 74954	Plant/Wood	4100 +/- 45	4472-4446	0.045	
					4730-4515	**0.719**	**4,580 BP**
					4743-4733	0.009	
					4821-4749	0.227	
HAUL 2C	124	OS- 74955	Plant/Wood	4200 +/- 35	**4765-4619**	**0.711**	**4,845 BP**
					4846-4785	0.289	

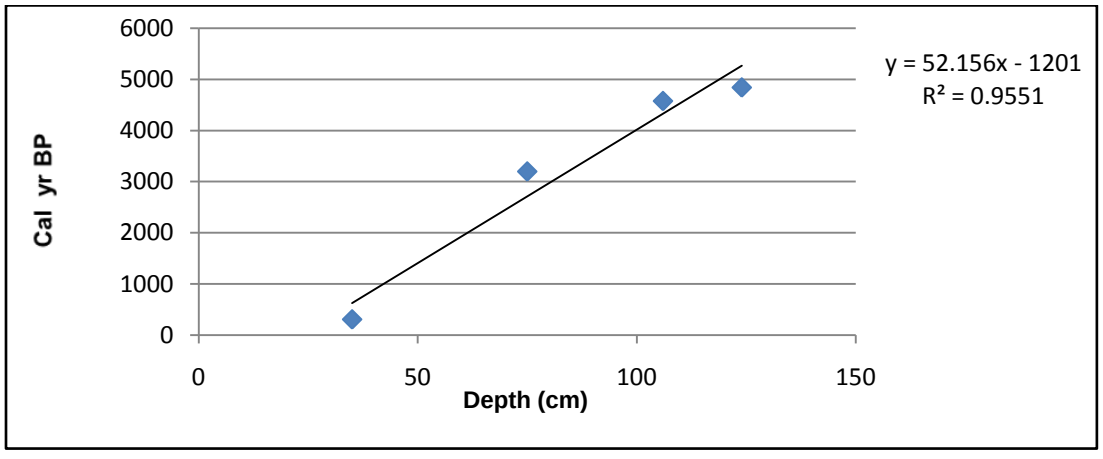

Figure 6.19: Depth-age graph for HAUL 2, showing the linear trend line and R^2 value for plotting of calibrated intercept dates.

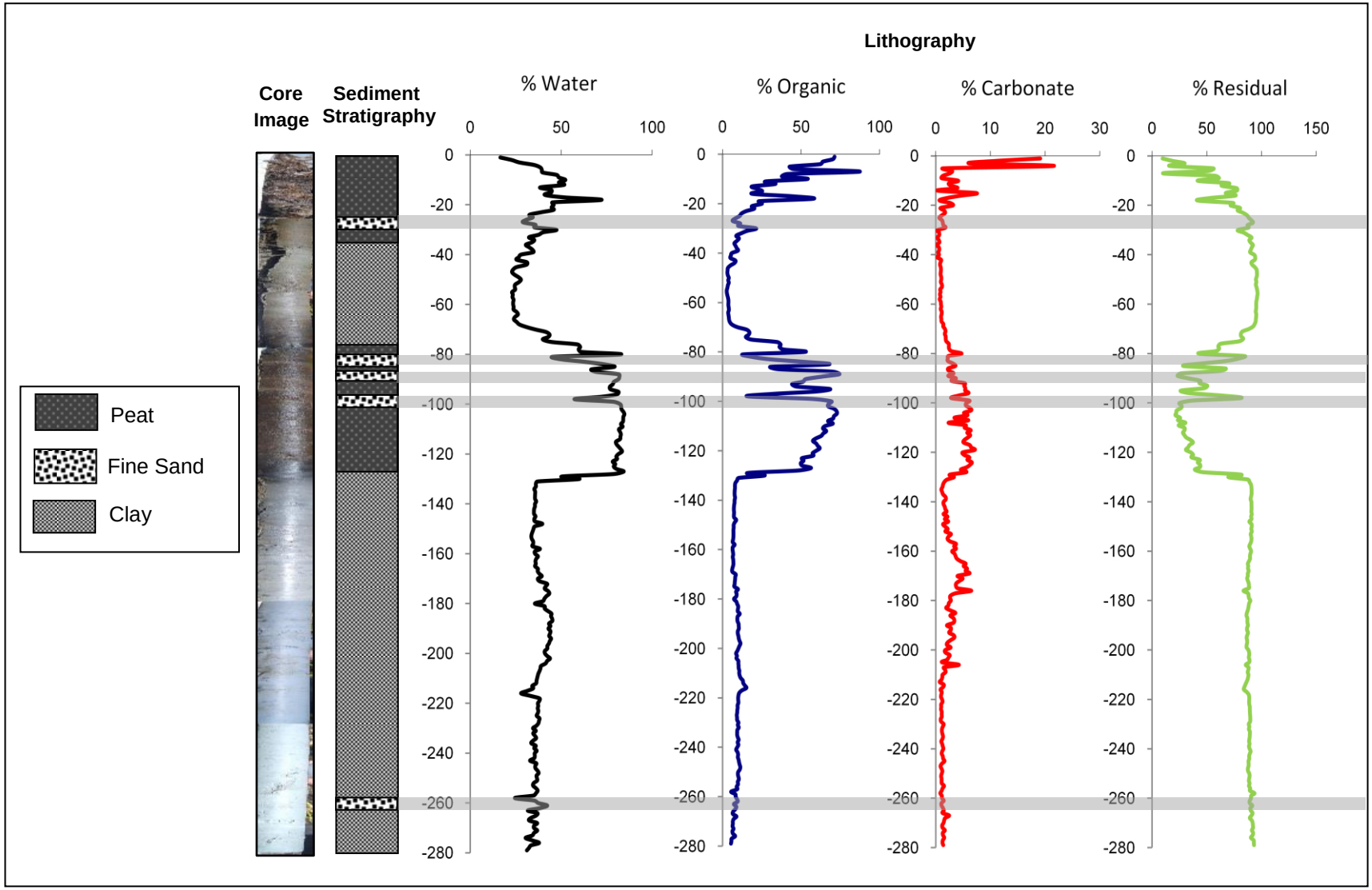

Figure 6.20: Loss-on-ignition and sedimentological analysis of Haulover core HAUL 1.

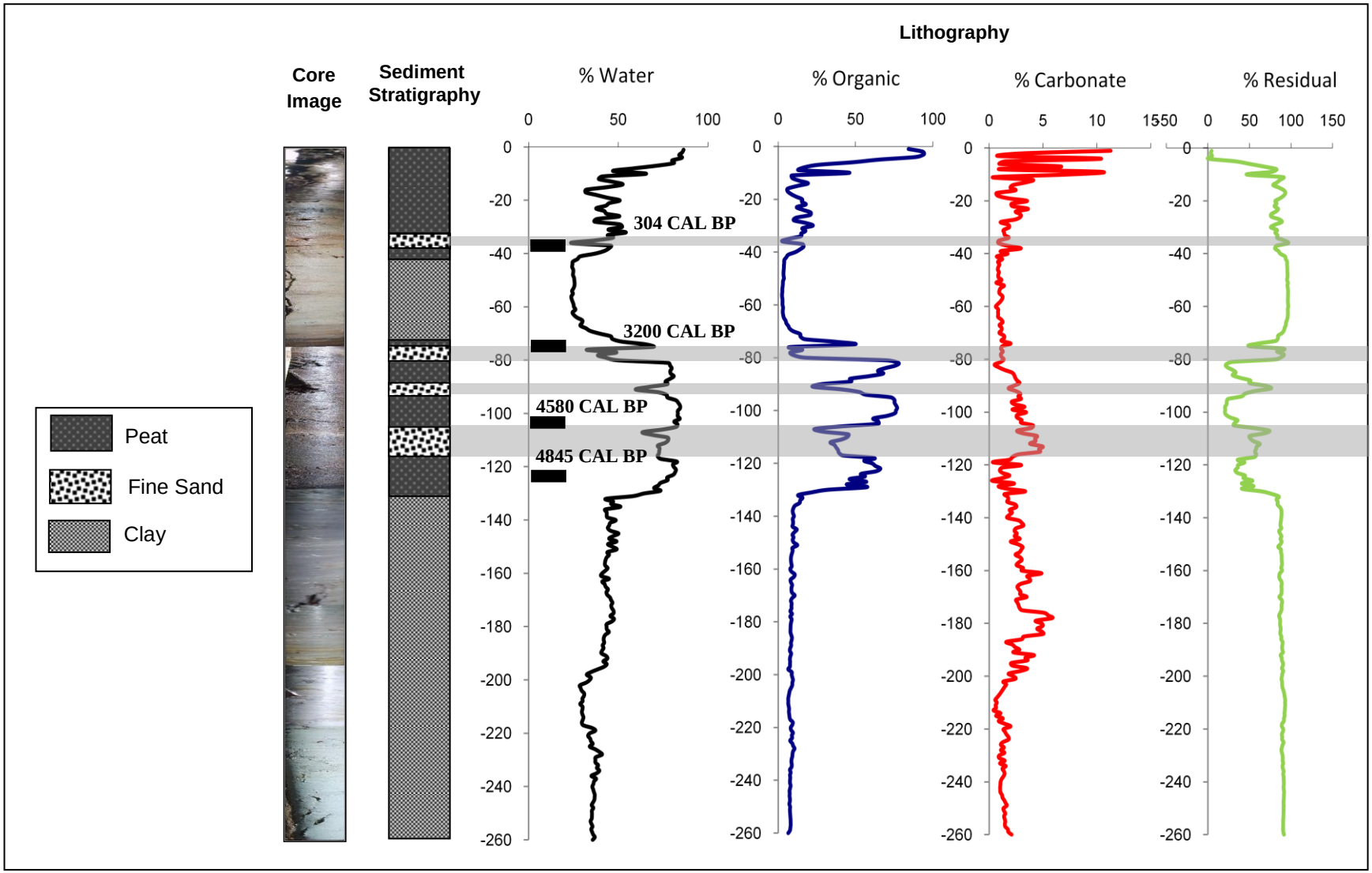

Figure 6.21: Loss-on-ignition and sedimentological analysis of Haulover core HAUL 2.

6.5.4 Puerto Isabel

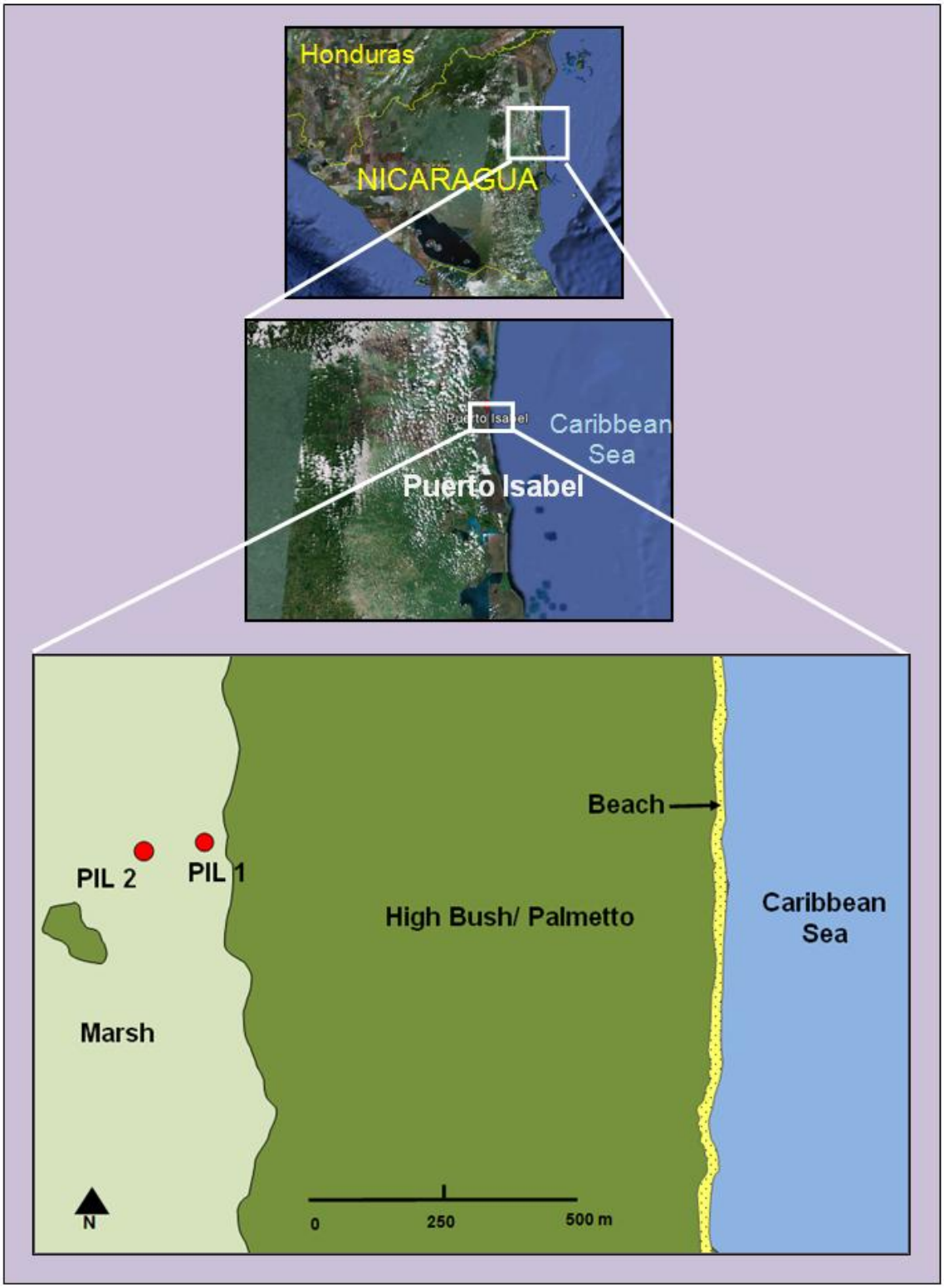

Figure 6.22: Coring locations for PIL 1 and PIL 2 near Lake Dakura.

Puerto Isabel site (Figure 6.22) is in a marsh close to the town of Puerto Isabel which is now abandoned. This was a big dock earlier but is not in operation now. The extensive marsh, where the cores were taken, is about 400 m wide and 2 km long. This is a *Typha* marsh with some Palmetto and high bush on the east of the marsh (Figure 6.23.A). This area burns a lot as is evident from the burnt palmetto stumps (Figure 6.23.B).

Figure 6.23: (A) Coring site for Puerto Isabel cores dominated by *Typha* vegetation (B) Burned Palmetto stumps indicating frequent fires.

Two cores were extracted from this site. The first core, PIL 1, was obtained from a spot that is 430 m from the sea and it is a 290 cm long core (Figure 6.25). This core consists of peat and clay with 8 layers of sand (Figure 6.25). The sand layers that indicate overwash events are at: 5-13 cm, 22-32 cm, 35-45 cm, 46-50 cm, 96-105 cm, 110-119 cm, 274-273 cm, and 281-290 cm.

PIL 2 was the longest and the oldest core obtained from RAAN, Nicaragua. It was cored farther inland, at 480 m from the sea (Figure 6.22), and is 470 cm long. This core has a similar sedimentary composition as core PIL 1 and comprises of peat and clay with 9 layers of sand in it (Figure 6.26). The sand layers are at: 11-18 cm, 20-25 cm, 27-31 cm, 121-129 cm, 135-148 cm, 163-170 cm, 210-218 cm, 232-246 cm, and 384-389 cm.

Five samples were sent for radiocarbon dating to NOSAMS (Table 6.5). The first sample at 35 cm was dated at the radiocarbon age of 1,030 +/-25 ^{14}C BP and the calibrated date of 950 cal yr BP. Second at 120 cm was dated in the radiocarbon age of 3,100 +/-40 ^{14}C BP and calibrated to 3,350 cal yr BP. Third was extracted at 238 cm and was dated at 3,460 +/- 35 ^{14}C BP This was calibrated to 3,750 cal yr BP. The fourth sample was obtained at 320 cm and dated at 2,120 +/-40 ^{14}C BP in radiocarbon years and 2,080 cal yr BP (Table 6.5). *(This date is younger than the age of the samples above the depth of 320 and thus was not considered reliable.) The fifth organic second sample was collected at 390 cm and was dated by NOSAMS at 6,550 +/- 40 ^{14}C BP and calibrated to 7,455 cal yr BP. Using this date of 7,455 cal yr BP and an indication of 9 events from sand proxy layers in the PIL 2 core, a return period of 828 years is calculated. Plotting of age versus depth revealed an R^2 value of 0.9341 (Figure 6.24).

Four activity regimes emerge from the LOI analysis (Figure 6.26) and dating of this core: (a) 0 to 950 cal yr BP (high activity), (b) 950 cal yr BP to 3,350 cal yr BP (low activity),

(c) 3,350 cal yr BP to 3,750 cal yr BP (high activity), (d) 3,750 cal yr BP to 7,750 cal yr BP (low activity), and >7,550 cal yr BP (not recording, submerged).

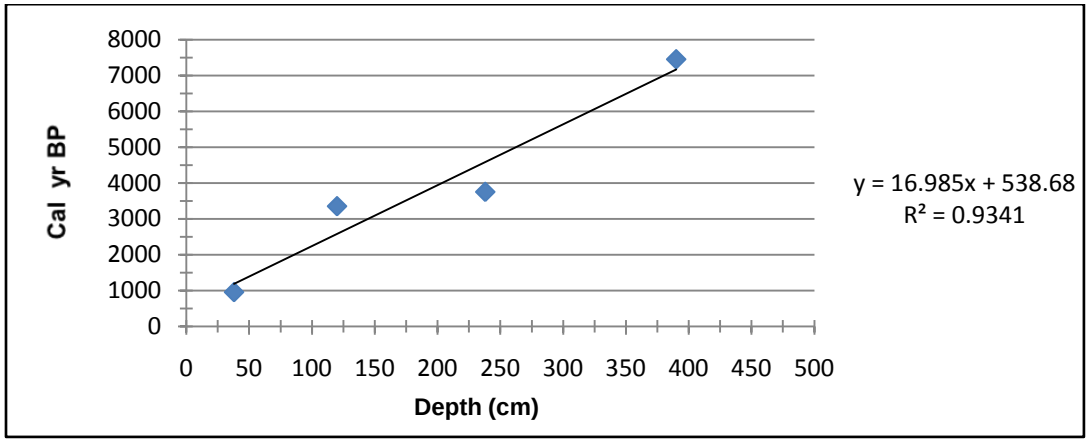

Figure 6.24: Depth-age graph for PIL 2, showing the linear trend line and R^2 value for plotting of calibrated intercept dates.

These results are in agreement with the study done by McCloskey (2009) in the southern part of the Mosquito Coast - at Falso Bluff Marsh. McCloskey's results also indicate a high activity period in the last millennium and a low activity period between 1,000 cal yr BP till 3,000 cal yr BP (McCloskey, 2009).

Table 6.5: Calibration results for PIL 2 at 38 cm, 120 cm, 238 cm, 320 cm, and 390 cm, depths using Calib 6.0 (Reimer *et al.*, 2009).

Core	Depth (cm)	Laboratory Number	Material Dated	Radiocarbon Age BP	Cal BP (2σ)	Relative Area under Probability Distribution	Intercept Date
PILL 2	38	OS- 80889	Plant/Wood	1030+/-25	**978-918**	**0.993**	**950 BP**
					1043-1039	0.007	
PILL 2	120	OS - 80988	Plant/Wood	3100+/-40	**3395-3215**	**1**	**3,350 BP**
PILL 2	238	OS - 74956	Plant/Wood	3460+/-35	**3831-3640**	**1**	**3,750 BP**
PILL 2	*320*	*OS - 80872*	*Plant/Wood*	*2120+/-40*	***2160-1991***	***0.878***	***2,080 BP****
					2178-2169	*0.009*	
					2301-2244	*0.113*	
PILL 2	390	OS - 74957	Plant/Wood	6550+/-40	7344-7346	0.002	
					7518-7418	**0.924**	**7,455 BP**
					7535-7563	0.074	

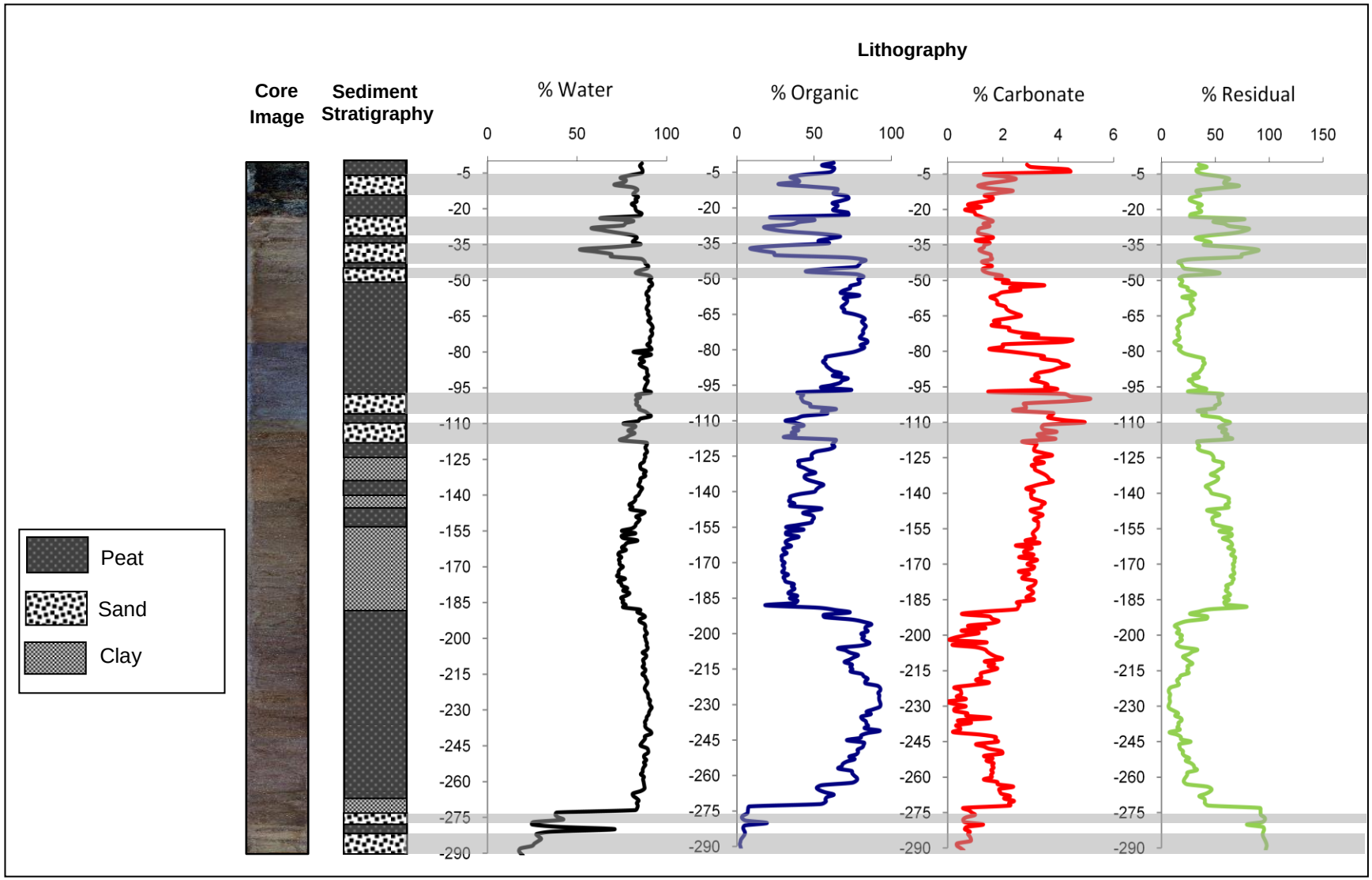

Figure 6.25: Loss-on-ignition and sedimentologial analysis of Puerto Isabel core PIL 1.

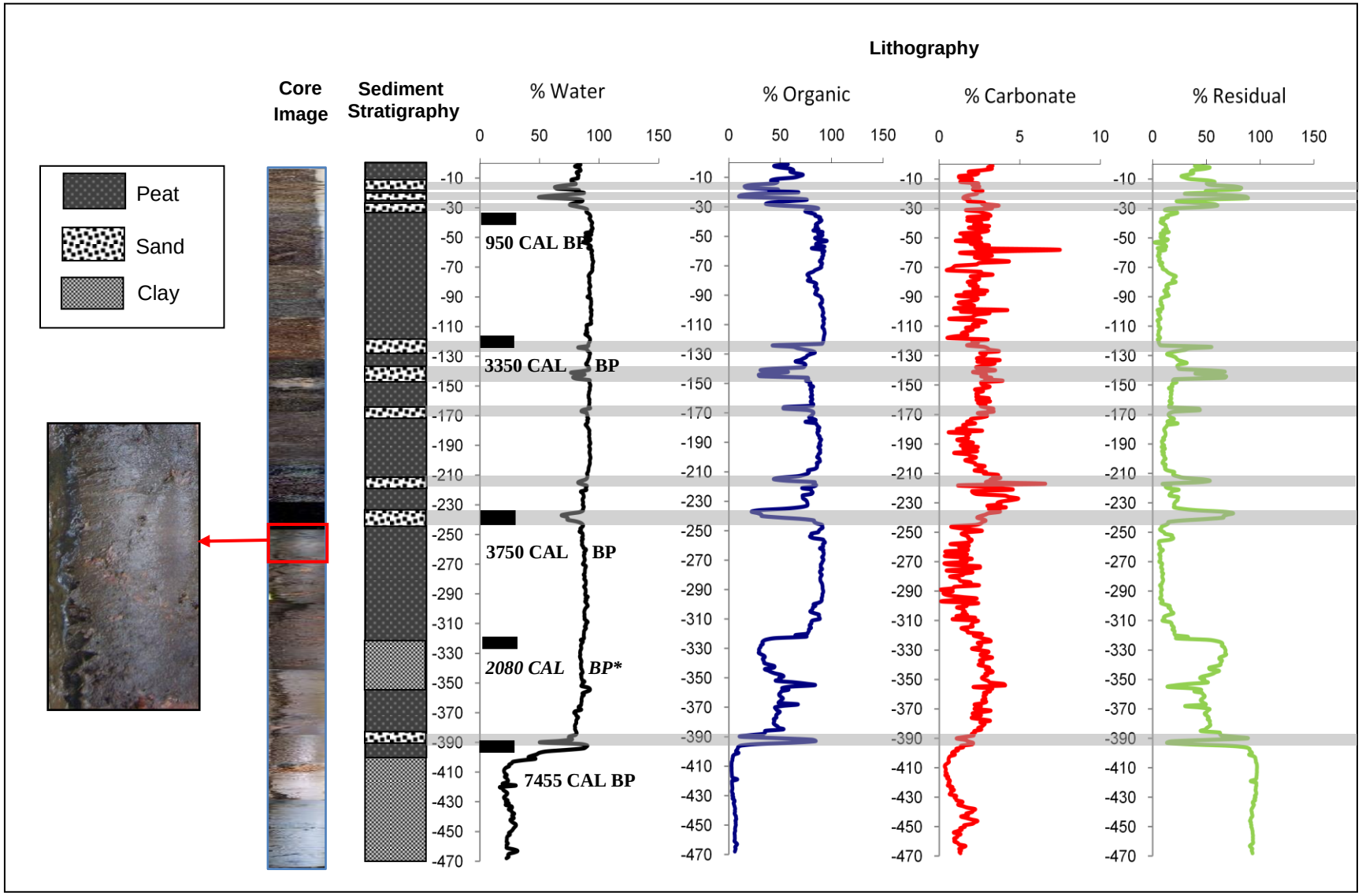

Figure 6.26: Loss-on-ignition and sedimentologial analysis of Puerto Isabel core PIL 2.

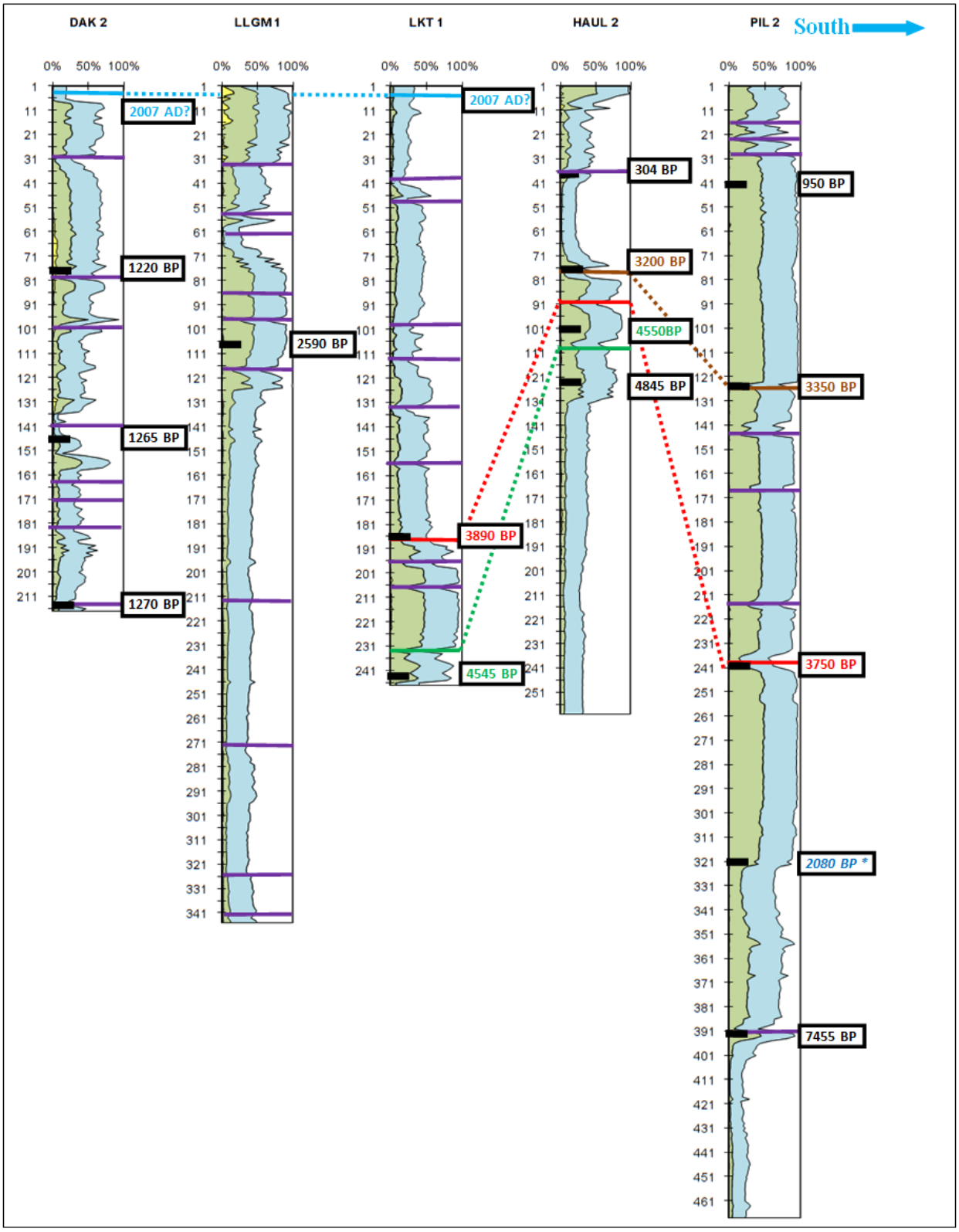

Figure 6.27: Transect showing cores from 5 locations in RAAN, arranged from north to south.

Correlation of cores from RAAN

The overwash layer visible on top of Dakura core DAK 2 is presumably from Hurricane Felix and it is also visible on top of Lakun Tara core LKT 1 (Figure 6.27) which is about 100 km south of the Dakura location (Figure 6.4). The Haulover site is about 70 km south of Lakun Tara (Figure 6.4) and cores LKT 1 and HAUL 2 have two layers that seem to be deposits from the same events. They are: 182-187 cm in LKT 1 correlates with 90-94 cm in HAUL 2, and 228-234 cm in LKT 1 correlates with 105-115 cm in Haul 2 (Figure 6.27).

Haulover and Puerto Isabel locations (Figure 6.4) are close to each other (~80 km) and cores Haul 2 and PIL 2 have two layers that are most likely from the same events. They are: 90-94 cm in HAUL 2 correlates with 232-246 cm in PIL 2, and 75-80 cm in HAUL 2 correlates with 121-129 cm in PIL 2. The event layer at 182-187 cm in LKT 1 is visible in 2 other cores; at 90-94 cm in HAUL 2 and 232-246 cm in PIL 2 (Figure 6.27).

6.6 Summary

All coring locations selected in RAAN had indication of multiple events, one going back 7,455 years. None of these layers were found to be tsunami deposits based on the two preliminary and visual criteria discussed in Chapter 2. Additionally, sediment composition of the event layers matches the composition of sand from the beach which has a low percentage of carbonates (Appendix A-2) supporting the view that sand was transported from the beach.

Cores from Lake Dakura site, DAK 2 and DAK 3 (Figures 6.7 and 6.8) have a storm deposit on the top indicating overwash from a recent event. This event is most likely Hurricane Felix (Figure 6.3.A) which made landfall in the Puerto Cabezas municipality (and very near the coring site) as a Category 5 storm in 2007.

Because only one modern analog was found in the Dakura core, and it was the highest

intensity hurricane - a Category 5, it is not possible to set a threshold for the minimum intensity needed to leave a record at the Dakura site. Consequently, it is difficult to ascertain the intensities of prehistoric hurricanes without analyzing new cores which may capture records of recent hurricanes with known intensities.

Four activity regimes emerged from the analysis of PIL 2 core as discussed in section 6.5.4. A high activity period until~1,000 cal yr BP and then a low activity period from 1,000 cal yr BP till about 3,300 cal yr BP are in agreement with a study done by McCloskey (2009). The return periods estimated from these cores ranged from 140 years to 1,211 years.

The probability of hurricane strike for Dakura is 0.4%, 0.24% for Lakun Tara, 0.19% for Llano de German, 0.08% for Haulover, and 0.12% for Puerto Isabel. This range indicates the varying sensitivity of the coring sites in RAAN. Using this information as a "prior" for Bayesian statistical analysis (Elsner and Bossak, 2001) of the historical storm records, future probability or "posterior" of landfall of hurricanes has been computed for RAAN in Chapter 7.

CHAPTER 7
RISK ANALYSIS OF RAAN, NICARAGUA

7. 1. Background

Nicaragua is at risk from multiple perils including volcanoes, earthquakes, and hurricanes. While the western part of the country is more prone to seismic hazards, the eastern coast is susceptible to hurricanes. This area lies in the zone of low activity (ranges from 1% -5% annual probabilities) for hurricanes (Pielke *et al*., 2003).

The coastal *Región Autónoma del Atlántico Norte* (RAAN) is part of the Mosquito Coast which runs on the eastern coast of Honduras and Nicaragua. The largest ethnic group in RAAN is that of the Miskitos who have lived in the Mosquito Coast for more than 300 years (Dodds, 2001). There are 120,817 Miskitos living in the Mosquito Coast of Nicaragua (INIDE, 2006). Of this 102,806 (INIDE, 2006) live in RAAN and the rest in *Región Autónoma del Atlántico Sur* (RAAS). They are part of a "contact culture" (Dodds, 2001) which has grown with the intermingling of the native American, African, and European people.

The Miskito communities were not prepared for a hurricane like Felix as Nicaragua does not regularly get affected by hurricanes. In a trip undertaken in February of 2009, coastal Miskito communities hit hardest by Hurricane Felix were visited. One and half years after the hurricane, these communities still hadn't recovered from the damage (Figure 7.1.A and 7.1.B). They alleged that they did not get warning about the approaching storm. Since there is a lack of road infrastructure and transportation leading to and out of these communities, evacuation and rescue work was also impeded for days.

7.2. Hurricane History

RAAN has been hit by 5 hurricanes in the last two centuries. Of these, the most

destructive were Edith in 1971 and Felix in 2007 making landfall as Category 5 storms. Hurricane Edith struck Nicaragua causing $380,000 (USD in 1971 dollars) in damage and killing 35 people.

Figures 7.1: (A) Tarp being used for roofs one and half years after Hurricane Felix (Sisin Village), and (B) School being held in open due to lack of proper structure.

The costliest hurricane in the history of the country was Hurricane Felix which caused extensive damage in the municipality of Puerto Cabezas (Figure 7.2.A-D). Hurricane Felix made landfall in the northern Mosquito Coast of Nicaragua on the 4th of September, 2007. According to the National Hurricane Center (NHC) advisory, the maximum sustained winds were of 160 mph (NHC, 2007). More than 130 people died in Nicaragua and more than 25,000 people were affected. The *Organización de las Naciones Unidas para la Agricultura y la Alimentación* (FAO) estimates agricultural losses alone to be $46.7 million USD (FAO, 2007).

Hurricane Mitch in 1998 hit Honduras but caused much damage and devastation in the neighboring RAAN. Since Mitch isn't considered a hurricane that made direct landfall in Nicaragua, it is not included in the analysis.

Figures 7.2: (A) Structure destroyed after Hurricane Felix. (B) Severe damage to Church from Hurricane Felix in Bilwi. (C) Wind damage to a Miskito home from Hurricane Felix in 2007. (D) Wind damage and roofs blown away in Bilwi, Puerto Cabezas (courtesy of INAFOR).

7.3 Socio-Economic Setting

The population of RAAN is 314,130 which include 158,169 men and 155,961 women (INIDE, 2006). Of the total population living in RAAN, 51,525 were children under the age of 5 and 7,784 over the age of 65 (Table 7.1). Both these groups are at the end of the age spectrum and are considered to be more vulnerable (Cutter *et al.*, 2003).

Three coastal municipalities in the department of RAAN that were considered for vulnerability analysis; they are Waspam, Puerto Cabezas and Prinzapolka. Most socio-economic

data available from the National Census of 2005 (INIDE, 2006) were collected at the departmental level and only limited information could be found at the municipal level.

Table 7.1: Demographic distribution of coastal municipalities in RAAN, Nicaragua.

Municipality	Total	Men	Women	Age<5	Age >65
Waspam	47,231	23,303	23,928	7,747	1,170
Puerto Cabezas	66,169	32,417	33,752	10,853	1,640
Prinzapolka	16,105	8,140	7,965	2,641	399
RAAN	**314,130**	**158,169**	**155,961**	**51,525**	**7,784**

Waspam is the northern-most municipality in RAAN and it borders Honduras. The population of Waspam is 47,231 of which 23,303 are men and 23,928 are women. Extrapolating from the population ratio of Waspam to RAAN, the number of children under 5 years and the number of aged over the age of 65 years were calculated (Table 7.1).

The municipality of Puerto Cabezas is south of Waspam, and Bilwi is the biggest town in this area. The population of this municipality is 66,169 making it the most populous municipality of the three coastal municipalities in RAAN. It also has the highest number of elderly and children under the age of 5 years (Table 7.1).

Prinzapolka is south of Puerto Cabezas and is relatively unpopulated. Its total population is 16,105 with most being Mikitos. The population of the elderly and children under the age of 5 is also the lowest of the three municipalities.

7.4 Calculation of Vulnerability Index

Women are more vulnerable to disasters because they are usually economically less stable and have to care for their children and family (Cutter *et al.*, 2003). The elderly and young children are less capable for caring for themselves during disasters this makes them more

vulnerable (Cutter *et al.*, 2003). They also may less mobile and dependent on other people. Thus all of these indicators - population, gender, children, and the elderly- contributed towards increasing vulnerability.

Census data obtained from *El Instituto Nacional de Información para el Desarrollo* (INIDE, 2006) provided information about the indicators of vulnerability that were used for calculations and mapping. Using this information, coastal areas were analyzed and mapped at the municipal level.

Puerto Cabezas has the highest score for all the vulnerability indicators (Figure 7.3). This municipality has almost 21% of the total population of RAAN and is vulnerable due to its high population (Table 7.1). The second most vulnerable municipality is Waspam which is north of Puerto Isabel. Prinzapolka is the least vulnerable due to its low population.

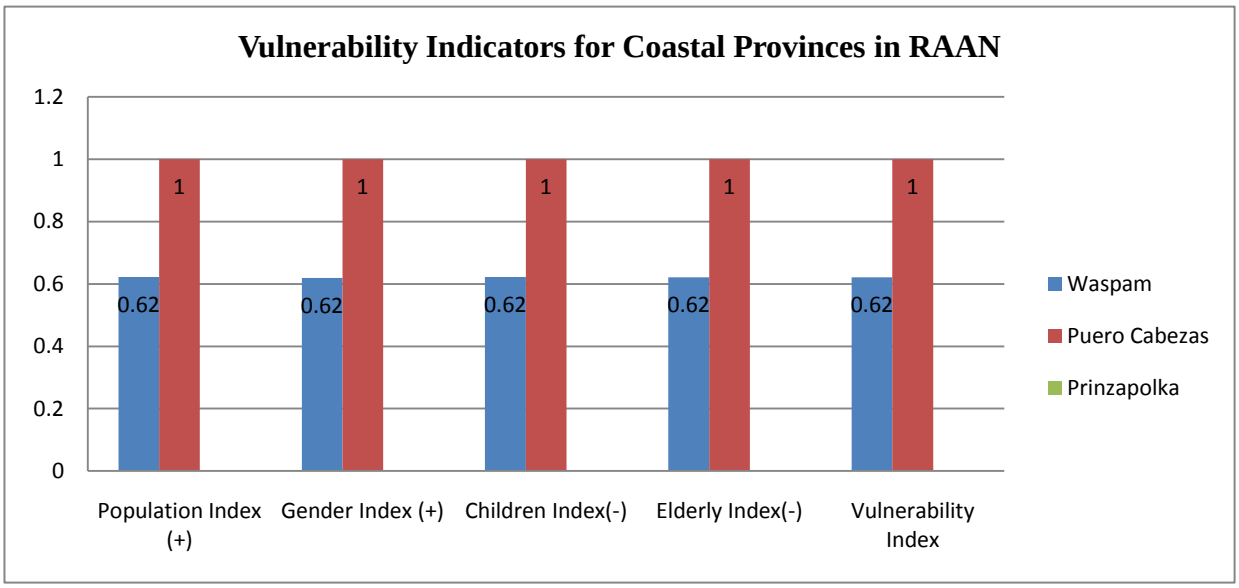

Figure 7.3: Histogram showing normalized indicators of vulnerability for each coastal province.

Other indicators such as poverty, access to roads, medical facilities etc., could not be found for either the departmental or the municipal level. Information for extremes in age cohorts

and gender were available for RAAN but not for the municipalities within it. A simple ratio method was used to deduce these indicators for the 3 municipalities based on the ratio of the municipal to the departmental population.

Using a rescaling methodology proposed by Brugglio (2003), the indicators were standardized such that each ranged from 0 to 1 and then combined and normalized again to create a composite index for each coastal province (Figure 7.4). This technique assigns equal weights to all indicators (Cutter *et al.*, 2003) before adding them up (Appendix B-3).

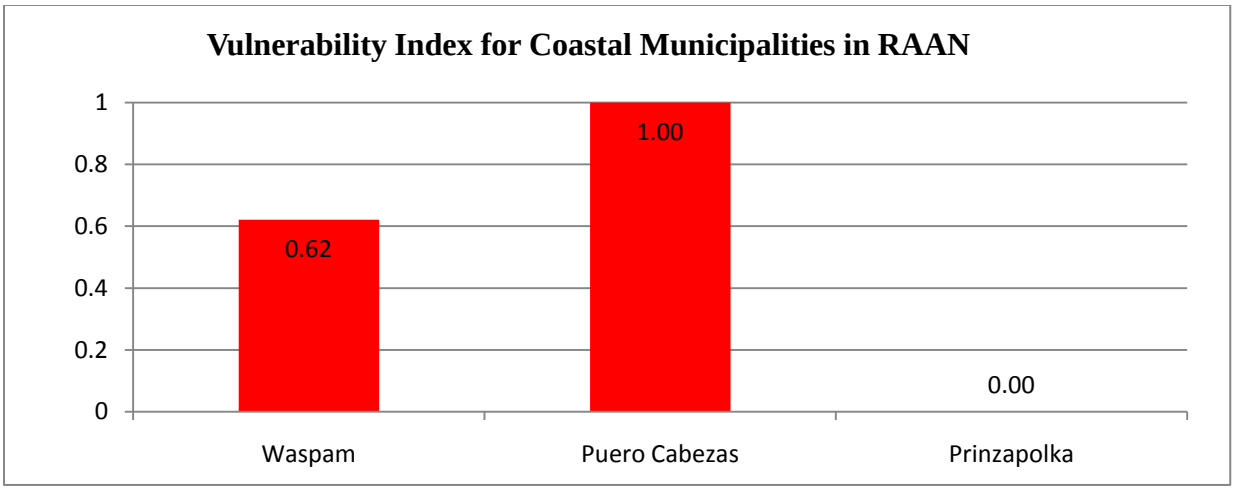

Figure 7.4: Histogram showing normalized total vulnerability score for each coastal municipality.

7.5 Calculation of Probability of Strike

Five hurricanes have made landfall in RAAN since 1851 (CSC, 2010). Using these past strikes, an average rate of return was derived for future hurricane landfall for RAAN. The number of strikes divided by the number of years gave an average rate of hurricane landfall for the last 160 years. Prehistoric records were obtained from cores from coastal lake sites in RAAN and an average rate of return for these hurricane events was treated as a separate Poisson process.

A Poisson distribution model to predict hurricanes was built on past hurricane data from the coastal municipalities in RAAN (Table 7.2). This distribution was calculated from the superposition of historic and prehistoric data (where available). By using the prehistoric record, a probability estimate was established especially for areas that have not had a hurricane in the last 160 years, for example, the municipality of Prinzapolka.

Table 7.2: Annual probability of occurrence of a hurricane. (NA represents locations where no paleo-records were found and/or dated.)

Municipality	Historic Landfalls	Rate of Return	Prehistoric Hurricanes	Rate of Return (Including Prehistoric Hurricanes)	Poisson Probability
Waspam	4	0.025	NA	0.025	0.024382748
Puerto Cabezas (Dakura)	1	0.0063	4	0.003952569	0.003936977
Prinzapolka (Puerto Isabel)	0	0	9	0.001207243	0.001205787

No coring was done in the municipality of Waspam and only the historic hurricanes were used for calculating the Poisson probability. Three sets of cores were extracted from the municipality of Puerto Cabezas from the following sites: Dakura, Llano de German, and Lakun Tara. But hurricane records from the Dakura core, DAK 2, were chosen for probability analysis as it also shows the presence of overwash sand from Hurricane Felix on the top of the core. This makes it an ideal core to separate the historic hurricane from the prehistoric record for the superposition of timelines for Poisson probability calculations (see Chapter 3).

Puerto Isabel cores were extracted from the municipality of Prinzapolka. The longer of the two cores, PIL 2, which is 7,455 years old and has recorded 9 overwash events, was used for estimating the rate of return of prehistoric storms. Historic hurricanes could not be separated as Cesium-137 and Lead-210 analysis was not done on this core to establish modern timeline.

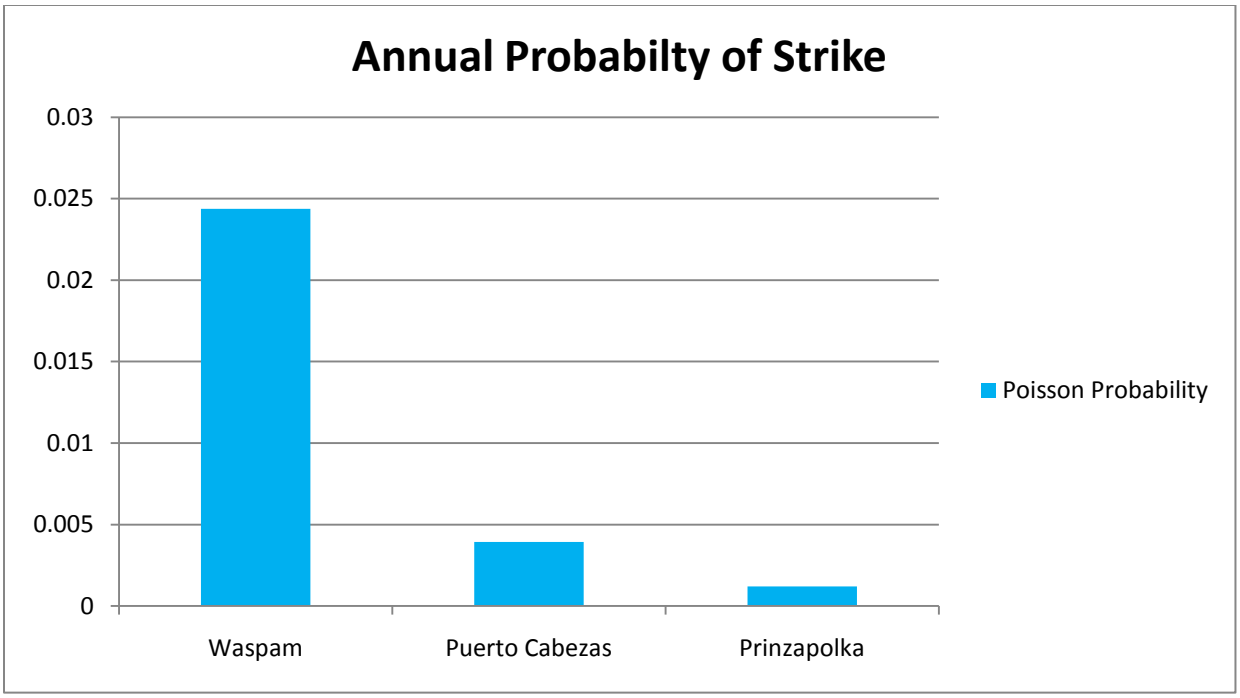

Figure 7.5: Annual probability of occurrence of a hurricane.

The probability of strike is the highest for the municipality of Waspam (Figure 7.5) because this municipality has had 4 hurricanes in the last 160 years. This figure may change if we add the information obtained from prehistoric records. However since no coring was done in this municipality, the likelihood of hurricanes is based on only the historic data.

Calculation of longer time frames and of multiple hurricane strikes is useful for insurance and building industry (Elsner and Kara, 1999). These calculations are used to estimate damage and loss from single and multiple hurricane strikes for varying time periods. Long term calculations for hurricanes in this region were done for multiple time periods using the likelihood of varying number of storms making a landfall (Appendix B–4).

7.6 Spatial Components of Risk for coastal RAAN

7.6.1 Mapping of Vulnerable Populations

Coastal population in RAAN consists of small villages and Miskito communities (Figures

7.6.A and 7.6.B) which rely on fishing for their livelihood. Coastal municipalities were ranked from highest to lowest in terms of their aggregate vulnerability score. These scores are represented spatially in Figure 7.7.

Puerto Cabezas is very vulnerable as it is the most populous municipality in RAAN. Hurricane Felix made direct landfall in this municipality in 2007 and caused extensive damage and loss of lives. The town of Bilwi in Puerto Cabezas municipality is the seat of the RAAN government. Damage to the only airport in the region which is in the town of Bilwi, impeded response and delivery of aid after the hurricane.

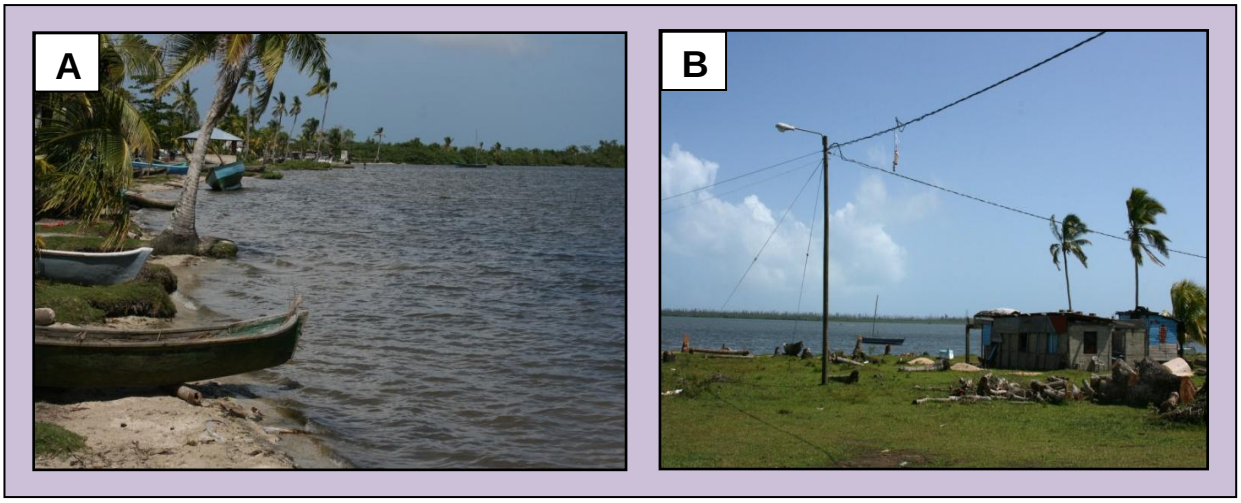

Figures 7.6: A and B. Fishing village near Dakura known as Krukira.

7.6.2 Mapping of Surge Inundation Potential

Hurricane surge potential was created for all five categories of storms using a flooding model discussed earlier in Chapter 3. This model uses a cost-distance analysis technique available in ArcGIS 9.3 to arrive at the inundation areas for different surge thresholds based on the 5 categories of storms (Figure 7.9).

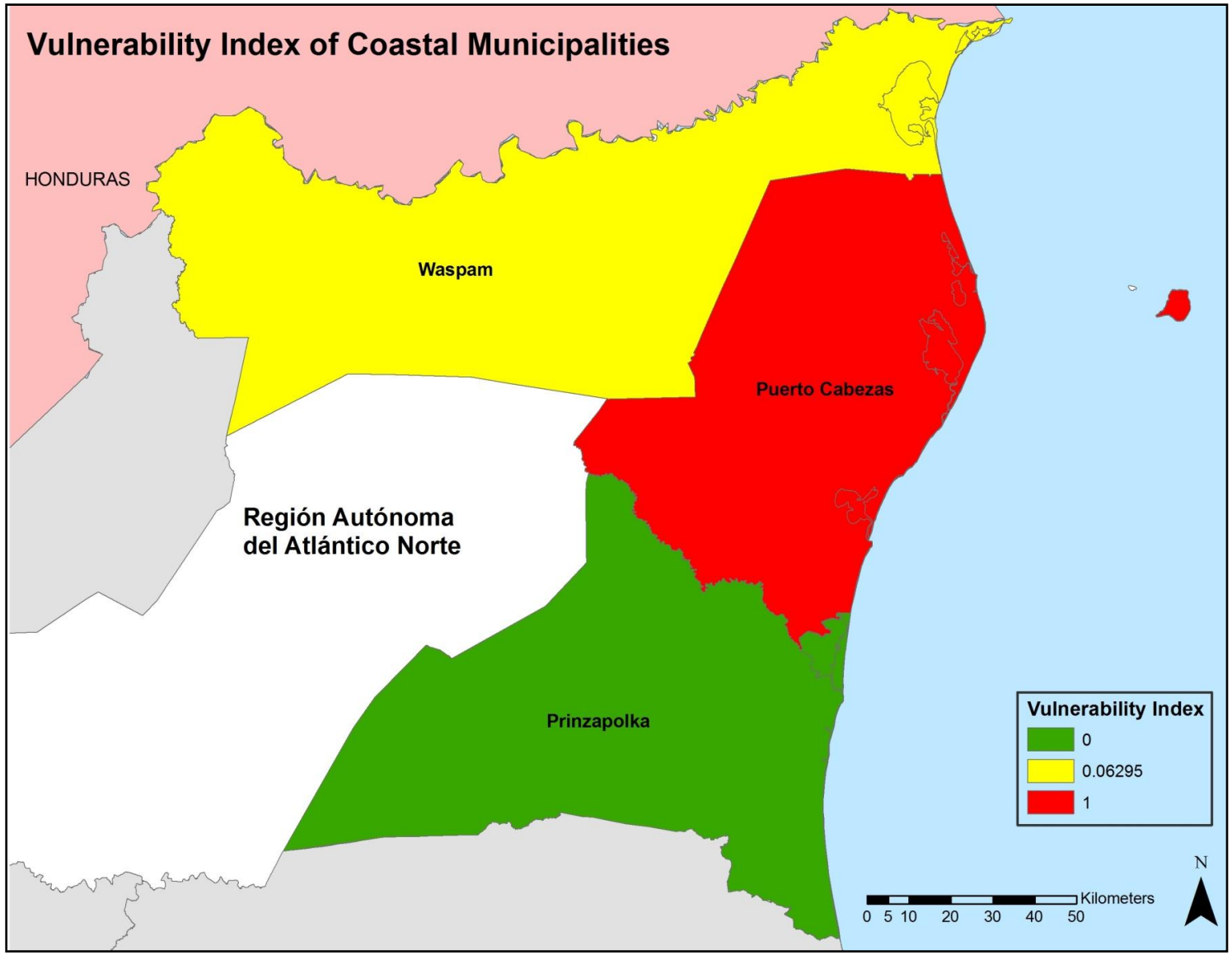

Figure 7.7: Composite vulnerability score of 3 coastal Municipalities in RAAN. Puerto Cabezas has the highest vulnerability.

The potential surge model is a simplified view of the inundation after the surge has reached land. It does not take into consideration the bathymetry of the coast, the pressure, or wind speed of the hurricane. Its goal is to help display the flooding potential of the coastal areas in RAAN.

A map like this helps delineate areas for mitigation efforts before a hurricane makes landfall. Because the Mosquito Coast is a flat coastal plain enabling the inundation to go farther inland, there is vast area that can flood from hurricanes in all three municipalities. Since the model only uses elevation values and does not consider other obstacles like trees and man-made features, the surge distance is considerably high at 75 km.

Puerto Cabezas has the most number of communities that can be affected by storm surge (Figure 7.10). This is followed by Prinzapolka which does not have a big population but has numerous small Miskito communities that are in low lying areas. Waspam has the least number of communities that can be directly impacted by a storm surge.

Flooding of roads

Most of the coastal roads in RAAN are not asphalted and are thus easily flooded during storm events. In some parts they can also flood from heavy rains. There is a general lack of public transportation in this area; some Miskito villages get bus service only once a week (Figure 7.8.B) which could make evacuation difficult for the coastal population.

Puerto Cabezas has the maximum number of roads that can be inundated from a potential surge. Prinzapolka does not have asphalted roads but most roads are made of compacted earth (Figure 7.8.A) which can get easily washed away. Road network in Waspam, while limited, is not entirely in the low lying areas and thence not as vulnerable to inundation as the other two

municipalities. Figure 7.11 illustrates the road network in RAAN and the areas that can be flooded during hurricanes. Road networks are sparse outside of Bilwi in Puerto Cabezas because it is the only urbanized area in the region.

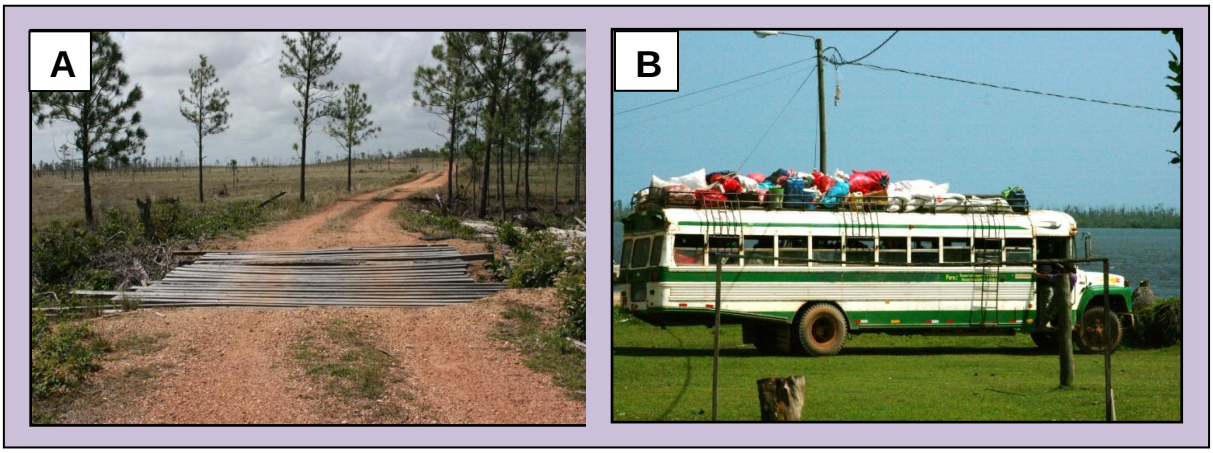

Figures 7.8: (A) Road built out of compacted earth. (B) Once-a-week bus service to Krukira.

7.6.3 Mapping of Potential Wind Speed

Wind speeds were interpolated using historic hurricane landfalls (Figure 7.12) as intensities of paleo-hurricanes were not known. An Inverse Distance Weighting (IDW) technique was used which assigns the highest weight to the nearest values and lowest to the farthest while interpolating missing data points.

Puerto Cabezas shows the highest wind speed potential due to its proximity to the landfall location of Hurricane Felix, a Category 5 storm. Hurricanes dissipate as they travel inland and not expected to affect the interior part of RAAN directly. Thus likelihood of strike shown for the coastal area is limited to 75 km based on the maximum distance of the potential surge inundation.

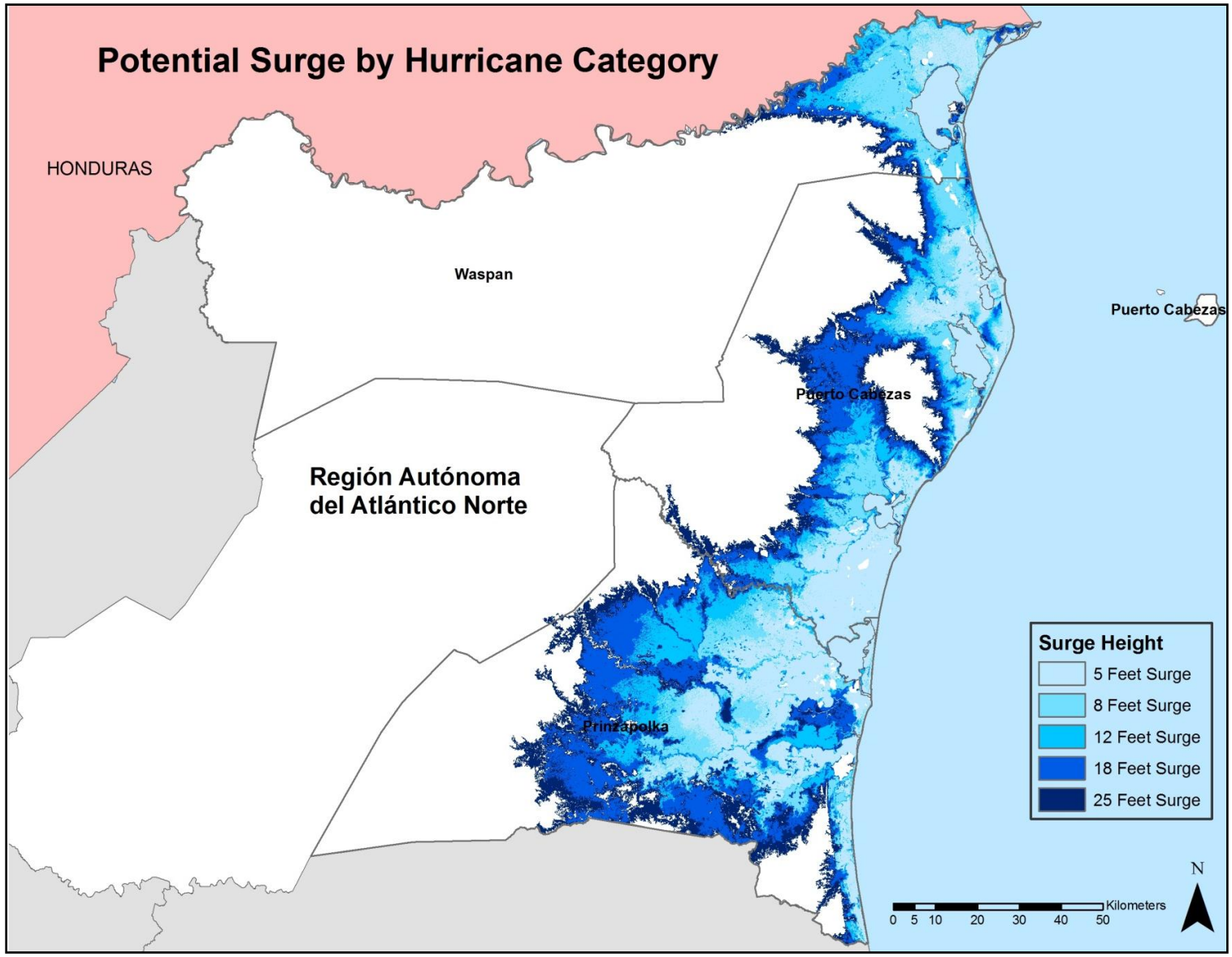

Figure 7.9: Potential inundation by storm surge from different categories of hurricanes.

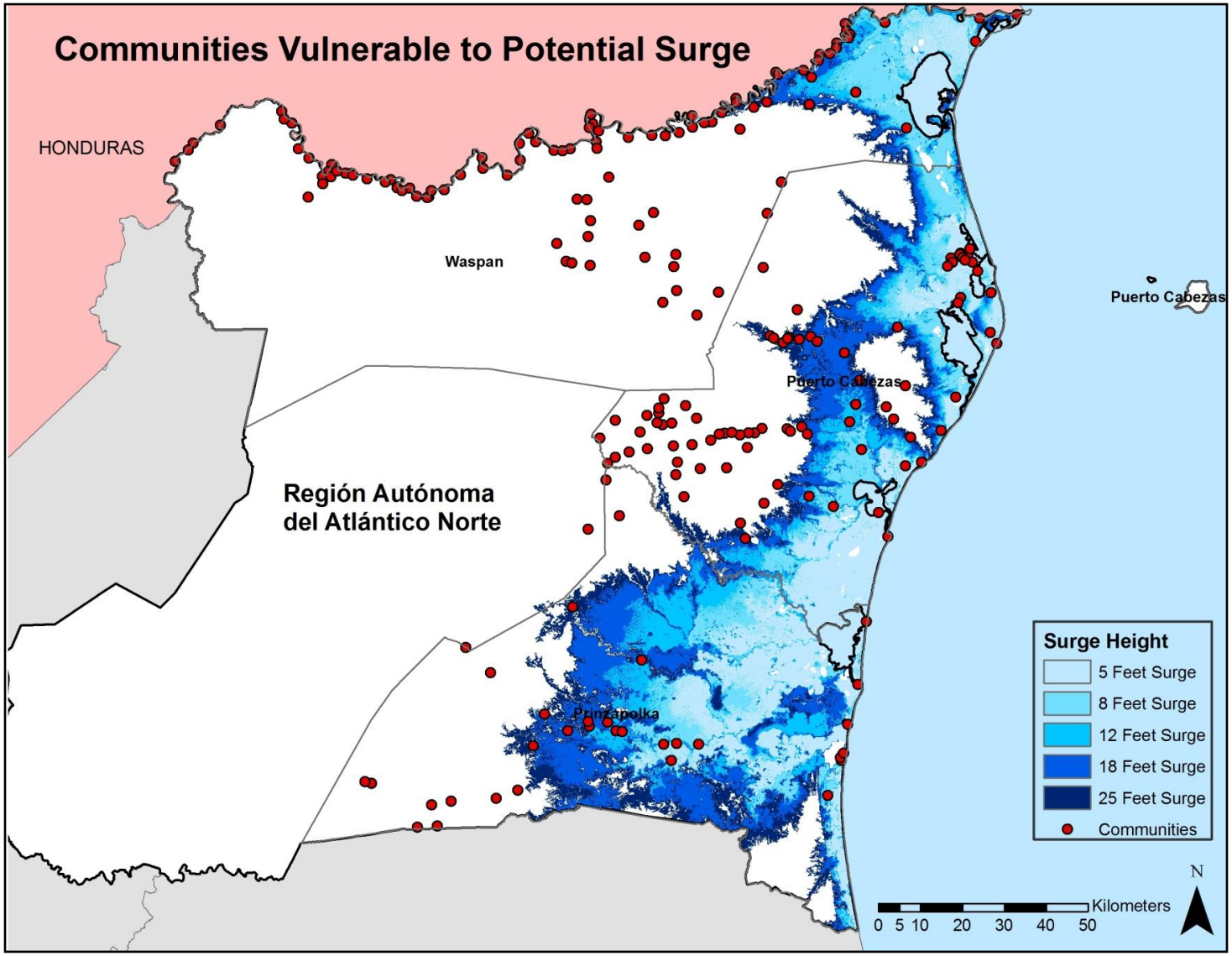

Figure 7.10: Communities that will be affected by potential storm surge inundation. Most are in Puerto Cabezas municipality followed by Prinzapolka.

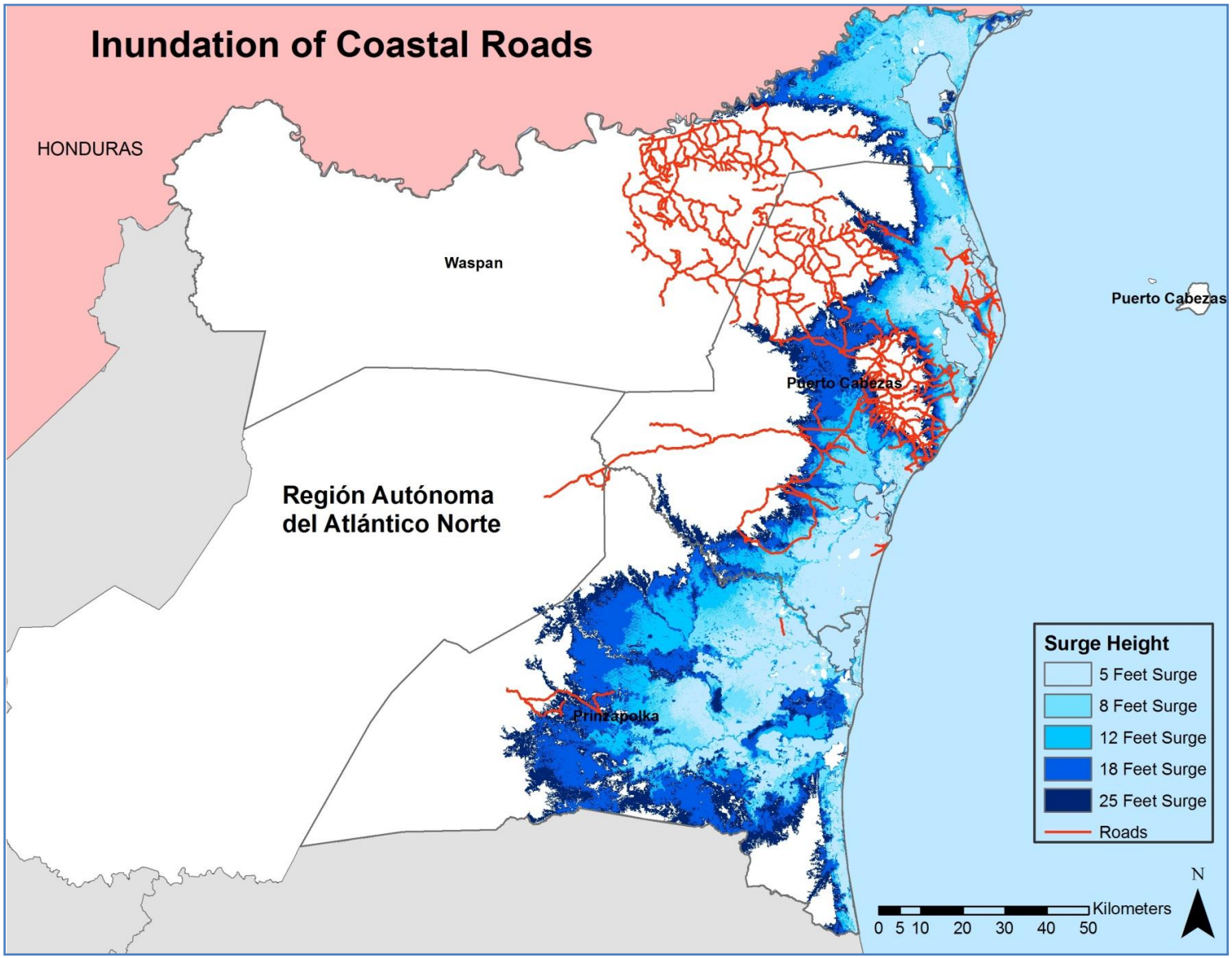

Figure 7.11: Flooding of coastal roads from hurricane surge.

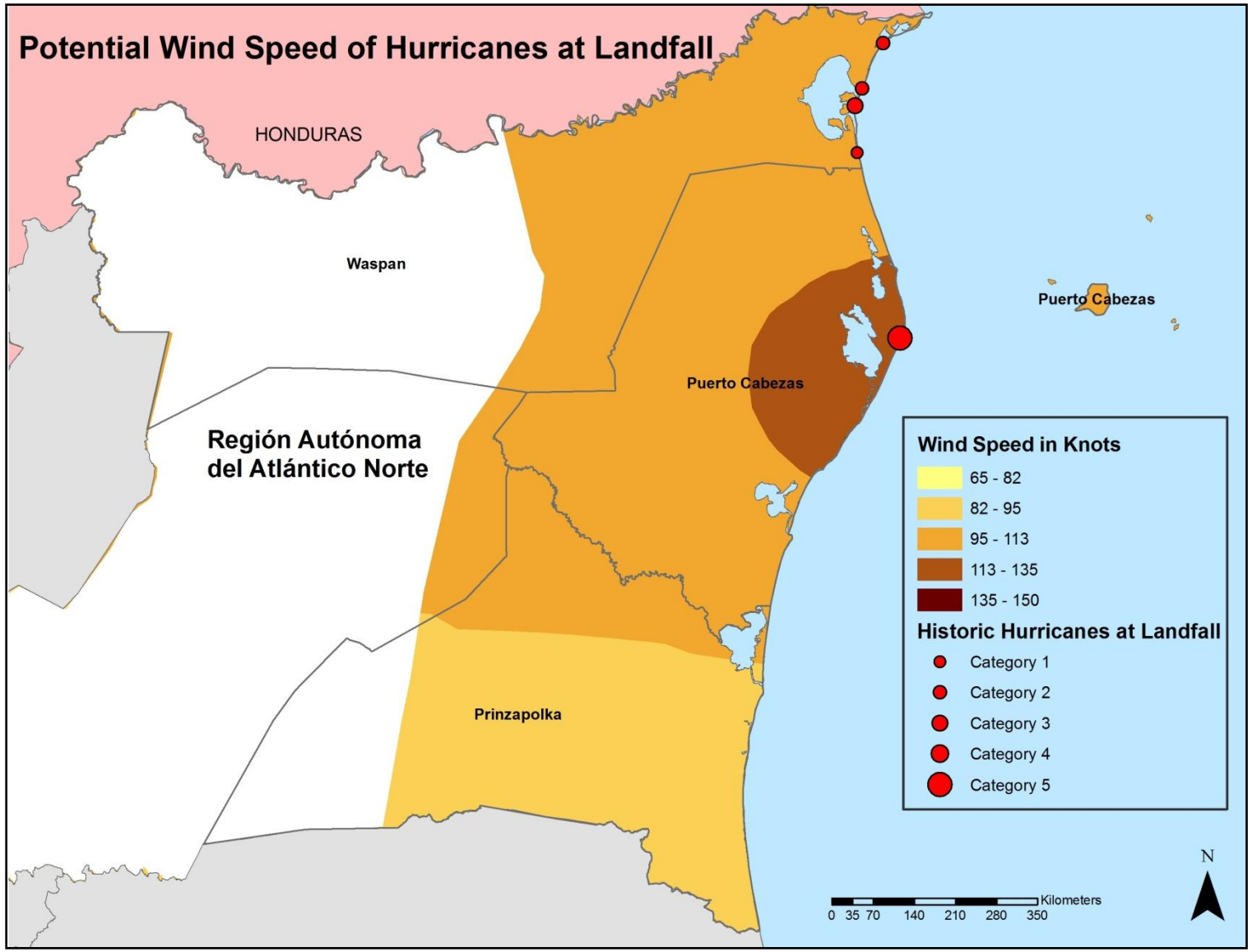

Figure 7.12: Potential inundation by storm surge from different categories of hurricanes.

7.6.4 Mapping of Hurricane Strike Probability

Strike probabilities were calculated for each municipality using a Poisson distribution model and mapped (Figure 7.13). Based purely on the historical strikes, the municipality of Waspam has the highest probability of strike followed by Puerto Cabezas. When paleo-hurricane records are included, Prinzapolka, which hasn't had any hurricane strikes in the last 160 years, has a small but quantifiable probability of future strike based on the 9 paleo-hurricane records from the Puerto Isabel core PIL 2. After adding the prehistoric records, Waspam still has the highest probability followed by Puerto Cabezas and then Prinzapolka.

7.6.5 Hurricane Risk Mapping for the Coastal Population

An amalgamation of the three components of risk (vulnerability, likelihood of hurricane landfall, wind, and storm surge hazard) results in athe comprehensive risk map (Figure 7.14) which shows areas that are most susceptible to the hurricane peril by virtue of their population, demographic composition, location, and topography.

The highest probability of hurricane strike is in the Waspam area. This municipality has moderately high vulnerability but a smaller area that can be inundated thus the risk is moderate in this municipality. Puerto Cabezas, while having a moderate likelihood of strike, is at greater risk from hurricanes (Figure 7.14) due to its high vulnerability. Prinzapolka has the lowest probability of strike and due to its moderate vulnerability, it is at a moderate risk as well.

LandScan grid data were utilized for population and based on different levels of surge, population that would be affected by each was identified (Lam *et al*., 2009). There are 37,533 people who would be impacted by a the surge of 5 feet; 65,174 by a surge of 8 feet; 74,940 by a surge of 12 feet; a surge of 18 feet will affect 86,003 people; and finally, a surge of 25 feet plus created by a Category 5 hurricane will affect 91,726. This means that 12% of the department's

population will be directly impacted by a Category 1 hurricane; 21% by a Category 2 hurricane; 24% by a Category 3 hurricane; 27% by a Category 4; and a 29% by a Category 5 hurricane.

Figure 7.15 shows coastal risk for the population of the RAAN that is directly impacted by the surge accompanied by hurricanes. This population is not limited by jurisdictional boundaries as this map uses LandScan population data for population count. Population in this data base is counted for each pixel illustrating the total population that would be in harm's way.

7.7 Summary

The municipality of Waspam has had the highest number of hurricane strikes (4) in the last two centuries. Puerto Cabezas has had one and Prinzapolka none. Based purely on historical data, the likelihood of hurricane strike for Waspam is the highest. When prehistoric records are considered for these municipalities, Waspam still has the highest probability of strike of hurricanes followed by Puerto Cabezas and lastly, Prinzapolka. Bilwi, the seat of the government of RAAN as well as the largest urban area in the region, is in the municipality of Puerto Cabezas. This makes the municipality more vulnerable than the other coastal municipalities. Also the population of this municipality is high, raising its total vulnerability to hurricanes.

The hurricane strike probability based on past hurricane record (Figure 7.13) is moderate, and the potential storm surge inundation map (Figure 7.9) illustrates that a large area in this municipality can be flooded. The municipality with the lowest vulnerability is Prinzapolka which has the lowest population and thus low scores on each of the demographic characteristics of vulnerability. It also has a lower likelihood of hurricane strikes based on empirical data. This makes the total risk of hurricanes in the municipality low. Waspam has a medium vulnerability (Figure 7.7) but a high probability of strike based on empirical data (Figure 7.13) thus increasing the total risk for this municipality.

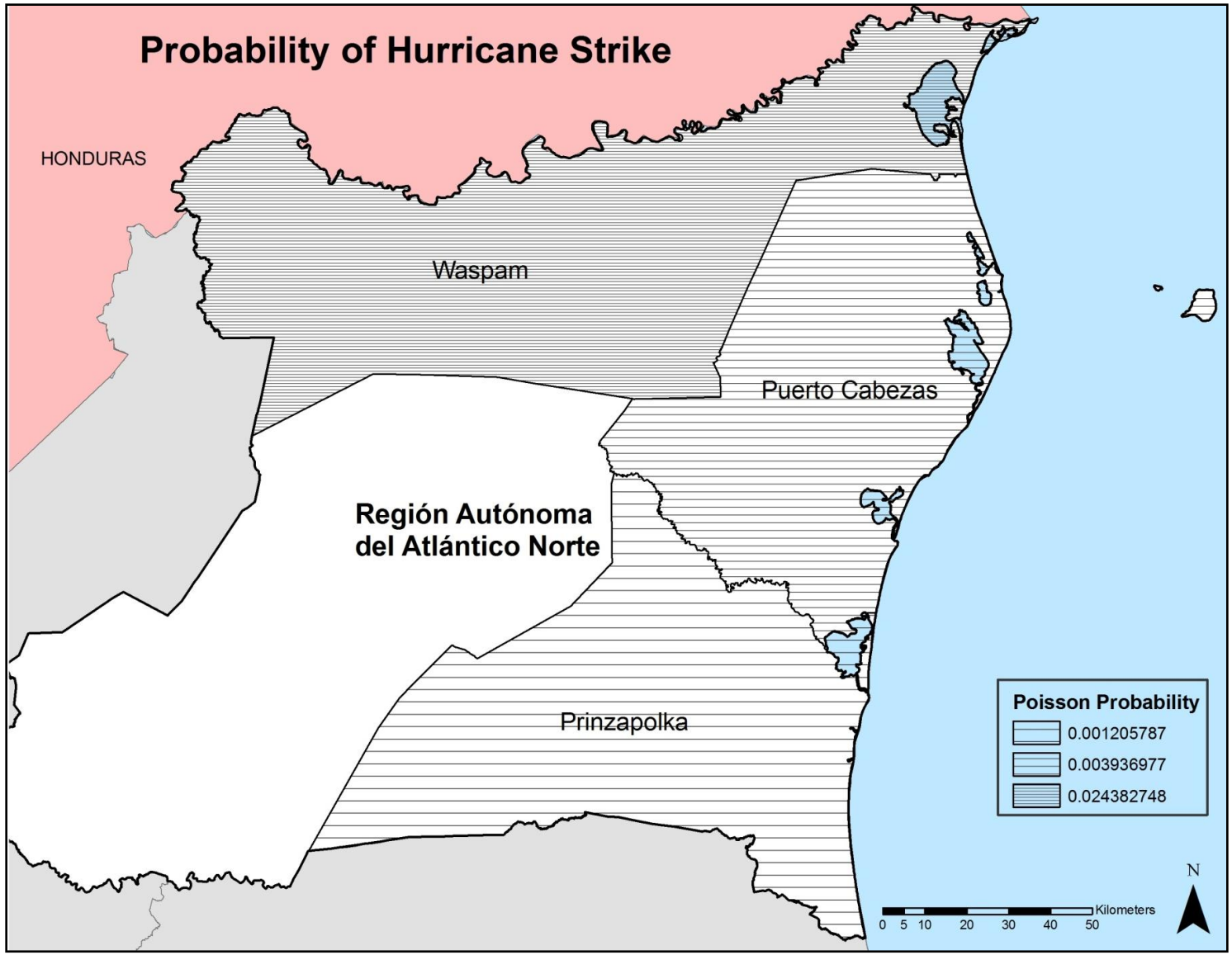

Figure 7.13: Poisson probability of strike based on historic and prehistoric hurricane records.

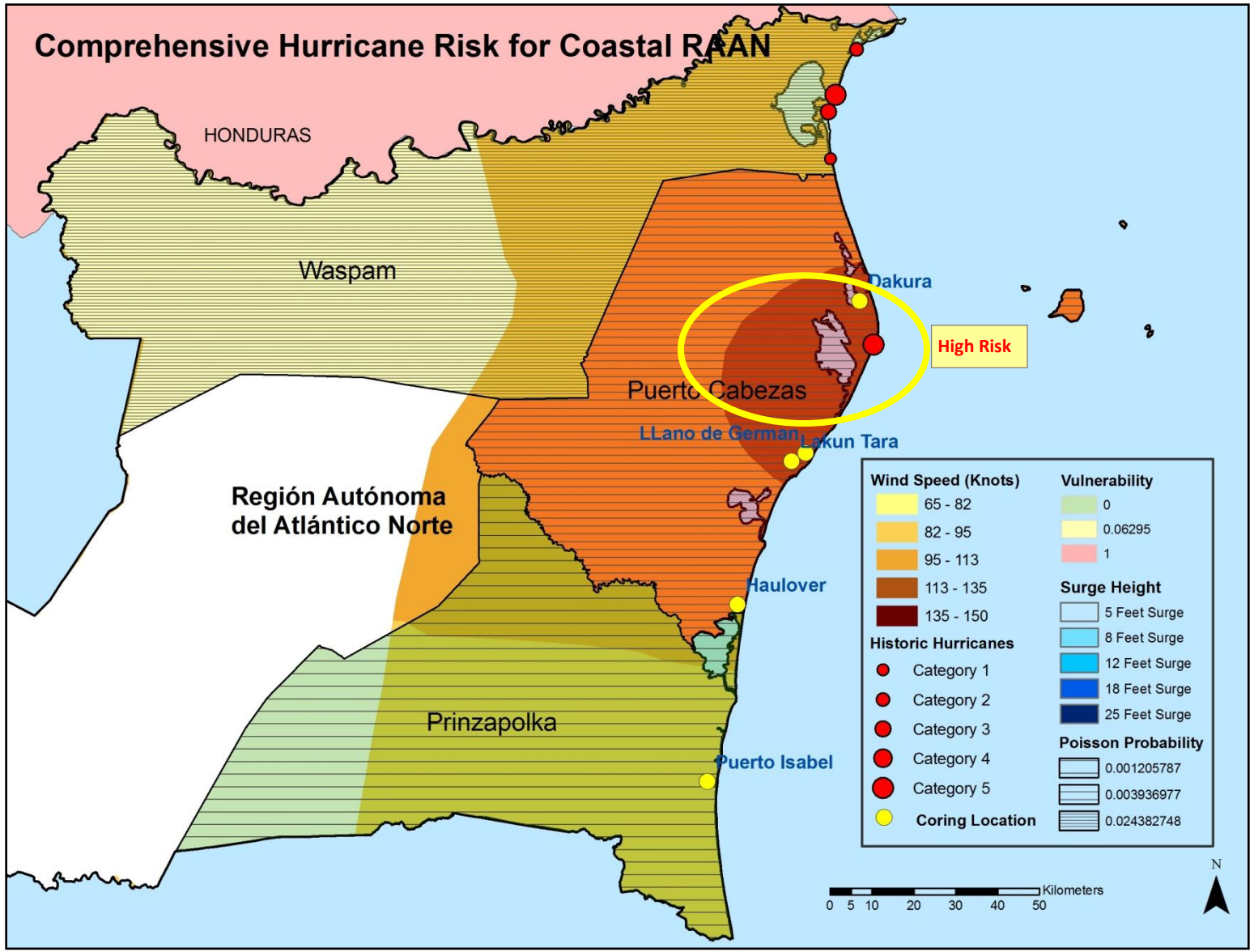

Figure 7.14: Comprehensive risk for coastal RAAN. Puerto Cabezas faces the highest risk.

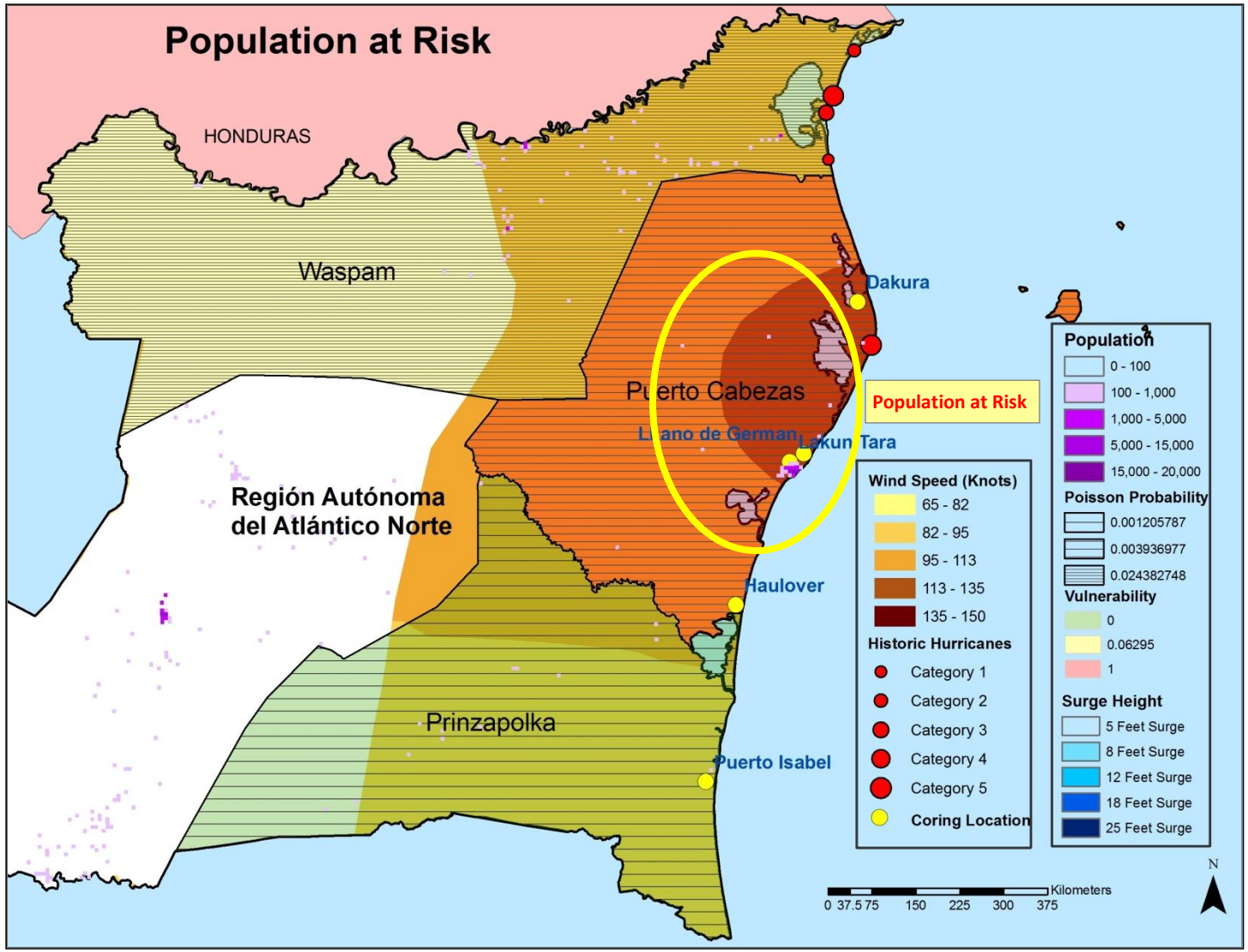

Figure 7.15: Population at risk from hurricanes and storm surge. There is a high population concentration in the Puerto Cabezas which is at most risk.

CHAPTER 8
DISCUSSION

8.1 Research Questions

The primary goal of this study was to analyze signatures left in coastal lakes by past hurricanes and to utilize that information in determining the likelihood of future hurricane strikes. This was closely followed by the task to provide a comprehensive view of the risk for coastal populations in the study areas. The two research questions corresponding to the above are:

1. **How does forecasting of future storm probability based on historic and prehistoric proxy data differ from forecasting based solely on historic data?**

Traditional forecasting of future hurricanes is based on historic data collected since 1851 AD (CSC, 2010). While this data capture decadal changes, longer-term hazard regimes are not apparent. The prehistoric hurricane strike data presented in this study can be used to refine estimates of future probabilities. In one example from the Dominican Republic, based on historical data, the likelihood of a hurricane strike for Pedernales province was 2.5 % (Table 5.1).

However, after combining with prehistoric records, the distribution suggests a considerably lower strike probability of 0.2% thus reducing the long-term risk for the province. Similarly, in another example, the province of El Seibo in the Dominican Republic, which has a 1.25 % strike probability based on historical records, sees a decrease in the likelihood of hurricane strike to 0.2% when prehistoric records are factored in (Table 5.1).

Conversely, in an example from RAAN, Nicaragua, the likelihood of hurricane strike for Prinzapolka is 0.0 but when prehistoric records are considered, Poisson probability of strike

increases to 0.0012 or 0.12% (Table 7.2).

A core obtained from Puerto Isabel, PIL 2 (Figure 6.26), is the longest and the oldest core in this study. This core shows alternating activity regimes: 0 – 925 cal yr BP (active); 925-3,350 cal yr BP (quiet); 3,350 cal yr BP – 3,750 cal yr BP (active); and then from 3,750 cal yr BP - 7,455 cal yr BP (quiet). In the period before 7,455 cal yr BP, no activity was recorded. These results are consistent with a similar study from the southern Mosquito Coast which reports an active period in the last millennium preceded by a quiet period from 1,000 cal yr BP to 3, 000 cal yr BP (McCloskey, 2009).

The Poisson probability of strike of a hurricane is calculated within a jurisdictional boundary based on historic and prehistoric landfall data. The shortcoming of this method is that jurisdictions such as provinces and municipalities with longer coastlines will have more strikes and thus lower return periods than those that have a shorter coastline. Secondly, if a hurricane strike is close to the border between two counties, the strike location will be counted in one county even though the neighboring county might have been equally affected.

Based on the chronology established by radiocarbon dating and grain size analysis, the western part of the Dominican Republic has seen at least 3 storms that have left records in the last 3,460 years and the eastern part has seen at least 5 in the last 2,330 years. The available data indicate a Poisson probability of 0.14% for the western and 0.2% for the eastern part. These probabilities are much less than the ones estimated based on historical records, i.e. at least 10% for the Dominican Republic (Pielke *et al.*, 2003).

RAAN, Nicaragua, shows a similar gap between the probability calculated from historical records and those from prehistoric records. All coring locations selected in RAAN, Nicaragua had indication of multiple hurricane events dated until 7,455 BP. In case of Dakura,

when the prehistoric data are added, the Poisson probability is 0.4% which is again much less than the range estimated by using only historical records which is 1% to 5% (Pielke *et al.,* 2003).

The wide gap between historic and prehistoric probability estimates for the two case studies are due to the following:

1. The probability based on the historical records is calculated for the regions based on latitudes, whereas this study focuses narrowly on the Dominican Republic and RAAN in Nicaragua.

2. This may be a reflection of the varying sensitivity of the coring sites. Selected sites may not have recorded all the storms that have occurred in the past.

3. Limited coring of coastal sites further reduces the chance of capturing all the hurricanes to have made landfall in this area.

These variations might lead one to question the utility of using paleo-hurricane records to understand future likelihood of hurricane strikes. But the intent of this study is not to substitute but rather supplement historic records in that a complete story is told.

2. How is risk and vulnerability distributed spatially for the Dominican Republic and Nicaragua?

Spatial distributions of vulnerability, probability of strike, potential inundation, and wind speed, as well as overall risk, are functions of location, topography, and demographic, characteristics of the coastal areas. Not surprisingly, the most "at risk" areas of both the case studies are urbanized and contain the capital city of the country/department. Distrito Nacional in the Dominican Republic has the highest risk (Figure 5.10) mainly due to its coastal location and high population. Distrito Nacional is the seat of the central government and a hurricane landfall in this area could cripple the whole country. Province with the lowest vulnerability is Pedernales

which has the lowest population and thus low scores on each of the demographic characteristics of vulnerability.

Bilwi, which is the seat of the government of RAAN as well as the largest urban area in the region, is in the municipality of Puerto Cabezas making this municipality more vulnerable than the other two coastal municipalities (Figure 7.7). The population of this municipality is high thus raising its total vulnerability to hurricanes. Municipality with the lowest vulnerability is Prinzapolka which has the lowest population and thus low scores on each of the demographic characteristics of vulnerability.

8.2 Origin of Overwash Layers in Cores

It is noted by researchers in the field that mainly events of great magnitude and intensity (Category 3-5) leave a signature in the sedimentary record (Nott, 2003). This theory may not be true if the lake was closer to the shore and therefore sensitive even to minor storms. Question then arises, were the records left by *only* major storms or storms of varying intensities?

When we look at the sea level curves provided for this region (Toscano and Macintyre, 2003; Digerfeldt and Hendry, 1989) it is apparent that the sea level has been rising albeit at a slower pace in the latter part of the Holocene and therefore a coastal lake could only move closer to the shore and would be more sensitive now to minor storms than in the past. Hence, an assumption is made that *all* categories of hurricane are capable of leaving a record based on the orientation of landfall and the sensitivity of the lake site.

Consequently, for the sake consistency, this project considers all categories of storms (i.e. Categories 1- 5) from the hurricane track data available from National Oceanic and Atmospheric Administration's (NOAA) historic storm database – HURDAT (CSC, 2010). While a threshold can be set based on modern analogs to determine the minimum intensity of hurricanes, it is

debatable to assume that the site conditions would have remained unchanging though thousands of years. A case of establishing a modern analog is from cores from Dakura in RAAN, Nicaragua. A distinct layer of sand was visible on top of both cores from Dakura, DAK 2 and DAK 3. This layer is 7 cm thick In DAK 2 and 8 cm thick in DAK 3. It is most likely from Hurricane Felix that made landfall as a category 5 hurricane in this region in 2007 as coring was done in 2008 and there is no sedimentation above these sand layers.

The second question that comes to mind regarding the origin of overwash records is that whether the records are from hurricane events or tsunamis deposits. While tsunami and hurricane deposits can be differentiated under ideal conditions as seen in the recent studies (Moya, 2006; Nayanama *et al.*, 2000; Scheffers *et al.,* 2005; Kelletat *et al.,* 2004; Dawson and Stewart, 2007; Morton *et al.,* 2007) described in Chapter 2, it is not easy to determine the origin of the overwash layer in the core. Kortekaas and Dawson (2007) found in a study done in Puerto Rico that it was only possible to identify hurricane deposits as separate from tsunami deposits by using multiple methods of differentiation. This becomes even more difficult in older cores as the sediment is considerably compacted and some of these methods become harder to apply.

In this study, a preliminary analysis of the overwash deposits in the cores extracted from the Dominican Republic and Nicaragua, did not exhibit the two characteristics that are visually apparent in defining tsunami deposits, such as large sized materials including coral (Scheffers *et al*., 2005) and deposits from alternating landward and seaward flow (Nayanama *et al.*, 2000, Dawson and Stewart, 2007; Morton *et al.,* 2007).

The third question that comes up is regarding the lateral extent of the overwash deposit. Some sand layers are visible in one core at a site and not in others at the same site. This can be explained by the particular attributes of the hurricanes and of the coring site such as the angle of

strike, position of the site in relation to the eye wall, and presence of ample sand in front of the site to be carried by the surge.

8.3 Future Work

This dissertation is only the first step in creating an integrated hurricane risk framework for the Caribbean area by utilizing paleotempestological, statistical, and visualization techniques. Much work needs to be done in the future to complete the picture for the entire circum-Caribbean region. Some of the future efforts are described below:

a. More dating to establish regime change

Not all event layers that were identified could be dated using radiocarbon dating technique due to budget and time constraints. Long term trends and changes will be better identified in the cores with improved dating control which can help understand and address long term shifts in regimes such as the Bermuda High Hypothesis (see Chapter 2).

b. ^{137}Cs and ^{210}Pb analysis of all cores

A comprehensive modern analog is pertinent in setting an intensity threshold for each site and will help select the storm categories that are above this threshold. ^{137}Cs and ^{210}Pb analysis of all cores would correlate known recent hurricanes with their signatures found in the cores.

c. Grain size analysis of all cores

As was evident in the LPE 2 core (see Chapter 4), not all sand layers from events are detectable in the LOI profile if there is negligible organic matter. Grain size analysis in addition to LOI analysis for all cores would help determine the presence of overwash sand. This type of analysis would also help in distinguishing hurricane deposits from tsunami deposits by revealing the sedimentary structure.

d. Further analysis to differentiate between hurricane and tsunami deposits

One of the important foundations of paleotempestological studies is proper identification of hurricane proxies. By using the multiple techniques covered in Chapter 2 to distinguish tsunami and hurricane deposits, a better deduction could be made as to the origin of overwash material.

e. More coring sites

Due to limited time and resources, only certain locations could be cored. Coring more locations at regular intervals and within smaller distance along the coast will improve the resolution of the cored data and possibly capture the prehistoric hurricanes records which may have gone undetected.

CHAPTER 9
CONCLUSION

Hurricanes account for a significant portion of the damages, injuries, and loss of life every year in the Caribbean. While hurricanes cannot be forecasted with absolute certainty, the ongoing target is to work towards reducing the vulnerability in areas that are most exposed to hurricanes. This project accomplishes this by providing extensive information about probability of strike, hazard, and vulnerability, such that mitigation measures can be taken to reduce impacts.

This dissertation examines hurricane records from the late Holocene and their importance in understanding the hurricane risk faced by the coastal population in the Dominican Republic and the Caribbean coast of northern Nicaragua. The two study areas are diverse in many ways thus providing a range of applicability of the multi-criteria risk assessment model provided in this dissertation. The paleotempestological findings from these areas provide a broader scientific foundation for estimating future hurricanes. The outcome of this study is a synthesis of the spatial and temporal dimensions of hurricane hazard with the vulnerability distribution of the coastal population. The results identify risk-prone zones in the study areas which are then spatially represented.

It is understood that there are constraints in using paleo data for future predictions, mainly due to the lack of knowledge about storm tracks for spatial reconstruction and about past conditions surrounding the recorded event. These gaps make it difficult to use only paletempetological data in predicting future events. Nonetheless, with careful use of modern analogs for calibration and knowledge of sea level changes in the Caribbean basin, paleotempestology is a powerful tool that complements historic and modern records.

This work taps into one of the many potential applications of paleotempestology and much more needs to be done in understanding the comprehensive hurricane risk in the Caribbean region. Considering this is the first paleo-hurricane proxy record for the Dominican Republic and the Mosquito Coast of northern Nicaragua, the paleotempestological findings from these areas suggest a need for more information from these sites to better understand the temporal and spatial patterns of hurricane strikes in the region. Although focused on two countries, it is hoped that this methodology can be applied in disaster planning and policy formulation by decision makers in other Caribbean locations as well.

REFERENCES

Adger, W. N, Brooks, N., Bentham,G., Agnew, M., Eriksen, S., 2004. New indicators of vulnerability and adaptive capacity. Norwich, UK: Tyndall Centre for Climate Change Research.

Alexander, D. 2000. *Confronting Catastrophe*. New York, NY: Oxford University Press.

Birkmann, J., 2007. Risk and vulnerability indicators at different scales: applicability, usefulness and policy implications. *Environmental Hazards* 7(1): 20-31

Blaikie, P., Cannon, T., Davis I., Wisner B., 1994. At Risk: Natural hazards, People's vulnerability, and disasters. London, Routledge.

Boose, E., 2004. A method for reconstructing historical hurricanes. In *Hurricane and Typhoons: Past Present and Future*, eds., Murnane, R.J., Liu, K.B., Columbia University Press, New York.

Boruff, B.J., 2005. A multiple hazards assessment of two Caribbean nations: Barbados and St. Vincent. *PhD Dissertation.* University of South Carolina. Columbia, SC.

Boruff, B.J. and S.L. Cutter. 2007. The environmental vulnerability of Caribbean island nations. *Geographical Review* 97(1): 24-45.

Briguglio, L., 2003. The vulnerability index and Small Island Developing States: a review of conceptual and methodological issues. Small Island Developing States Network (SIDS). http://www.sidsnet.org/docshare/other/20030909152131_capverde_paper_03Sep.doc (accessed on May 20, 2010).

Briguglio, L., 1995. Small Island States and their Economic Vulnerabilities. *World Development* 23: 1615-1632.

Bender, M.A., Knutson, T.R., Tuleya, R., Sirutis, J.J., Vecchi, G.A., Garner, S.T., Held, I.M., 2010. Modeled Impact of Anthropogenic Warming on the Frequency of Intense Atlantic Hurricanes. *Science* 327: 454-458.

Birks, H. J. B., 1993. Quaternary palaeoecology and vegetation science - current contributions and possible future developments. *Review of Palaeobotany and Palynology* 79: 153-177.

Cardona, O. D., 2005. Indicators of disaster risk and risk management. Washington D.C.: Inter-American Development Bank.

Carrara, A., M. Cardinali, R. Detti, F. Guzzetti, V. Pasqui, and P. Reichenbach. 1991. GIS techniques and statistical models evaluating landslide hazards. *Earth Processes and Landforms* 16: 427-445.

Central Intelligence Agency (CIA) 2010. The World Factbook.

https://www.cia.gov/library/publications/the-world-factbook/geos/dr.html (accessed on March 3, 2010).

Cheung, K.F., Tang, T., Donnelly, J.P., Scileppi, E.M., Liu, K.B., Nao, X.J., Houston, S.H., Murnane, R.J., 2007. Numerical modeling and field evidence of coastal overwash in southern New England from Hurricane Bob and implications for paleotempestology. *Journal of Geophysical Research* 112.

Chu, P.S., 2004. A method for reconstructing historical hurricanes. In *Hurricane and Typhoons: Past Present and Future*, eds., Murnane, R.J., Liu, K.B. Columbia University Press, New York.

Coastal Services Center (CSC) NOAA, 2010. Historical Hurricane Tracks. http://csc-s-maps-q.csc.noaa.gov/hurricanes/viewer.html (accessed on May 20, 2010).

Cutter, S. L., Boruff, B.J., Shirley W. L., 2003. Social Vulnerability to Environmental Hazards. *Social Science Quarterly* 84(2).

Cutter,S.L., 1996. Societal Vulnerability to Environmental Hazards. *International Social Science Journal* 47 (4): 525-536.

Cutter, S. L., J.T. Mitchell, and M.S. Scott. 2000. Revealing vulnerability of people and places: A case study of Georgetown county, South Carolina. *Annals of the Association of American Geographer* 90: 713-737.

Cutter, S. L., 2003a. The Changing Nature of Risks and Hazards. *American Hazardscapes,* National Academy of Sciences. http://books.nap.edu/catalog/10132.html (accessed on September 29, 2008).

Cutter, S.L. 2003b. GI science, disasters, and emergency management. *Transactions in GIS* 7(4): 439-445.

Dawson, A. G., and Stewart, I. 2007. Tsunami deposits in the geological record. *Sedimentary Geology* 200: 166-183.

Dengo, G., 1969. Problems of tectonic relations between Central America and the Caribbean. *Transactions: Gulf Coast Association of Geological Societies* 19: 311-320.

Dean, W. E. Jr., 1974. Determination of carbonate and organic matter in calcareous sediments and sedimentary rocks by loss on ignition: Comparison with other methods. *Journal of Sedimentary Petrology* 44: 242–248.

Desjardins, A.A., 2007. Paleoenvironmental Reconstruction of a Coastal Lagoon in Southwestern Dominican Republic. *MS Thesis,* Virginia Polytechnic Institute and State University, Blacksburg, Virginia.

Dix, G.R., Patterson, R.T, and Park, L.E. 1999. Marine saline ponds as sedimentary archives of late Holocene climate and sea-level variation along a carbonate platform margin: Lee

Stocking Island, Bahamas. *Palaeogeography, Palaeoclimatology, Palaecology* 150: 223-246.

Digerfeldt, G., Hendry, M.D., 1987. An 8000 year Holocene sea-level record from Jamaica: implications for interpretation of Caribbean reef and coastal history. *Coral Reefs* 5(4): 165-169.

Dodds, D.J., 2001. The Miskito of Honduras and Nicaragua. In Stonich, S.C., ed., *Endangered Peoples of Latin America: Struggles to Survive and Thrive*, Greenwood Press, Westport, CT.

Donnelly, J.P., 2005. Evidence of past intense tropical cyclones from backbarrier salt pond sediments: A case study from Isla de Culebrita, Puerto Rico, USA. *Journal of* Coastal Research 42: 201-210.

Donnelly, J.P., Bryant, S.S., Butler, J., Dowling, J., Fan, L., Hausmann, N., Newby, P., Shuman, B., Stern, J., Westover, K., and Webb III, T., 2001a. 700 yr sedimentary record of intense hurricane landfalls in southern New England. *Geological Society of America* 113: 714-727.

Donnelly, J.P., Roll, S., Wengren, M., Butler, J., Lederer, R., Webb III, T., 2001b. Sedimentary evidence of Intense Hurricane strikes from New Jersey. *Geology* 29 (7): 615-618.

Donnelly, J.P., Butler J., Roll, S., Wengren , M., Webb III, T., 2004. A backbarrier overwash record of intense storms from Brigantine, New Jersey. *Marine Geology* 210:107-121.

Douglas, B.C., Kearney, M.S., & Leatherman, S.P., 2001. Sea Level Rise: History and Consequences. *National Geophysics Series* 75.

Draper, G., Mann, P., Lewis, J. F., 1994. Hispaniola. In *Caribbean Geology: an introduction*, eds., Donovan S.K. and Jackson, T. A. University of the West Indies Publishers Association/University of the West Indies Press, Kingston, Jamaica: 129-150..

Emanuel, K., 2005. Increasing destructiveness of tropical cyclones over the past 30 years. *Nature* 436: 686-688.

Emanuel, K., 2006. Anthropogenic Effects on Tropical Cyclone Activity. http://wind.mit.edu/~emanuel/anthro2.htm (accessed on September 27, 2008).

El Instituto Nacional de Información para el Desarrollo (INIDE), 2006. http://www.inide.gob.ni/censos2005/censo2005.html (accessed on June 12, 2010).

Elsner, J.B., Kara, A.B, 1999. Hurricane of the North Atlantic. Oxford University Press, New York.

Elsner, J.B., 2000. Changes in the rates of North Atlantic major hurricane activity during the 20th Century. *Geophysical Research Letters* 27: 1743-1746.

Elsner, B., Bossak, B.H., 2001. Bayesian Analysis of U.S. Hurricane Climate. *Journal of Climate* 14: 4341-4350.

Elsner, J. B., Jagger, T. H., 2004. A hierarchical Bayesian approach to seasonal hurricane modeling. Journal of Climate 17: 2813–27.

Elsner, B., Bossak, B.H., 2004. A method for reconstructing historical hurricanes. In *Hurricane and Typhoons: Past Present and Future*, eds., Murnane, R.J., Liu, K-b, Columbia University Press, New York.

Elsner, J. B., 2006. Evidence in support of the climate change-Atlantic hurricane hypothesis. *Geophysical Research Letters* 33.

Elsner, J.B., Jagger, T.H., Liu, K.B., 2008. Comparison of hurricane return levels using historical and geological records. *Journal of Applied Meteorology and Climatology* 47:368-374.

Epstein, E. S., 1985. Statistical Inference and Prediction in Climatology: A Bayesian Approach. Meteor. *Monographs* 42.

Fairbanks, R.G. 1989. A 17,000-year glacio-eustatic sea level record: influence of glacial melting rates on the younger Dryas event and deep ocean circulation. *Nature* 342: 637-642.

FAO, Organización de las Naciones Unidas para la Agricultura y la Alimentación Nicaragua, 2007. Evaluación de Daños Causados por el Huracán Félix en el Caribe de Nicaragua. http://www.fao.org/fileadmin/templates/tc/tce/pdf/Nicaragua_FAO_Evaluacion_2007.pdf (accessed in Spanish on January 31, 2009).

Government of the Dominican Republic, 1958. Final Report of the Caribbean hurricane seminar, 1956. Ciudada Trujillo, Dominican Republic.

Fletcher, C.H., Richmond, B.M., Barnes, G.M., and Schroeder, T.A. 1995. Marine flooding on the coast of Kauai during hurricane Iniki – hindcasting inundation components and delineating washover. *Journal of Coastal Research* 11(1): 188-204.

Folk R.L.,Ward W.C., 1957. Brazos river bar: a study of significance of grain size parameters. *Journal of Sedimentary Petrology* 27: 3-26.

Frank ,W.M. & Young, G.S., 2007. The interannual variability of tropical cyclones. *American Meteorological Society* 135: 3587-3598.

Frappier, A.B**.**, Sahagian, D**.,** Carpenter, S.J., González, L.A., Frappier, B.R., 2007a. A stalagmite proxy record of recent tropical cyclone events. *Geology* 7(2): 111-114.

Frappier, A., Knutson, T., Liu, K-B., Emanuel, K., 2007b. Perspective: coordinating paleoclimatic research on tropical cyclones with hurricane –climate theory and modeling. *Tellus.*

Geerts, B., Heymsfield, G.M., Tian, L., Halverson, J. B., Guillory, A., Mejia, M. 2000. Hurricane Georges's Landfall in the Dominican Republic: Detailed Airborne Doppler Radar Imagery. *Bulletin of the American Meteorological Society* 81(5): 999-1018.

Geophysics Study Committee, Commission on Physical Sciences, Mathematics, and Resources**,**1990. *Sea-Level change.* National Research Council**,** National Academy Press**,** Washington DC**.**

Goldenberg, S.B., Christopher, L.W., Mestas-Nuñez, A.M. & Gray, W. M., 2001. The recent increase in Atlantic hurricane activity: causes and implications. *Science* 293: 474-479.

Gonzales, F.I., 1999. Tsunami! *Scientific American* 280: 56–65.

Hartwell, E., 1930. The Santo Domingo Hurricane of September 1 to 5, 1930**.** *Monthly Weather Review*, September 1930. http://docs.lib.noaa.gov/rescue/mwr/058/mwr-058-09-0362.pdf (accessed on March 24, 2010).

Hebert, P.J., 1980. Atlantic Hurricane Season of 1979. *Monthly Weather Review* 108: 973-990. http://www.aoml.noaa.gov/general/lib/lib1/nhclib/mwreviews/1979.pdf (accessed on March 24, 2010).

Heiri, O., Lotter, A. F., Lemcke, G., 2001. Loss on ignition as a method for estimating organic and carbonate content in sediments: reproducibility and comparability of results. *Journal of Paleolimnology* 25: 101–110.

Helwege, A., Birch, M.B.L., 2007. Declining Poverty in Latin America? A Critical Analysis of New Estimates by International Institutions. Global Development and Environment Institute, Tufts University, Medford MA 02155, USA.

Hewitt, K., 1997. *Regions of risk: A geographical introduction to disasters.* Addison Wesley Longman Limited: London, England.

Hodell, D. A., Curtis, J. H., Jones, G. A., Higuera-Gundy, A., Brenner, M., Binford, M.W. & Dorsey, K. T. 1991. Reconstruction of Caribbean climate change over the past 10,500 years. *Nature* 352: 790–793

Hsu, S. A., 2004. A Wind-Wave Interaction Explanation for Jelesnianski's Open-Ocean Storm Surge Estimation Using Hurricane Georges' (1998) Measurements. *National Water Digest* 28.

Inter American Institute for Global Climate Change, 2010. Current Project Summaries: CRN2050 http://iaibr1.iai.int/cgi-bin/SCI_Projects_Dynamic_Pages/CRN2/Factsheets/CRN2_50.pdf (accessed on May 10, 2010).

Intergovernmental Panel on Climate Change (IPCC), 2007. Climate Change 2007: Synthesis Report. http://www.ipcc.ch/pdf/assessment-report/ar4/syr/ar4_syr_spm.pdf (accessed on

September 29, 2008).

Islebe G., S´anchez O., 2002. History of Late Holocene vegetation at Quintana Roo, Caribbean coast of Mexico. *Plant Ecology* 160: 187–192.

Jagger, T. H., and J. B. Elsner, 2006. Climatology models for extreme hurricane winds in the United States. *J. Climate* 19: 3220–3236.

Keim, B.D., Muller, R.A., Stone, G.W., 2007. Spatiotemporal Patterns and Return Periods of Tropical Storm and Hurricane Strikes from Texas to Maine. *Journal of Climate* 20(14): 3498-3509.

Kelletat, D., Scheffers, A., Scheffers, S., and Scheffers, E. 2004. Holocene tsunami deposits on the Bahamian Islands of Long Island and Eleuthera. *Z.Geomorph. N.F.* 48(4): 519-540.

Kerr, R.A., 2010. Foreshadowing Haiti's Catastrophe. *Science* 327: 398.

Kikuchi, M., Kanamori, H., 1995. Source characteristics of the 1992 Nicaragua tsunami earthquake inferred from teleseismic body waves. *Pure and Applied Geophysics* 144(3-4): 441-45.

Klotzbach, P, Gray, W., Shama, U., Harman, L., Fitch., D., 2004. Methodology: Central America/Caribbean Landfall Probability Calculations. Colorado State University and GeoGraphics Laboratory, Bridgewater State College. http://www.e-transit.org/hurricane/welcome.html (accessed on May 1, 2010).

Kortekaas, S., and Dawson, A.G., 2007. Distinguishing tsunami and storm deposits: an example from Martinhal SW Portugal. Sedimentary *Geology* 200: 208-211.

Knowles, J.T., Leitner, M., 2007. Visual representations of spatial relationship between Bermuda High strengths and hurricane tracks. *Cartographic Perspectives* 56: 37-48.

Knowles, J.T., 2008. A 5000-year history of Caribbean environmental change and hurricane activity reconstructed from coastal lake sediments of the West Indies. *A Dissertation.* Louisiana State University. Baton Rouge, LA.

Knutson,T.R. & Tuleya, R.E., 2004. Impact of CO2-Induced Warming on Simulated Hurricane Intensity and Precipitation: Sensitivity to the Choice of Climate Model and Convective Parameterization. *Journal of Climate* 17(18): 3477-3495.

Krumbein, W.C., Sloss, L. L., 1963. *Stratigraphy and Sedimentation*, 2nd edition. Freeman, San Francisco.

La Oficina Nacional de Estadística, http://www.one.gob.do (accessed on March 22, 2010).

Lam, N. S.-N. 1983. Spatial interpolation methods: A review. *The American Cartographer* 10(2): 129-149.

Lam, N.S.-N., Arenas, H., Li, Z., and Liu, K.B., 2009. An estimate of population impacted by climate change along the U. S. coast. *Journal of Coastal Research* 56: 1522-1526.

LandScan™ Global Population Database. 2010. Oak Ridge, TN: Oak Ridge National Laboratory. http://www.ornl.gov/landscan/ (accessed on February 20, 2010).

Landsea, C.W., Harper, B.A., Hoarau K., Knaff. J. A., 2006. Climate Change: Can We Detect Trends in Extreme Tropical Cyclones? *Science* 313 (5786): 452 – 454.

Landsea, C.W., 2005. Hurricanes and global warming. *Nature* 436: 686-688.

Leatherman, S.P. 1983. Barrier dynamics and landward migration with Holocene sea-level rise. *Nature* 301, 415-417.

Lewis, J.F., Draper, G., 1990. Geological and tectonic evolution of the northern Caribbean margin. In: *The Geology of North America, The Caribbean Region*. eds., Dengo, G., Case, J. Boulder, Geological Society of America H: 77-140.

Liu, K.B., Fearn, M.L., 1993. Lake-sediment record of Late Holocene hurricane activities from coastal Alabama. *Geology* 21: 793-796.

Liu, K.B., Fearn, M.L., 2000a. Holocene History of Catastrophic Hurricane Landfalls along the Gulf of Mexico Coast Reconstructed from Coastal Lake and Marsh Sediments. In Ning, Z.H. and Abdollahi, K.K. eds., *Current Stresses and Potential Vulnerabilities: Implications of Global Change for the Gulf Coast Region of the United States*, Gulf Coast Regional Climate Change Council, Franklin Press, Baton Rouge.

Liu, K.B. and M.L. Fearn, 2000b. "Reconstruction of Prehistoric Landfall Frequencies of Catastrophic Hurricanes in Northwestern Florida from Lake Sediment Records," *Quaternary Research* 54: 238-45.

Liu, K.B. 2004. Paleotempestology: Principles, methods, and examples from Gulf Coast lake-sediments. In Murnane, R. and Liu, K.B., eds., *Hurricanes and Typhoons: Past, Present, and Future*, Columbia University Press, New York.

Liu, K.B., 2007. Paleotempestology. In *Encyclopedia of Quaternary Science*, eds. Elias, S., Elsevier, Amsterdam.

Liu, K.B., Lu, H., Shen, C., 2008. A 12000-year proxy record of hurricanes and fires from the Gulf of Mexico coast: Testing the hypothesis of hurricane-fire interactions. *Quaternary Research* 69: 29-41.

Lu, H.Y., Liu, K.B., 2005. Phytolith assemblages as indicators of coastal environmental changes and hurricane overwash deposition. *The Holocene* 15(7): 965-972.

Marshall, J.S., 2007. Geomorphology and Physiographic Provinces of Central America. In Bundschuh, J. and Alvarado, G., eds., *Central America: Geology, Resources, and Hazards*, Taylor and Francis, London, 75-122.

Mangerud, J, 1972. Radiocarbon dating of marine shells, including a discussion of apparent age of recent shells from Norway. *Boreas* 1:143-172.

McCann, W.R., 2006. Estimating the threat of tsunamigenic earthquakes and earthquake induced –landslide tsunami in the Caribbean. In *Caribbean Tsunami Hazard*, eds., Liu, P., Mercado-Irizarry, A. World Scientific Publishing, Singapore.

McCloskey, T.A., 2009. Proxy records of paleohurricanes for the western and southern Caribbean. *PhD Dissertation*, Louisiana State University, Baton Rouge, LA.

Miller, D.L., Mora, C., I., Grissino-Mayer H.D., Mock, C. J., Uhle, M., E., Sharp Z., 2006. Tree-ring isotope records of tropical cyclone activity. *Proceedings of the National Academy of Sciences* 103(39): 14294–14297.

Mimura, N., Nurse, L., McLean, R.F. Agard, J., Briguglio, L., Lefale, P., Payet, R., Sem, G., 2007. Small islands. Climate Change 2007: Impacts, Adaptation and Vulnerability. *Contribution of Working Group II to the Fourth Assessment Report of the Intergovernmental Panel on Climate Change*, eds., M.L. Parry, O.F. Canziani, J.P. Palutikof, P.J. van der Linden and C.E. Hanson. Cambridge University Press, Cambridge, UK, 687-716.

Mills, R. A., and Hugh, K.E., 1974. Reconnaissance group map of Mosquitia region, Honduras and Nicaragua Caribbean coast. The Association of American Petroleum Geologist Bulletin 58: 189-207.

Milne, G.A, Antony J. Long, A.J., Bassetta**, S**.E., 2005. Modelling Holocene relative sea-level observations from the Caribbean and South America. *Quaternary Science Reviews* 24(10-11): 1183-1202.

Morton, R. A., Gelfenbaum, G., Jaffe, B. E., 2007. Physical criteria for distinguishing sandy tsunami and storm deposits using modern examples. *Sedimentary Geology* 200: 184-207.

Morton, R.A., Sallenger, A.H., 2003. Morphological impacts of extreme storms on sandy beaches and barriers, *Journal of Coastal Research*, 19(3): 560–573.

Moya, J.C., 2006. Geomorphologic and stratigraphic investigations on historic and pre-historic tsunami in northwestern Puerto Rico: implications for long term coastal evolution. In *Caribbean Tsunami Hazard*, eds., Liu, P., Mercado-Irizarry, A. World Scientific Publishing, Singapore.

Murnane, R.J., 2004. Introduction. In *Hurricane and Typhoons: Past Present and Future*, eds., Murnane, R.J., Liu, K.B., Columbia University Press, New York.

Nardo, M., Saisana, M., Saltelli, A., Tarantola, S., 2005. Tools for composite indicators building. Working Paper, EUR 21682 EN. Ispra, Italy: European Commission Joint Research Centre.

National Hurricane Center (NHC), 2007. Hurricane Felix Tropical Cyclone Report. http://www.nhc.noaa.gov/pdf/TCR-AL062007_Felix.pdf (accessed on January 31, 2008).

National Oceanic and Atmospheric Administration, Coastal Services Center (NOAA), 2009. Coastal Inundation Mapping Guidebook. Charleston, SC. http://csc.noaa.gov/digitalcoast/inundation/pdf/guidebook.pdf#page=24 (accessed on April 28, 2010).

Nayanama, F., Shigeno, K., Satake, K., Shimokawa, K., Koitabashi, S., Miyasaka, S., Ishii, M., 2000. Sedimentary differences between the 1993 Hokkaido-nansei-oki tsunami and the 1959 Miyakojima typhoon at Taisei, southwestern Hokkaido, northern Japan. *Sedimentary Geology* 135(1-4): 255-264.

Nelson, R., 1995. Probability, Stochastic Processes, and Queuing Theory: The Mathematics of Computer Performance Modeling. Springer, New York.

Nott, J., 2003.The importance of Prehistoric Data and Variability of Hazard Regimes in Natural Hazard Risk Assessment – Examples from Australia. *Natural Hazards* 30: 43-58.

Nott. J., 2004. Paleotempestology: the study of prehistoric tropical cyclones – a review and implications for hazard assessment. *Environmental International* 30: 433 -447.

O' Loughlin, K.F., Lander, J.F., 2003. *Caribbean Tsunamis: A 500 –Year History from 1498-1998*. Kluwer Academic Publishers, The Netherlands.

Parsons, J. J., 1955. The Miskito pine savanna of Nicaragua and Honduras. *Annals of the Association of American Geographers (*45): 36-63.

Pempkowiak, J., Skiba, D., 1988. The determination of accumulation rates in the recent Baltic Sea sediments on the basis of ^{210}Pb and ^{137}Cs profiles. In Proceedings, XVI Conference Baltic Oceanographers 2**:** 824-832**.**

Pielke, R.A., Rubiera, J., Landsea, C., Fernandez, M.L., Klein, R., 2003. Hurricane vulnerability in Latin America and the Caribbean: normalized damage and loss potential. *Natural Hazards Review* 4(3): 101-114.

Pielke, R.A., 2007. Future economic damage from tropical cyclones: sensitivities to societal and climate changes. *Philosophical Transactions of the Royal Society* 365: 2717–2729.

Pielke R.A., Gratz, J., Landsea, C.W., Collins, D., Saunders, M.A., Musulin, R., 2008. Normalized Hurricane Damage in the United States: 1900–2005. *Natural Hazards Review* 30: 29–42.

Reimer, P.J., Baillie, M.G.L., Bard, E., Bayliss, A., Beck, J.W., Bertrand, C., Blackwell, P.G., Buck, C.E., Burr, G., Cutler, K.B., Damon, P.E., Edwards, R.L., Fairbanks, R.G., Friedrich, M., Guilderson, T.P., Hughen, K.A., Kromer, B., McCormac, F.G., Manning, S., Bronk Ramsey, C., Reimer, R.W., Remmele, S., Southon, J.R., Stuiver, M., Talamo, S Taylor, F.W., van der Plicht, J., Weyhenmeyer C.E., 2009. IntCal09 and Marine09 Radiocarbon Age Calibration Curves, 0–50,000 Years cal BP. *Radiocarbon* 51(4): 1111–1150.

Ritchie, J.C., McHenry, J.R., 1990. Application of radioactive fallout cesium-137 for measuring soil erosion and sediment accumulation rates and patterns: a review. *Journal of Environmental Quality* 19: 215- 233.

Ritchie, W., Penland, S., 1990. Coastline Erosion and Washover Penetration along the Bayou Lafourche Barrier Shoreline Between 1978 and 1985 with Special Reference to Hurricane Impacts. *O'Dell Memorial Monograph* 23, Department of Geography, University of Aberdeen.

Roy, P.S., Cowell, P.J., Ferland, M.A., Thom, B.G., 1997. Wave Dominated Coasts. In *Coastal Evolution: Late Quaternary Shoreline Morphodynamics,* eds., Carter, R. W. G., Woodroffe C. D., Cambridge University Press, UK.

Scheffers, A., Scheffers, S., and Kelletat, D. 2005. Paleo-tsunami relics on the southern and central Antillean Island arc. *Journal of Coastal Research* 21(2): 263-273.

Scott, D.B., Collins, E.S., Gayes, P.T., and Wright, E. 2003. Records of prehistoric hurricanes on the South Carolina coast based on micropaleontological and sedimentological evidence, with comparison to other Atlantic Coast records. *Geological Society of America* 115 (9): 1027-1039.

Sluijs, A., Pross, J., Brinkhuis, H., 2005. From greenhouse to icehouse; organic-walled dinoflagellate cysts as paleoenvironmental indicators in the Paleogene. *Earth-Science Reviews* 68(3-4): 281-315.

Solow, A., Moore, L., 2000. Testing for a Trend in a Partially Incomplete Hurricane Record. *Journal of Climate* (13): 3696-3699.

Stone, G.W., Walker, N.D., Hsu, S.A., Babin, A., Liu, B., Keim, B.D., Teague, W., Mitchell, D., and Leben, R. 2005. Hurricane Ivan's impact along the northern Gulf of Mexico. *EOS, Transactions, American Geophysical Union* 86(48): 497-501.

Stuiver, M., and Reimer, P.J., 1993. Extended 14C data base and revised CALIB 3.0 14C age calibration program. Radiocarbon 35: 215-230.

Tobin, G.A., Montz, B.E., 1997. *Natural hazards: explanation and integration.* The Guilford Press: New York, NY.

Torrescano, N., Islebe, G.A., 2006. Tropical forest and mangrove history from southeastern Mexico: a 5000 yr pollen record and implications for sea level rise. *Vegetation History Archaeobotany*15: 191-195.

Toscano, M.A., Macintyre, I.G., 2003. Corrected western Atlantic sea-level curve for the last 11,000 years based on calibrated C-14 dates from Acropora palmate framework and intertidal mangrove peat. *Coral Reefs* 22 (3): 257-270.

Turner, B.L., Kasperson, R.E., Matson, P.A., McCarthy,J.J, Corell, R.W., Christenson, L.,

Eckley, N., Kasperson, J.X., Luers, A., Martello, M.L., Polsky, C., Pulsipher, A., Schiller, A., 2003. A framework for vulnerability analysis in sustainability science. *PNAS* 100(14): 8074-8079.

Tylmann, W., 2004. Estimating Recent Sedimentation Rates Using 210pb on the Example of Morphologically Complex Lake (Upper Lake Raduñskie, N Poland. *Geochronometria* (23): 21-26.

USAID, 2005. An economic snapshot. http://www.usaid.gov/our_work/cross-cutting_programs/wid/pubs/DominicanRepublic_Economic_Snapshot_Dec2005.pdf (accessed on March 19, 2010).

Woodruff, J. D., Donnelly, J. P., Emanuel, K., Lane, P., 2008a. Assessing sedimentary records of paleohurricane activity using modeled hurricane climatology. *Geochemistry ,Geophysics, Geosystems* 9(9).

Woodruff, J. D., Donnelly, J. P., Mohrig, D., Geyer, W., 2008b. Reconstructing relative flooding intensities for hurricane induced deposits from Laguna Playa Grande, Vieques, Puerto Rico. *The Geological Society of America* 36(5): 391-394.

APPENDIX A

COMPOSITION OF BEACH SAND SAMPLES

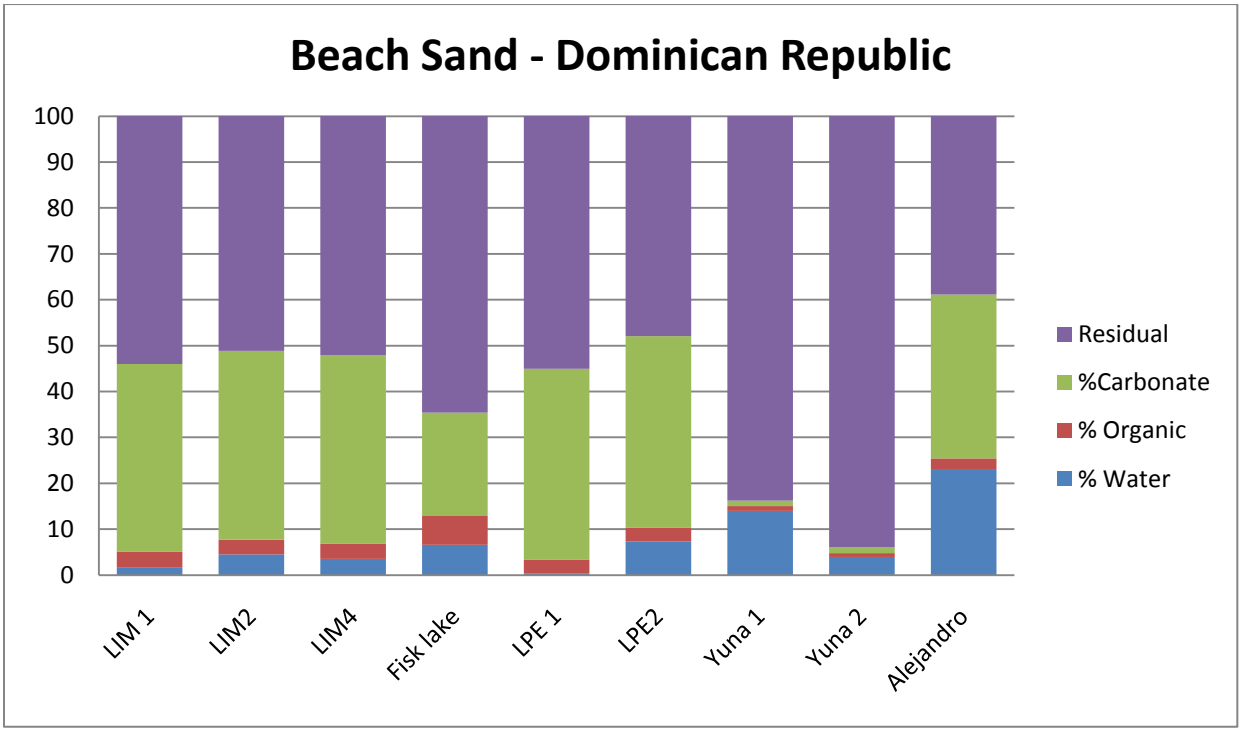

Appendix A-1: Loss-on-ignition compositions for beach sand samples. Note the high carbonate levels in the Dominican Republic samples.

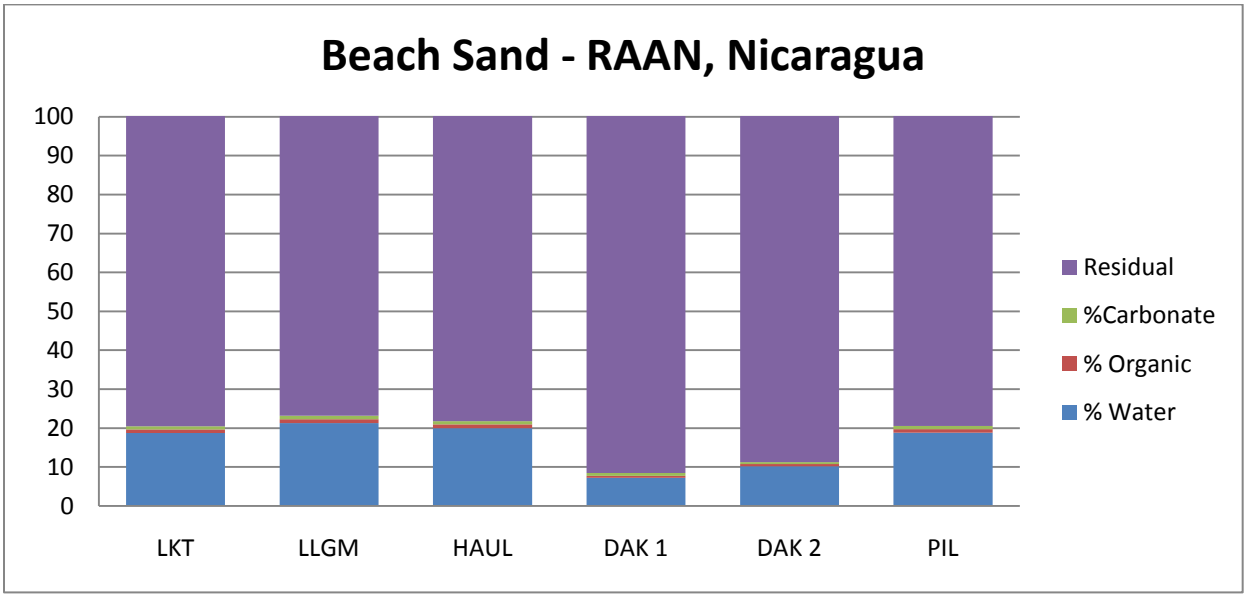

Appendix A-2: Loss-on-ignition compositions for beach sand samples. Note the low carbonate percentage in RAAN, Nicaragua samples.

APPENDIX B

VULNERABILITY AND PROBABILITY CALCULATIONS

Coastal Provinces	Population Index (+)	Gender Index (+)	Children Index (+)	Disability Index (+)	Poverty Index (+)	Building Index (+)	Connectivity Index (-)	Medical Index (-)	Vulnerability (∑Indices)	Normalized Vulnerability
Distrito Nacional	1.00	1.00	1.00	1.00	1.00	1.00	1.00	0.25	4.75	1.00
San Cristobal	0.19	0.18	0.21	0.17	0.33	0.29	0.04	0.08	1.26	0.38
La Altagracia	0.06	0.06	0.06	0.08	0.13	0.07	0.01	0.00	0.45	0.24
Puerto Plata	0.11	0.10	0.10	0.11	0.21	0.16	0.02	0.39	0.38	0.22
San Pedro de Macoris	0.11	0.10	0.11	0.09	0.20	0.15	0.02	0.41	0.34	0.22
Azua	0.07	0.06	0.07	0.06	0.15	0.10	0.02	0.29	0.22	0.19
Espaillat	0.08	0.07	0.07	0.10	0.12	0.07	0.01	0.29	0.20	0.19
La Romana	0.08	0.07	0.08	0.07	0.13	0.07	0.02	0.35	0.14	0.18
Peravia	0.06	0.05	0.06	0.06	0.09	0.03	0.02	0.37	-0.03	0.15
El Seibo	0.03	0.02	0.02	0.03	0.08	0.02	0.00	0.25	-0.05	0.15
Hato Mayor	0.03	0.02	0.02	0.03	0.07	0.01	0.00	0.25	-0.07	0.14
Maria Trinidad Sanchez	0.05	0.04	0.04	0.06	0.10	0.04	0.01	0.42	-0.11	0.14
Barahona	0.06	0.06	0.07	0.05	0.14	0.08	0.01	0.86	-0.42	0.08
Samana	0.03	0.02	0.02	0.03	0.06	0.00	0.00	0.62	-0.45	0.08
Monte Cristi	0.04	0.03	0.03	0.04	0.09	0.03	0.01	1.00	-0.76	0.02
Pedernales	0.00	0.00	0.00	0.00	0.00	-0.07	0.00	0.82	-0.88	0.00

Appendix B-1: Vulnerability scores for coastal districts in the Dominican Republic.

Province		0 Hurricanes					1 Hurricane				
	Mean	**1 Y**	**5 Y**	**10 Y**	**20 Y**	**50 Y**	**1 Y**	**5 Y**	**10 Y**	**20 Y**	**50 Y**
San Pedro de Macoris	0.0067	0.9933555	1.0000	1.0000	1.0000	1.0000	0.0066	0.0327	0.0643	0.1244	0.2827
San Cristobal	0.0267	0.9736857	1.0000	1.0000	1.0000	1.0000	0.026	0.1233	0.2313	0.4091	0.7316
Samana	0.0067	0.9933555	1.0000	1.0000	1.0000	1.0000	0.0066	0.0327	0.0643	0.1244	0.2827
Puerto Plata	0.0067	0.9933555	1.0000	1.0000	1.0000	1.0000	0.0066	0.0327	0.0643	0.1244	0.2827
Peravia	0.0200	0.9801987	1.0000	1.0000	1.0000	1.0000	0.0196	0.0943	0.1796	0.3270	0.6284
Pedernales	0.0032	0.9967699	1.0000	1.0000	1.0000	1.0000	0.0032	0.0160	0.0318	0.0626	0.1491
Monte Cristi	0.0000	1	1.0000	1.0000	1.0000	1.0000	0	0.0000	0.0000	0.0000	0.0000
Maria Trinidad Sanchez	0.0067	0.9933555	1.0000	1.0000	1.0000	1.0000	0.0066	0.0327	0.0643	0.1244	0.2827
La Romana	0.0000	1	1.0000	1.0000	1.0000	1.0000	0	0.0000	0.0000	0.0000	0.0000
La Altagracia	0.0400	0.9607894	1.0000	1.0000	1.0000	1.0000	0.0384	0.1779	0.3242	0.5433	0.8591
Hato Mayor	0.0000	1	1.0000	1.0000	1.0000	1.0000	0	0.0000	0.0000	0.0000	0.0000
Espaillat	0.0000	1	1.0000	1.0000	1.0000	1.0000	0	0.0000	0.0000	0.0000	0.0000
El Seibo	0.0014	0.9985724	1.0000	1.0000	1.0000	1.0000	0.0014	0.0071	0.0142	0.0281	0.0689
Distrito Nacional	0.0000	1	1.0000	1.0000	1.0000	1.0000	0	0.0000	0.0000	0.0000	0.0000
Barahona	0.0133	0.9867552	1.0000	1.0000	1.0000	1.0000	0.0132	0.0641	0.1240	0.2327	0.4843
Azua	0.0200	0.9801987	1.0000	1.0000	1.0000	1.0000	0.0196	0.0943	0.1796	0.3270	0.6284
Country	**0.1733333**	**0.8408573**	**0.9999**	**1.0000**	**1.0000**	**1.0000**	**0.1457**	**0.5451**	**0.7931**	**0.9572**	**0.9996**

Appendix B-2: Poisson probability of strike for varying number of hurricanes in the varying number of years in the future.

Province		2 Hurricanes					3 Hurricanes				
	Mean	**1Y**	**5 Y**	**10 Y**	**20 Y**	**50 Y**	**1Y**	**5 Y**	**10 Y**	**20 Y**	**50 Y**
San Pedro de Macoris	0.0067	0.0000	0.0001	0.0002	0.0004	0.0011	0.0000	0.0000	0.0000	0.0000	0.0000
San Cristobal	0.0267	0.0003	0.0017	0.0035	0.0069	0.0172	0.0000	0.0000	0.0000	0.0001	0.0002
Samana	0.0067	0.0000	0.0001	0.0002	0.0004	0.0011	0.0000	0.0000	0.0000	0.0000	0.0000
Puerto Plata	0.0067	0.0000	0.0001	0.0002	0.0004	0.0011	0.0000	0.0000	0.0000	0.0000	0.0000
Peravia	0.0200	0.0002	0.0010	0.0020	0.0039	0.0098	0.0000	0.0000	0.0000	0.0000	0.0001
Pedernales	0.0032	0.0000	0.0000	0.0001	0.0001	0.0003	0.0000	0.0000	0.0000	0.0000	0.0000
Monte Cristi	0.0000	0.0000	0.0000	0.0000	0.0000	0.0000	0.0000	0.0000	0.0000	0.0000	0.0000
Maria Trinidad Sanchez	0.0067	0.0000	0.0001	0.0002	0.0004	0.0011	0.0000	0.0000	0.0000	0.0000	0.0000
La Romana	0.0000	0.0000	0.0000	0.0000	0.0000	0.0000	0.0000	0.0000	0.0000	0.0000	0.0000
La Altagracia	0.0400	0.0008	0.0038	0.0077	0.0153	0.0377	0.0000	0.0001	0.0001	0.0002	0.0005
Hato Mayor	0.0000	0.0000	0.0000	0.0000	0.0000	0.0000	0.0000	0.0000	0.0000	0.0000	0.0000
Espaillat	0.0000	0.0000	0.0000	0.0000	0.0000	0.0000	0.0000	0.0000	0.0000	0.0000	0.0000
El Seibo	0.0014	0.0000	0.0000	0.0000	0.0000	0.0001	0.0000	0.0000	0.0000	0.0000	0.0000
Distrito Nacional	0.0000	0.0000	0.0000	0.0000	0.0000	0.0000	0.0000	0.0000	0.0000	0.0000	0.0000
Barahona	0.0133	0.0001	0.0004	0.0009	0.0018	0.0044	0.0000	0.0000	0.0000	0.0000	0.0000
Azua	0.0200	0.0002	0.0010	0.0020	0.0039	0.0098	0.0000	0.0000	0.0000	0.0000	0.0001
Country	**0.173333**	**0.0126**	**0.0616**	**0.1194**	**0.2245**	**0.4704**	**0.00073**	**0.0036**	**0.0073**	**0.0145**	**0.0358**

Appendix B-2 (contd.): Poisson probability of strike for varying number of hurricanes in the varying number of years in the future.

	Population Index (+)	Gender Index (+)	Children Index(-)	Elderly Index(-)	Vulnerability Score	Vulnerability Index
Waspam	0.621724193	0.619033	0.621773015	0.621273	2.483803221	0.620950805
Puero Cabezas	1	1	1	1	4	1
Prinzapolka	0	0	0	0	0	0

Appendix B-3: Vulnerability scores for coastal municipalities in RAAN, Nicaragua.

Municipality		0 Hurricanes					1 Hurricane				
	Mean	1 Y	5 Y	10 Y	20 Y	50 Y	1 Y	5 Y	10 Y	20 Y	50 Y
Waspam	0.025	0.97531	1.0000	1.0000	1.0000	1.0000	0.024382748	0.1161	0.2187	0.3896	0.7089
Puerto Cabezas	0.01085	0.989206	1.0000	1.0000	1.0000	1.0000	0.010735569	0.0525	0.1023	0.1942	0.4171
Prinzapolka	0.001956	0.998046	1.0000	1.0000	1.0000	1.0000	0.001952178	0.0097	0.0194	0.0383	0.0931

Municipality		2 Hurricanes					3 Hurricanes				
	Mean	1Y	5 Y	10 Y	20 Y	50 Y	1Y	5 Y	10 Y	20 Y	50 Y
Waspam	0.0067	0.0003	0.0015	0.0030	0.0061	0.0151	0.0000	0.0000	0.0000	0.0001	0.0001
Puerto Cabezas	0.0267	0.0001	0.0003	0.0006	0.0012	0.0029	0.0000	0.0000	0.0000	0.0000	0.0000
Prinzapolka	0.0067	0.0000	0.0000	0.0000	0.0000	0.0001	0.0000	0.0000	0.0000	0.0000	0.0000

Appendix B-4: Poisson probability of strike for varying number of hurricanes in the varying number of years in the future.

VITA

Devyani Kar was born in August 1978, in Cuttack, a city in the state of Orissa in India. She was awarded a Bachelor of Planning degree from the School of Planning and Architecture, New Delhi, India in 2001. She graduated from Nicholas School of the Environment and Earth Sciences, Duke University, in 2003 with a Master of Environmental Management degree. After graduation, Devyani worked as a Hazard Mitigation Planner for North Carolina Emergency Management before starting her doctoral studies at Louisiana State University. During her doctoral program, she also worked full-time as a Disaster Risk Analyst for Innovative Emergency Management, Inc., a disaster management company that was based out of Baton Rouge, Louisiana. Under the advisorship of Dr. Kam-biu Liu in the Department of Oceanography and Coastal Sciences, and with funding from the IAI Grant, Devyani travelled to the Dominican Republic and Nicaragua for her research in 2008. This dissertation is the culmination of that research. She expects to receive her Doctor of Philosophy degree in December 2010.